IJEST

ISSN: 0973-6255
Vol. 4 No. 1
January - June 2010

Indian Journal of Engineering, Science, and Technology

A Refereed Research Journal

BANNARI AMMAN
INSTITUTE OF TECHNOLOGY
Stay Ahead

BANNARI AMMAN INSTITUTE OF TECHNOLOGY
Sathyamangalam - 638 401 Erode District Tamil Nadu India

Indian Journal of Engineering, Science, and Technology

IJEST is a refereed research journal published half-yearly by Bannari Amman Institute of Technology. Responsibility for the contents rests upon the authors and not upon the IJEST. For copying or reprint permission, write to Copyright Department, IJEST, Bannari Amman Institute of Technology, Sathyamanagalam, Erode District - 638 401, Tamil Nadu, India.

Special Issue

Published from the Proceeding of National Conference

"Advancements and Futuristic Trends in Mechanical and Materials Engineering"
AFTMME'10

February 19-20, 2010

Organized by

Mechanical Engineering Section
Yadavindra College of Engineering
Punjabi University Guru Kashi Campus
Talwandi Sabo - 151 302, Bathinda, Punjab

Sponsored by

Department of Science and Technology
New Delhi

and

Council of Scientific and Industrial Research
New Delhi

Preface

It is our immense pleasure to publish the special issue of the journal from the proceedings of National conference on "Advancements and Futuristic Trends in Mechanical and Materials Engineering" (February 19-20, 2010) organized by Mechanical Engineering Section, Yadavindra College of Engineering, Punjabi University Guru Kashi Campus, Talwandi Sabo.

Mechanical engineers over the next two decades will be called upon to develop technologies that foster a cleaner, healthier, safer and sustainable global environment and will continue to lead the world in providing significant contributions to the essential sectors including energy, environment, manufacturing, transportation, waste management and health & medical care. Trends in the scientific and technological world indicate rapid transformations in the scope of mechanical engineering. The world of engineering is rapidly changing in its content, scope and expectations. Advancements in the engineering tools required for the growth of technological know-how has been catalytic in the recent achievements and the ones to come in the near future. The success of engineers and our profession depends on how well we can adapt to these changes and thus excel in facing the challenges ahead.

Futuristic trends in mechanical engineering, in the domains of energy, power generation, manufacturing, materials, and transportation are the need of the hour. The parameters that determine the standard of achievement in any subdivision are precision, quality, efficiency, economy, reliability and acceptability. Technology and its applications tend to become increasingly automated to maintain these standards and thus survive in the intense competition. To put it in a nutshell, it's going to be the survival of the fittest in a world of exceptional technologies. This conference provides a common platform for further training the mechanical engineers in the emerging interdisciplinary areas and recent technologies to meet the future challenges.

We are greatly indebted to Department of Science & Technology, New Delhi and Council of Scientific &Industrial Research, New Delhi without whose assistance, it would not have been possible to organize such a resourceful event. A special thanks to all the individuals and institutions who contributed to the success of the conference, the authors for submitting papers, the invited speakers for accepting our invitation and lending us their insight into recent developments in their research areas as well as the sponsors for their generous financial and logistical support. We are also thankful to the editor of IJEST, for publishing some of the selected papers in a special issue of the journal.

We are also highly thankful to the authorities of Punjabi University, Patiala for extending their support at each and every step to organize the conference. The help and co-operation received from the members of various committees is gratefully acknowledged. Lastly, we are also extending a word of gratitude to our chief patron, humble Dr. Jaspal Singh, Vice- Chancellor, Punjabi University, Patiala.

Organizing Committee

Indian Journal of Engineering, Science, and Technology

ISSN: 0973-6255

Volume 4 Number 1 **January - June 2010**

CONTENTS

Experimental Investigations for Tool Life Enhancement using Cryogenic Treatment

Rupinder Singh, Bhupinder Singh and Harpuneet Singh
Department of Production Engineering, Guru Nanak Dev Engineering College, Ludhiana, Punjab -141 006, India
E-mail:- rupindersingh78@yahoo.com

Abstract

Electrical discharge machining (EDM) is a potential process for commercial machining of tough materials like titanium and its alloys. This paper reports investigation on effect of cryogenic treatment for enhancing life of EDM tool while machining titanium alloys using Taguchi technique. The output parameters are tool wear rate (TWR) and surface roughness (SR) of machined surface. The results of the study suggest an improvement of 58.77% in TWR and 8.0% in SR.

Keywords: *Cryogenic treatment, EDM, Surface roughness, Titanium alloy, Tool wear rate*

1. INTRODUCTION

Electrical Discharge Machining (EDM) is a controlled metal-removal process that is used to remove metal by means of electric spark erosion [1]. In this process an electric spark is used as the cutting tool to cut (erode) the workpiece to produce the finished part to the desired shape [2]. The metal-removal process is performed by applying a pulsating (ON/OFF) electrical charge of high-frequency current through the electrode to the workpiece [3]. This removes (erodes) very tiny pieces of metal from the workpiece at a controlled rate [1-3]. Figure 1 shows schematic of EDM process [4].

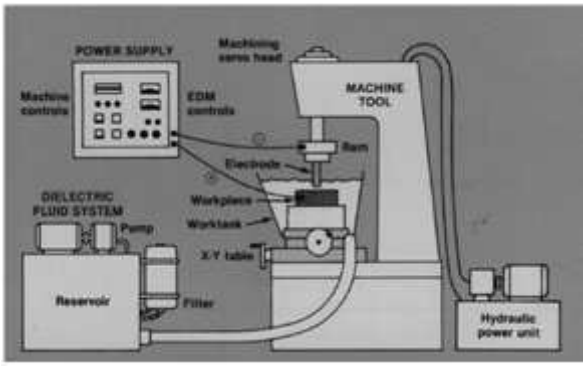

Fig. 1 Schematic of EDM process

Titanium (Ti) and its alloys exhibit excellent corrosion resistance and have high strength to weight ratio which make them ideal candidates for use in primarily two areas of application: corrosion resistant service and specific strength for efficient structures [5]. Normally, low strength, unalloyed, commercially pure (CP) Ti is used in the fabrication of tanks, heat exchangers and reactor vessels for chemical processing and power generation plants. High strength Ti alloys are used in high performance applications such as aerospace [6].

Cryogenics deals with the branches of science physics and engineering that study very low temperatures, how to produce them, and how materials behave at those temperatures [7]. Figure 2 shows schematic of cryogenic equipment. Figures 3 and 4 shows cryogenic and tempering cycle.

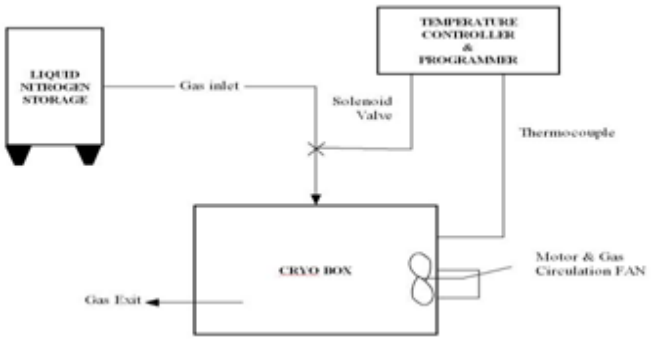

Fig. 2 Schematic of cryogenic equipment

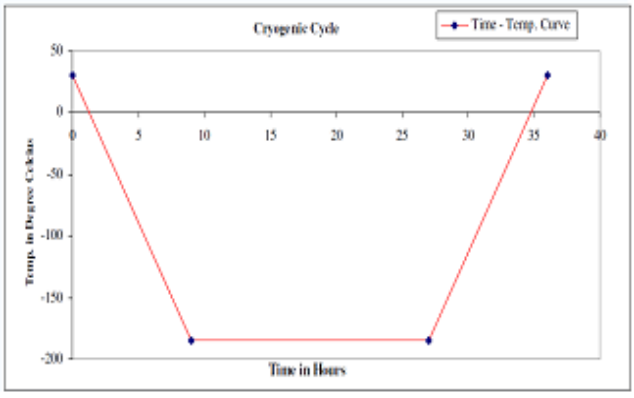

Fig. 3 Cryogenic cycle

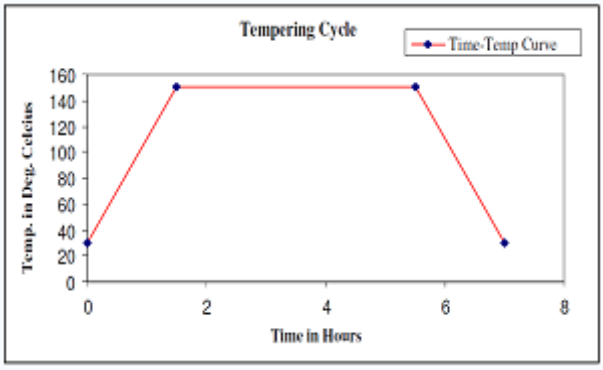

Fig. 4 Tempering cycle

The objective of the present work is to compare the machining characteristics of titanium with EDM, before and after cryogenic treatment of tool and work piece using Taguchi design approach. The output parameters for study are tool wear rate (TWR) and surface roughness (SR).

2. EXPERIMENTAL DETAILS

2.1 Substrate Materials

The substrate material selected for the study was commercially pure Ti (Titan 15), ASTM Gr.2 as workpiece and Ti, copper (Cu) and copper chromium (CuCr) as electrode. The workpiece samples were cut into 20 mm x 12 mm x 12mm and electrodes were of 6mm diameter and 100mm length for the experiments.

2.2 Input-Output Parameters

This research work was carried out with selected combinations of electrode and workpiece (pure Ti) by selecting three different current levels using L9 orthogonal array of Taguchi design approach. Cryo-treatment was performed at -80°C. Other input parameters for study were:

Work Materials

i. Ti (Plain)
ii. Ti (Cryogenic)

Tool Materials

i. CuCr (Plain)
ii. CuCr (Cryogenic)
iii. Cu (Plain)
iv. Cu (Cryogenic)
v. Ti (Plain)
vi. Ti (Cryogenic)

Current (I) level

i. 2, 4, 6(Ampere)

The output parameters were TWR and SR.

2.3 Experimental Setup

The experimentation was conducted on a CNC EDM machine. The different combinations of workpiece and electrode were made by taking cryogenic electrode with cryogenic workpiece and cryogenic electrode with plain workpiece. Whereas when the electrode was taken as plain then the workpiece were plain in one case and cryogenic in another case (Ref. Table 1).
Mathematically TWR = $(V_1-V_2)/t$

Where:

'V_1' initial weight of tool in gm (before machining)
'V_2' final weight of tool in gm (after machining)
't' machining time in min for '01mm' fixed depth of cut in work-piece measured with stopwatch.

The values of TWR have been put up to four decimal place by using the concept of significant figures. The accuracy of weighing balance was up to 10^{-4}gm. SR was measured as 'Ra value' expressed in microns by using a surface roughness measuring instrument (Talysurf).

3. RESULTS AND DISCUSSION

The results obtained from pilot experimental data were optimized by using Taguchi L9 orthogonal array to get optimized conditions of TWR and SR. With the help of MINITAB 15 software the ANOVA analysis of the above data was performed to attain the plots for TWR and SR. The results are valid with 95% accuracy level. Final experimentation was conducted in four sets. In the first set cryogenically treated electrode and cryogenically treated workpiece were machined using EDM. In the second setup non-cryo treated electrode and non-cryo treated workpiece was selected. In third setup non-cryo treated workpiece were machined with cryogenically treated electrode. In final setup non-cryo treated electrode and cryogenically treated workpiece combination was selected. Detailed analysis for set1 is given as below:

Table 1Experimental Observations

Input parameters				Output Parameters	
Tool		Work Piece	I	TWR	SR
Cryogenic	Ti	Cryogenic Titanium	2	0.0094	0.587
			4	0.0103	0.599
			6	0.0097	0.618
	Cu		2	0.0187	0.593
			4	0.0218	0.605
			6	0.0168	0.628
	CuCr		2	0.0145	0.591
			4	0.0187	0.603
			6	0.0161	0.624
Non-Cryogenic	Ti	Non-Cryogenic Titanium	2	0.0104	0.591
			4	0.0112	0.606
			6	0.0105	0.622
	Cu		2	0.0199	0.597
			4	0.0228	0.612
			6	0.0218	0.629
	CuCr		2	0.01735	0.594
			4	0.0195	0.609
			6	0.0189	0.627
Cryogenic	Ti	Non-Cryogenic Titanium	2	0.0109	0.595
			4	0.0114	0.609
			6	0.0114	0.628
	Cu		2	0.0185	0.603
			4	0.0215	0.613
			6	0.0194	0.632
	CuCr		2	0.0183	0.599
			4	0.0216	0.612
			6	0.0185	0.631
Non-Cryogenic	Ti	Cryogenic Titanium	2	0.0107	0.601
			4	0.0129	0.617
			6	0.0122	0.633
	Cu		2	0.0178	0.607
			4	0.0209	0.623
			6	0.0206	0.638
	CuCr		2	0.0189	0.605
			4	0.0232	0.618
			6	0.0223	0.635

Set 1: Workpiece Cryogenic Titanium

Model: TWR, SR versus Current, Tool

Factor	Type	Level	Values
Current	Fixed	3	2,4,6
Tool	Fixed	3	Cryogenic Cu, Cryogenic CuCr, Cryogenic Ti

Analysis of Variance for TWR, using Adjusted SS for Tests

Source	DF	Seq SS	Adj MS	F	P
Current	2	0.0000149	0.0000074	3.96	0.113
Tool	2	0.0001369	0.0000684	36.39	0.003
Error	4	0.0000075	0.0000019	-	-
Total	8	0.0001593			

S = 0.00137150

Analysis of Variance for SR, using Adjusted SS for Tests.

Source	DF	Seq SS	Adj MS	F	P
Current	2	0.0016740	0.0008370	627.75	0.000
Tool	2	0.0000827	0.0000413	31.00	0.004
Error	4	0.0000053	0.0000013	-	-
Total	8	0.0017620			

S = 0.00115470

Figures 5 and 6 shows main effects plot for SR and TWR.

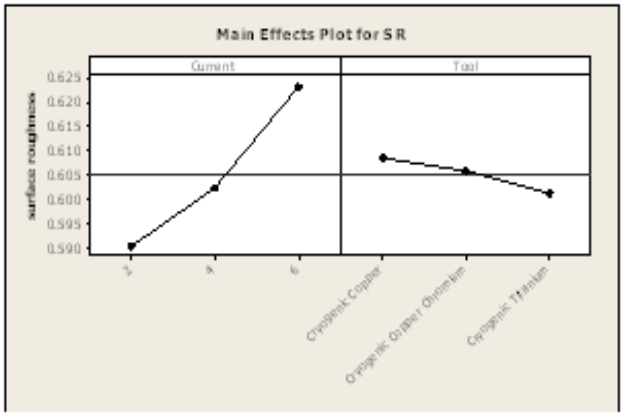

Fig. 5 Main effects plot for SR (for set1)

Similarly for set 2, 3 and 4 main effect plots for TWR and SR was developed.

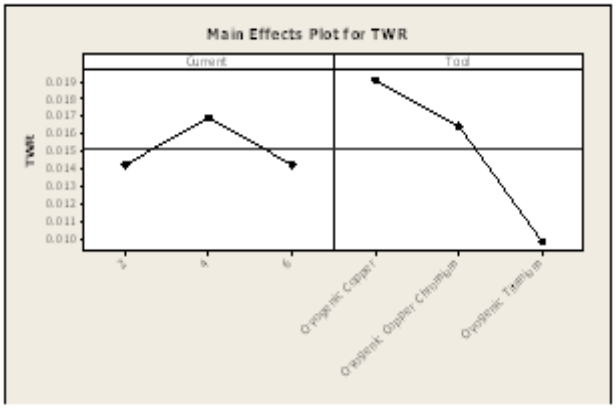

Fig. 6 Main effects plot for TWR (for set1)

3.1 Tool Wear Rate

For cryogenic Ti workpiece minimum value of TWR (i.e. 0.00943443 gm/min) was achieved with cryogenic Ti as tool and value of current was 2 Ampere. For Plain Ti workpiece minimum value of TWR (i.e. 0.010418803 gm/min) was achieved with plain Ti as tool and value of current was 2 Ampere. For Cryogenic Ti workpiece minimum value of TWR (i.e. 0.010778846 gm/min) was achieved with plain Ti as tool and value of current was 2 Ampere. For Plain Ti workpiece minimum value of TWR (i.e. 0.010935185 gm/min) was achieved with cryogenic Ti as tool and value of current was 2 Ampere.

The overall optimized value of TWR has been achieved at combination of cryogenic Ti workpiece, cryogenic Ti tool and 2 ampere current (Ref. Figure 7).

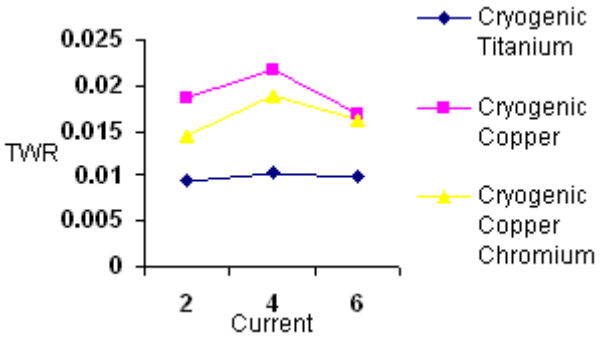

Fig. 7 Optimized TWR values at different values of current

The increase in TWR with increase in current from 2 to 4 ampere is but obvious, because with increase in current more ionization of dielectric fluid occurs which means more number of ions/ electrons are striking on the workpiece/ tool surface resulting in more TWR. The decreasing trend of TWR from 4 to 6 ampere may be explained on the basis of strain hardening of tool as a result of cryogenic treatment. That is why with Cu tool more TWR was observed as compared to Ti and CuCr.

3.2 Surface Roughness

For Cryogenic Ti workpiece minimum value of SR (i.e. 0.587 ìm) was achieved with Cryogenic Ti as tool and value of current was 2 Ampere. For Plain Ti workpiece minimum value of SR (i.e. 0.591 ìm) was achieved with plain Ti as tool and value of current was 2 Ampere. For Cryogenic Ti workpiece minimum value of SR (i.e. 0.601 ìm) was achieved with plain Ti as tool and value of current was 2 Ampere. For Plain Ti workpiece minimum value of SR (i.e. 0.595 ìm) was achieved with Cryogenic Ti tool and value of current was 2 Ampere. The overall optimized value of SR has been achieved with combination of cryogenic Ti workpiece, cryogenic Ti tool and 2 ampere current (Ref. Figure 8).

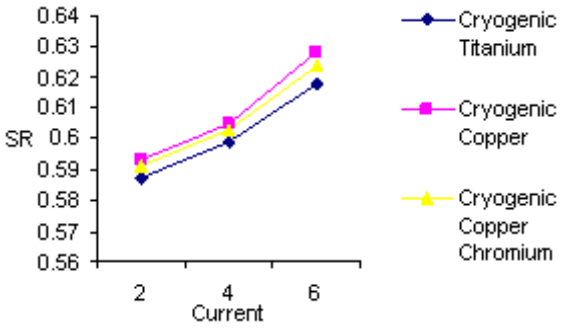

Fig. 8 Optimized SR values at different values of current

The cost of cryogenic treatment is commercially not high. It is available at the cost of Rs. 200/- only per kg. So this does not add much amount in final cost of machining with EDM process.

4. CONCLUSION

The results of the present study highlights that with the help of cryogenic treatment the machining parameters TWR and SR improves significantly when machined with EDM. Overall TWR and SR shows an improvement of 58.77% and 8% respectively with cryogenic treatment.

ACKNOWLEDGEMENT

The authors would like to thank Dr. M.S.Saini (Director, GNDEC Ludhiana) for providing laboratory facilities. The authors are also thankful to AICTE, New Delhi for financial support under CAYT.

REFERENCES

[1] R. Ramakrishnan and L. Karunamoorthy, “MUlti Response Optimization of Wire EDM Operations Using Robust Design of Experiments”, International Journal of Advance Manufacturing Technology, Vol. 29, 2006, pp.105-112.

[2] Shabgard, M. Reza, A. Ivanov and A. Rees , “Influence of EDM Machining on Surface Integrity of WC-Co”, Manufacturing Engineers Centre, Cadrif University, 2006, pp 1-5.

[3] M.Z. Zahiruddin, E.A. Rahim and S. Hasan, “Effect of Electrical Parameters on the EDM

Performances of Titanium Alloy" Proceedings of the 1st International Conference and 7th AUN/ SEED-Net Fieldwise Seminar on Manufacturing and Material Processing, 2006, pp. 147-150.

[4] B. Singh, "Effect of Cryogenic Treatment for Enhancing life of EDM Tool While Machining Pure Titanium", M.Tech Thesis PTU, Jalandhar, 2009.

[5] S. Sarkar, S. Mitra and B. Bhatacharyya, "Parametric Optimisation of Wire Electrical Discharge Machining of ã Titanium Aluminide Alloy Through an Artificial Neural Network Model", International Journal of Advance Manufacturing Technology, Vol. 27, 2006, pp.501-508.

[6] A. Luciana, "Superplasticity of Titanium Alloys", "Metalurgia (Bucharest)", Vol. 56, 2004, pp 26-31.

[7] J.Y. Huang, X.T. Zhu, X.Z. Liao, I.J. Beyerlein, M.A. Bourke and T.E. Mitchell, "Microstructure of Cryogenic Treated M2 Tool Steel", Journal of Materials Science and Engineering, Vol. 339, 2003, pp 241-244.

[8] W. Reitz and J. Pendray, "Cry-processing of Materials- A Review of Current Status", Journal of Materials and Manufacturing Processes, Vol. 16, 2001, pp 829-840.

Comparison of Simulated and Practical Results of a Gravity Filling Sand Casting Process using Aluminium Metal

Harvinder Singh and Ravinderpal Singh
Department of Mechanical Engineering, Chitkara Institute of Engineering & Technology, Rajpura,
Punjab - 151 302, India
E-mail: harvinder.shera@chitkara.edu.in, ravinderpal.singh@chitkara.edu.in

Abstract

Simulation has become an indispensable part of the engineering world. It has brought revolutionary changes in all the fields of mechanical engineering especially metal casting. The present paper analyzed and compared the casting of aluminum metal in real and simulated conditions using a modular software, PROCAST. The paper examined porosity, casting defects etc. in real as well as simulated conditions. The findings indicated that simulation of casting process is an economical, swift and flexible process than the conventional one. It has been further reported that simulation reduces the traditional trial and error casting methods resulting in improvement of the yield, product characteristics and quality within a short time. The future implications of the simulation technique have also been outlined.

Keywords: *Casting, Casting defects, Simulation, Quality*

1. INTRODUCTION

The simulation of casting process saves time, effort and labour, and we can know the loop holes of any design without even casting in foundry shop practically. More over fluid dynamics and various time temperature graphs can be plotted before hand . All most major defects like shrinkage, fraction of solid, porosity etc can be studied in advance.

There are a number of simulation software's like SolidCAST, Calsoft, ProCAST etc .We have chosen ProCAST as software for simulation of U shape pattern. Proper learning of the software is a very tedious one. But once you are thorough with the software you can easily simulate any casting process. It may be very valuable thing if this technique is used in the foundries, where the mould design is made by error and trail method hence they may save time and labour.

2. EXPERIMENTAL DETAILS

2.1 Test Shape

U shape aluminium casting was decided to be taken as test piece for this experimentation.

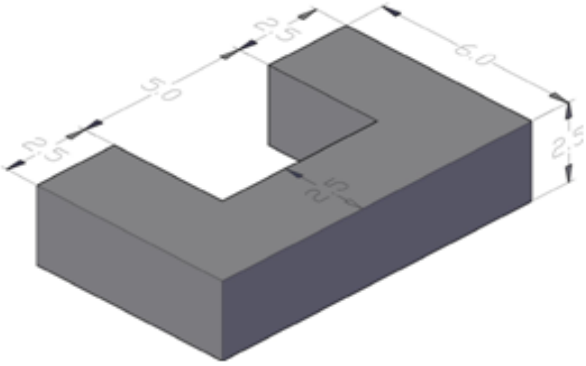

Fig.1

2.2 Cases

Following are the five cases which were taken on which simulation was done. And out of five three cases were actually casted in the foundry shop.

Fig. 2

CASE I

In this case the riser is absent and the cross section area of runner is taken as 2.5 square cm. Rest all dimensions of the required casting are same as the pattern

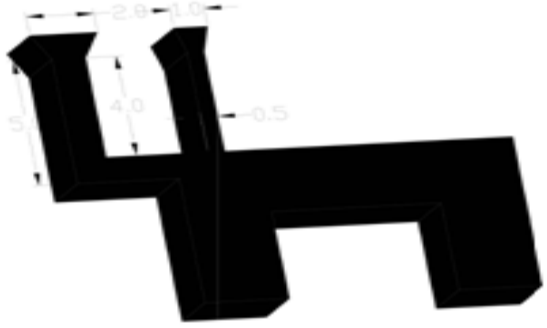

Fig. 3

CASE II

In this case the riser is placed near the ingate of the runner and the cross section area of runner is taken as 2.5 square cm. The cross section area of riser is 2.5*.5 square cm. Rest all dimensions of the required casting are same as the pattern.

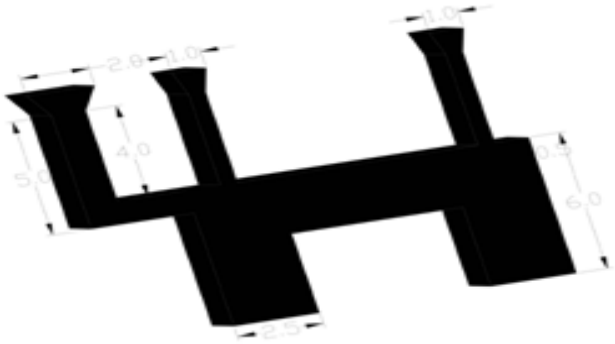

Fig. 4

CASE III

In this case one riser is placed near the ingate of the runner and another riser is placed on the other end. The cross section area of runner is taken as 2.5 square cm. The cross section area of riser is 2.5*.5 square cm. Rest all dimensions of the required casting are same as the pattern.

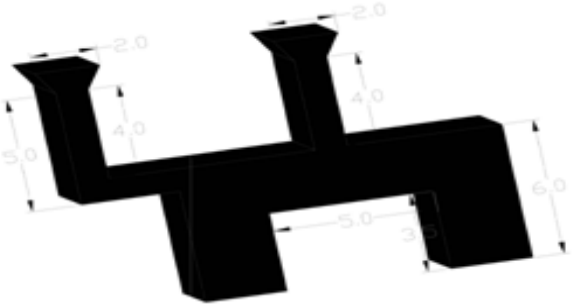

Fig. 5

CASE IV

In this case the riser is placed at the centre and the cross section area of runner is taken as 2.5 square cm. The cross section area of riser is 2.5 square cm. Rest all dimensions of the required casting are same as the pattern.

Fig. 6

CASE V

In this case the riser is placed on the opposite side of the runner and the cross section area of runner and riser is taken as 2.5 square cm. Rest all dimensions of the required casting are same as the pattern.

2.3 Drafting 3d Model and Generating Surface and Volume Mesh

All the five cases were drafted in Mesh cast module. When all the geometry construction, repairing and surface meshing is completed by clicking on the GENERATE TET MESH button the volume meshing process begins and is based on the specified ASPECT RATIO. We have taken aspect ratio as 1. GENERATE TET MESH is used to generate a 3-D tetrahedral mesh from a triangular surface mesh of the model. The quality of the tet mesh may also be enhanced by using the SMOOTH MESH function.

The functions available in the GENERATE TET MESH component may be used on an iterative basis in order to generate the tet mesh and enhance its quality. The normal sequence of steps for using TET MESH is as follows:

i. Generate the tet mesh
ii. Plot the quality of the generated tet mesh
iii. Smooth the tet mesh.

MeshCAST adds interior nodes to the model in iterations. Hence volume mesh is generated and the all the 5 cases were saved as .mesh file, which was ready to be imported in Pre CAST software.

2.4 Constraints Assignment in PreCAST Module Assignment of Virtual Mould

Since the U shape pattern was decided to be kept upside down as per the drawing. The mould box selected to be the size of 22cm*17cm*20 cm. ProCAST offers the capability of modeling a mold without meshing it, with the Virtual Mold option. This is especially useful in the case of large sand casting. It can also be used in permanent mold casting, if one is mainly interested in the filling behavior. When a Virtual mold is used, one should define the dimension of the mold (which is an orthogonal box, aligned with X, Y and Z, the material properties of the mold and the interface heat transfer coefficient between the different part of the casting and the mold. Values which were given were X min = 0, X max = 22 and Y min=0, Ymax=17, Z min=-10 and max=10.

2.4.1 Boundary Conditions Assignment

Since the material used is aluminium which is having melting point as 660^0 C ,the temperature of pouring metal must be high. Temperature boundary condition is given as 900^0C. Inlet point has to be defined .This ensures that temperature at inlet is taken as 900^0 C.

Then the Inlet point is defined. Select tools are used to specify the inlet point. The area is automatically calculated.

Then velocity is defined at that inlet area. The velocity is calculated by velocity calculator. Velocity calculator works when time and area is given. That velocity is assigned as the boundary condition. Then type of cooling is specified by using the boundary condition as heat. By selecting the whole body, area is automatically calculated.

2.4.2 Process Conditions Assignment

For Thermal problems (as well as for flow), the gravity vector should be defined in the “Process” menu

2.4.3 Gravity

For Thermal only problems, it is important to define the gravity direction for the calculation of the porosity (using the POROS=1 model). Value given in Y direction was -9.8 m sq/sec.

2.4.4 Initial Conditions Assignment

The initial temperature of each material should be defined in the initial condition menu.Value of Material Aluminium is given as 900^0C and value of virtual silca mold was taken as 20^0C.

2.4.5 Run Parameters Assignment

The thermal module was activated with THERMAL = 1. The fluid flow module was activated with FLOW =1. Some other more parameters were defined and the the file was saved as Restart file.

2.5 Running the Solvers

DataCAST

DataCAST converts the input data stored in ASCII in the prefixd.dat file into binary data ready for the solver.

ProCAST

Main solving part is done in ProCAST module. During the calculation, the status of the model can be monitored. To do so, the “Status” button of the Manager is used.

3. RESULTS AND DISCUSSION

3.1 Simulation Results

Case Without Riser

Following figures shows tempertature variation and flow at different times in secs:

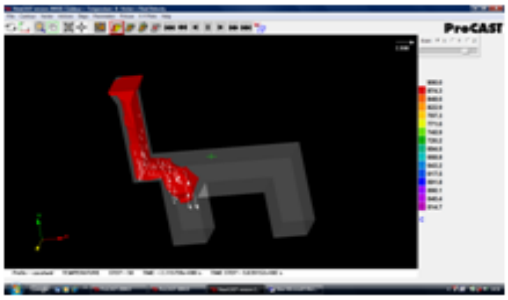

Fig. 7

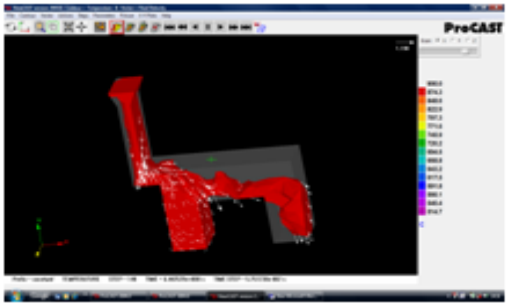

Fig. 8

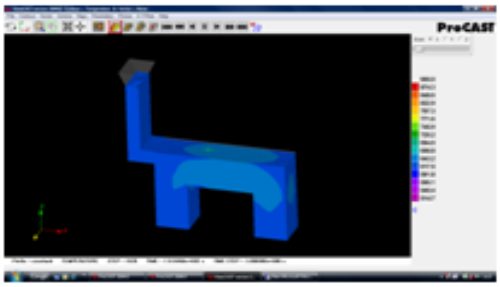

Fig. 9

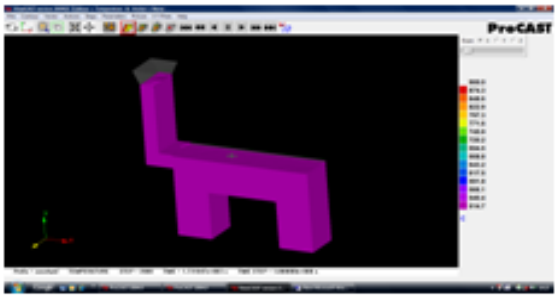

Fig. 10

Following figures shows solid fraction at different times in sec:

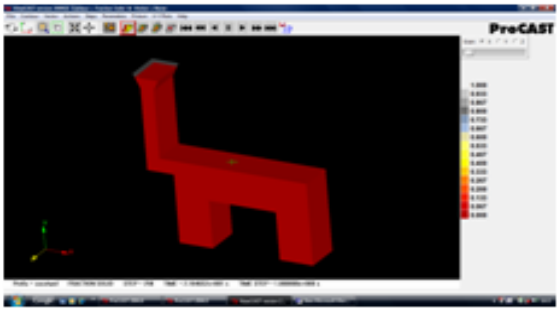

Fig. 11

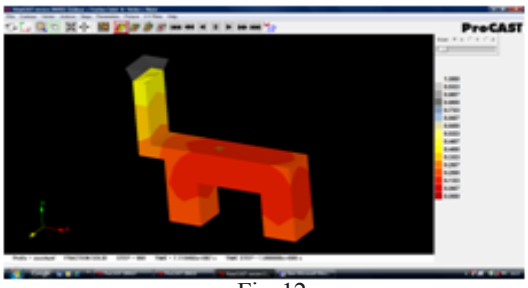

Fig. 12

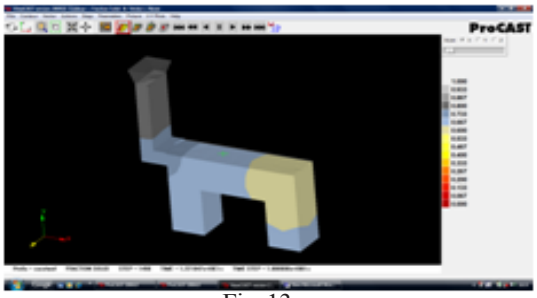

Fig. 13

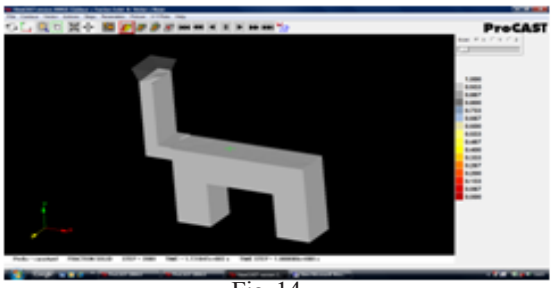

Fig. 14

Following figures shows shrinkage porosity at diff sections:

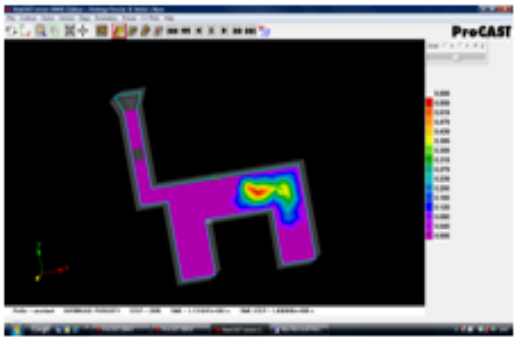

Fig. 15

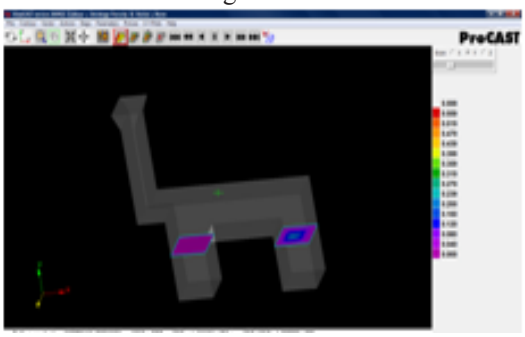

Fig. 16

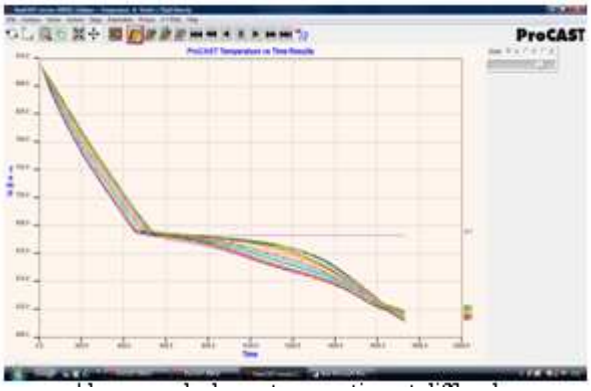

Fig. 17 Shows temp vs time at diff nodes

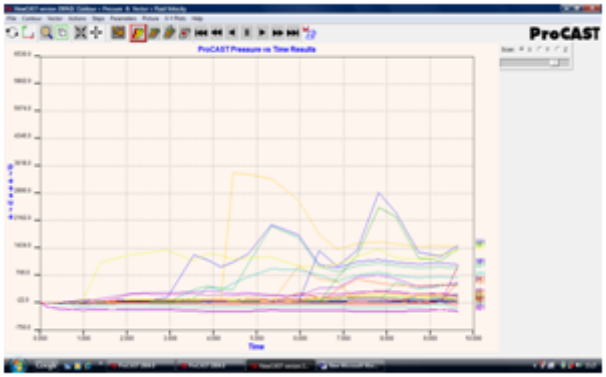

Fig. 18 Shows pressure vs time at diff nodes

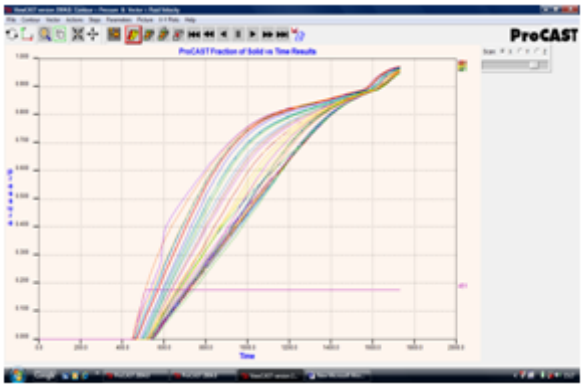

Fig. 19

3.2 Visual Analysis and Comparison with Simulated Results

Out of five cases three cases were casted in the foundry shop and the simulated and real results were compared . They actual casted cases are visually analized in the following section

CASE I

By visually analysing we come to know that CASE without riser is having defect at near about same positions.

On the upper side material could not be filled. And shrinkage defect lies .

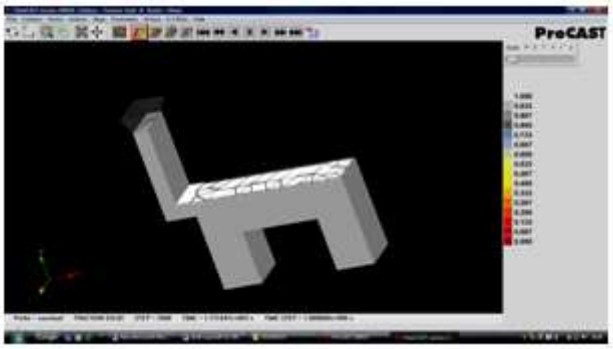

Fig. 20

Fig. 21

CASE II

By visually analysing we come to know that CASE one riser near runner is having defect at near about same positions. On the upper as well as right side shrinkage defect lies .

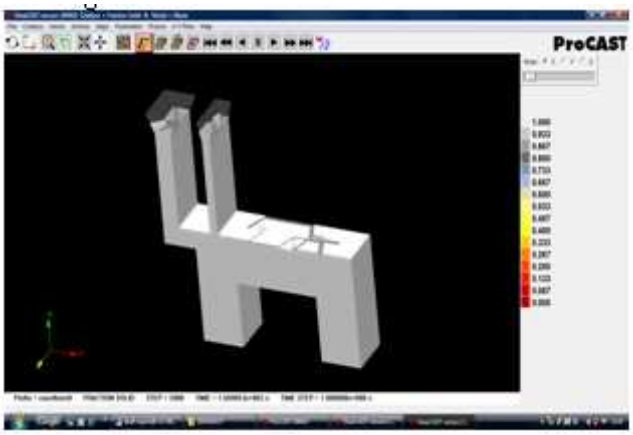

Fig. 22

Fig. 23

CASE III

By visually analysing we come to know that CASE one riser at the centre of the inverted U is having defect no where except very small shrinkage defect at the upper face.

Fig. 24

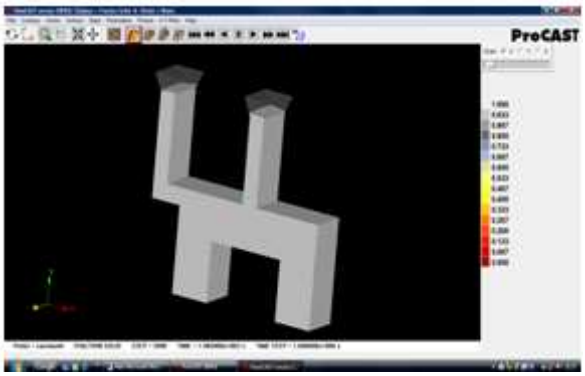

Fig. 25

3.3 Discussion (Comparison)

Comparison practical and simulated results of case I,II,III:

The results have varied in case one and two cases. By visually analysing we come to know that CASE one (riser near runner) and CASE two (without riser) having defected at near about same positions. Some of the unexpected results which have come on practical basis are:-

In the case one unexpected excess shrinkage of metal has taken place near the runner and the small projection has occurred near the leg of U shape outside the tolerance limits.

In the case two small unexpected excess of shrinkage of metal has taken place near the runner. Case one which is without riser was subjected to destructive testing by cutting the sample and it was found that their was no blow hole or any other defect inside , which has not occur in simulated results.

Reason behind the small variation in case one and case two

The main reason behind the variation of simulated and actual results might be that the followings:

i. The heat assignment in the PreCAST module is air cooling which is uniform at all the areas of the casting. But in actual case it is not the same. The rate of cooling of actual mold in the lab condition may not be same at each point. The permeability of the sand may not be uniform at all the point.
ii. The pouring time taken in the software was 10 second. But in Actual the time varied for 2-3 minutes. More over it depends upon the skill of the foundry man.
iii. The silica sand assigned in the software has properties as per the manufacturers. But their might be the variation in the composition of the silica sand used in the foundry.
iv. The mould formed in foundry had moisture content, and was made to dry for 2 days. There could be possibility that moisture content was not completed removed. There for some unexpected defects might have come.

v. The rate of ramming of sand might have varied. Hence rate of cooling could be affected by rate of rammed sand at different area.

4. CONCLUSION

This project gives an idea that simulation can be an important tool for foundry shops to find the near about optimized mold design of any casting. The results of all the practical as well as the simulated analysis are near about same. The simulated results can further refined if actually real values of the parameters are fed into the proCAST software. Casting process simulation helps in solving fluid mechanics and thermodynamic problems during filling and solidification process in the mold. Simulation reduces the casting trial and error traditional methods, improve yield, product characteristics, quality within a short time.

REFERENCES

[1] E. Abhilash and M.A. Joseph, "Modelling and Simulation of Casting Process", Department of Mechanical Engineering, National Institute of Technology, Calicut, India, Technical Paper from IndianFoundry Journal, October 2009.

[2] Dr.S.Shamasundar, Damayanthi Ramachandran, N.S.Shrinivasan and T.M. Manjunatha Paper on " Computer Simulation and Analysis of Investment Casting Process".

[3] Yi-tao Yang , Wei Luo, Meng Chen, Guang-jie Shao paper on "Simulation Analysis of Thermal Stress during Casting Process of Large-sized Alloy Steel Ingot", School of Materials Science and Engineering, Shanghai University, Shanghai 2007.

[4] Maria Jose Marques, Portugal, "CAE Techniques for Casting Optimisation", Case Study of Procast Simulation.

[5] Milek M. Tomovic, Purdue University, "USA Simulation Software Makes Metal Casting Course More Interesting and Challenging".

[6] Matthias Guamann and Adi Sholapurwalla, "Investment Casting Simulation", Case Study of Calcom Casting Simulation.

The Effects of Process Variables on the Penetration of Submerged - Arc Weld Deposits

Vinod Kumar[1], Narendra Mohan[2] and J.S.Khamba[3]
[1]University College of Engineering, Punjabi University, Patiala, India
[2]Production Engineering Department, Punjab Engineering College, Chandigarh, India
[3]University College of Engineering, Punjabi University, Patiala, India
E-mail:- vk_verma5@rediffmail.com

Abstract

The results of bead-on-plate weld measurements are presented to determine the effects of the process variables on the penetration for the submerged-arc welding process using developed fluxes. Response surface methodology (RSM) has been applied to derive mathematical models for penetration for submerged arc welding process (SAW) using developed fluxes. More the penetration less is the number of welding passes required to fill the weld joint and consequently results in higher production rate. Therefore penetration is an important consideration in SAW process. The ANOVA technique has been adopted to check the level and degree of the direct or interactive effect of process variables like welding current, operating voltage, welding speed and flux basicity index on the penetration. Main and interaction effects of the process variables on the penetration are presented in graphical form. By selecting appropriate process parameter values it is possible to predict as well as control the penetration.

Keywords: *Design of experiment, RSM, Submerged arc welding*

1. INTRODUCTION

Submerged arc welding (SAW) is characterized by its high reliability, deep penetration, smooth finish and high productivity especially for welding of pipes and boiler joints. The relationship between SAW parameters and weld bead geometry is complex, since a number of factors are involved. Extensive studies have been carried out to determine the effect of the various process variables on the weld bead geometry. This is necessary since in practice all variables must be selected before a weld can be specified for a given welding situation, especially where automated welding equipment is used. Shinoda and Doherty [1] summarized the work of various authors concerning weld bead shape, prior to 1978. McGlone [2], and McGlone and Chadwick [3] carried out further studies on the work of Shinoda and Doherty to review on submerged-arc welding, the variables included in these studies were being welding current, welding voltage, welding speed, joint preparation angle and electrode diameter. The effects of these variables on deposit area, fusion area, and bead width and bead height were studied. Chandel *et al.* [4] extended the study to include the effects of electrode polarity and electrode extension on weld penetration, total fusion area and electrode melting rate. However, the Chandel study did not include penetration.

Researchers McGlone [5] and Gupta *et. al* [6] observed that bead width increases with an increase in current until it reaches critical value and then decreases with an increase in welding current. Yang [7] observed that the bead width was not affected significantly by the types of the power source, constant voltage or constant current, when an acidic flux was used. However, when a basic flux was used constant current operation showed some what larger bead width than acidic fused flux welds. Pandey [8] observed that welding current increases with increase in welding wire feed rate and it interacts with open circuit voltage and nozzle to plate distance. According to Parmar [9], in order to automate a welding process it is essential to establish the relationship between process parameters and weld bead geometry to predict and control weld bead quality. Mohan & Pandey [10] studied the effect of welding current in submerged arc welding. Too low or high current causes the arc instability. Rayes [11] reported that arc power and consequently, the mode of metal transfer had a great influence on bead shape parameters in hybrid welding (GMAW-CO_2 laser beam welding). They observed that an increase in arc power caused to raise the bead width.

The primary function of the flux in SAW is to protect the weld pool from atmospheric contamination. It facilitates

in a slower cooling rate resulting in the desired mechanical properties as well as metallurgical characteristics of the weldment. In submerged arc welding significant percentage of the flux gets converted into very fine particles termed as flux dust before and after welding, due to transportation and handling. If welding is performed without removing these very fine particles from the flux, the gases generated during welding are not able to escape, thus it may result into surface pitting (pocking) and even porosity. Vinod *et al.* [12] developed agglomerated fluxes by utilizing wasted flux dust with the addition of potassium silicate as binder and aluminium powder as deoxidizer. The solution of potassium silicate binder (90 ml in 550 grams of flux dust) was added to the dry mixed powder of the flux dust and aluminum powder (4% of the weight of the flux dust) and it was wet mixed for 10 minutes and then passed through a 10 mesh screen to form small pellets.

Weld bead penetration is the maximum linear distance between the base plate surface and depth to which the fusion has taken place. The more the penetration, the less is the number of welding passes required to fill the weld joint which consequently results in higher production rate. The present study investigates the effect of using developed fluxes prepared from waste flux dust on the penetration through experiments based on design of experiment.

2. EXPERIMENTAL PROCEDURE

Design of experiments is a powerful analysis tool analyzing the influence of process variables over some specific variable, which is unknown function of these process variables. It is the process of planning the experiments that appropriate data can be analyzed by statistical methods, resulting in valid and objective conclusions. Statistical approval to experiment design is necessary if we wish to draw meaningful conclusions from the data [13]. Various process parameters influencing bead geometry, bead quality as well as mechanical-metallurgical characteristics of the weldment include welding current, voltage, traverse speed, electrode diameter, type of flux, height of flux layer, etc. In a full factorial design, the number of experimental runs exponentially increases as the number of factors as well as their level increases. This results in huge experimentation cost and considerable time. So, in order to compromise these two adverse factors, the present study has been planned to use only four process parameters. It has been reported by previous researchers that among the conventional process parameters in SAW welding, current, voltage and welding speed are the most significant factor that influences different quality characteristics of submerged arc weldment. Flux basicity index is related to the chemical composition of flux, which affects mechanical properties and metallurgical features of the weld, and is also an important factor. Therefore, welding current, voltage and speed have been chosen as conventional process parameters along with flux basicity index.

Response Surface Methodology (RSM) is a collection of statistical and mathematical methods that are useful for modeling and analyzing engineering problems. RSM also quantifies the relationship between the controllable input parameters and the obtained response [14]. Based on Box Behnken Design of RSM experiments have been conducted with three different levels of process parameters to obtain bead on- plate weldment on mild steel plates having dimension 200 x 75x 12 mm (Montgomery, 2001; Myers, R. and Montgomery, D. 2004). Based on the effect on weld bead geometry, ease of control and capability of being maintained at the desired level, four independently controllable process parameters were identified namely, the open circuit voltage (A), current (B), welding speed (C) and Basicity Index (D). Trial runs were conducted by varying one of the process parameters at a time while keeping the rest of them at constant value. The working range was fixed by inspecting the bead for a smooth appearance and the absence of visible defects. The upper and lower limits were coded as +1 and -1, respectively. The selected process parameters and their upper and lower limits together with notations and units are given in Table 1.

3. MATHEMATICAL MODEL OF THE PENETRATION

The necessary data required for developing the response models have been collected by designing the experiments based on Box-Behnken Design (BBD) using state ease 6.0 version of design of experiment. Two transverse specimens were cut from each welded plate.

These specimens were prepared by the usual metallurgical polishing methods and etched with 2% nital. The profiles of the beads were traced by using optical profile projector.

Table 1 Process Control Variables and their Limits

Parameters	Notations	Limits		
		-1	0	+1
Voltage (volts)	A	32	35	38
Current (amperes)	B	375	425	475
Welding Speed (m/hr)	C	24	27	30
Basicity Index	D	0.6	0.9	1.2

The Penetration (P) results for the 29 experiments are given above in Table 2. The response equations for Penetration (P) so obtained is given below:

$$\text{Peneration(P)} = 6.99-0.30*A+0.95*B-0.70*C-1.53*D+0.30*A^2+0.29*B^2+0.18*C^2+1.07*D^2-0.025*A*B-0.20*A*C+0.088*A*D-0.58*B*C-0.48*B*D+0.44*C*D \quad \text{..... (2)}$$

4. RESULTS AND DISCUSSION

The analysis of variance (ANOVA) was applied to study the effect of input parameters on penetration. It reveals that the quadratic model is the best suggested model. So, for further analysis this model was used.

4.1 The effect of Process Variables on Penetration (P)

As shown in Figure 1, the penetration (P) increases from 6.33 to 8.22 mm with the increase in welding current from 375 to 475 amperes. Increase in current gives rise to enhanced line power per unit length of the weld bead and higher current density, causing larger volume of the base material to melt and hence, deeper penetration. As current increases the temperature, the heat content of the droplets also increases, which results in more heat being transferred to the base material. Increase in current also increases momentum of the droplets, which on striking the weld pool causes a deeper penetration. An increase in welding current, with other variables remaining constant, results in increased depth of penetration, increased deposition rate and increased weld bead size and shape at a given cross-section. It is also attributed to the increase in digging power of the arc with the increase in welding current. As the current increases, the intensity of the arc and hence the digging power of the arc and penetration increases.

The penetration decreases from 7.86 to 6.47 mm with the increase in welding speed from 24 to 30 m/hr. This could obviously be due to the reduced line power per unit length of weld bead as speed increases. Also, at higher welding speeds, the electrode travels faster and covers more distance per unit time. The combined effects of lesser line power and faster electrode travel speed result in decreased metal deposition rate per unit length of weld bead [15]. It is also attributed to decrease in heat input, metal deposition rate and digging power of the arc with the increase in welding speed resulting in decrease in weld metal penetration.

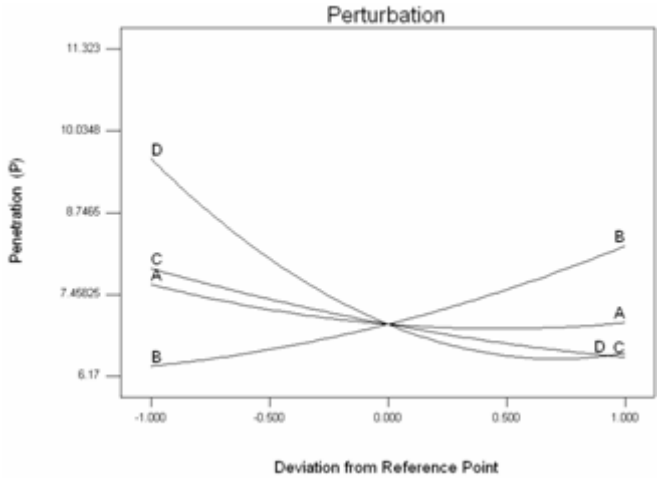

Fig. 1 Effect of process variables on penetration

4.2 Interaction Effect

From the Figure 2, it is evident that P increases with the increase in welding current for all values of welding speed. It shows that the weld metal penetration increases from 6.63 to 9.67 mm and from 6.38 to 7.12, with the increase in current, at the welding speed of 24 to 30 m/hr respectively. The rate of increase in P with the increase in current decreases gradually as speed increases. These effects on P are due to the reasons that current has positive effect but speed has a negative effect on P as discussed already in the direct effects of current and speed on P. It is found that at lower values of speed, the positive effect of current on P is stronger but at higher values of speed, the negative effect of speed on P is stronger.

From Figure 3, it is observed that penetration increases from 8.45 to 11.31 mm and from 6.38 to 7.28 mm, with increase in current, at the basicity index of 0.6 and 1.2

respectively. These results can be explained with the help of effects of welding variables such as welding speed and basicity index on penetration. Figure 4, that penetration decreases form10.91 to 8.63 and from 6.97 to 6.45 with increase in welding speed from low basicity index to higher value of basicity index. These results can be explained with the help of effects of welding variables such as welding speed and basicity index on penetration.

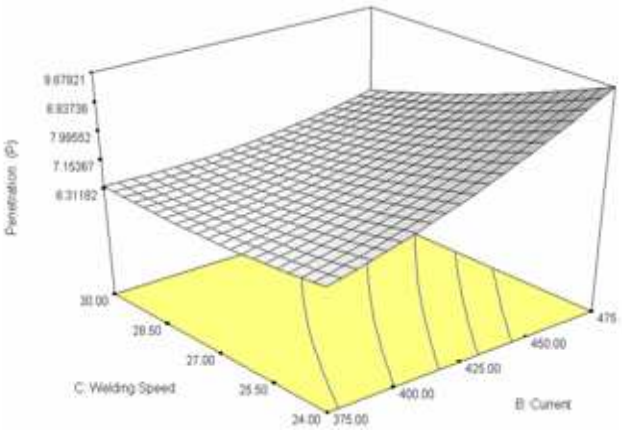

Fig. 2 Response surface due to interaction of current and speed on penetration

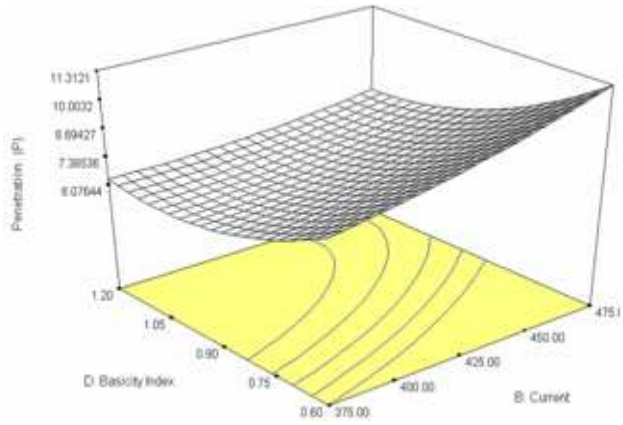

Fig. 3 Response surface due to interaction of current and basicity index on penetration

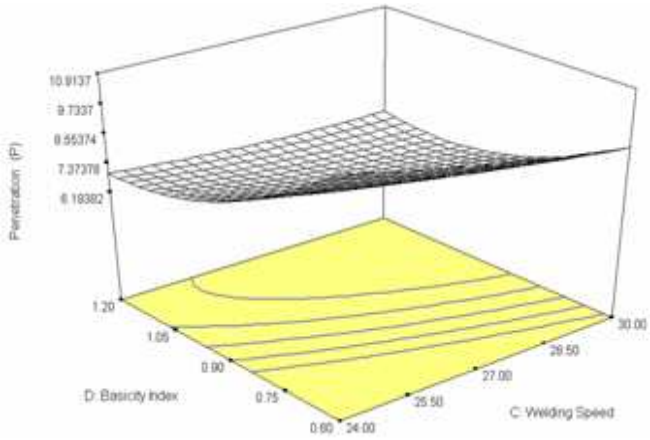

Fig. 4 Response surface due to interaction of weldin speed and basicity index on penetration

5. CONFIRMATION TEST

In order to confirm the accuracy of the model developed, confirmation experiment was performed (Table 3). The predicted value and the associated experiment value were compared and the percentage error was calculated. The error percentage is within permissible limits. So the response equations for the penetration evolved through RSM can be used successfully to predict the bead geometry for any combination of process parameters within the range of the experimentation conducted.

The interaction of welding current and speed had an appreciable effect on penetration. Penetration increased with the increase in current for all values of welding speed but this increasing rate of the penetration with the increase in current gradually decreased with the increase in welding speed.

Thus it is seen that within the present experimental domain, using the developed flux prepared from waste flux dust had no adverse effect on penetration. Detailed experimentation on the effect of developed flux on mechanical properties and metallurgical characteristics of the weldment to be rigorously done. If the outcome becomes positive, then developed flux prepared this way can be recommended to use as an alternative to fresh flux in practical situations to yield “waste to wealth”.

6. CONCLUSION

A RSM model can successfully relate the above process parameters with the response namely penetration.

The verifying experiment has shown that the predicted values agree with the experimental value. The models developed can be employed easily in automated or robotic welding in the form of a program, for obtaining the desired weld bead dimensions.

The penetration in submerged arc welding is affected by voltage, welding current and welding speed. Out of the four process variables considered, voltage had a negative effect on penetration. The penetration decreased with the increase in welding speed. Penetration decreased with increase in basicity index.

Table 2 Design values and Observed Values of Penetration

Expt. Run No.	Process Parameters				Response Factor
	A Voltage (volts)	B Current (amperes)	C Welding Speed (m/hr)	D Basicity Index	Penetration
1	1	-1	0	1	6.545
2	-1	0	0	0	7.349
3	0	0	0	1	6.735
4	0	-1	1	1	6.671
5	-1	0	0	-1	10.455
6	0	-1	0	0	6.389
7	0	0	0	1	6.17
8	0	1	-1	1	8.56
9	0	0	0	1	6.66
10	-1	0	-1	1	7.115
11	0	0	0	1	6.4
12	1	0	0	0	7.53
13	0	0	1	-1	8.75
14	0	0	1	0	6.525
15	0	1	0	-1	11.323
16	1	1	0	1	7.355
17	1	0	0	-1	9.285
18	0	1	0	0	7.895
19	0	1	1	1	6.6
20	-1	1	0	1	7.935
21	1	0	1	1	6.34
22	0	0	-1	0	7.835
23	-1	0	0	1	7.255
24	1	0	-1	1	6.99
25	-1	-1	0	1	7.025
26	0	0	-1	-1	11.07
27	0	0	0	1	6.7
28	0	-1	-1	1	6.32
29	0	-1	0	-1	8.272

Table 3 Comparison of Actual and Predicted Values of Weld Bead Parameters

Sl.No.	Predicted Values of Penetration	Actual Values of Penetration	% Error
1	6.48	6.54	1
2	6.53	6.51	-0.003
3	7.30	7.12	-2.46
4	7.37	7.39	0.002
5	6.33	6.51	2.84
6	8.23	7.99	-2.91

REFERENCES

[1] Shinoda T., Doherty J. (1978) "The relationship between arc welding parameters and weld bead geometry—A literature survey", The Welding Institute Report 74/1978/PE.

[2] McGlone J. C. (1978) "The submerged arc butt welding of mild steel, Part 1: The prediction of weld bead geometry from the procedure parameters", The Welding Institute Report80/1978/PE.

[3] McGlone J.C. Chadwick D. B. (1978) "The submerged arc butt welding of mild steel, Part 2: The prediction of weld bead geometry from the procedure parameters", The Welding Institute Report80/1978/PE.

[4] Chandel R.S., Bala S.R.(1987) Relationship between saw parameters and weld bead size, Physical Metallurgy Research Laboratories Report: PMRL 86-38 (J), Canmet, Ottawa, Canada.

[5] McGlone J.C.(1982) "Weld bead geometry prediction-A review", Metal Construction, Vol.14(7), pp.378-384.

[6] Gupta, S. R., Arora, N. (1991), "Influence of Flux Basicity on Weld Bead Geometry and HAZ in Submerged Arc Welding", Indian Welding Journal, Vol.7, pp.127-133.

[7] Yang, L. J., Chandel, R.S. Bibby, M.J. (1992) "The effects of process variables on the bead width of submerged-arc weld deposits", Journal of Materials Processing Technology, Vol. 29(1), pp. 133-134.

[8] Pandey S. (2004) "Welding current and welding rates in submerged arc wielding: An approach", Australian Welding Journal, Vol.2, pp.34-42.

[9] Parmer R. S. (1992), Welding Processes and Technology, Khanna Publishers, New Delhi.

[10] Mohan N., Pandey S. (2003) "Welding current in submerged arc wielding", Indian Welding Journal, Vol.36(1), pp.18-22.

[11] Rayes M. El. (2004) "The influence of various hybrid welding parameters on bread geometry", Welding Journal, Vol.85(5), pp.147s-155s.

[12] Vinod K., Mohan N.,Khamba J. S. (2009) "Development of cost effective agglomerated fluxes from waste flux dust for submerged arc welding", Proceedings of World Congress on Engineering, Imperial college, London, 1-3 July 2009.

[13] Myers R., Montgomery D. (2004) Response surface methodology", John Wiley & Sons, New York.

[14] Kwak, Jae-seob. (2005) "Application of Taguchi and response surface methodologies for geometric error in surface grinding process", Int. J. Mach. Tools Manuf, Vol. 45, pp. 327-334.

[15] Box G.E.P., Hunter W.G., Hunter J.S. (1976) "Statistics for Experimenters: An Introduction to Design', Data Analysis, and Model Building, New York, John Wiley & Sons.

Life Enhancement of Single Point Cutting Tool by Hard Facing and Cryogenic Treatment

Hazoor S. Sidhu[1], Kumar Gaurav[2] and Rakesh Bhatia[1]

[1]Department of Mechanical Engineering, Yadvindra College of Engineering, Punjabi University Guru Kashi Campus, Talwandi Sabo, Bathinda, Punjab - 151 302, India

[2]Department of Mechanical Engineering, G.T.B.Khalsa Institute of Engineering & Technology, Chhapianwali (Malout) - 152 107, Punjab, India

E-mail: hazoors@yahoo.co.in

Abstract

Hard turning is an attractive replacement for many grinding operations, but implementation in industry remains low, particularly for critical surfaces. This is because cutting tools required for hard turning are much more expensive. Therefore, tool life must be investigated to assure the economic justification for replacing grinding operations with hard turning. This paper present the work done with an objective to improve tool life by hard facing the surface of the tool with a hard facing material i.e. Hard Alloy LH-III. The scope of the study has been enhanced by the introduction of a cryogenically treated HSS tool. Micro Structural, Micro Hardness and Chemical Analysis of hard faced tool & simple High Speed Steel tool has been carried out to analyze the reasons for improved tool life. The results show that the tool hard faced with Hard Alloy LH-III showed better tool performance as compared to simple HSS tool.

Keywords: *Cryogenic treatment, Hard facing, Hard alloy, Tool life*

1. INTRODUCTION

Engineers continue to design materials that are capable of longer service lives, and processes for shaping these materials into finished products. Traditionally, finished surfaces have been ground from near net shape hardened steel parts. Recent improvements in machine tool rigidity and the development of Ceramic and Cubic Boron Nitride (CBN) cutting tools have allowed the machining of hardened steel with geometrically defined cutting edges to become a reality. There are numerous advantages of replacing grinding with hard turning operations. Even though small depth of cut & feed rates are required for hard turning but the material removal rates in hard turning can be much higher than grinding for same applications [1]. Recently, one of the new methods of surface modification to improve tool life is evolved by using the tools with their surfaces hard faced. The basic objective of this paper is to compare the performance of a hard faced tool to that of a simple HSS tool.

2. RELATED WORKS

The tribological properties of a single tool material never satisfy all performance requirements. Coated tools can produce high wear resistance on the surface with high toughness in the substrate material. Properly applied coatings increase the surface hardness of cutting tools at high cutting temperatures, thus minimizing abrasive wear. The coating provides a chemical barrier to decrease diffusion or reaction between the tools and the work piece, thus reducing tool wear. Most of the heat generated during machining goes into the chips, and the coated tool substrate stays cooler as compared to with uncoated tools. The high lubricity of most coatings reduces the coefficient of friction between the cutting tool and the work piece, which also reduces cutting temperature. Lubricity and the chemical–thermal barriers provided by coatings reduce adhesion and welding of chips to the tools. The formation of Build-Up-Edge (BUE) and cratering of the work piece are also minimized [2-3].

While coating increases initial cost, the benefits of coatings are often more than their cost. Coated tools generally have longer tool life, fewer tool changes, with improved work piece surface finish, etc. and hence cost of production is lowered. These advantages are the driving force for developing coating techniques [2-3]. The results produced by using coated tools in terms of process characteristics such as material removal rate (MRR),

surface roughness (SR) & tool wear rate (TWR) are quite encouraging. However, little research work has been carried out to study the effect of hard facing on the process characteristics of a single point cutting tool during the hard turning operations.

3. TOOL LIFE

Tool life can be defined as the time interval for which the tool works satisfactorily between two successive grindings (sharpening). Thus, it can be basically conceived as functional life of the tool.The tool is subjected to wear continuously while it is operating. Obviously, after some time, when the tool wear is increased considerably, the tool loses its ability to cut efficiently and must be reground [4].

The life of cutting tool is affected by the factors like: cutting speed, feed and depth of cut, tool geometry, tool material, work material and nature of cutting [4].

During the cutting operation, cutting tool is subjected to static & dynamic forces, high temperatures, wear & abrasion [5]. The main characteristics of a good cutting tool material are its hot hardness, wear resistance, impact resistance, abrasion resistance, heat conductivity, strength, etc. What is important to tool life is the likely changes in these characteristics at high temperature because the metal cutting process is always associated with generation of high amount of heat and, hence, high temperatures. Cutting speed has the maximum effect on tool life, followed by feed rate and depth of cut. All these factors contribute to the rise of temperature. That is why it is always said that an ideal tool material is the one which will remove the largest volume of work material at all speeds. It is, however, not possible to get a truly ideal tool material. The tool material which can withstand maximum cutting temperature without losing its principal mechanical properties (especially hardness) and geometry will ensure maximum tool life, and, hence, will answer the most efficient cutting of metal [4].

4. EXPERIMENTATION

In the experiments, all the parameters except the tool material are kept constant & experiments are conducted using three different tool materials- a simple HSS tool, cryogenic heat treated tool & a tool hard faced with hard alloy LH-III. The scope of the study has been enhanced by the introduction of a cryogenically treated HSS tool. This has been done to analyze the effect of cryogenic treatment on the tool material properties.

4.1 Preparation of Cutting Tool

Hard facing material was deposited on to the HSS tool shanks. For this purpose, commercially available hard facing electrode- Hard Alloy LH-III was used. The material was deposited onto the tool shanks with the help of Manual Metal Electric Arc welding using DC Reverse polarity. The current during the deposition was 180 amperes & voltage was 60 volts.

The desired tool angles are cut with the help of the Electrical Discharge Machining & the Surface Grinder. The desired nose radius is cut with the help of Electrical Discharge Machining.

One of the tools was cryogenically treated at Institute of Auto Parts, Ludhiana. The equipment is such that it could completely control the thermal cycle in terms of temperature and time. A recommended thermal cycle for this tool material was used, consisting of a cooling to a temperature of -196^{o}C followed by three cycles of heating to temperatures in the order of +196^{o}C for tempering, lasting a total of 43 h.

The following steps were taken for the cryogenic treatment, after the tools were conventionally quenched and tempered:

Step 1: Cooling to -196 ^{0}C (4 h at a rate of 1 æ%C/min).
Step 2: Cold stabilization at “196 ^{o}C (20 h).
Step 3: Heating to +196 ^{o}C (8 h at a rate of 1 æ%C/min).
Step 4: Hot stabilization at +196 ^{o}C (2 h).
Step 5: Cooling to room temperature (1 h average).
Step 6: Stabilization at room temperature (2 h).
Step 7: Heating to +196 ^{o}C (1 h average).
Steps 5-7 were repeated three times.

4.2 Estimation of Wear

The various steps involved in the estimation of wear during the machining process are:

Step 1: The initial profile of the tool is measured with the help of the Universal Measuring Machine manufactured by Nikon, Japan.

Step 2: Turning operation is performed on the lathe machine to remove a specified volume of the material. For each experiment the various input parameters like speed, feed & depth of cut are kept constant & the work material used for machining was mild steel.
Step 3: The profile of the tool is again measured after each step of machining. The same procedure is followed as given in Step 1 to determine the final profile of the tool. Change in nose radius is reported in Table 1.

4.3. Microstructural Analysis

The microstructure analysis is carried to study the micro structural changes after the HSS tool is hard faced with hard facing electrode (Hard Alloy LH-III) and cryogenic treatment. The results of microstructure analysis are presented in Figure 1.

4.4. Microhardness Analysis

This part of the work had the objective of analyzing the hardness of the simple HSS tool & Tool hard faced with hard facing alloy LH-III .The analysis has been done to check the hardness values of the hard facing electrode. The results are presented in Table 1.

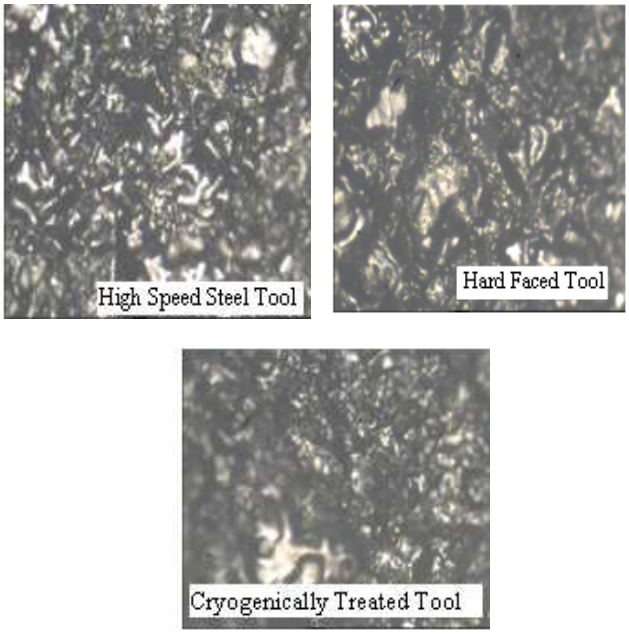

Fig. 1 Optical micrographs of tool material

4.5. Chemical Analysis

The chemical analysis is necessary to determine how the presence of certain elements as well as their percentage composition can influence the properties of the tool material thereby affecting the wear rate. The results are presented in Table 2.

5. RESULTS

The parameter chosen for study was the change in the nose radius of the cutting tools used in the experimental set-up to remove a fixed volume of the material from the surface of the work-piece.

In laboratory tests the wear of the different tools was found to be significantly different. The results for the change in the nose radius after the removal of a definite amount of the metal are presented in the Table 1 and Figure 2. The wear of a regular tool was slightly higher than that of the hard faced tool. The change in nose radius of the cryogenically treated HSS tool was lowest as compared to that of the simple HSS tool. There is no difference in the hardness values of both the tools. So, hardness cannot be factor for the difference in the change in nose radius of the cryogenically treated HSS tool and simple HSS tool. Also, the chemical composition of both the tools is same.

6. DISCUSSIONS

The results for the wear i.e. change in nose radius of the tools used for experiments vary widely. From the analysis of the change in nose radius in Table 1 and Figure 2. It was found that the hard faced tool has a lower wear as compared to that of the Simple High Speed Steel tool, although the hardness of the hard facing material i.e. Hard alloy LH-III was less as compared to the Simple HSS tool.

Table 1 Change in Tool Profile and Hardness Values

Tool Material	Initial Nose Radius	Nose Radius After final Machining	Change in Nose Radius	Observed Harness
High Speed Steel (HSS)	1.0022 mm	1.2902 mm	0.2880 mm	65 HRC
Hard faced HSS Tool	1.0022 mm	1.1919 mm	0.1897 mm	49 HRC
Cryogenically Treated HSS Tool	1.0022 mm	1.1422 mm	0.1400 mm	65 HRC

Table 2 Percentage Chemical Composition of Hard Alloy LH-III

Element %	HSS	Hard Alloy-III
C	0.900	1.000
S	0.044	0.016
P	0.030	0.020
Si	0.350	1.100
Mn	0.280	0.320
Cr	4.000	4.110
Mo	4.640	1.190
V	1.600	0.920
W	5.500	2.200
Co	1.190	0.220

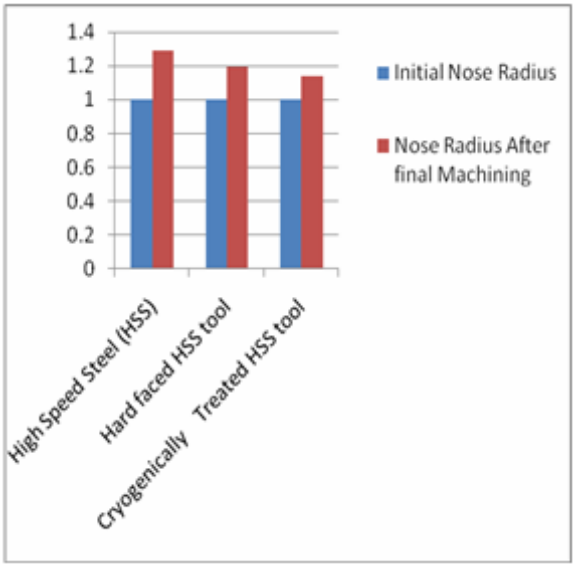

Fig.2 Result of tool wear after final machining

Metallurgical variables, such as hardness, toughness, microstructure and chemical composition, are an important influence on abrasive wear [5]. Though the hardness of a hard alloy LH-III electrode was low, the rate of wear was not high as expected. Not only hardness has an effect on wear but also parameters such as toughness, microstructure and chemical composition also influence the wear characteristics of any material. Hard alloy LH-III has a higher composition of carbon and manganese than simple HSS tool. Wear rate has decreased by increasing the Carbon (C) and the Manganese (Mn) proportion in the chemical composition of the hard facing material. The wear rate is related to both hardness and chemical composition of the materials. Mainly, carbon and manganese proportions of the steels are effective on the wear rate [6]. After hard facing, in the welding metal and the heat-affected zone (HAZ) of specimen, there often occurs martensite with high hardness, which is quite sensitive to formation of cold crack. The sensitivity of martensite to crack formation is mainly dependent on its carbon content, which will not be changed in matrix metal during welding, but, in welding metal, it can be controlled by adjusting the chemical compositions of used electrode. Nevertheless, the carbon content in welding metal should be kept on a needed level to guarantee the wear resistance of the hard facing layer. The microstructure analysis of the hardfaced samples shows the presence of the fine alloy carbides in tempered martensite, which is expected from the composition of the alloy LH-III. Thse carbide believed to increase the wear resistance and tool life.

The improvement of the wear resistance i.e. lowest change in nose radius of the cryogenically treated tool may be attributed to the mechanism of transformation of the retained austenite into martensite. The tool steels submitted to conventional heat treatment presented only a small amount of retained austenite, but those submitted to cryogenic treatment showed better performance during machining. This new mechanism would be time and temperature dependent due to the long period (8 h or more) during which the tools would have to stay at cryogenic temperatures. Before the cryogenic treatment the microstructure showed relatively large carbides dispersed in the matrix. After the cryogenic treatment, smaller carbide particles were found. The carbide refinement could in such a way contribute to the improvement of the wear resistance of the tool. The lowest change in nose radius may be due to austenite transformation and to the presence of hard and small carbide particles well distributed among the larger carbide particles within the martensite matrix.

7. CONCLUSION

Hard alloy LH-III performed quite well because of the increased content of Carbon, Manganese and Molybdenum resulting in the formation of carbides, which further increased the wear resistance and tool life. Microstructure of the cryogenically treated tool is very fine. The presence of hard and small carbide particles well distributed among the larger carbide particles within the martensite matrix attributed to lowest change in nose radius. The reduction in nose radius i.e. improvements in the wear resistance of the tool represents some of the major challenges in this current research field.

REFERENCES

[1] T.G. Dawson and T.R. Kurfess, “Hard Turning, Tool Life and Surface Quality”, Manufacturing Engineering, 2007.

[2] J. Gu, G. Barber, S. Tung and R. Gu, “Tool Life and Wear Mechanism of Uncoated and Coated Milling Inserts”, Wear 225 - 229, 1991, pp. 273-284.

[3] M.V. Kowstubhan and P.K. Philip, “On the Tool Life Equation of TiN Coated High Speed Steel Tools”, Wear, Vol.143, 1991, pp. 267-275.

[4] B.S. Raghuwanshi, “A Course in Workshop Technology, Volume II (machine tools)”, Dhanpat Rai & Company Ltd., New Delhi, 2001, pp.140-218.

[5] H.J. Yu and SD. Bhole, “Development of a Prototype Abrasive Wear Tester for Tillage Tool Materials”, Tribology International, Vol. 23, No.5, 1990, pp. 309-16.

[6] Y. Bayhan, “Reduction of Wear Via Hard Facing of Chisel Ploughshare”, Tribology International Vol. 39,2006, pp. 570-574.

A Study on MECD-Machining during Drilling of Electrically Non-conductive Ceramic

Kanwaljit Khasa[1] and A. Manna[2]

[1]Department of Mechanical Engineering,GGS College of Modern Technology, Kharar, Punjab - 140 301

[2]Department of Mechanical Engineering, Punjab Engineering College, Deemed University, Chandigarh - 160 012, India

Email: kjitkhas@yahoo.co.in; kgpmanna@rediffmail.com;

Abstract

In this study a combined technique of electrochemical (ECM) and electric discharge machining (EDM) has been utilized to machine the electrically non-conductive high-strength high-temperature-resistant aluminium-oxide (Al_2O_3) ceramics. A Micro Electrochemical Discharge Machining (MECDM) setup has been designed and fabricated for the purpose. The developed ECDM has been used to machine Al_2O_3 ceramics. From the test results, it is found that at higher setting value of supply DC voltage e.g. 90 volts and at moderate setting values of gap between electrodes e.g. 200 mm the Material Removal Rate (MRR) is maximum. Utilizing the test results mathematical models for MRR is developed to predict the setting value of MECDM parameters in advance.

Keywords: *Al_2O_3 ceramics, MECDM, MRR*

1. INTRODUCTION

Advance engineering materials are gradually becoming very important material for their scope and use in advance manufacturing industries due to their high fatigue strength, thermal shock resistance, high strength to weight ratio etc. Because of such superior properties, engineering ceramics have got wide industrial applications in the production of cutting tool, electrical and thermal insulators, turbine blades, electronic devices, fighter jet and other defense related products. Hence, it is essential for developing an efficient and accurate machining method for processing advanced ceramic materials. However, electrochemical machining (ECM) and electrical discharge machining (EDM) combined together is used for machining of Al_2O_3 ceramics. Keep in view, to machine Al_2O_3 ceramic a combined technique of ECM and EDM is known as electrochemical discharge machining (ECDM) has been developed.

Zhang, *et al* [1] studied on electrolytic interval-dressing grinding and concluded that the method has a potential to produce micro-diameter with high-quality holes on hard and brittle materials. Jain, *et al* [2] studied on the electrochemically spark abrasive drilling (ECSAD) and reported that electrochemical spark machining with abrasive cutting tools gives the improved performance (both in terms of material removal and machined depth) related to machining of electrically non conducting materials, alumina and borosilicate glass. Kaminski and Capuano [3] studied the parameters that affect the micro hole machining process utilizing conventional penetration electrical discharge machine. They concluded that the process is technically and economically viable and the quality of the generated hole directly depends on the cleaning process. Bhattacharyya and Munda [4] studied on electrochemical micromachining (EMM) process and observed that due to several advantages and wider range of applications, electrochemical micromachining (EMM) is considered to be one of the most effective advanced future micromachining techniques. Peng and Liao [5] studied on electrochemical discharge machining (ECDM) to slice the small size (10–30 mm diameter) optical glass and quartz bars.

However, from the past literature survey, it is evident that some research on electrochemical discharge machining have been carried out but still a lot of applied research in the above field is required so as to explore the successful utilizations of the process in the area of machining of non conductive ceramics. Keeping in view, the developed micro electrochemical discharge machine has been utilized to machine micro holes on aluminium oxide ceramic materials and subsequently analyzes the machining performance characteristic with respect to various parameters of ECDM.

2. EXPERIMENTAL PLANNING

A micro electrochemical discharge machining setup was designed and fabricated for conducting the experimental investigation. Different drilling tests were performed on Al_2O_3 ceramics using developed ECDM setup. Table 1 shows the detail experiment

Table 1 Details of Experimental Conditions

1	Machine tool used:	Fabricated Micro Electrochemical Machining (MECDM) setup
2	Electrolyte used:	Sodium Hydroxide (NaOH)
3	Work-piece:	Electrically non-conductive aluminium oxide (Al_2O_3) ceramics.
4	Work-piece thickness:	2.8 mm.
5	Electrode used:	IS-3748 / T35Cr5Mo1V30 Steel with varying 250 µm to 600

The following parameters such as DC supply voltage (Volt), electrolyte concentration (g/l), and gap between tool and anode (mm) are considered for experimental investigation. Figure 1 shows micro tool feed motion unit. The other equipment are utilized (not shown here) such as (i) tank for electrolyte concentration (ii) work-piece holder (iii) DC generator with regulator to supply the constant D.C voltage at various levels and (iv) step down transformer for supply of 18 volts to run the stepped motor mounted on fabricated micro-ECDM set up. A bench vice is designed and fabricated to hold the work-piece. condition used. The material removal rates are determined by difference of weight of work-pieces before and after each micro hole. Contech (Instrument) Electronic Balance of resolution 0.001 g was used to weight the work-pieces before and after each run. The depths of micro holes were measured by utilizing a digital depth gauge, Mitotio, Japan, of resolution 0.001mm. Different micro graphs of the micro holes were taken utilizing Scanning Electro Micrograph (SEM) to analyze the surface texture of the machined hole.

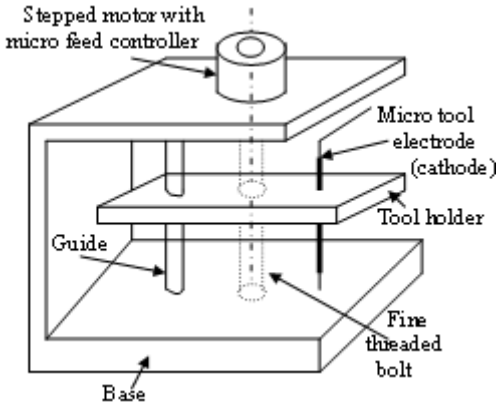

Fig.1 Micro-tool feed motion unit

3. RESULTS AND DISCUSSION

The test results are analyzed to identify the effect of various parameters of the developed ECDM setup on material removal rate(mg/min). Figure 2 shows the effect of gap between electrodes (mm) and supply D.C. voltage (Volts) on material removal rate (MRR, mg/min). From the Figure 2, it is observed that the material removal rate initially increases with the decrease in gap between electrodes thereafter material removal rate decreases with slight decrease in gap between electrodes. It is also observed that material removal rate (MRR) increases with the increase of supply D.C. voltage. From the Figure 2, it is clear that at higher setting value of supply DC voltage e.g. 90 volts and at moderate setting values of gap between electrodes e.g. 200 mm the MRR is maximum. It is also observed that MRR is minimum when the gap between electrodes is maximum e.g. 250mm and supply DC voltage is minimum e.g. 50 volts.

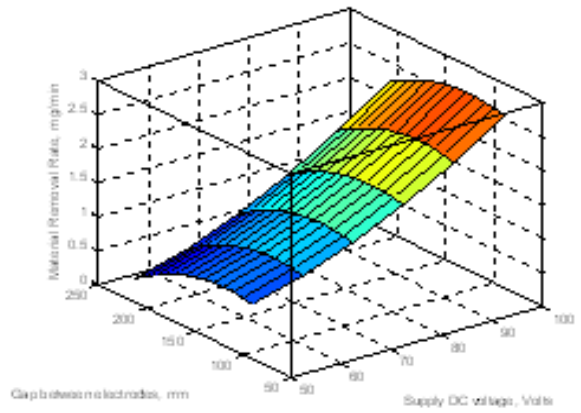

Fig. 2 Effect of gap between electrodes and supply voltage on MRR

4. DEVELOPMENT OF MATHEMATICAL MODEL FOR MRR

Considering the developed ECDM parameters mathematical models for MRR is developed. The additivity test results show that the predicted determined values utilizing developed mathematical model make a good agreement with the experimental results.
Mathematical model for material removal rate (MRR), mg/min is

$$Y_{MRR} = - 1.740083 - 0.030967. X_1 + 0.013337. X_2 + 0.0254299.X_3 + 0.0001558.X_1X_2 + 0.0000193.X_1X_3 - 0.00015296.X_2X_3 + 0.0003409\ X_1^2 + 0.0001204\ X_2^2 - 0.0000598.X_3^2$$

$R2 = 0.9789$

Where, X_1= D.C. supply voltage, X_2 = electrolyte concentration, X_3 = gap between tool and anode.

5. CONCLUSIONS

On the basis of the experimental results during drilling on Al_2O_3 ceramics utilizing the developed electrochemical discharge machining (ECDM) setup and thereafter analyzed the test results and concluded the following remarks as listed below.

i. The electrolyte concentration and DC supply voltage have most influential parameters on micro hole depth.
ii. For maximum material removal rate the recommended parametric combination is 90 volts DC supply voltage, 110 g/l electrolytic concentration and 100 mm gap between anode and cathode.
iii. During drilling it is observed that at the initial stage of drilling the shape of the generated micro hole was conical. Even after 5 minutes of continuous machining the shape of the micro hole still was conical in style.
iv. The mathematical models for material removal rate is successfully proposed for evolution of parametric value in advance for effective machining of electrically non-conducting Al_2O_3-ceramic material.

REFERENCES

[1] Chunhe Zhang, Hitoshi Ohmori and Wei Li, "Small-Hole Machining of Ceramic Material with Electrolytic Interval-dressing (ELID-II) Grinding", Journal of Material Processing Technology , Vol. 105, 2000, pp.284-293.
[2] V.K.Jain, S.K.Choudhury and K.M.Ramesh, "On the Machining of Alumina and Glass", International Journal of Machine Tools and Manufacture, Vol 42, 2002, pp.1269-1276.
[3] Paulo Carlos Kaminski and Marcelo Neublum Capuano, "Micro Hole Machining by Conventional Penetration Electrical Discharge Machine", International Journal of Machine Tools and Manufacture, Vol 43, 2003, pp.1143-1149.
[4] B Bhattacharyya and J Munda, "Experimental Investigation into Electrochemical Micromachining (EMM) Process", Journal of Materials Processing Technology, Vol 140, No.1-3, 2003, pp.287-291
[5] W. Y. Peng and Y. S. Liao, "Study of Electrochemical Discharge Machining Technology for Slicing Non-Conductive Brittle Materials", Journal of Material Processing Technology Vol 149, 2004, pp.363-369.

Resource Sharing in Indian Scenario: A Critical Review

V.K.Bansal[1], Sandeep Grover[2] and Ashok Kumar[3]

[1]Department of Training and Placement, Y.M.C.A. Institute of Engineering, Faridabad, India

[2]Department of Mechanical Engineering, Y.M.C.A. Institute of Engineering, Faridabad, India

[3]Department of Electrical Engineering , Y.M.C.A. Institute of Engineering, Faridabad, India

E-mail: vijaybansal1012@gmail.com

Abstact

With mushrooming of technical institutions in India many of the new institutions are unable to find students as per sanctioned capacity. Their revenue generation is quite low and some of them are unable to reach break even point. Such institutions hesitate to invest more money to improve infrastructure and to employ experienced faculty, which demands higher salaries. Government sector is already known for lack of infrastructure due to financial constraints. Indian industrial sector is also passing through highly competitive phase and battling for its survival. Financial constraints are looming large on both of them. Faced with the obvious impossibility of remaining totally self-sufficient, the role of industrial resource sharing is being assessed, with a purpose to understand its present status on sharing of software's, labs, libraries, training centers, recreation centers and to analyze its impact in improving research and development activities, generation of money, hunting best talents for managing manpower and industrial projects, getting local recognition and improving industry academia relations.

Keywords: *Industry-academia interface,Infrastructure facilities,Resource sharing, Survey analysis*

1. INTRODUCTION AND LITERATURE SURVEY

Education is a good indicator of the development and socio economic condition of a nation [1]. In government institutions student fee is very nominal and it is probably just sufficient to meet only the faculty salary expenses. In absence of sufficient funds from state governments, most of the institutions face financial crunch and lacks infrastructure facilities, which have direct bearing on student education quality.

Recently number of institutions has come up in a big way in every state. Some are doing quite well, but many others do not have experienced faculty and proper infrastructure. Faculty is considered as the main asset of any institution and a well developed dedicated and devoted in its pursuits of excellence in education, students are automatically developed and achieve high standards [2]. Lack of faculty and infrastructure is a great hindrance in achieving high standards of quality education. Mindless expansion of technical education without concern for quality would only lead to ill educated technical workforce misfit in the present age of competition [3].

These institutions avoid investing more money in improving infrastructure and employing experienced faculty which demands high salaries. Student expects good returns of their investment in terms of proper placement. Quality has become a decisive factor in attracting students and faculty to an institution. The institution which offers quality education will survive present scenario [4].

Indian industries too are passing through bad phase. With global competition few industries have already perished and some are on verge of closure. Survival has become a great issue. Industries are unable to invest huge resources to create strong infrastructure. Similar is the condition with most of the institutions.

Under these circumstances, best solution for an industry and academia may be to join hands and share resources. Apart from better resource utilizations and cost reduction, it will improve industry-academia relations, industrial training, student employment, consultancy and understanding about needs of each others. To become successful global player in technology, industry-institute-interaction must be more intensive [5]. Creating and maintaining relationships between academic and industrial

organizations is a highly recognized mechanism to manage the changing demands of industrial society [6]. Industry-academia-interface can be a logical alternative to march on path of quality education and to manage better manpower. Quality education can be supplemented through various industry-academia-interface (IAI) modes i.e. industrial training, curriculum development, evaluation, seminar/expert lectures, adjunct faculty, placement and personality development program [7].

2. SURVEY ANALYSIS

2.1 Purpose of Study

In the present work, the purpose of the study through survey is to have the feed back on present status on the extent of sharing of industrial resources, its impact in improving- industry academia relations, research and development activities, generation of money, locating potential viable candidates for managing manpower and industrial projects/ training. This paper may possibly provide an opportunity to industry and academia to understand the importance of their intimate bonding through resource sharing in cost cutting, preparing students as per industrial needs and managing manpower and organizations effectively.

2.2 Methodology of Study

Based on industrial interaction, feed back from student community, literature review and personal experience, questionnaires on resources sharing under development of a system based model for improving industry-academia-interface was prepared. In all five questions with parts were prepared for survey to be carried out. With a view to have fair assessment of the study, industries having different type of business were approached. Questionnaires prepared on resource sharing were sent to 110 industries through post, e-mail and students undergoing industrial training with a request to return the completed questionnaires with in two month. The survey spread over six months. Out of 110 approached industries only 63 industries responded. Most of the industries belong to Delhi, Haryana and Uttar Pardesh. Some of the industries are from Maharashtra, Himachal Pradesh and Chandigarh.

3. PRESENTATION AND ANALYSIS OF STUDY

Industries and institutions are passing through highly competitive phase. Cut throat competition is predominant. Survival is of the fittest. Financial constraints are looming large on both of them. No organization is able to satisfy all the needs of its clientele. The purpose of resource sharing is to have access to those resources which fall outside their scope. Resource sharing is not merely mutual sharing of infrastructure, but it is a concept which is developed to include many cooperative activities between industry and academia in meeting their needs. There are significant barriers to the widespread take-up of resource sharing, which is not just of a technical nature. Through literature it is recognized that resource sharing throughout higher studies has not reached the level of maturity. The extent of sharing various industrial facilities, donation of industrial equipments, industrial visits, its effectiveness and advantages of resource sharing are analyzed as such.

3.1 Sharing of Software

Software's use age is quite common in industries. It makes work simpler and enhances performance, visualization and analyzing strength of an individual. Different industries many times use different software's. Institutions may not be able to purchase all of them. Utilization of software's to its full capacity is normally not happening. Sharing of software's can ease the problem and students will be able to pick up the use of software's which are very much locally in use. Through study an attempt is made to understand the extent of use age of industrial software by students. Figure 1 indicates that around 13% industries allow sharing of software's from little to great extent. This includes sharing during industrial/project training also.

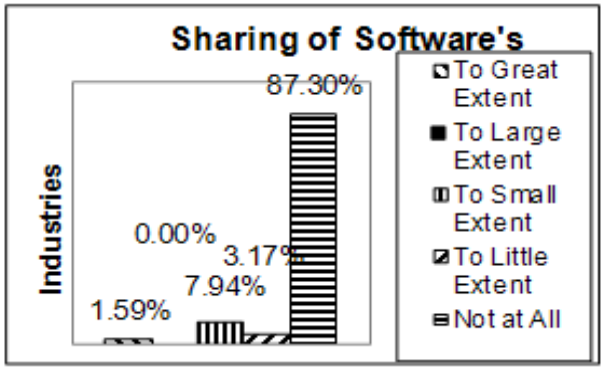

Fig. 1 Sharing of software's

3. 2 Sharing of Testing Labs

Large industries employ hi-tech labs for highly specialized applications to combine the highest levels of accuracy and precision with design innovations. These are necessary for producing innovative and high-performance products. It is state of the art facility employed to conduct tests on existing and new products. Development of these labs needs plenty of experience and finance. Through resource sharing, if students are allowed to work in these labs, they will be more technology driven professionals. Figure 2 reveals that around 21% industries permit students to make use of their labs from little to great extent.

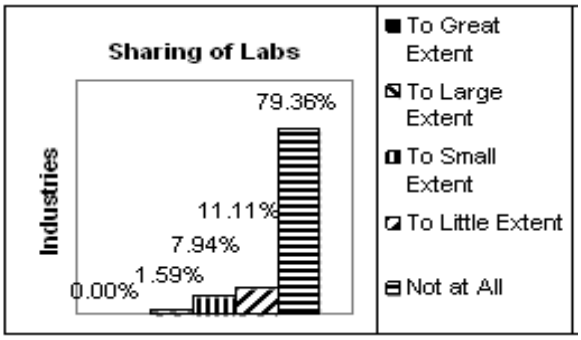

Fig.2 Sharing of labs

3.3 Sharing of Library

Library is a source of information and industrial library mostly contains the books, catalogue related to industrial products. These books are written in simple and straight language. It usually contains cut section details and step by step information about various parts through assembly and disassembly. It improves conceptualization, application and makes the technology easier and faster to understand. It helps to understand what current technologies are presently in use. Survey indicates that in around 16% industries students do make use of industrial libraries from little to large extent. Figure 3 projects the overall library sharing facilities available to students.

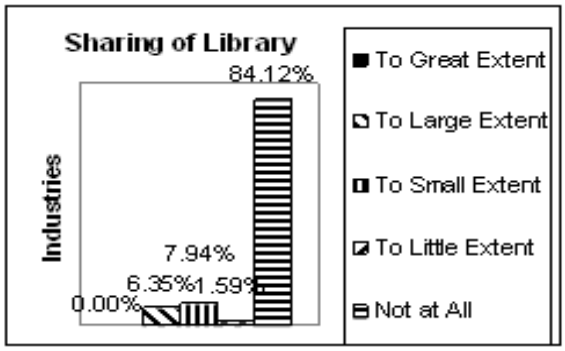

Fig.3 Sharing of Library

3.4 Sharing of Training Centers

Indian technical education system lays more weight age to theory against practice. Technology innovative countries are opposite to this. Institutions in the name of workshop, have kept just few old machines, where as industries are extensively making use of CNC based machines. Most of the foreign joint ventured training centers in India too have employed state of the art machines through which they not only impart best training to their students, but generate money for their organization by doing production jobs. This sort of training not only creates better placement opportunities for their students, but brings greater satisfaction to their stake holders. Sharing of such training centers will definitely make students industrial friendly, improve their confidence level apart from cost cutting and better employment. Figure 4 reveals that in around 7% industries students work in industrial training centers from large to great extent.

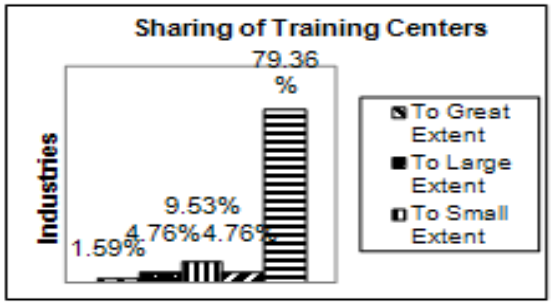

Fig.4 Sharing of training centers

3.5 Sharing of Recreation Centers

Sharing of recreation centers helps to develop intimate relations between industry and academia. This opens platform for further interactions which may bring qualitative changes and open up avenues in consultancy, industrial training, student projects, seminars, adjunct faculty, personality development and permanent recruitment. Figure 5 reveals that around 5% industries permits use of their recreation centers to institutions from large to great extent.

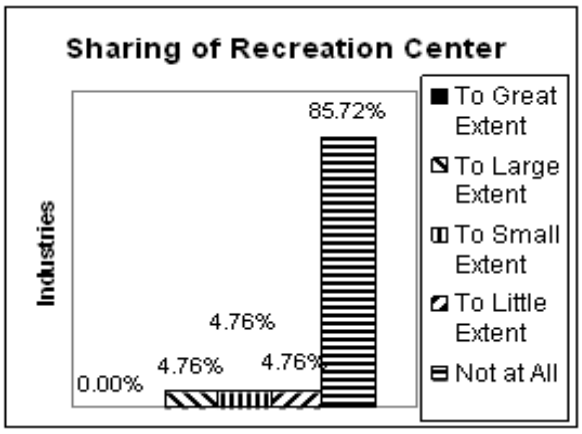

Fig.5 Sharing of recreation center

3.6 Donation Status of Industrial Equipments

Industries look to institutions for their manpower requirements. Industrial quality is based on the institutional input. Quality can be strengthened with better faculty and infrastructure. Industries keep on adding state of the art equipment to enhance quality and reliability. Some of the industries prefer to donate their old equipments, instead of selling it in scrap, so that institutions can make use of these equipments to strengthen teaching learning process. Figure 6 reveals that less than 8% industries donate their equipment either free of cost or on nominal cost to the institutions

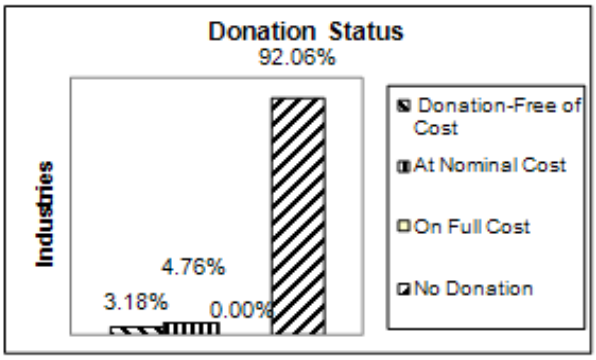

Fig.6 Donation status

3.7 Permission to Visit Industries

Industrial visits carry lot of significance. Learning in class rooms gets strengthened during industrial visits. Visualization gives boost to analyzing power. This helps to co-relate theory with application much better. Visits keep people abreast with what new is going on in an industrial sector. Figure 7 reveals that around 82% industries support this activity.

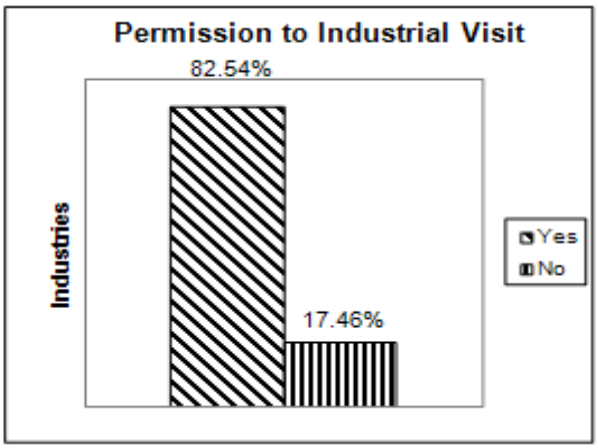

Fig.7 Permission to visit industries

3.8 Effectiveness of Industrial Visits

Many years back, practice of taking final year students on industrial tour was quite common. The purpose of this visit was to acquaint the students with the industrial atmosphere, to make them learn about various technological practices being followed in different industries and to have interaction with the industries about students industrial training and their placement. These process some how discontinued few years back. Literature indicates that many educational experts still advocate for frequent industrial visits. Industries views through survey were gathered about effectiveness of student industrial visits. Figure 8 reveals that around 51% industries are of the opinion that these visits are quite effective from large to great extent for student's academic growth.

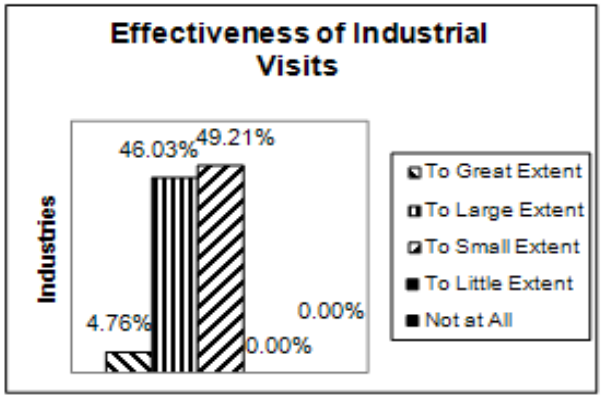

Fig.8 Effectiveness of industrial visits

3.9 Advantages of Sharing Resources

Through industrial survey feed back is taken on benefits of sharing resources. The opinion of industries about interaction, generation of money, local recognition, industrial research and development and hunting best talents is as such:

3.9.1 Improvement in Interaction

Resource sharing is need based, which requires lot of interaction initially to start with. Interaction brings people closer through frequent exchange of thoughts. Through resource sharing perhaps people may be able to understand each other much better. Figure 9 projects the status of interaction through resource sharing. It indicates that around 58% improvements in interaction from large to great extent may occur through resource sharing.

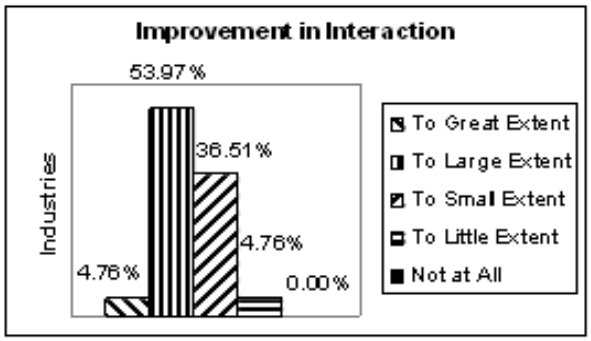

Fig.9 Improvement in interaction

3.9.2 Money Generation

The purpose of resource sharing is to make use of the better facilities which one do not have, but are available with someone else. This will improve utilization capacity and generate money for the organization. Figure 10 projects the status of money generation with resource sharing. It indicates that around 24% resource sharing industries feel that they will be able to generate money from small to large extent.

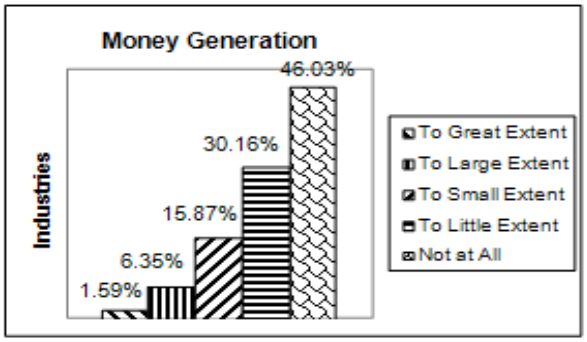

Fig.10 Money generation

3.9.3 Local Recognition

Resource sharing brings people closer. When resource sharing is between large numbers of organizations, the interaction becomes extensive and it makes the people or organizations more locally known. Figure 11 indicates that around 56% industries feel that they will get local recognition from small to great extent through resource sharing.

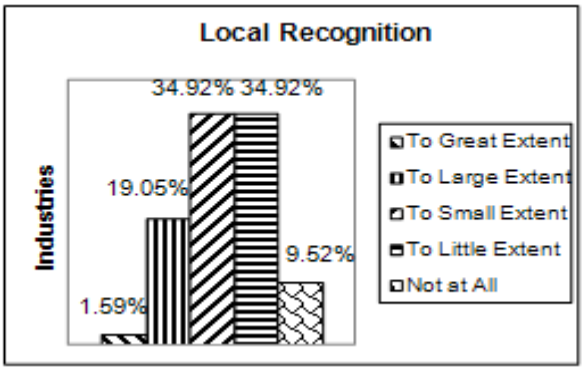

Fig.11 Local recognition

3.9.4 Improvement in Industrial Research and Development

Through resource sharing industrial people gets a chance to interact with various faculty members, through whom they understand their strengths, competencies and areas of specialization. This help to improve industrial research and development with involvement of appropriate faculty. Figure 12 indicates that around 14% improvement in research and development activities can take place from large to great extent through resource sharing.

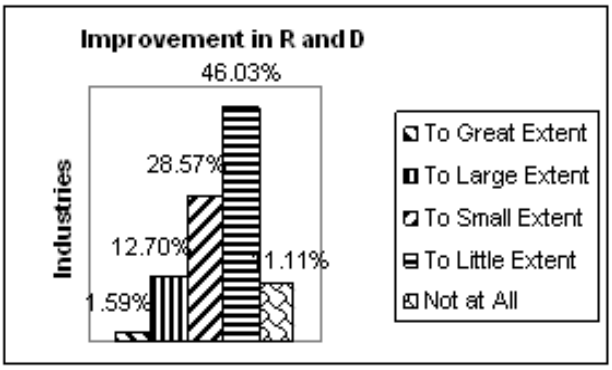

Fig.12 Improvement in R & D

3.9.5 Talent Tracking

Talent is natural abilities, qualities or unusual innate ability which a person possesses. Talent gives an instant access to the right candidates and a rich vein of competitive information. Talent tracking is one of an important and difficult task before any human resource department. In order to effectively tap the best talent, large industries employ best human resource professionals, who are able to understand the psychology, needs, expectations and satisfaction levels of interested people, which play a very constructive role in organizational development. Industries and institutions during resource sharing come closer to each other and this interaction creates a platform both for an industry and institute to understand each other strengths and to look for more collaborative activities including student's industrial projects and man power recruitment. Figure 13 indicates that around 50% industries are of the opinion that resource sharing helps in talent hunt from large to great extent.

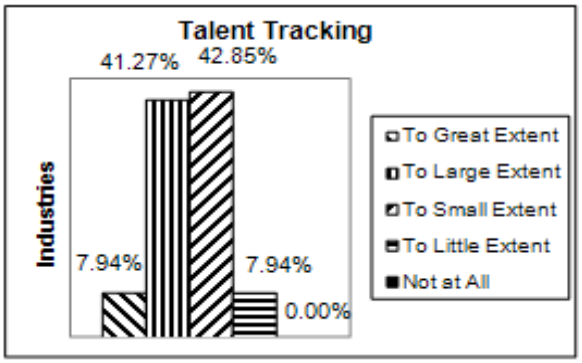

Fig.13 Talent tracking

4. CONCLUSION

The present work has highlighted the importance of resource sharing and its impact on industry-academia interaction. Based on survey analysis following conclusions may be drawn:

i. Sharing of industrial software's, labs, libraries, training centers and recreation centers is minimal.
ii. Very small percentage of industries donates their old equipments to institutions to strengthen teaching learning process.
iii. Large percentage of industries highly recommends industrial visits as they feel student's visits are quite effective in their academic growth.

Resource Sharing Helps to

i. improve industry-academia ties to great extent.
ii. recover infrastructure cost to certain extent through generation of money.
iii. improve industrial research and development to certain extent.
iv. track talents to large extent.
v. provide local recognition to great extent.

In India resource sharing has not developed in true sense, but it appears to be a strong viable tool to improve education quality through industry-academia- interface. The proposed work suggests that faced with the obvious impossibility of remaining totally self-sufficient turning towards resource sharing may be an answer to the problems.

REFERENCES

[1] R.S. Sirohi and P.C. Sinha, "Technical Education Programmes and Quality Assurance Process", the Indian Journal of Technical Education, Vol. 26, No.2, 2003, pp.15-18.
[2] N.K. Mittal, "Twenty Point Program for Implementing TQM in Technical Education", Proceedings of National Conference on TQM in Technical Education, 1996, pp. 15-25.
[3] Manoj Pandey, "Towards a World Class Technical Force", Press Information Bureau, Govt. of India, 2003.
[4] Pandi, A. Pal, Rao and U.Surya, "Implementation of Total Quality Management in Engineering Institution", the Indian Journal of Technical Education, Vol.30. No.2, 2007, pp. 82-86.
[5] S.S. Murthy, "Industry Institute Interaction", the Indian Journal of Technical Education, Vol. 25, No. 2, 2002, pp. 32-35.
[6] Nanda, Tarun and T.P.Singh, "A Comprehensive Strategy for Technology Generation through Effective Industry-Institute Bonding", the Indian Journal of Technical Education, Vol.31, No.2, 2008, pp. 1-6.
[7] V.K. Bansal, Sandeep Grover, and Ashok Kumar, " Enhancement of Quality through Industry-Academia-Interaction", All India Conference on Recent Developments in Manufacturing and Quality Management, Chandigarh, India, 2007, pp. 325-331.

Biomass Gasifier-Based Power Generation System Back to Basics, with a Difference

Ashok J. Keche
Department of Mechanical Engineering, Maharashtra Institute of Technology, Aurangabad (M.S.)
E-mail: kecheashokj@rediffmall.com

Abstract

Modern agriculture is an extremely energy intensive process. However, high agricultural productivities and subsequently the growth of green revolution have been made possible only by large amount of energy inputs, especially those from fossil fuels. With recent price rise and scarcity of these fuels there has been a trend towards use of alternative energy sources like solar, wind, geothermal etc. However, these energy resources have not been able to provide an economically viable solution for agricultural applications.One biomass energy based system, which has been proven reliable and had been extensively used for transportation and on farm systems during World War II is wood or biomass gasification. Biomass gasification offers most attractive alternate energy system for agricultural purposes and also biomass gasification can provide an economically viable system.

India being a large agrarian economy, biomass-wood, agricultural residues, animal dung, etc. is available in enormous quantities. And, hence, over 40% of India's total energy requirement can be met through biomass burning. However, biomass burning has been characterized with energy inefficiency and environmental hazards. Working towards a sustainable solution to the energy scarcity in rural India. "This biomass-based power generation system for rural applications could effectively make up for the absence of grid electricity supply in many remote areas.This paper deals with a case study of design, development fabrication and testing of biomass gasifier and technological innovation to exploit the vast biomass resource and generate power in an environment-friendly and profitable proposition.

Keywords: *Alternate energy system,Biomass gasification,Sustainable solution*

1. INTRODUCTION

Biomass energy based system, which has been proven reliable and had been extensively used for transportation and on farm systems during World War II is wood or biomass gasification. Biomass gasification offers most attractive alternate energy system for agricultural purposes and also biomass gasification can provide an economically viable system.

India being a large agrarian economy, biomass – wood, agricultural residues, animal dung, etc. is available in enormous quantities. And, hence, over 40% of India's total energy requirement can be met through biomass burning. However, biomass burning has been characterized with energy inefficiency and environmental hazards.Working towards a sustainable solution to the energy scarcity in rural India. The down draft gasifier have been developed as shown in Figure 5. "This biomass-based power generation system for rural applications could effectively make up for the absence of grid electricity supply in many remote areas.

2 TYPES OF GASIFIERS

2.1 Updraught or Counter Current Gasifier

The oldest and simplest type of gasifier is the counter current or updraught gasifier shown schematically in Figure 1. The air intake is at the bottom and the gas leaves at the top. Near the grate at the bottom the combustion reactions occur, which are followed by reduction reactions somewhat higher up in the gasifier. In the upper part of the gasifier, heating and pyrolysis of the feedstock occur as a result of heat transfer by forced convection and radiation from the lower zones. The tars and volatiles produced during this process will be carried in the gas stream. Ashes are removed from the bottom of the gasifier.

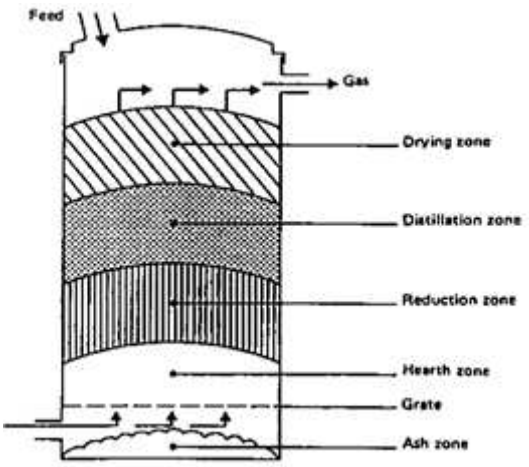

Fig.1Updraught or counter current gasifier

The major advantages of this type of gasifier are its simplicity, high charcoal burn-out and internal heat exchange leading to low gas exit temperatures and high equipment efficiency, as well as the possibility of operation with many types of feedstock (sawdust, cereal hulls, etc.) Major drawbacks result from the possibility of "channeling" in the equipment, which can lead to oxygen break-through and dangerous, explosive situations and the necessity to install automatic moving grates, as well as from the problems associated with disposal of the tar-containing condensates that result from the gas cleaning operations. The latter is of minor importance if the gas is used for direct heat applications, in which case the tars are simply burnt.

2.2 Downdraught or Co-Current Gasifiers

A solution to the problem of tar entrainment in the gas stream has been found by designing co-current or downdraught gasifiers, in which primary gasification air is introduced at or above the oxidation zone in the gasifier. The producer gas is removed at the bottom of the apparatus, so that fuel and gas move in the same direction, as schematically shown in Figure 2. The air intake is at the bottom and the gas leaves at the top. Near the grate at the bottom the combustion reactions occur, which are followed by reduction reactions somewhat higher up in the gasifier. In the upper part of the gasifier, heating and pyrolysis of the feedstock occur as a result of heat transfer by forced convection and radiation from the lower zones. The tars and volatiles produced during this process will be carried in the gas stream. Ashes are removed from the bottom of the gasifier.

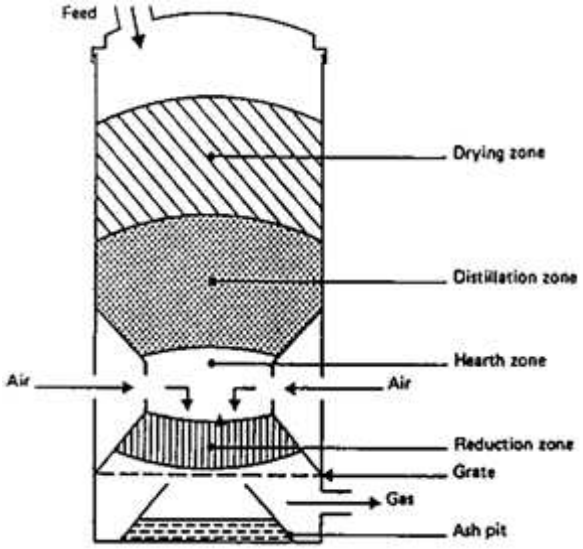

Fig.2 Downdraught or co-current gasifier

The major advantages of this type of gasifier are its simplicity, high charcoal burn-out and internal heat exchange leading to low gas exit temperatures and high equipment efficiency, as well as the possibility of operation with many types of feedstock (sawdust, cereal hulls, etc.)Major drawbacks result from the possibility of "channeling" in the equipment, which can lead to oxygen break-through and dangerous, explosive situations and the necessity to install automatic moving grates, as well as from the problems associated with disposal of the tar-containing condensates that result from the gas cleaning operations. The latter is of minor importance if the gas is used for direct heat applications, in which case the tars are simply burnt.

Cross-draught gasifiers, schematically illustrated in Figure 3 are an adaptation for the use of charcoal. Charcoal gasification results in very high temperatures (1500 °C and higher) in the oxidation zone which can lead to material problems. In cross draught gasifiers insulation against these high temperatures is provided by the fuel (charcoal) itself. Advantages of the system lie in the very small scale at which it can be operated. Installations below 10 kW (shaft power) can under certain conditions be economically feasible. The reason is the very simple gas-cleaning train (only a cyclone and a hot filter) which can be employed when using this type of gasifier in conjunction with small engines. A disadvantage of cross-draught gasifiers is their minimal tar-converting capabilities and the consequent need for high quality (low volatile content) charcoal.

2.3. Cross-Draught Gasifier

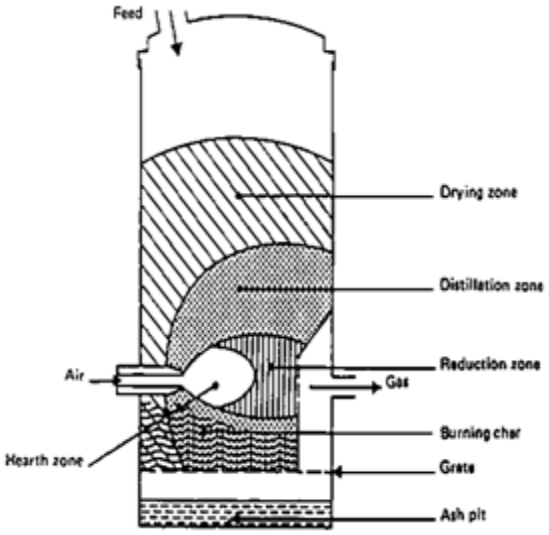

Fig.3 Cross-draught gasifier

It is because of the uncertainty of charcoal quality that a number of charcoal gasifiers employ the downdraught principle, in order to maintain at least a minimal tar-cracking capability.

2.4 Fluidized Bed Gasifier

The operation of both up and downdraught gasifiers is influenced by the morphological, physical and chemical properties of the fuel. Problems commonly encountered are: lack of bunker flow, slagging and extreme pressure drop over the gasifier.

A design approach aiming at the removal of the above difficulties is the fluidized bed gasifier illustrated schematically in Figure 4. Air is blown through a bed of solid particles at a sufficient velocity to keep these in a state of suspension. The bed is originally externally heated and the feedstock is introduced as soon as a sufficiently high temperature is reached. The fuel particles are introduced at the bottom of the reactor, very quickly mixed with the bed material and almost instantaneously heated up to the bed temperature. As a result of this treatment the fuel is paralyzed very fast, resulting in a component mix with a relatively large amount of gaseous materials. Further gasification and tar-conversion reactions occur in the gas phase. Most systems are equipped with an internal cyclone in order to minimize char blow-out as much as possible. Ash particles are also carried over the top of the reactor and have to be removed from the gas stream if the gas is used in engine applications.

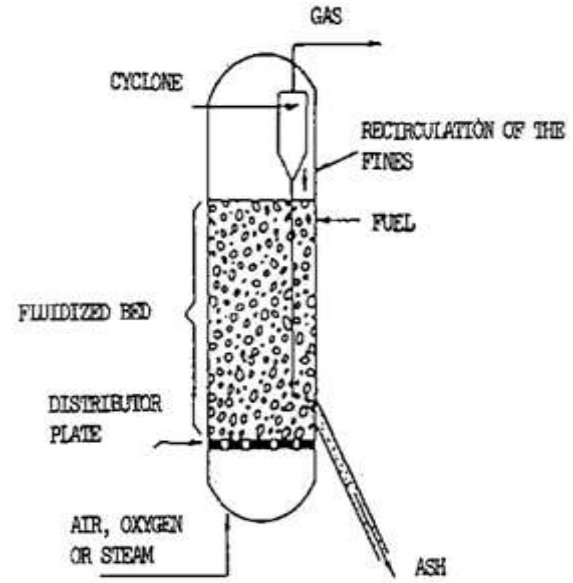

Fig.4 Fluidized bed gasifier

3. EXPERIMENTAL DETAILS

3.1 Objectives

i. The aim of developing a biomass gasifier which would cater to the needs of people of rural society.
ii. The biomass gasifier uses non polluting natural resources & so is eco-friendly.
iii. Developing a biomass gasifier is also aiming to provide an option for an automobile fuels.

3.2 Technology

i. Biomass technology today serves many markets that were developed with fossil fuels and modestly reduces their uses.
ii. Uses:
iii. Power generation
iv. Alternate fuels for transporting vehicles and other products.

3.3 Concept of Gasifier

i. Gasifier is device in which the use of heat to transforms solid biomass into a synthetic “natural gas like” flammable fuel through gasification.
ii. We can convert solid dry organic matter into a clean burning, carbon neutral and gaseous fuel.
iii. Starting with wood chips the end product is a flexible gaseous fuel.
iv. You can burn in your internal combustion engine, cooking stove and furnace.

3.4 Principle

A process that uses heat and pressure to convert materials directly into a gas composed primarily of carbon monoxide and hydrogen. The essence of gasification is the conversion of the solid fuel to gaseous fuel by thermo chemical reactions of a fuel with oxidizer under sub-stoichiometric conditions, the energy in biomass being realized in the form of combustible gases (CO, CH_4 and H_2). The generation of gas occurs in two significant Steps. The first step involves exothermic reactions of oxygen in air with the pyrolysis gas under fuel-rich conditions. The second step involves the endothermic reaction of these gases largely CO_2 and H_2O with hot char leading to product gases namely, CO, H_2 and CH_4.Have also been reported by Dasappa1 *et al* [11]

$$C + 2\,CO = 2CO$$
$$C + H_2O = CO + H_2$$
$$C + 2H_2 = CH_4$$

Gasification technologies rely on four key engineering factors:

1. Gasification reactor.
2. Reactor design.
3. Internal and external heating.
4. Operating temperature.

3.5 Raw Material Used for Gasification

Fig.5 Wooden chips

3.6 Downdraft Gasifier Set Up

Fig.6 Down draft gasifier setup

3.7 Main Parts of Gasifier

i. Gas cowling ii. Gas making reactor
iii. Hopper iv. Cyclone
v. Blower vi. Burner

3.8 Operating Procedure

i. The feedstock as shown in Figure 5 is prepared in adequate quantity and fed into a sealed reactor chamber called a gas cowling.
ii. The feedstock is subjected to high heat, pressure, and oxygen-starved environment within the gas cowling.
iii. Five nozzles are provided to which five circular pipes are attached which will supply proportionate quantity of pre-heated air for partial combustion.
iv. After partial combustion, the produced gas is supplied to cyclone and excess gas remains in the hopper.
v. From cyclone gas will be sucked by blower and supplied to the burner.
vi. Produced gas will be passed through fuel purifier and finally supplied to prime mover as shown in Figure 7.

3.9 Composition of Gas Obtained from Wood Gasification

i.	Carbon monoxide	18 - 22 %
ii.	Hydrogen	13 - 19 %
iii.	Methane	1 - 5 %
iv.	Heavier hydrocarbons	0.2 - 0.4 %
v.	Carbon dioxide	9 - 12 %
vi.	Nitrogen	45 - 55 %
vii.	Water vapour	4 %

3.10 Products of Gasification

i. Hydrocarbon gases (also called syngas).
ii. Char (carbon black and ash).
iii. Syngas is primarily carbon monoxide and hydrogen and smaller quantities of carbon dioxide and methane.

3.11 Proposed Biomass Gasification System

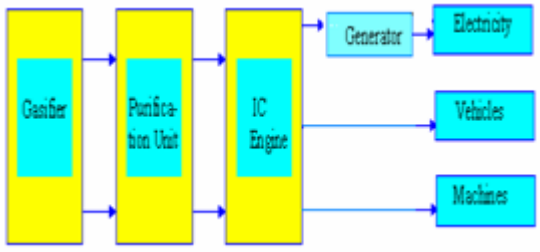

Fig. 7 Gasification System

3.12 Environmental Benefits

i. Reduction of waste.
ii. Extremely low emission of greenhouse gases compared to fossil fuels.

3.13 Socio-Economic Benefits

i. Helps developing economies by promoting agrarian communities.
ii. Increases job opportunities.
iii. Increase in trade balance (Indian perspective) due to lesser dependence on foreign resources

4. RESULTS AND CONCLUSION

The last two decades of R&D efforts at the Indian Institute of Science, in the area of biomass gasification have resulted in a technology package to meet the energy needs in various sectors. The gasification system has proved a reliable alternative for village electrification and industrial operations meeting thermal and electrical needs. The development relating to dual fuelling and gas alone operation of standard engines has resulted in field applications producing several million kilowatt-hours daily substituting fossil fuel. However, biomass burning has been characterized with energy inefficiency and environmental hazards.

India being a large agrarian economy, biomass- wood, agricultural residues, animal dung, etc.is available in enormous quantities. And, hence, over 40% of India's total energy requirement can be met through biomass burning. However, biomass burning has been characterized with energy inefficiency and environmental hazard.

Working towards a sustainable solution to the energy scarcity in rural India.This biomass-based power generation system for rural applications could effectively make up for the absence of grid electricity supply in many remote areas.The present designed and manufactured gasifier will give following out put:

If we burn 1kg of wood (15% moisture content) produces 2.185 cubic metres of gas.

or 3.165kW heat from burning gas direct
or 0.837kW of shaft power (i.e. engine)
Or 1.12HP of shaft power (i.e. engine)
Or 0.754kW of electric power generated.

REFERENCES

[1] U. Shrinivasa and H.S. Mukunda, "Wood Gas Generator for Small Power (5 HP) Requirements", Sadhana, Vol.7, 1984, pp.137-154.
[2] SERI, Generator Gas, "The Swedish Experience from 1938 to 1945 (translation)", Solar Energy Research Institute, Colorado,NTIS/S, 1979, pp.33-140.
[3] A. Kaupp and J.R. Goss, "Small Scale Gas Producer Engine Systems", GATE, Germany, 1984.
[4] T. Reed and M.Markson, "A Predictive Model for Stratified Downdraft Gasification of Biomass", Proceedings of the Fifteenth Biomass Thermo chemical Conversion Contractors Meeting, Atlanta, GA, 1983, pp. 217-254.
[5] N. Coovaththanachai, "Rural Energy", RAPA 10 Bulletin, FAO Office, Bangkok, 1990/1, Ed. 1986–1990, pp. 12-51.
[6] ABETS, "Biomass to Energy: The Science and Technology of the IISc Bio-energy Systems", CGPL, Dept of Aerospace Engineering Indian Institute of Science, 2003.
[7] H.S. Mukunda, S. Dasappa, P.J. Paul, N.K.S. Rajan and U. Shrinivasa, "Gasifiers and Combustors for Biomass - Technology and Field Studies", Energy for Sustainable Development: J. Int. Energy Initiative, 1994, Vol. 1, pp.27-38.
[8] H.S. Mukunda, *et al.,* "Results of An Indo-Swiss Programme for Qualification and Testing of a 300 kW IISc – DASAG Gasifier", Energy for Sustainable Development: J. Int. Energy Initiative, 1994, pp.1.22
[9] H.I. Somashekar, S. Dasappa and N.H. Ravindranath, "Rural Bioenergy Centers based on Biomass Gasifiers for Decentralized Power Generation: Case Study of Two Villages in Southern India", J. Int. Energy Initiative, Energy for Sustainable Dev., 2000, 4.
[10] N.H. Ravindranath,H. I.Somashekar, S. Dasappa, and C.N. Jayasheela Reddy, "Sustainable Biomass Power for Rural India: Case Study of Biomass Gasifier Power for Village Electrification", Curr. Sci., 2004, pp.87 (this issue).
[11] S. Dasappa1, P. J. Paul, H. S. Mukunda, N. K. S. Rajan, G. Sridhar and H. V. Sridhar, "Biomass Gasification Technology - A Route to Meet Energy Needs.
[12] www.allpowerlabs.org

Review Paper on Different Coating Techniques used for Hydroxyapatite Coating on Bioimplants

Gurbhinder Singh and Pawan Kumar Sapra
Department of Metallurgical and Materials, Indian Institute of Technology, Roorkee
E mail:gurbhinder@yahoo.com

Abstract

Hydroxyapatite (HA) is the main component of mineral bone. Due to its same Ca/P ratio of natural bone it has a property of Bio-Compatibility with the body. It is non toxic and stable when coated on the bio-implants. In this review paper different techniques which are used for the coating of Hydroxyapatite are discussed.

Keywords: *Coating techniques, Electropheretic technique, Hydroxyapatite, Sol gel, Thermal spray*

1. INTRODUCTION

Hydroxyapatite (HA), $Ca_{10}(PO_4)_6(OH)_2$, has been extensively used as biomedical material due to its bioactive properties and its chemical structure which is close to the structure of natural bone. Clinical tests have been showed that HA material is compatible with the tissue of the human body which makes it attractive materials to treat and replace the broken parts of human bones. However, HA material has poor mechanical properties such as low bending strength and fracture toughness, so it could not be used in bulk form for load bearing applications such as orthopedics. So it is a good idea to coat Hydroxyapatite on metals and alloys like SS-304L, SS-316L, Titanium and its alloys which are widely used for bio-implants due to their excellent mechanical properties [8].

To enhance mechanical properties and adhesion strength between coating and substrate some reinforced materials like silica, alumina, titania, zirconia, nanotubes and YSZ etc are added into hydroxyapatite by 7 to 15 % by weight better results are achieved by adding rainforest materials upto 15% by weight. As the percentage of reinforced materials increased than 15% decrease in mechanical properties has been observed. In this paper different coating techniques commonly used for Hydroxyapatite coating are discussed [1, 2].

2. THERMAL SPRAY

Thermal spraying techniques are coating processes in which melted or heated materials are sprayed onto a surface. The feedstock is heated by electrical (plasma or arc) or chemical means (combustion flame). Thermal spraying can provide thick coatings (approx. thickness range is 20 micrometers to several mm, depending on the process and feedstock), over a large area at high deposition rate as compared to other coating processes such as electroplating, physical and deposition. Their are so many techniques of Thermal spray but from literature review it has been found that work has been done by only Plasma spraying and High-velocity oxy-fuel coating spraying (HVOF).

2.1 Plasma Spray

Although there are many methods have been used to deposit HA coatings on metallic implants, thermal spraying processes (e.g. plasma and HVOF) are the fastest methods to deposit thick HA coatings with good adhesion with the substrate [10]. Plasma spray techniques has numerous advantages such as simplicity, high deposition rates, low substrate temperature, variable coating porosity, phases, and structure[6]. It is the only technique which is approved by Food & Drug Administration (FDA) USA.

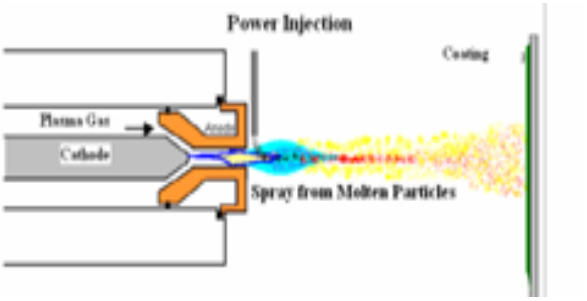

Fig.1 Plasma spray technique

Main weakness of this technique is the generation of amorphous calcium phosphate (ACP) and bioactive

calcium phosphate phase such as tetra calcium phosphate (TTCP), tri-calcium phosphate (TCP) and meta-stable crystalline products such as Oxy-hydroxyapatite which may cause mechanical and adhesive instabilities of the coating in vivo resorption [7]. Degradation of HA coatings with high amorphous phase content occurs by delamination of cracked lamellae and dissolution of the remaining lamellae during immersion tests [9]. In thermal spray technique spraying parameters are widely affect the properties of coating. From literature survey, optimum parameters of plasma spray coating are given as: [8].

Table 1 Parameters of Plasma Spray

Main Gas Pressure (Ar)	345 kPa
Auxiliary gas Pressure (He)	190-345 Kpa
Arc current	800 A
Arc voltage	32-35 V
Powder feed rate gm/min	10–20
Spraying distance (mm)	120-140

2.2 High Velocity Oxy Fuel (HVOF) Spray Technique

HVOF is a new thermal spray technique to obtain HA coatings onto metallic substrates. The HVOF thermal spraying process is based on the principle of combustion of fuel and oxygen gases in a chamber. Fuel gases used are hydrogen, propylene, propane, or acetylene. The combination of high gas flow rates and high pressure in the combustion chamber leads the generation of a supersonic flame which reaches a speed of 2000 m s)1 and the particle speed may reach 800 m s)1.

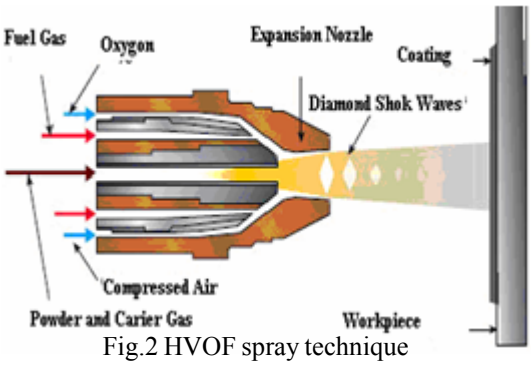

Fig.2 HVOF spray technique

This technique has the same advantages of Atmospheric Plasma Spray. However the drawback of this technique is that coating is not 100% crystalline [7]. Parameters for HVOF Spray are given in the table.

Table 2 Parameters of HVOF Spray

Oxygen(at 1.03 Mpa)L/min	235.96
Auxiliary gas Pressure (He)	190-345 Kpa
Fuel (at 1.03 Mpa)L/min	566.30
Carrier gas(at .69 Mpa)L/min	16.52
Powder feed rate gm/min	10–20
Spraying distance (mm)	300-310

3. SOL-GEL TECHNIQUE

The sol-gel process is a wet-chemical technique of coating. The method is based on the phase transformation of a sol obtained from metallic alkoxides or organometallic precursors. The sol-gel approach received more attention than others over the past 10 years because of its low temperature nature and ease of processing and forming.

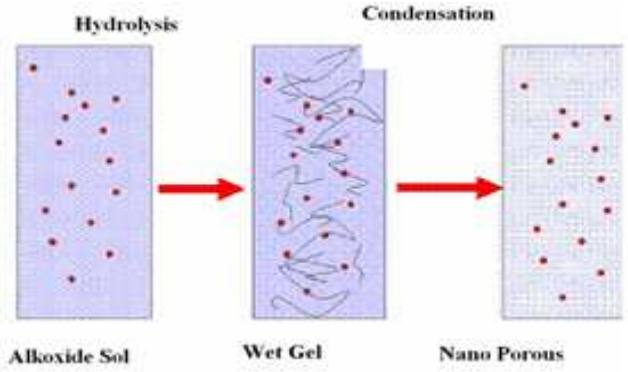

Fig.3 Sol gel technique

However, published reports regarding the adhesive strength of the sol–gel HA coating on metal or ceramic substrates are not extensive. Most reported works focused on structural evolution of sol-gel HA [11].The advantages of the sol-gel methods are its versatility and the possibility to obtain high purity materials [3].

4. ELECTRPHORETIC SPRAY TECHNIQUE

The development of HA coatings by electrophoretic deposition (EPD) is an area of increasing interest. EPD is achieved via the motion of charged particles dispersed in a liquid towards an electrode under an applied electric field [4]. It is a colloidal process which offers easy control of thickness and quality of coating through simple adjustment of the deposition time, applied potential and powder morphology. Nano-structured coatings fabricated by EDP have high chemical homogeneity, reduced flaw size and microstructural uniformity, and require a lower sintering temperature for densification.

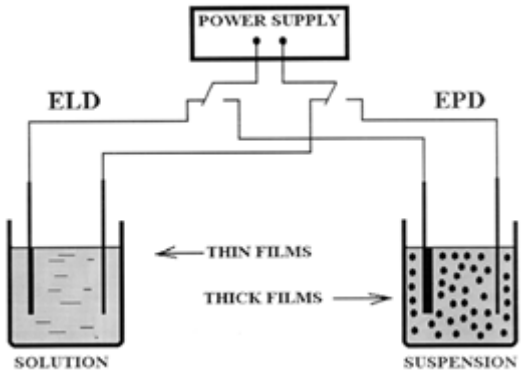

Fig. 4 Electrophoretic technique

Other advantages of this technique are short formation time, simplicity in instrumentation and capability of coating complex-shaped implants. But main limitation of this process is that coating thickness by this technique is limited to 10 micrometer. Adhesion strength is not comparable with thermal spray techniques and hence post spray sintering is required for better results. Another problem in this technique is that adsorbed water interferes with the electrophoretic transport of as precipitated HA nanoparticles [5]. Due to above problems it is in limited use.

4. CONCLUSION

Plasma spray is the only process which is clinically used now days due to its excellent properties as compared to other processes. However chemical processes like sol gel and electrophoretic techniques may also be used where high load bearing conditions are not present due to their simplicity.

REFERENCES

[1] A.E.Wen,Y.Yamada,K. Shimojima,Y. Chino, H. Hosokawa and M. Mabuchi, "Materials Letters", Vol.58, 2004, pp.357.

[2] B. Laxmidhar, L. Meili, "A Review on Fundamentals and Applications of Electrophoretic Depositions (EPD)", Prog. Mater. Sci., Vol.52, 2007, pp.1-61.

[3] C. Garcýa, S. Cere and A. Duran, "Bioactive Coatings Prepared by Sol-Gel on Stainless Steel 316L", Journal of Non-Crystalline Solids 348, 2004, pp.218-224.

[4] C.T. Kwok , P.K. Wong, F.T. Cheng and H.C. Man, "Characterization and Corrosion Behavior of Hydroxyapatite Coatings on Ti6Al4V Fabricated by Electrophoretic Deposition, Applied Surface Science, Vol.255, 2009, pp.6736–6744.

[5] P. Ducheyne, S.Radin, M.Heughebaert and JC.Heughebaert, "Calcium Phosphate Ceramic Coatings on Porous Titanium: Effect of Structure and Composition on Electrophoretic Deposition", Vacuum Sintering and in Vitro Dissolution. Biomaterials, Vol.11, 1990, pp.244-54.

[6] J. Fernandez, M. Gaona and J.M. Guilemany, "Effect of Heat Treatments on HVOF Hydroxyapatite Coatings", Journal of Thermal Spray Technology, Vol.16, 2007, pp.220-228.

[7] L. Sun, C.C. Berndt, K.A. Gross and A. Kucuk, "Material Fundamentals and Clinical Performance of Plasma-sprayed Hydroxyapatite Coatings: Review", J. Biomed. Mater. Res: Appl. Biomater., Vol.58, 2001, pp.570-592.

[8] M.F. Morks, "Structure Mechanical Performance and Electrochemical Characterization of Plasma Sprayed SiO2/Ti-Reinforced Hydroxyapatite Biomedical Coatings", J. Mech. Behav. Biomed. Mater, 2008, pp. 105.

[9] P. Chean and K.A. Khor, "Addressing Processing Problems Associated with Plasma Spraying of hydroxyapatite Coatings", Biomaterials, Vol.17, No.5, 1996, pp.537-544.

[10] P.L. Silva, J.D. Santos, F.J. Monteiro, J.C. Nowles, "Adhesion and Microstructural Characterization of Plasma-sprayed Hydroxyapatite/glass Ceramic Coatings onto Ti–6A1-4V Substrates", Surf. Coat. Technology, Vol.102, 1998, pp.191–196.

[11] SW.Russel and KA. Luptak, "Suchicital CTA, Alford TL", VB. Pizzicoui, "Chemical and Structural Evolution of Sol-Gel-derived Hydroxyapatite Thin Films under Rapid Thermal Processing", Journal of Amer Ceram Soc., Vol.79, No.4, 1996, pp.837-42.

An Overview on Cold Spray Process Over Competitive Technologies for Electro-Technical Applications

Tarun Goyal[1], T.S.Sidhu[2] and R.S.Walia[3]
[1]Punjab Technical University, Jallandhar, Punjab
[2]SBSCET, Ferozpur, Punjab
[3]PEC University of Technology, Chandigarh
E-mail: goyaltarun1@gmail.com, tarun_goyal2@rediffmail.com)

Abstract

Cold gas dynamic spray is a rapidly emerging coating technology, in which spray particles in a solid state are deposited on a substrate via supersonic velocity impact, at temperatures lower than the melting point of the powder material. Cold spray coatings have very low porosity, high density, high hardness, high abrasive resistance, good wear resistance with a strong ability to resist corrosion and wear. This paper briefly reviews the various competitive coating deposition processes and presents how the cold spray process benefits in comparison to other thermal spray coating processes.

Corrosion, wear and erosion phenomenon in electro-technical parts presents a serious damage resulting in repair or replacement of the components, which is very expensive. The purpose here is to summarise the performance of such coatings so as to avoid a loss of capital which runs into millions of dollars.

Keywords: *Coating Cold spray, Power-generating equipment, Thermal spraying*

1. INTRODUCTION

Coatings and surface engineering are used to protect manufactured components from thermal or corrosive degradation, impart wear resistance and hardness to the surface while retaining the toughness and ductility of the bulk component, and enhance the aesthetic and decorative appeal.

Many factors must be considered in selecting coatings for a given application. The process of selecting coatings must consider the operating conditions, material compatibility issues, nature and surface preparation of substrate, time or speed of application, cost, safety, environmental effects, coating properties, and structural design. Frequently the task of selecting the right coating is really a process of elimination rather than selection. Regardless of the coating process used, selecting the right coating for a given application usually requires considerable experience and judgment. The process of designing and developing coatings for modern technological applications is usually very complex [1].

2. OVERVIEW OF COMPETITIVE TECHNOLOGIES

The thermal spray coating process are based on a combination of thermal and kinetic energy transfer, i.e., the melting and acceleration of powder particles, to deposit the desired coating [2]. The main parameter affecting the deposition is temperature and velocity of coating particles. The plasma spraying, D-Gun and HVOF processes basically rely on high temperature of particles.

Figure 1 shows various coating deposition processes in commercial use. Figure 2 shows various thermal spray processes.

3. DEMAND FROM ELECTRO-TECHNICAL APPLICATIONS

The growth of power-generation facilities throughout the world has been unprecedented [2]. These facilities face numerous corrosion and/or wear issues, and maintenance must regularly be performed on various machines and systems [3]. In an effort to reduce downtime, thermal spray technology had emerged to extend the life of power-generating components and

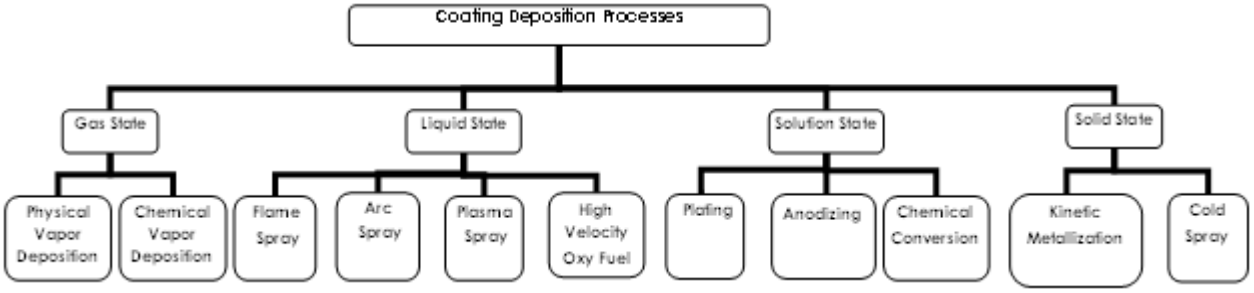

Fig. 1Various coating deposition processes in commercial use

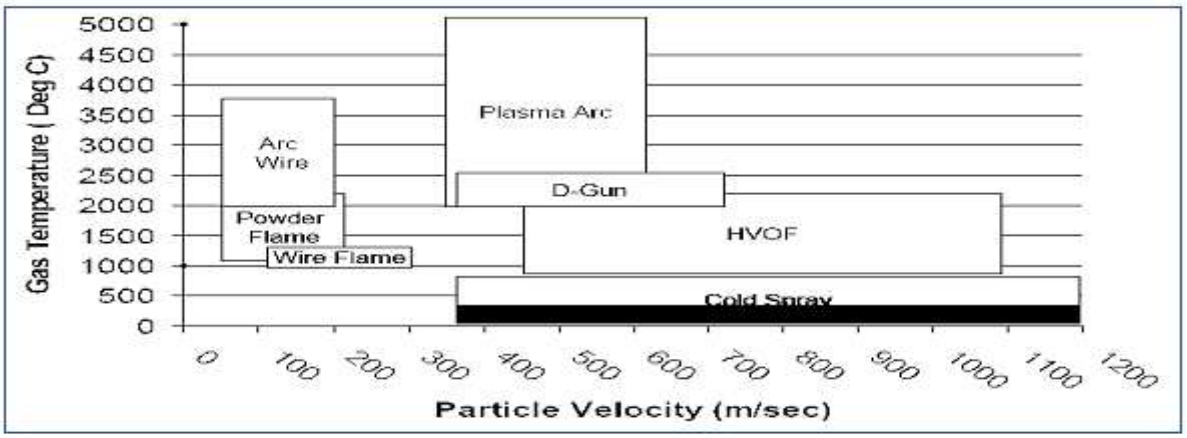

Fig. 2 Comparisons between different thermal spraying processes

systems. Coatings manufactured by this technology are being used throughout the power-generating industry in applications such as water pumps, conveyor screws, boiler tubes, coal crushers and contacting elements of electro-technical applications.

3.1 Pump Repair-Housings, Impeller Fins, Seal Sections, and Wear Rings

Pumps are used in almost every facet of a power-generating facility and must often endure abrasion as well as cavitation wear. The double suction pump is commonly used to move river water through a power plant. As river water commonly contains fine sand and even small stones, several sections of a pump can be attacked including the impeller fins, the pump housing, the impeller's seal section, and the wear ring.

The fins of the impeller are abrasively worn by the fine sand and the small stones and broken down by cavitations. Over time, pump efficiency will be reduced. Similarly, the housing of the pump also faces wear from the sand and/or rocks as water is pumped through it. If left unchecked, the housing will eventually wear away to the point where the pump may rupture. In both cases, the cold spray solution is to apply a very hard and wear-resistant tungsten carbide coating onto the fins.

The seal section of the impeller shaft undergoes abrasive wear when fine sand slips into the packing material and scores the journal. If the journal becomes too worn, water will eventually penetrate beyond the seal section and start corroding the bearings. An effective solution is to undercut the journal, cold spray a chromium oxide coating, and finish the journal to size. Lastly, the wear rings begin to erode as fine sand flows through the gap between the impeller and the housing. As it wears and widens, the efficiency of the pump is reduced. These wear rings can be efficiently reconditioned by applying bronze onto the rings and machining them to size.

3.2 Coal Crusher Roll Repair-Journals and Seal Sections

In this case, a coal crusher required repair on the seal section and the bearing section. A quick analysis of the seal section reveals that the coal dust generated during grinding penetrated the gap between the packing material and the journal, imbedding itself into the packing material and creating abrasion on the journal. The solution was to

undercut the section, cold spray chromium carbide, and then finish the journal to the size.

3.3 Reconditioning an Abrasively Worn Conveyor Screw

Conveyor screws are used in power plants to transport limestone into the boilers. Conveyor screw manufactured from carbon steel, needed to be replaced/repaired once a year due to the abrasion by the limestone. The thermal spray solution was to apply a thin layer of wear-resistant tungsten carbide on the shaft and both sides of the flights using the cold spray system.

3.4 Contacting Elements for Electro-Technical Applications

Important structural elements of power engineering systems are tips of connecting cables and connecting plates. The contact between the copper wire of the transformer and the aluminium tip of the cable of the electric mains is a typical situation as well. Under the action of atmospheric moisture and electric current, intense electrochemical oxidation processes occur in such a contact pair, which increases the resistance of the contact and leads to contact and circuit breakdown. Aqueous solutions of acids, alkali, and salts are electrolytes, i.e., liquids capable of conducting the electric current [4]. The problem is also common with the contact of copper wires and aluminium terminal in automotive batteries.

To prevent oxidation of contacting elements, it is necessary to avoid the presence of different materials in contacts. The same may be achieved by coating copper powder on aluminium tips/terminals by cold spray process.

4. COLD SPRAY PROCESS - A SOLUTION

The cold-gas dynamic-spray process, often referred to as simply "cold spray," is a high-rate material deposition process in which fine, solid powder particles (generally 1–50 μm in diameter) are accelerated in a supersonic jet of compressed (carrier) gas to velocities in a range between 500 and 1000 m/s. As the solid particles impact the target surface, they undergo plastic deformation and bond to the surface, rapidly building up a layer of deposited material. Cold spray as a coating technology was initially developed in the mid-1980s at the Institute for Theoretical and Applied Mechanics of the Siberian Division of the Russian Academy of Science in Novosibirsk [5, 6]. The Russian scientists successfully deposited a wide range of pure metals, metallic alloys, polymers, and composites onto a variety of substrate materials. In addition, they demonstrated that very high coating deposition rates of the order of 5m^2/min (~ 300 ft^2/min) are attainable using the cold-spray process [7].

Compressed gas of an inlet pressure of the order of 30 bar (500 psi) enters the device and flows through a converging/diverging nozzle to attain a supersonic velocity. The solid powder particles are metered into the gas flow upstream of the converging section of the nozzle and are accelerated by the rapidly expanding gas. To achieve higher gas flow velocities in the nozzle, the compressed gas is often preheated. However, while preheat temperatures as high as 900K are sometimes used, due to the fact that the contact time of spray particles with the hot gas is quite short and that the gas rapidly cools as it expands in the diverging section of the nozzle, the temperature of the particles remains substantially below the initial gas preheat temperature and, hence, below the melting temperature of the powder material. The actual mechanism by which the solid particles deform and bond during cold spray is still not well understood. The prevailing theory for cold-spray bonding postulates that, during impact, the solid particles undergo plastic deformation, disrupt thin (oxide) surface films and, in turn, achieve intimate conformal contact with the target surface. The intimate conformal contact combined with high contact pressures promotes bonding. This theory is supported by a number of experimental findings such as:

(a) A wide range of ductile (metallic and polymeric) materials can be successfully cold-sprayed while non-ductile materials such as ceramics can be deposited only if they are co-cold-sprayed with a ductile (matrix) material [6];
(b) The mean deposition particle velocity should exceed a minimum (material-dependent) critical velocity to achieve deposition which suggests that sufficient kinetic energy must be available to plastically deform the solid material and/or disrupt the surface film [8]; and
(c) The particle kinetic energy at impact is typically significantly lower than the energy required to melt the particle suggesting that the deposition mechanism is primarily, or perhaps entirely, a solid-state process [9-12].

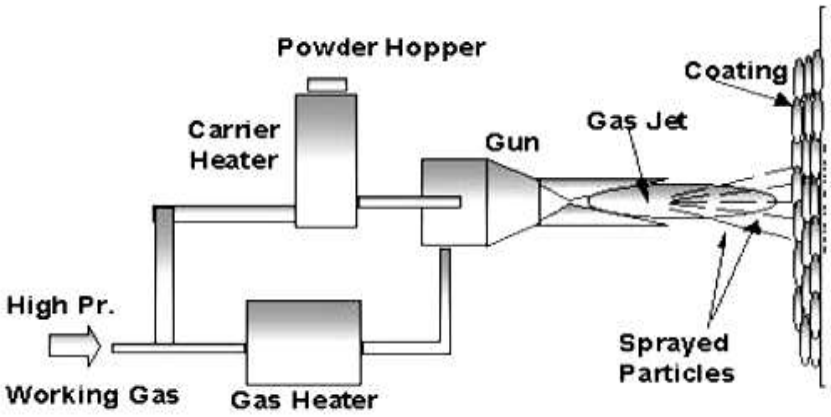

Fig. 3 Schematic diagram of cold spray process

4.1 Advantages of Cold Spray to other Competitive Technologies

As the cold-spray process does not normally involve the use of a high-temperature heat source, it generally offers a number of advantages over the thermal-spray material deposition technologies such as high velocity oxy-fuel, detonation gun, plasma spray, and arc spray. Among these advantages, the most important appear to be:

(a) The amount of heat delivered to the coated part is relatively small so that micro structural changes in the substrate material are minimal or nonexistent;
(b) Due to the absence of in-flight oxidation and other chemical reactions, thermally- and oxygen-sensitive depositing materials (e.g. copper or titanium) can be cold sprayed without significant material degradation;
(c) Nano-phase, intermetallic and amorphous materials, which are not amenable to conventional thermal spray processes (due to a major degradation of the depositing material), can be cold sprayed;
(d) Formation of the embrittling phases is generally avoided;
(e) Macro and micro-segregations of the alloying elements during solidification which accompany conventional thermal spray techniques and can considerably compromise materials properties do not occur during cold spraying. Consequently, attractive properties are retained in cold-sprayed bulk materials;
(f) "Peening" effect of the impinging solid particles can give rise to potentially beneficial compressive residual stresses in cold-spray deposited materials [6] in contrast to the highly detrimental tensile residual stresses induced by solidification shrinkage accompanying the conventional thermal-spray processes; and
(g) Cold spray of the materials like copper, solder and polymeric coatings offers exciting new possibilities for cost-effective and environmentally friendly alternatives to technologies such as electroplating, soldering and painting [13].

Table 1 makes a comparison of Cold Spray process to competitive technologies by listing out important process features.

5. CONCLUSION

A comparison of competitive spraying technologies clearly shows that cold gas dynamic spraying has been established as a viable coating technology in the thermal spray processes family for reconditioning worn components. The dense and oxide-free coatings that may be produced through Cold Spray have brought about a numerous new applications which, up to now, have not been feasible using traditional processes. As a result, practical solutions may be readily observed within industries such as automotive and electronics manufacturing.

REFERENCES

[1] Rajiv Asthana, Ashok Kumar and Narendra Dahotre, "Material Processing and Manufacturing Science", Chapter-5, Coating and Surface Engineering, pp.313.
[2] Wally Birtch, "Supersonic Spray Technologies Division Centreline (Windsor) Ltd.", Kinetic Spray for Corrosion Protection and Metalpart Restoration: 2007 , CTMA Symposium, San Antonio.
[3] Klaus Dobler and St. Louis Metallizing Co., "Reconditioning Power Generation Components with Thermal Spray//Welding Journal", May 2006.

Table 1Comparison of Cold Spray to Competitive Technologies

Process Feature	Cold Spray	HVOF	Plasma	Arc Spraying
Bonding Mechanism	Mechanical /Chemical	Mechanical	Metallurgical	Metallurgical
Max. Thickness (mm)	0.05 -10	< 1.5	< 0.5	0.1
Surface Finish (µm Ra)	<1	1.3 - 2.0	13.0	2.0
Deposition Rate (kg/hr)	1 - 10	1 - 5	2 - 7	5 - 60
Deposition Efficiency (%)	>95	50 - 70	30 - 60	55 - 65
Wear Resistance (mm^3)	50	27	10	6
Bond Strength (M Pa)	30-40	30-70	30-55	20-30
Equipment Cost (USD)	40000	60,000	50,000	10,000
Corrosion Rate (m p y)	0.25	3.5	1	2
Porosity (%)	0.15	1.6 – 2	5	10 - 20
Oxygen Content (%)	0.25	3	9	5 – 15
Conductivity (%)	85	45	15	60
Feedstock Size (µm)	5 - 60	5 – 60	5 – 20	5 – 100
Gas Consumption (m^3)	1 – 5	50	1 – 5	0.1 – 5
Power Consumption (kW)	5 - 15	1 – 2	30 - 100	5 – 10
Powder Feed Rate (kg/hr)	25 - 75	25	15	125-150
Spray Velocity (ft/sec)	2000	2200	1500- 2000	2300
Feedstock Capability	Metallics, Polymeric, Composites, Self Fluxing Alloys	Metallics, Tungsten Carbides, Chromium Carbides, Self fluxing Alloys	Metallics, Tungsten Carbides, Chromium Carbides, Self fluxing Alloys	Metallics, Tungsten Carbides, Chromium Carbides, Self fluxing Alloys
Typical Applications	Friction, Impact, Abrasion, Corrosion,	Friction, Abrasion, Corrosion	Friction, Impact, Abrasion, Corrosion, Cavitation	Friction, Impact, Abrasion, Corrosion, Cavitation

[4] Antolii Papyrin, Vladmir Kosarev, Sergey Klinkov and Antolii Alkhimov, "Vasily Fomin: Cold Spray Technology", Elsevier Publishers.

[5] A.P. Alkhimov, A.N. Papyrin, V.F. Dosarev, N.I. Nestorovich and M.M. Shuspanov, "Gas Dynamic Spraying Method for Applying a Coating", US Patent 5,302,414, 12, April 1994.

[6] A.O. Tokarev, "Structure of aluminum powder coatings prepared by cold gas dynamic spraying", // Met. Sci. Heat. Treat., Vol.35, 1996, pp.136.

[7] J. Karthikeyan, "Cold Spray Technology: International Status and USA efforts", ASB Industries, December 2004.

[8] R.C. McCune, A.N. Papyrin, J.N. Hall, W.L. Riggs, P.H. Zajchowski, C.C. Berndt and S. Sampath, (Ed.), "An Exploration of the Cold Gas-dynamic Spray Method for Several Material Systems// Thermal Spray Science and Technology", ASM International, 1995, pp.1-5.

[9] J. Vlcek, "A Systematic Approach to Material Eligibility for the Cold Spray Process, in: International Thermal Spray Conference and Exhibition", May 5 -8, Orlando, 2003, Florida, USA.

[10] D.G. McCartney, "Particle-substrate Interactions in Cold Gas Dynamic Spraying, in: International Thermal Spray Conference and Exhibition", May 5-8, Orlando, 2003, Florida, USA.

[11] H. Assadi, F. Gärtner, T. Stoltenhoff, H. Kreye// Acta Mater. 51, 2003, 4379.

[12] F. Gärtner, "Numerical and Microstructural Investigations of the Bonding Mechanisms in Cold Spraying, in: International Thermal Spray Conference and Exhibition", Orlando, Florida, May 5-8, 2003.

[13] C.V. Bishop, G.W. Loar// Plat. Surf. Finish 80, 1993, 37.

Metallic Biomaterials

T.P.S. Sarao[1], H.S. Sidhu[2], H.Singh[3]and R.Chhibber[4]
[1]Swami Vivekananad Institute of Engineering and Technology, Patiala, Punjab
[2]Yadavindra College of Engineering, Bathinda, Punjab
[3]IIT Ropar, Ropar, Punjab
[4]Thapar University, Patiala, Punjab
E-mail: tsarao@yahoo.com

Abstract

The materials used for biomedical applications are called biomaterials. Biomaterials is an important research area for material scientists and biomedical engineers as they helps to improve the quality and longevity of human life. Biomaterials can be classified as polymers ,composites, metals and ceramics. Metals and their alloys are used as biomaterials due to their excellent mechanical properties, reasonable biocompatibility and ease of manufacturing. Corrosion resistance is another important factor in selection of any metal for biomedical applications. Commonly used metallic biomaterials are stainless steel 316L, titanium and titanium alloys and cobalt-chromium alloys. These biomaterials are used in various biomedical application such as implants, crowns, bridges, dentures etc. This paper gives an overview of commonly used metallic biomaterials.

Keywords: *Biocompatibility,Biomaterials,Corrosion,Surface modification,Wear*

1. INTRODUCTION

Biomaterials can be defined as that branch of biomedical engineering which deals with the material aspects of medical devices and implants. The materials used for developing body implants or interfaces are commonly called biomaterials. According to Clemson advisory board for biomaterials "A biomaterial is a systemically, pharmacologically inert substance designed for implantation within or incorporation with a living system", a definition adopted at the sixth annual international biomaterials symposium, April 20-24, 1974. Williams has defined biomaterials as "any nonliving materials used in medical devices intended to interact with biological systems" [1,2].

The field of biomaterials is rapidly expanding. It is considered that this domain represents 2 to 3 % of the overall health expenses in developed countries. For example France spends every year 30 to 40 billions of French francs. World expenses could be estimated at 100 billions of dollars [3].

Each year in the United State there are around 250,000 age-related hip fractures, with an estimated health care cost approaching $10 billion and 700,000 age-related vertebral fractures, with costs of £1billion. In Britain, the equivalent overall costs approach £2 billion [4].

The field of biomaterials covers a lot of different materials: cardiac artificial valves, artificial vessels, cardiac stimulators, stents, artificial hips, knees, shoulders, elbows, materials for internal fracture fixation, scoliosis treatment, materials for urinary tract reconstruction, artificial crystalline, skin, ears ossicules, dental roots and so on [3]. Not all biomaterials are implanted within the body and there are several examples of medical devices that are used external to the body but which, nevertheless, come into critical contact with the tissues. These mostly involve external circulatory systems such as the heart lung machines used to support patients undergoing open-heart surgery, kidney dialysis machines and liver perfusion systems. These devices will have many components, often including tubing, blood reservoirs and heat exchangers in addition to the critical functioning component such as the dialysis membrane [6].

Biomaterials can be divided into two categories as metallic biomaterials and non metallic biomaterials (Figure 1).

2. A BRIEF REVIEW OF NONMETALLIC BIOMATERIALS

Nonmetallic Biomaterials fall in three categories polymers, ceramics and composites. Polymers, have covalent bonds within molecules and van-der-waals bonds between molecules with low melting point.

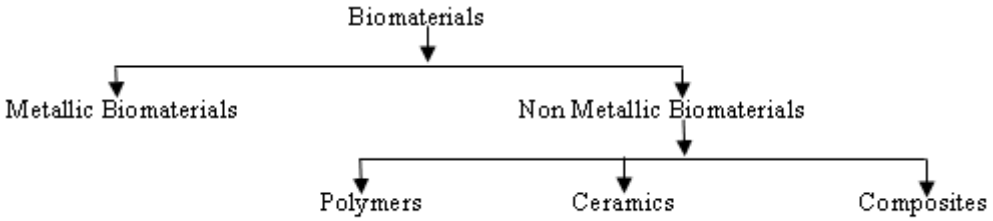

Fig.1 Types of biomaterials

Polymers undergo degradation in the body environment due to biochemical and mechanical factors. This results in ionic attack and formation of hydroxyl ions and dissolved oxygen, leading to tissue irritation and decrease in mechanical properties. Currently the polymers most widely used as biomaterials are: Ultrahigh molecular weight polyethylene (UHMWPE), Acrylic bone cements, polyether ether ketone (PEEK), Bioabsorbables [5, 6]. Ceramic, have predominantly ionic bonds but also covalent bonds. They are heat resistant with various electric and magnetic properties. They have low fracture toughness and are brittle. The class of ceramics used for repair and replacement of diseased and damaged parts of musculoskeletal systems are termed bioceramics. Bioceramics became an accepted group of materials for medical applications, mainly for implants in orthopaedics, maxillofacial surgery and for dental implants. The main ceramic used as biomaterials are Alumina, Zirconia, and Hydroxyapatite [5, 6].

Composites are materials obtained by combining two or more materials or phases with a view to take advantage of the salient features of each constituent. It is essential that each component of the composite be biocompatible to avoid degradation between interfaces of the constituents. Mainly used composites as biomaterials are Fiber-reinforced polymers, polymethyl methacrylate (PMMA) [5, 6].

3. METALLIC BIOMATERIALS

Materials in medicine date back to ancient civilizations (India, China, Egypt etc), where the medicine was practiced as part of the religious and mystical activities. Metallurgical tools were used for surgical treatment, tendons for suture etc [7].

The first metallic alloy "vanadium steel" was developed in the early 1900's for human use. The first successful implants were bone plates, introduced in the early 1900s. With the introduction of these implants, surgeons identified material and design problems that resulted in premature loss of implant function, as evidenced by mechanical failure, corrosion, and poor biocompatibility. In 1926, 18-8SMo stainless steel was introduced which contained a small percentage of molybdenum, to improve the corrosion resistance in salt water. Later on this alloy became to be known as stainless steel316. In 1936, Vitallium (19-9 stainless steel) was introduced, which laterally changed to CoCr alloys. In late 1940's the titanium and its alloys were considered for applications in surgical implants. The titanium and its alloys had shown excellent corrosion resistance in the human environment. In 1950's, the carbon content of stainless steel 316 was reduced from 0.08% to 0.03% for better corrosion resistance and it was known as 316L stainless steel [8].

Metals have metallic bonds, free electrons distributed throughout lattice, high thermal and electrical conductivity, high fracture toughness and ductility, and reflection of light.

The three major classes of metallic biomaterials for biomedical applications are: stainless steel, cobalt-chromium alloys and titanium (as alloys and commercially pure). In addition, dental casting alloys are based on precious metals (gold, platinum, palladium or silver), nickel and copper and may contain smaller amounts of many other elements, added to improve the alloys' properties.

Austenitic stainless steels, especially AISI (American Iron and Steel Institute) Type 316L stainless steel is the most widely used material for implant fabrication in India for orthopedic applications because of its lower cost, ease of fabrication and welding as compared to Co–Cr alloys and Ti and its alloys. Austenitic type 316L stainless steel possesses reasonable corrosion resistance, biocompatibility, tensile strength, fatigue resistance and suitable density for load-bearing purposes thus making this material a desirable surgical implant material [5]. Recently, titanium alloys are getting much attention for biomaterials because they have excellent specific strength

and corrosion resistance, no allergic problems and the best biocompatibility among metallic biomaterials. Pure titanium and Ti–6Al–4V are still the most widely used ones for biomedical applications among the titanium alloys. They occupy almost whole of the market of titanium biomaterials. The titanium alloys composed of non-toxic elements that have been developed in the early stage are mainly α+β type ones. Recently, mechanical biocompatibility of biomaterials is regarded as important factor, and therefore the research and development of â types titanium alloys, which are advantageous from that point, are increasing [9, 10, 11]. The proper functioning of the implant depends on whether it possesses the strength necessary to withstand loading within the expected range [12].

Table 1 Mechnical Properties of Current Implant Materials and Cortical Bone

Material	E (GPa)	σ (MPa)	ε (%)	K_{IC} (MN $m^{-3/2}$)
Co-Cr alloy	230	900-1540	10-30	~100
316L stainless steel	200	540-950	6-70	~100
Ti-6Al-4V alloy	106	900	12.5	~80
Alumina	400	450	~0.5	~3
Zirconia (Mg-PSZ)	200	450-700		7-15
Hydroxyapatite	45-116	60-190		~1
Polyethylene (high density)	1	30		>300
Cortical bone	7-30	50-150	1-3	2-12

E : Young's modulus σ : tensile strength ε: elongation at fracture K_{IC} : fracture toughness

Current implant materials such as Co-Cr alloys and alumina are much stiffer than human cotical bone (Table 1). The modulus mismatch between an implant material and the host tissue can cause bone to resorb at the implant bone interface, leading to implant instability and hence its eventual failure. Failure is one of the most important aspects of implant materials behavior and directly influences the choice of materials and production methods in manufacturing. Because of the many variables involved, implant failure analysis is a complex area of study.

3.1 Requirements for Metallic Biomaterials

The important requirements for metallic biomaterials are that they must be corrosion resistant, biocompatible, wear resistant, fatigue resistant, non allergic, and a young's modulus as close to that of bone as possible depending upon their biomedical applications.

3.1.1 Biocompatibility

Biocompatibility is the ability of a material to perform with an appropriate host response in a specific application. It is the primary characteristic of any biomaterial. What this means is that for the intended function, in the location where an implant is located, the material should be compatible with its surroundings, and should be integrated with the surrounding tissue without deleterious effects. Biocompatibility is not controlled by one process but is the sum of many different processes. There are two compartments in this system, the material and the host tissue, and it is usual to consider the reactions that occur within these separate parts [6]. Many materials are not compatible in vivo.Biocompatible materials must release substance in non toxic concentrations after their implantation in body [13].

3.1.2 Wear

Wear is the main cause of failure of implants in the case of knee and hip joint prosthesis. Any use of the joint, such as walking in the case of knees or hips, results in cyclic articulation of the polymer cup against the metal or ceramic ball. Over time, sufficient bone is resorbed around the implant to cause mechanical loosening, which necessitates a costly and painful implant replacement, or revision. The metal to plastic system will exhibit a lower coefficient of friction but a higher volumetric wear rate. The volumetric wear of stainless steel–polyethylene combination is greater than cobalt–chromium–polyethyle systems. The only combination used extensively in the metal-to-metal system is cobalt–chromium to cobalt–chromium because of its high wear resistance [16, 5].

Fatigue wear also plays a significant role in ultimate

failure of medical devices. Materials used in medical devices are subjected to high stresses and high cycle loading. This very demanding condition coupled with the aggressive body environment leads to fatigue failure of metallic, polymer and ceramic implants. A fatigue wear process involving fretting causes the generation of wear debris which invokes acute host–tissue reactions which tend to aggravate the fatigue problems of the biomaterial by producing enzymes and chemicals that are highly corrosive. Fatigue failure may also occur due to improper installation and the presence of gap between the fractured bone fragments after implantation [21].

3.1.3. Metal Allergy

In biomaterials, metal allergy is also a significant problem. Metal allergy is caused by the metallic ions, which are released from an alloy through sweat and other body fluids. In dentistry, Co, Cr, and Ni have been pointed out to be highly associated with metal allergy, and the use of Ni is rapidly being abandoned. It is important to omit metallic elements that cause metal allergy [14]. The metallic alloys used for fabrication of artificial joints undergo corrosion and release metallic ions into the patient's body. The metallic ions of these metals (Cobalt, Chromium, Nickel, but also the relatively inert Titanium) may combine with patient's proteins and trigger allergic immune response. One such allergy reaction is skin rash observed (very seldom) in patients with orthopedic metal devices implanted in their bodies. Interest in nickel-free stainless steel and cobalt alloys is high for biomedical applications because nickel is an allergen so high-nitrogen stainless steel has been developed [15].

3.1.4 Corrosion

Corrosion of metals is a complex phenomenon that depends on geometric, mechanical, and chemical solution parameters. During the corrosion process, a coupled oxidation-reduction reaction takes place, in which one species gains electrons (oxidizing agent) while the other donates electrons (reducing agent). This reaction occurs spontaneously when energy is released by the reaction. Most implanted metals, such as titanium, cobalt-chromium, and stainless steels, have a tendency to lose electrons in solution, and as a result, they have a high potential to corrode. The result is dissolution of the metal and formation of metallic ions [17]. Two essential features determine how and why a metal corrodes. The first characteristic involves thermodynamic driving forces, which cause corrosion (oxidation and reduction) reactions, and the second involves kinetic barriers, which limit the rate of these reactions. The thermodynamic driving forces that cause corrosion correspond to the energy required or released during a reaction. The kinetic barriers to corrosion are related to factors that impede or prevent corrosion reactions from taking place [18].

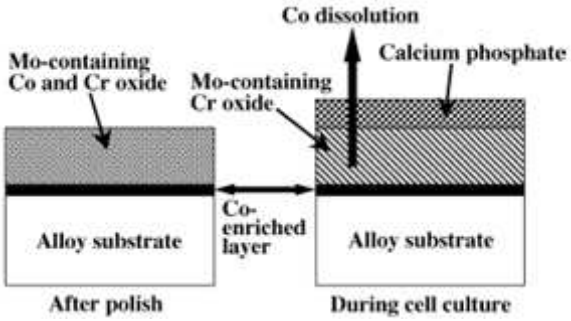

Fig.2 A schematic illustration of the reconstruction of surface oxide film on a Co-Cr-Mo alloy after polishing and during cell culture

The human body is a harsh environment for metals and alloys having to be in an oxygenated saline solution with salt content of about 0.9% at pH 7.4, and temperature 37.1^{0}C. Changes in the pH of body fluids are small because the fluids are buffered solutions and the pH usually remains between 7.0 and 7.35 [16]. All the surgically implantable metallic materials, including the most corrosion-resistant materials, undergo chemical or electrochemical dissolution at some finite rate, due to the complex and corrosive environment of the human body. The body fluid acts as a electrolyte .Metallic implants can interact with living tissue in three ways: by electron exchange (redox reaction), by protonexchange (hydrolysis), and by complex formation (metal ion-organic molecule binding). The behavior of stainless steel is dominated by its nickel component, which induces all three reactions, whereas none have been observed with titanium [19]. All main metallic biomaterials comes under category of passive metals i.e they owe their corrosion resistance to the presence of a stable oxide layer on their surface. Stainless steel and Cobalt-Chromium alloys are protected by a chromium oxide layer,Cr_2O_3 whereas titanium and its alloys are protected by a titanium oxide layer i.e TiO_2.Despite their good corrosion resistance, ion release in vivo is still of some concern. Chromium and nickel are known carcinogens, and cobalt is a suspected carcinogen [19, 14]. A schematic illustration of surface oxide film on a Co-Cr-Mo alloy during cell culture is shown in Figure 2 [16].

3.2 Surface Modification

Surface modification is one of the major research areas in biomaterials. It is an important technique for obtaining biofunction, bioactivity, corrosion resistance and biocompatibility in metals for biomedical applications. The surface modification technique is a process that changes the surface composition, structure and morphology of a material, leaving the bulk mechanical properties intact. There are many surface modification methods such as chemical methods, thermal spray methods, ion implantation, biomimetic coatings, functionally graded coatings etc. Metallic implants are mostly coated with hydroxyapatite for biomedical applications. Hydroxyapatite has a chemical formula $Ca_{10}(Po_4)6(OH)_2$ is commonly referred as HA. The concept of applying HA on to metallic implants as a coating was developed due to its biocompatibility and bioactive properties.

4. CONCLUSION

The effect of materials on tissues and vice versa needs to be understood and tissue engineering is one major research area in this field. For mechanical reliability, metallic materials must be used and cannot be replaced with ceramics or polymers though composite biomaterial is another alternative. Corrosion is one major reason of metallic implant failure. In vitro and In vivo testing in simulated body fluids is recommended for the safe use of biomaterials. Besides developing novel biomaterials, surface modification of the biomaterials, for improving their corrosion resistance and bioactivity is emerging area of research. The conclusion is that much research is needed in these areas to improve the lives of human beings.

REFERENCES

[1] Park J B (1981), Biomaterials science and Engineering, Plenum Press, New York,Vol.1(1).

[2] Williams D F (1987), Definitions in Biomaterials, New York, Elsevier.

[3] Sadel L (2004), Biomaterials: Medical Viewpoint in Materials, Hospital Laribeùrlere Universite Paris 7, UFR Lariboisiere – Saint – Louis 75475 Paris Cedex 10, France, pp 76.

[4] Bonfield W ,Behiri J C, Doyle C, Bowman J and Abram J (1984), "Hydroxyapatite Reinforced Polyethylene Composites for Bone Replacement," Biomaterials and Biomechanics, Elsevier, pp 421-426.

[5] Kamachi M U, Sridhar T M and Raj B (2003), "Corrosion of Bio Implants," Sâdhana, Vol. 28, (3 & 4), pp 601-637.

[6] Williams D F (2003), "Biomaterials and Tissue Engineering in Reconstructive Surgery," Sadhana, Vol. 28(3 & 4), pp 562-574.

[7] Sivakumar R (1999), "On the Relevance and Requirement of Biomaterials," Bulletin of Material Science, Vol. 22(3), pp 647-655.

[8] http://www.ece.uprm.edu/m goyal/home.htm

[9] Kovacs P, Davidson J A (1993), "The Electrical Behavior of a New Titanium Alloy,"Titanium'92, The Institute of Materials, pp 2705.

[10] Ahmed T, Lomg M, Silvestri J, Ruiz C, Rack H J (1996), "A New Low Modulus, Biocompatible Titanium Alloy," Proceedings of Titanium'95, The Institute of Materials, pp 1760.

[11] Kuroda D, Niinomi M, Morinaga M, Kato Y and Yashiro T (1998), "Design Mechanical Properties of New â Type Titanium Alloys for Implant Materials," Material Science and Engineering, pp 244–249.

[12] Wang M (2003), "Developing Novel Biomaterials for New Challenges," Proceedings of Conference Material Science and Technology in Engineering, Hong kong.

[13] Itiravivong P (2001), "Biomaterial : An Overview," Journal of Metals, Materials and Minerals, Vol. 11(1), pp 15-21.

[14] Minomi M (2002), "Recent Metallic Materials for Biomedical Applications," Metallurgical and Materials Transactions, Vol. 33A, pp 477-486.

[15] Niinomi M, Hanawa T and Narushima T (2005), "Japanese Research and Development on Metallic Biomedical, Dental, and Health Materials," Journal of the Minerals, Metals and Materials Society, Vol.57(4), pp 18-24 .

[16] Hanawa T (2002), Evaluation Techniques of Metallic Biomaterials in Vivo," Science and Technology of Advanced Materials, Vol. 3, pp 289-295.

[17] Sharan D (1999), "The Problems of Corrosion in Orthopedic Implant Materials," Orthopaedic Update, Vol. 9(1), pp 1-5.

[18] Jacobs J J, Gilbert J L, Urban R M (1998), "Corrosion of Metal Orthopedic Implants," The Journal of Bone and Joint Surgery , Vol. 8, pp 268-282.

[19] Bombaè D, Brojan M, Krkoviè M, Turk R, Zalar A (2007) "RMZ -Characterization of Titanium and Stainless Steel medical implants surfaces," Materials and Geo Environment, Vol. 54 (2), pp 151-164.

Electrostatic Spraying of Biocompatible UHMWPE Reinforced with Alumina (Al_2O_3) and HA (Hydroxyapitite) Nanocomposites

S. Srivastava[1] and K Balani[2]

[1]Department of Materials Science and Metallurgical Engineering, UIET, CSJM University, Kanpur - 208 024, India

[2]Department of Materials and Metallurgical Engineering, IIT Kanpur - 208 016, India

E-mail:- 100rabhmishra@gmail.com.

Abstract

Electrostatic spraying is a useful way to produce fine coatings with a simple apparatus. Bioactive coating on Ti alloy facilitates biological fixation between the prosthesis and the hard tissue, and increase the long-term stability and integrity of the implants. It produces an intermediate region between bone and implant, and enhances the transition of stress between them. Polymer coating on the Ti alloy substrate which is used as an implant for the bones and hip joints. UHMWPE as the matrix polymers and added biocompatible HA and alumina for increasing the strength and stiffness of the coating. The coated samples showed excellent wear results under the pin on disc apparatus.

The coated materials were characterized by X-ray diffraction(X-RD), scanning electron microscopy (SEM), wear test (pin on disc), and Vickers hardness test. Bacterial culture study of the coatings showed excellent cell growth properties.

Keywords: *Alumina, HA,UHMWPE, Wear test*

1. INTRODUCTION

Electrostatic spraying is a useful way of producing fine powder coatings. In medical field many a time replacement of body parts is being done due to many reasons like accidental bone failure .Implant prototype normally made of Ti alloy having coating of other materials such that it makes implant compatible to body. These coatings provide lubrication, hardness, anti-corrosion property, reduce wear and also make implant compatible to body [1-8].

Our main aim is to replace Ti-6Al-4V alloy by steel.Ti alloy generally used in implants but its cost is high and replacing it with steel lead to reduction in cost of replacement (like hip joint, knee joint). So we have to investigate whether coatings of these bio materials can be develop on steel with the same integrity as for Ti alloy.

Our interest area is to produce LDPE and UHMWPE reinforced with Alumina and HA on the Ti6V4Al alloy for use as an implant in the body.Although the Ti alloy is itself very inert still the coating is done because it releases toxic ions under the body environment.We have chosen electrostatic spraying as the coating technique for the coating because of the ease at which the powder coating is done using this process.Powder coating is applied as a free flowing fine powder through the electrostatic gun.The main advantage of the powder coating is that it does not require a binder in the liquid suspension form. The coating is typically applied electrostatically and is then cured under heat to allow it to flow and form a fine adhesive layer. It is usually used to create a hard finish that is tougher than conventional paint [9].

Alumina is used as a reinforcing element because of its excellent corrosion resistance in the body environment, excellent biocompatibility, high hardness and wear properties. The Young Modulus of Alumina is 300 times greater than bone. HA material is highly biocompatible and it closely resembles the composition of the bone[10].The high molecular weight of UHMWPE makes it a very tough material and because of its outstanding toughness and its cut, wear and excellent chemical resistance it is used here as the matrix material.

After depositing a thick adhesive coating on the substrate the wear study of the Sample was done by the pin on disc set up and hardness of the samples was calculated using the vicker hardness test. The comparison

between the hardness and wear values showed that the alumina addition increases the hardness and wear properties of the coatings.

2. EXPERIMENTAL DETAILS

2.1 Selection of the Materials

The LDPE powder,UHMWPE powder, hydroxyapitite (HA) powder (Aldrich 99.9%) and alumina (99.85 Merck) (nano and micro size) were selected for coating on the steel substrate. Ball milling operations were used to mix powders homogeneously the required amount of the powder.

2.2 Coating Composition

Alloy Powder	Chemical Composition (wt %)
LDPE-Al_2O_3	98LDPE,2Al_2O_3
LDPE-Al_2O_3-HA	95LDPE,2Al_2O_3, 5HA
LDPE-HA	95LDPE, 5HA
UHMWPE-Al_2O_3	98UHMWPE, 2Al_2O_3

2.3 Coating on the Substrate

2.3.1 Coating of LDPE on the Mild Steel Substrate

The required amounts of the powder were weighted form electrical pan balance. The ball milling procedure was used to mix the weighted amount of the powder.The ethanol solution was used as the solvent. The powder was dried in oven at 55°C for 20 hrs. Electrostatic spraying is by far the widest spread deposition system used for powder coatings in finishing of conductive surfaces. The system is based on the propulsion of painting powders through a spraying gun by using compressed air at moderate pressure. The temperature in the oven was maintained as per the requirement (190°C for LDPE coatings). After coating the powders with the gun the coated substrate were kept in the furnace at optimum temperature for an optimum amount of time.The purpose of our experiments was to find the optimum curing temperature and time for the LDPE coatings. Figure 1(a) and 1(b) shows the LDPE coating on the surface. At temperature 235°C and time 25 min, the coating is uniform but non homogeneous. Keeping the temperature same but reduce the time from 25 to 20 minutes the LDPE coating was uniform and still non-homogenous. Again reducing the temperature from 235 to 190°C and time from 20 minutes to 10 minutes the coating was successfully done on the mild steel substrate. Finally, 190°C temperature and 10 minutes were selected as the curing temp and time respectively for further LDPE coatings (Figure 1c).

2.3.2 Coating of LDPE Reinforced with Alumina on the Mild Steel Substrate

The LDPE reinforced with different amount of nano-alumina was coated on the steel surface. In this case the temperature is 190°C and curing time is 10 minutes. At 10% alumina the appearance of the coated surface contains large peels. But the appearance of the coated surface was changed with reducing the amount of the alumina in the LDPE matrix. At 5% alumina small voids still appear as shown in figure 2a. It was observed that due to deagglomerated nano size Al_2O_3, peel formation occurred. Reducing the Al_2O_3 % the problem was reduced. Thus it was concluded that more Al_2O_3 % is causing peel formation. Thus, Al_2O_3 % was reduced in the coatings to follow and the substrate was grinded rough. Despite reducing the Al_2O_3 % and rough grinding still some voids are still appearing. It can be seen in the Figure 3a.Finally two step coating was done. In the first step the LDPE coating was done with curing temperature 190°C and time 10 minutes. In the second step LDPE reinforced with 2% alumina was coated on the already LDPE coated substrate. The coating was homogeneous and uniform after the two step coating as shown in Figure 3(b).

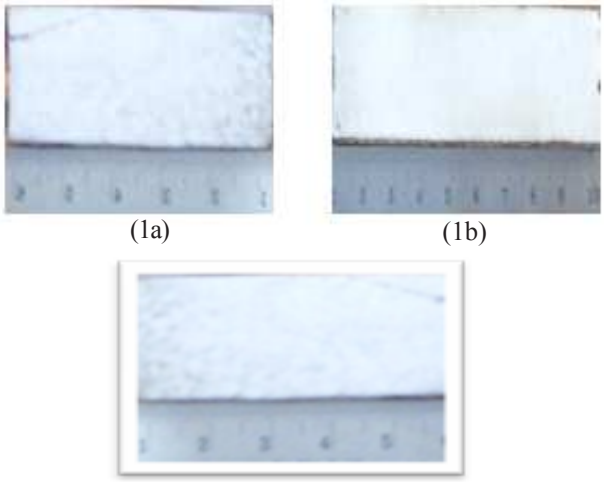

(1a) (1b)

(1c)

Fig. 1 LDPE coating on the mild steel surface (a) Temp-235°C and time 25min (b) Temp-235°C and 20min and (c) Temp-190°C for 10min

(2a)

Fig. 2.a LDPE reinforced with 5% nano-alumina coating on the mild steel surface (a) Initial weight =56.4852g (b) Coating Thickness = 0.1896mm

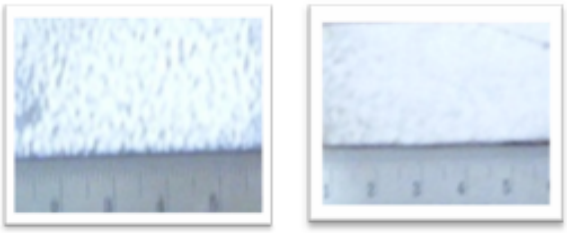

(3a) (3b)

Fig.3 LDPE reinforced with nano-alumina coating on the mild steel surface (a) 2% alumina uniform Non-homogeneous, large voids, Initial weight =56.185g and Coating thickness = 0.1803mm (b)Two step coating (i)LDPE (ii)LDPE and2%alumina, homogeneous and uniform coating. Initial weight =56.896g and Coating thickness = 0.1833mm.

2.3.3 Coating of UHMPWE Reinforced with Alumina and HA on the Mild Steel Substrate

Now, the substrate is again coated with UHMWPE powder as the matrix and Al_2O_3, HA are the reinforcements. This coating is transparent in nature. During curing period it was observed that after 20 minutes by the addition 2% alumina UHMWPE decolorized (see Figures below).

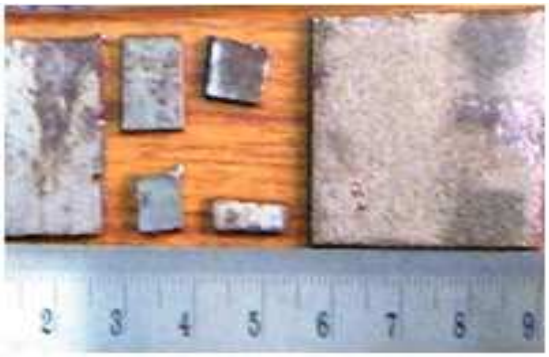

UHMPWE reinforced with nano-alumina and HA coating on the mild steel surface.

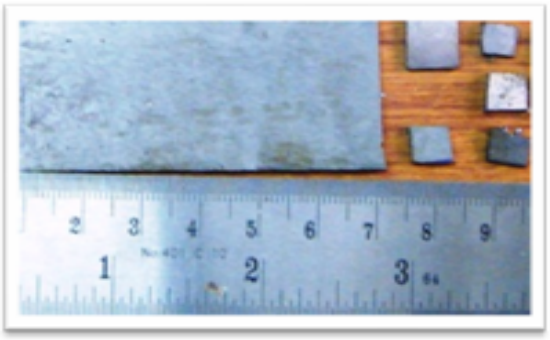

UHMPWE reinforced with nano-alumina coating on the mild steel surface.

2.3.4 Characterization of the Coating

XRD measurements were performed in the 2θ range of 20º- 90º in a Rich-Seifert ISO Debyflex 2002 Diffractometer using Cu K_α (λ=0.154 nm) target at a scan rate of 1º/min. The spectra were analyzed using JCPDS database. The optical Microscope (SEM) was used to observe the basic feature of the specimen.

The Scanning Electron Microscopy (SEM) images were obtained on thin film of the sample in a CARL-ZEISS EVO 50 XVP Low Vacuum Scanning Electron Microscope (LVSEM) equipped with the Everhart–Thornley SE detector. The samples were coated with gold to make surface conductive. Thickness of the sample is determined by using optical microscope.

Wear study is done by using pin on disk tribometer. In all the the experements, testing was carried out with 50 grams load.

2.3.5 Wear Test Load

Pin on disc methods was used to study the wear behavior of the material. Their schematic diagram is shown below.

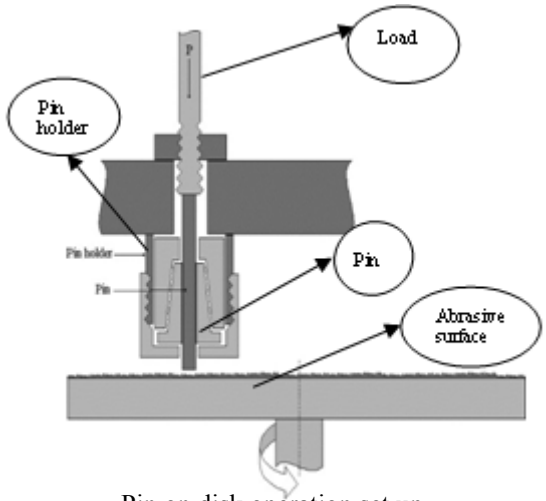

Pin on disk operation set up

3. RESULTS AND DISCUSSION

3.1 Characterization of Ball Milled Powders

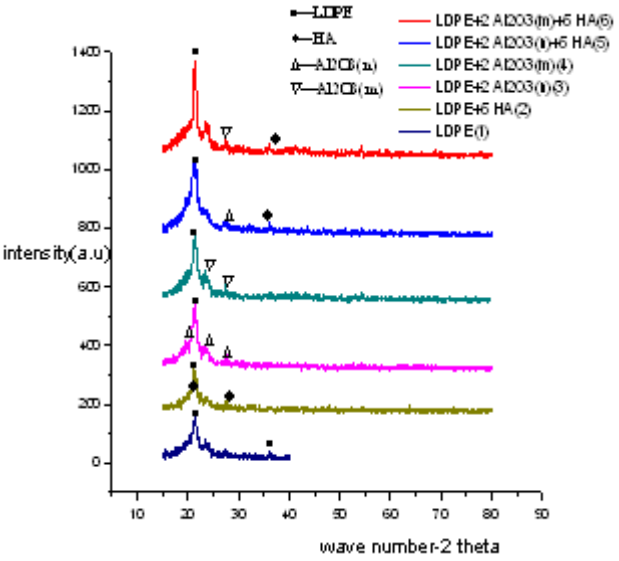

In all the plots LDPE is the dominant group.

3.2 Examine the Coss Section View of Coating and its Thickness

For determining the thickness of the coated sample the Optical Microscope was used. Mount the cross-sectioned part of the sample by the acrylic polymer on the mild steel subtract, the sample were polished with different emery papers (500, 1200, 2000mesh respectively) & then fine polishing with aluminum slurry. Figure3.2(a) LDPE and 5% HA and 3.2(b) UHMWPE+2% Al_2O_3 shows the optical photograph of the coated sample on mild steel subtracts by using selected coating materials. It can be obviously seen that the gray region are the mounting materials and darks regions shows the coated materials coated on the surface. The surface in this case is seen as white.

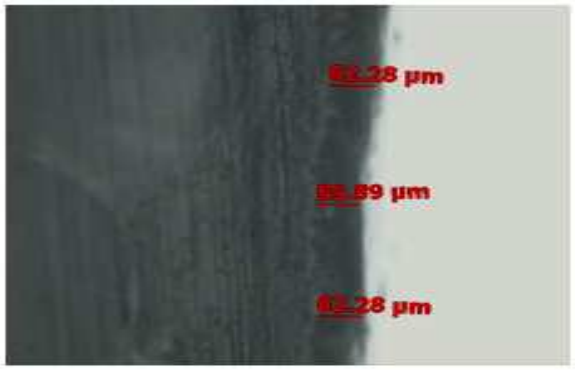

(a)

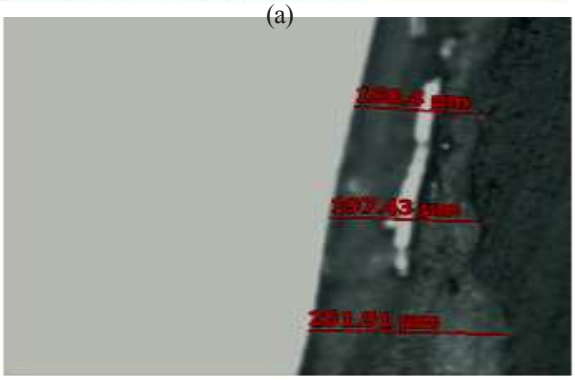

(b)

Fig. 3.2 Optical Micrograph of the (a) LDPE +5% HA and (b) UHMWPE+2% Al_2O_3 of ball milled

3.3 Wear Study (Pin on Disc Tribometer)

One of the main important characteristics of materials behavior is wear and friction. For wear study by pin on disc methods of the materials the selected parameters are given in table1. The wear results are tabulated in Table 1. Figure 3.3(a) shows the variation of the coefficient of the friction with variable time. It can be seen from the figure the coefficient of friction increase suddenly but certain periods of time trends are almost constant.

Parameters

Load=50 gm
Time interval=60 sec
r.p.m=300
Sliding distance = 3.925 cm
Here we are taking three samples.
Sample A:Two step coated sample (i)LDPE(ii)LDPE+2%Al_2O_3+5%HA
Sample B : UHMWPE
Sample C :UHMWPE+2%Al_2O_3

Table 1 Wear Results

Sample	Wt. with-out pin (gm)	Wt. with pin before test (gm)	Wt.with pin after test (gm)	$\Delta w = w_1 - w_2$ wt.loss (gm)	Density (gm/cm^3)	Wear volume (Δw in cm^3)	Specific wear rate(k_0 in cm^2/N)
A	1.0876	59.6414	59.6411	0.0003	0.95887	0.00073	0.00092
B	0.6019	61.4098	61.3930	0.0168	0.93	0.01806	0.0189
C	0.6552	61.2560	61.2430	0.0130	1.03953	0.00028	0.00045

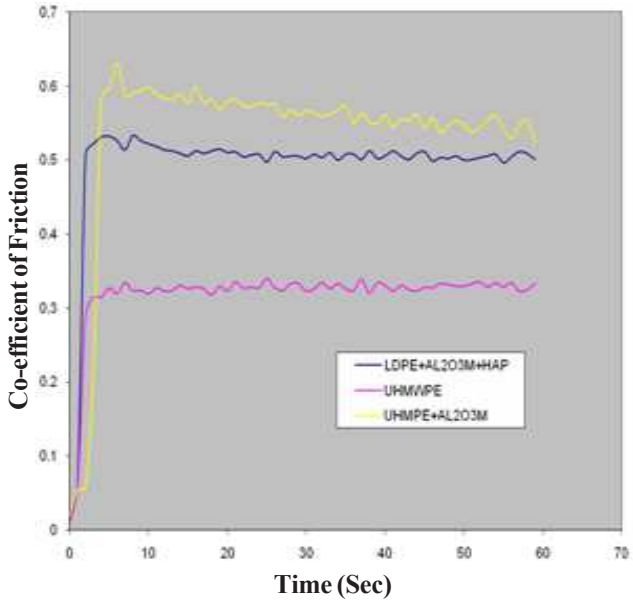

3.4 Hardness test

The hardness of the entire composite was measured using a Vickers hardness testing machine. A Vickers test for microhardness uses light loads between 1g and 2kg to test the small or thin materials. The maximum hardness (see Table 2) is observed in UHMWPE+2% Al_2O_3 coating and minimum in LDPE.

Formula used in calculation of Vickers micro hardness:

Sample cross section = 10 mm×10 mm
F = Load in kgf
d = Arithmetic mean of two diagonals,d_1 and d_2 in mm
HV = Vickers hardness

$$HV = \frac{2F\sin\frac{136^\circ}{2}}{d^2} \qquad HV = 1.854\frac{F}{d^2} \text{ approximately}$$

Table 2 Hardness Measurement

Sample Coating	Load (in gm)	d_1 (in mm)	d_2 (in mm)	Hardness (in MPa)
LDPE	20	0.0953	0.0926	4.200
LDPE+5%HA	20	0.0946	0.0915	4.300
UHMWPE+2% Al_2O_3	20	0.0842	0.0833	4.413

3.5 SEM Observation

Figure 3.5 (a) to (c) shows the SEM micrographs of the all coated sample. From these figures it can be seen that the morphology of the coated sample is not uniform because some cracks shown in the fig that makes this coating non-uniform. This coating was done by same electrostatic spraying methods of this powder mixture cure it for 10 minutes and curing temperature 190ºC.After this operation sample was taken out from the oven.The film were obtained of the order of 0.15mm thick.

4. CONCLUSION

Curing parameters were optimized at 190ºC, 10 minutes for LDPE matrix and 180ºC, 40 minutes for UHMWPE matrix.Curing parameters were optimized at two step process. In view, uniform and homogeneous coatings were obtained. The HA/Al_2O_3 in LDPE and UHMWPE matrix were successful incorporated. From the graph of Intensity v/s 2-theta LDPE shows dominating peaks because % of this compound in the mixture is more. The Al_2O_3 shows peak due to its very fine 0.05µm size due to this reason.

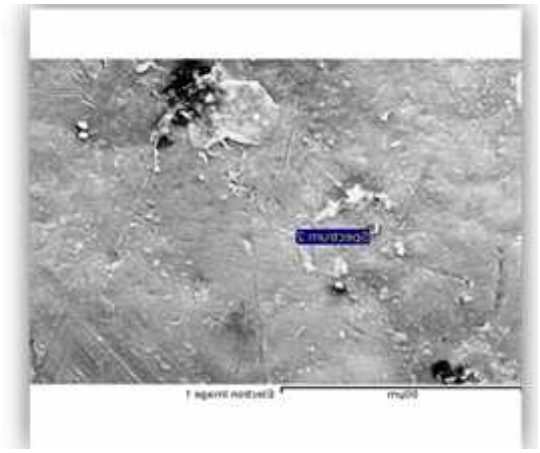

(a)

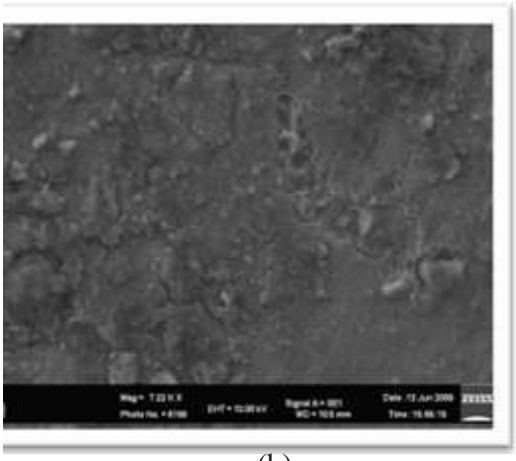

(b)

(c)

Fig 3.5 SEM image of (a) LDPE+5%HA+2% Al_2O_3 (b) LDPE+5%HA coating (c) UHMWPE+2%Al_2O_3 coating

It can easily be mixed up with the matrix compound. Every compound present in the mixture shows their respective peak means mixture is homogeneous and they can easily mixed without any reaction. It shows that properties of the compound retained in the matrix. Out of this the specific wear volume for sample UHMWPE+2%Al_2O_3 coating is found to be minimum. Presence of Al_2O_3improves the wear resistance of the coating. From Vicker micro hardness study, this result shows that hardness value for UHMWPE+2%Al_2O_3 is maximum.This suggests that after curing UHMWPE is harder than LDPE.

5. ACKNOWLEDGEMENT

We gratefully acknowledge mental support by Dr.Kantesh Balani (Asst. Professor, IIT Kanpur) of MME Department. We would also like to thank our friends Ram Krishna Mishra, Shubhra Bajpai, Manish Jain, Somya Mehrotra and Vatsala Chaturvedi for their support throughout our work.

REFERENCES

[1] M. S. Donley, P.T. Murray, S. A. Barber and T. W. Haas, "Surface and Coatings Technology", Deposition and Properties of MO and Thin Films Grown by Pulsed Laser Evaporation, Vol.36, 1988, pp.329 - 340.

[2] V. Sundar, R.P. Rusin and C.A. Rutiser (Eds.), "Bio Ceramics", Materials and Applications IV (Ceramic Transactions, Vol.147, The American Ceramic Society, 2003.

[3] J.F. Shackelford, "Bio Ceramics (Advanced Ceramics Vol. 1)", Gordon and Breach Science Publishers, 1999.

[4] J.F. Shackelford (Ed.), "Bio Ceramics (Applications of Ceramics and Glass Materials in Medicine)", Trans. Tech. Publication Ltd, 1999.

[5] K. Shimizu, A. Ito and H. Honda, Journal of Bioscience, Bioengineering, Vol.104, 2007, pp.171.

[6] H. Wu, T. Wang, J. Sun, W. Wang and F. Lin, Nanotechnology, Vol. 18, 2007, pp.1.

[7] J. Zhang, M. Iwasa, N. Kotobuki, T. Tanaka, M. Hirose, H. Ohgushi, D. Jiang, J. Am. Ceram. Soc. Vol.89, 2006, pp.3348.

[8] Z. Shen, E. Adolfsson, M. Nygren, L. Gao, H. Kawaoka and K. Niihara, Adv. Mater., Vol.13, 2001, pp.214.

[9] www.jotun.com

[10] 4th Lecture Bioceramics and Polymers MTKD-CT-2004-517226,Dr Christos S. Ioakimidis Gdansk University of Technology, Faculty of Ocean Engineering and Ship Technology

[11] http://www.gordonengland.co.uk/hardness/vickers.htm.

Erosion - Corrosion Resistance of Carbide Based Thermal Spray Coatings: A Review

Rakesh Bhatia, Sukhpal S. Chatha, Hazoor S. Sidhu and Buta S. Sidhu
Department of Mechanical Engineering, Yadavindra College of Engineering, Punjabi University Guru Kashi Campus, Talwandi Sabo, Bathinda, Punjab -151 302, India
E-mail:- Rakesh_lit@yahoo.co.in

Abstract

Degradation of metal is a severe problem in the world today. Understanding the behaviour of metals and alloys has been an object of investigation for long, as it is not possible for a single material to have different properties to meet the demand of today's industry. So, a composite system of a base material is required to provide the necessary mechanical properties and a protective surface layer which immune the substrate from hot corrosion, erosion and wear. Carbide based coatings have reported to be used for combating erosion and corrosion problems. In this article a brief review of the performance of carbide based coatings has been made to understand their hot corrosion and erosion behaviour.

Keywords: *Carbide coatings,Erosion, Hot corrosion,Thermal spray process*

1. INTRODUCTION

Advances in material development and cooling schemes will lead to increased operation temperature of gas turbine, boilers and industrial waste incinerators. The components working at elevated temperatures in contaminated environment and low grade fuels such as sulphur, sodium, vanadium and chlorine require special attention due to the phenomenon of hot corrosion and erosion which is the main cause of failure of these components [1].

Hot corrosion is an accelerated form of oxidation, which occurs when metals are heated in the temperature range of 700^0-900^0C in the presence of sulphate deposits formed as a result of the reaction between sodium chloride and sulphur compounds in the gas phase around the metals [2-3].

Hot corrosion was a serious problem in boiler tubes, internal combustion engines, fluidized bed combustion, industrial waste incinerators, power generation equipment, gas turbines in ships and aircraft [4-6].

In a case study done by Parkash et al it was observed that corrosion resulted in more than 50% of the failures in boiler tube in span of one year [7].

Erosion is the removal of material from a surface by high velocity fluids containing solid particles, or small drops of liquid or gas. According to ASTM standard G76-04, erosion is the progressive loss of original material from a solid surface due to mechanical interaction between that surface and a fluid, a multi-component fluid, or impinging liquid or solid particles. Erosion is a serious problem in many engineering systems, including steam and jet turbines, pipelines and valves used in slurry transportation of matter and fluidized bed combustion system [8].

It is not possible for a single material to have different properties to meet the demand of today's industry [9]. The desire for higher operating temperature, improved performance, extended component lives, and cleaner and more fuel-efficient power plant/processes places severe demands on the structural materials used to construct such a high-temperature plant. As a result, many components operating at high temperature within such plants are coated or surface treated [10]. Coatings provide a way of extending the limits of use of materials at the upper end of their performance capabilities, by allowing the mechanical properties of the substrate materials to be maintained while protecting them against wear or corrosion [11]. Coating can be deposited by thermal spraying (flame spraying, vacuum plasma spray, low pressure plasma spray, high velocity oxy fuel), by sputtering or by evaporation. However thermal spray coatings are generally preferred for industrial applications.

The use of protective coatings for the superheater/ re-heater components of boiler where the material severely suffers on fireside corrosion have also been reported [12]. A few earlier attempts have been made on the thermal sprayed protective coatings for fossil power plants though the thermal spray process is extensively used for gas turbine applications [13]. Sundararajan et al also advocate the need for applying thermal spray coatings on the boiler components [14-15].

Scrivani *et al* [20] conducted experiments on six thermal sprayed coatings where they found that HVOF sprayed chromium carbide metal cermet coatings showed much higher erosion resistance than 1018 steel. N. Espallargas *et al* [27] compared the performance of HVOF thermal spray coatings (Cr_3C_2–NiCr and WC–Ni) under the two erosion–corrosion conditions with different erosivity. It was observed that Cr_3C_2–NiCr coatings were superior with respect to corrosion resistance as compared to WC–Ni.

In this paper author has made the efforts to compile the literature as it is reported.

2. CARBIDE BASED COATINGS

Erosion-corrosion resistances of HVOF Cr_3C_2-NiCr coating was compared by Wang [16] with several other thermal sprayed coatings in an elevated temperature blast nozzle erosion tester. An attempt had been made to simulate erosive conditions with the refractory-waterwall interface and in the convection pass region in tubular heat exchangers of FBC boilers. HVOF sprayed Cr_3C_2-NiCr coating showed excellent E-C behavior as compared with 1018 steel, A213, T22 steel and other thermal sprayed coatings tested under both shallow and steep angles. High compactness, fine grain size structure, and a homogeneous distribution of the skeletal network of hard carbides within a ductile, corrosive-resistant metal binder results in high E-C resistance of HVOF Cr_3C_2-NiCr coating.

Erosion of HVOF Cr_3C_2/TiC-NiCrMo and Cr_3C_2-NiCr coatings, were studied by Wang et al [16] at the elevated temperature, it was observed that thickness loss for both coating increased with increase in impact angle and reached a maximum at 900.The erosion behavior of the HVOF Cr_3C_2/TiC-NiCrMo coating was found to be more sensitive to temperature than the HVOF Cr_3C_2-NiCr coating. The results indicated that the thickness loss decreases from room temperature to 300^0C, then increases from 300 to 750^0C for both coatings.

Stein *et al* [17] have investigated different carbide levels ranging from 0–100% in the pre-sprayed powder of FeCrAlY–Cr_3C_2 and NiCr–Cr_3C_2 cermet coatings in order to investigate the optimum ceramic content for the best erosion resistance and it was suggested that by decreasing the carbide content and overall hard phase content oxides and carbides, results in decrease in the erosion rate for 90^0 impacts. It was observed that the lower carbide levels in the coatings are caused by a combination of poor carbide spray efficiency and reduction/oxidation of the carbide particles in the HVOF jet, resulting in the formation of various oxides and metal rich carbides. Further Lih *et al* [18] and Wirojanupatump *et al* [19] reported that at elevated temperature, up to approximately 850^0C, CrC/NiCr is one of the best coating materials to combat wear owing to its oxidation-resistance.

Wirojanupatump *et al* [19] concluded in his study that characteristics of the powder feed stock have a strong influence on the coating microstructure and the wear resistance of the coatings depends critically upon the microstructure of the coating.

Scrivani *et al* [20] conducted experiments on six thermal sprayed coatings where they found that with the addition of chromium to a cobalt matrix in WC-Co cermets coatings, erosion-corrosion resistance increases. Further with the addition of hard phase particle (Cr_3C_2) in place of the WC, can result in enhancement of resistance of the material in terms of erosion performance. Wang *et al* [21] reported that the HVOF chromium carbide metal cermet coatings showed much higher erosion resistance than 1018 steel.

The wear resistance of various sliding components in automotive application can be decreased by thermal sprayed Cr_3C_2-NiCr coatings instead of hazardous hard chromium plating technology [22].

Murthy *et al* [23] deposited WC–10Co–4Cr and Cr_3C_2–20(NiCr) coatings by HVOF and pulsed DS processes, and compared low stress abrasion wear resistance of these coatings. The abrasion tests were

done using a three-body solid particle rubber wheel test rig using silica grits as the abrasive medium. The study shows that the HVOF coating resulted in higher residual compressive stresses; hence DS coating performs slightly better. Further it was reported that WC-based coating has higher wear resistance in comparison to Cr_3C_2-based coating.

T.S.Sidhu [24] used thermogravimetric technique to establish the kinetics of corrosion of HVOF sprayed Cr_3C_2–NiCr and Ni–20Cr coatings on a Ni-based superalloy (Superni 600) in a molten salt environment of Na_2SO_4–60%V_2O_5 at 900 °C under cyclic conditions. X-ray diffraction, scanning electron microscopy/energy-dispersive analysis and electron probe microanalysis techniques were used to analyse the corrosion products. The hot corrosion resistance of Cr_3C_2–NiCr coating might be due to the formation of protective phases like NiO, Cr_2O_3 and $NiCr_2O_4$, whereas Ni–20Cr coating showed the formation of alternative Ni- and Cr-rich layers. The Ni–20Cr wire coating has better hot corrosion resistance than the Cr_3C_2–NiCr powder coating.

J. Vicenzi [25] investigated three different high velocity oxygen fuel (HVOF) sprayed coatings (WC–12Co, Cr_3C_2–NiCr and WC–CrC–Ni) to improve the material performance under high temperature (~310^{0}C) erosion by means of an apparatus that simulated real conditions using fly ash from coal which causes erosive wear in equipments in thermoelectric power plants. The results showed that under these tests conditions the WC–12Co coating worn less followed by WC–CrC–Ni and Cr_3C_2–NiCr coatings, respectively than bare SAE 1020 steel.

M. Suarez *et al* [26] investigated the corrosion resistance of, as coated and post treated Cr_3C_2–NiCr coating of 450 ìm thickness, deposited by a vacuum plasma spray process (VPS) on a steel substrate. The post-heat treatment of coating was done by heating as-deposited coating in Ar at 400 °C and 800 °C, respectively. Electron probe micro analyzer (EPMA) with wavelength dispersive X-ray spectrometers (WDS) was used to characterize the coatings. Results showed that no significant changes were produced by heat treatment at 400°C whereas the coating annealed at 800°C has a better corrosion resistance than the as-deposited coating due to the microstructural changes that take place in the coating and the diffusion of Ni into Fe at the coating-substrate interface, which ensures the presence of a metallurgical bond.

N. Espallargas et al [27] studied the erosion corrosion behaviour of two types of HVOF thermal spray coatings (Cr_3C_2–NiCr and WC–Ni) obtained with different spray conditions and compared with conventional micro-cracked hard chromium coatings under two erosion–corrosion conditions with different erosivity. It was observed that Cr_3C_2–NiCr coatings were superior with respect to corrosion resistance compared to WC–Ni under both erosive conditions. Further, tungsten carbide coatings due to its high hardness showed better performance under the most erosive condition, while chromium carbide coatings were superior under less erosive conditions.

S. Matthews [28] investigated erosion behaviour of Cr_3C_2–NiCr thermal spray coatings at 700^{0}C and 800^{0}C with erodent impact velocities of 225–235 m/s to characterize the variation in oxides erosion response as a function of Cr_3C_2–NiCr coating microstructure. It was observed that the erosion behavior of the oxide scales formed on these coatings was influenced by the coating microstructure and erosion temperature. At 700^{0}C and 800^{0}C, the thinner Cr_2O_3 matrix oxide exhibited a ductile response on the blended coating whereas oxidised as-sprayed HVAF coating exhibited a brittle scale response at 700^{0}C after 48 h preoxidation due to the limited matrix ductility and at 800^{0}C the ductility of the matrix is increased and oxide prevented brittle spallation in the as-sprayed and heat treated coatings. The spallation of oxide carbide scale was more in magnitude at 700^{0}C than 800 ^{0} C. Larger carbide features were more prone to oxide spallation wheras smaller carbide features retained their oxide scales. Development in the carbide microstructure with extended heat treatment leads to variations in the erosion–corrosion response of Cr_3C_2–NiCr coatings.

R.C. Souza [29] compared the influence of Cr_3C_2–25NiCr and WC–10Ni coatings applied by HVOF process and hard chromium electroplating on the fatigue strength, abrasive wear and corrosion resistance of AISI 4340 steel. S–N curves were obtained in axial fatigue tests for base material, chromium plated and HVOF coated specimens. HVOF coated specimens showed higher axial fatigue resistance and better performance in wear weight loss in comparison to electroplated chromium. Further for Cr_3C_2–25NiCr HVOF coating, results indicate clearly the higher salt spray resistance and higher microhardness than for chromium electroplated.

Subhash Kamal[30] investigated detonation-gun thermal sprayed Cr_3C_2–NiCr cermet coatings deposited on two Ni-based superalloys, namely superni 75, superni 718 and one Fe-based superalloy superfer 800H. The cyclic hot-corrosion studies were conducted on uncoated as well as D-gun coated superalloys in the presence of mixture of 75 wt.% Na_2SO_4+25 wt.% K_2SO_4 film at 900 °C for 100 cycles. Thermogravimetric technique was used to establish the kinetics of hot corrosion of uncoated and coated superalloys. Characterization was done using X-ray diffraction, FE-SEM/EDAX and X-ray mapping techniques. Results showed that due to the formation of continuous and protective oxides of chromium, nickel and their spinel, Cr_3C_2–NiCr-coated superalloys showed better hot-corrosion resistance than the uncoated superalloys in the presence of 75 wt.% Na_2SO_4+ 25 wt.% K_2SO_4 in all cases.

Subhash Kamal[32] studied the cyclic oxidation behavior of detonation-gun-sprayed Cr_3C_2–NiCr coating on three different superalloys namely Superni 75, Superni 718 and Superfer 800H at 900^0C for 100 cycles in air under cyclic heating and cooling conditions. The thermogravimetric technique was used to analyse kinetics of oxidation of coated and bare superalloys. Further X-ray diffraction, FE-SEM / EDAX and X-ray mapping techniques were used to analyse the oxidation products of coated and bare superalloys. It was found that the Cr_3C_2–NiCr coatings on the alloys resulted in providing better oxidation resistance due to formation of Cr_2O_3 scale on the surface of the sample. In the subscale region, the phases revealed in EDAX analysis of the oxidised specimens were oxides of Cr and Ni, and their spinels and Ni in the splats remained unoxidised and provided protection on the superalloys against high temperature oxidation. It is shown that the Cr_3C_2–NiCr coatings on Ni- and Fe-based superalloy substrates are found to be very effective in decreasing the corrosion rate in the given molten salt environment at 900^0C. Weight gain data for Cr_3C_2–NiCr coated superalloys indicated less weight gain compared to bare super alloys, hence the hot corrosion protection of Cr_3C_2–NiCr coated superalloy is of the order Superfer 800H > Superni 75 > Superni 718.

S. Matthews [31] investigated relative erosion rate of Cr_3C_2-NiCr coatings at 700^0C and 800^0C under impact velocity of 225-235m/s, under simulated conditions of turbine environment. HVAF and HVOF sprayed coatings produced comparable erosion rates in both as sprayed and heat treated coatings, which can be related to the complex transition in influence of the brittle matrix phase in the as-sprayed state and impact of the three dimensional carbide network following in heat treated samples. However the ductility of the NiCr matrix phase significantly increased for both coatings at 800^0C, but the erosion rate of heat treated samples increased due to the increasing constraint imposed upon the matrix by the developing carbide microstructure.

S. Matthews [33] investigated mechanism of erosion as a function of coating composition and microstructure variation of High Velocity Air Fuel (HVAF) and High Velocity Oxygen Fuel (HVOF) thermal spray Cr_3C_2–25% NiCr coatings at an impact velocity of 150 m/s by 20–25 ìm alumina grit. It was observed that the HVOF coatings underwent significant in-flight dissolution of the carbide phase whereas the erosion response of the supersaturated NiCr matrix was characterised by brittle cracking and fracture. Further it was observed that the HVAF coatings retained high carbide content with minimal phase dissolution however, the rapid solidification of the matrix material made the coating prone to brittle interphase cracking during impact. It was also observed that spalt based erosion mechanisms played a significant role, especially in HVOF coatings because HVOF spray parameters promote carbide dissolution resulted in reduced inter-splat adhesion on a scale comparable with the erosion impact damage which resulted in significant localised mass loss through splat based erosion mechanism on a single impact scale. Comparison of the steady state eroded surfaces of both coatings suggested that the HVAF coating was more erosion resistant.

S. Matthews [34] investigated high velocity erosion response of High Velocity Air Fuel (HVAF) and High Velocity Oxygen Fuel (HVOF) thermal spray Cr_3C_2–25% NiCr coatings which were heat treated for 30 days at 900^0C so as to generate a range of coating microstructure up to steady state. The erosion tests were performed at an impact velocity of 150 m/s by 20–25 ìm alumina grit. Heat treatment of the samples increased the ductility of NiCr matrix phase which enable ductile deformation rather than brittle interphase cracking. Moreover inter spalt sintering which occurred during heat treatment of samples increases the inter spalt cohesive strength resulting in mass loss occurrence due to standard erosion mechanism than typically observed spalt based erosion observed in thermal spray coatings. It was observed that these developments improved the quantified

erosion resistance of both coating systems relative to the as-sprayed conditions.

3. CONCLUSION

Erosion and hot corrosion is a serious problem in energy conservation processes. Carbide Coatings were found to be very effective in dealing with the erosion and corrosion problem in the components working at elevated temperatures in contaminated environment and low grade fuels such as sulphur, sodium, vanadium and chlorine.

Carbide coatings can be successfully deposited over the substrate material by HVOF, Detonation gun Spray and Plasma Spray processes.

It is learnt from the literature that Cr_3C_2–NiCr had in-flight dissolution of the carbide phase which results in combating with erosion problem and due to formation of Cr_3C_2 scale on the surface of the base metal it provides oxidation resistance.

Although different authors have made the efforts to understand the mechanism of hot corrosion using carbide coatings but still long term exposure of the failure mechanism are essential for estimating the protection capabilities of these coatings.

REFERENCES

[1] Bala N., Singh H., Parkash S., (2007), "An overview of Characterization and high temperature behaviour of Thermal spray NiCr coatings," International Jouranal of material science, Vol.2, pp.201-218.

[2] Hancock, P., (1987), "Vanadic and Chloride Attack of Superalloys," Mater. Sci. Technol., Vol. 3, pp. 536-544.

[3] Eliaz, N., Shemesh, G. and Latanision, R.M., (2002), "Hot Corrosion in Gas Turbine Components," Eng. Fail. Anal., Vol. 9, pp. 31-43.

[4] Rapp, R. A., (2002), "Hot Corrosion of Materials: A Fluxing Mechanism," Corros. Sci, Vol. 44, No. 2, pp. 209-221.

[5] Rapp, R. A. and Zhang, Y. S., (1994), "Hot Corrosion of Materials: Fundamental Studies," JOM, Vol. 46, No. 12, pp. 47-55.

[6] Pettit, F. S. and Giggins, C. S., (1987), "Hot Corrosion, Ch. 12," in 'Superalloys II,' Eds. Sims, C. T., Stollof, N. S. and Hagel, W. C., Pub. Wiley Pub., N. Y.

[7] Singh, B., Studies on the role of coatings in improving resistanceto hot corrosion and degradation, Ph D thesis, Metallurgical and Material Eng. Dept., IIT Roorkee, 2003.

[8] Kosel, T. H., (1992) "Friction, Lubrication and Wear Technology," ASM Handbook, Vol. 18, pp. 199-213.

[9] Sidhu, B.S., Puri, D. and Prakash, S., (2004), "Characterisations of Plasma Sprayed and Laser Remelted NiCrAlY Bond Coats and Ni3Al Coatings on Boiler Tube Steels," Mater. Sci. Eng. A-Struct., Vol. 368, No. 1-2, pp. 149-158.

[10] Nicholls, J.R., (2000), "Designing Oxidation-Resistant Coatings," JOM, pp.28-35.

[11] Sidky, P.S. and Hocking, M.G., (1999), "Review of Inorganic Coatings and Coating Processes For Reducing Wear and Corrosion," Brit. Corros. J., Vol. 34, No. 3, pp. 171-183.

[12] Porcayo-Calderon, J., Gonzalez-Rodriguez, J.G. and Martinez, L., (1998), "Protection of Carbon Steel against Hot Corrosion using Thermal Spray Si- and Cr-Base Coatings," J. Mater. Eng. Perform., Vol. 7, pp. 79-87.

[13] Taylor, M.P. and Evans, H. E., (2001), "The Influence of Bond Coat Surface Roughness and Structure on the Oxidation of a Thermal Barrier Coating System," Mater. Sci. Forum, Vol. 369-372, pp. 711-717.

[14] Sundararajan, T., Kuroda, S., Itagaki, T. and Abe F., (2003A), "Steam Oxidation Resistance of Ni-Cr Thermal Spray Coatings on 9Cr-1Mo Steel. Part 1: 80Ni-20Cr," ISIJ Int., Vol. 43, No.1, pp. 95-103.

[15] Sundararajan, T., Kuroda, S., Itagaki, T. and Abe, F., (2003B), "Steam Oxidation Resistance of HVOF Thermal Sprayed Ni-Cr Coatings," Thermal Spray 2003: Advancing the Science & Applying the Technology, (Ed.) C, Moreau and B. Marpie, pp. 495-502.

[16] Wang B., (1996), "Erosion-corrosion of thermal sprayed coatings in FBC boilers," Wear, Vol. 199, pp. 24-32.

[17] Stein K. J., Schorr B. S. and Marder A R, (1999), "Erosion of Thermally Sprays MCr-Cr3C2 cermet coatings," Wear, Vol. 224, pp 153-159.

[18] Lih, W.C., Yang, S.H., Su, C.Y., Huang, S.C., Hsu I.C. and Leu, M.S., (2000), "Effects of process parameters on molten particle speed and surface temperature and the properties of HVOF CrC/NiCr coatings" Surf. Coat. Technol., Vol. 133-134, pp. 54-60.

[19] Wirojanupatump, S., Shipway, P.H. and McCartney, D.G., (2001), "The influence of HVOF powder feedstock characteristics on the abrasive wear behaviour of CrxCy–NiCr coatings," Wear, Vol. 249, pp. 829–837.

[20] Scrivani, A., Ianelli, S., Rossi, A., Groppetti, R., Casadei, F. and Rizzi, G., (2001), "A contribution to the surface analysis and characterisation of HVOF coatings for petrochemical application," Wear, Vol. 250, pp. 107-113.

[21] Wang, C.J. and Lin, J.S. (2002), "The oxidation of MAR M247 superalloy with Na2SO4 coating," Materials Chemistry and Physics, Vol.76, pp. 123-129.

[22] Picas, J.A., Forn, A., Igartua, A. and Mendoza, G., (2003), "Mechanical and tribological properties of high velocity oxy-fuel thermal sprayed nanocrystalline CrC-NiCr coatings," Surf. Coat. Technol., Vol.174 –175, pp. 1095–1100.

[23] Murthy, J.K.N. and Venkataraman, B., (2006), "Abrasive wear behaviour of WC–CoCr and Cr3C2–20(NiCr) deposited by HVOF and detonation spray processes," Surf. Coat. Technol., Vol. 200, pp. 2642– 2652.

[24] Sidhu, T.S., Prakash, S. and Agrawal, R.D., (2006D), "Hot corrosion studies of HVOF sprayed Cr3C2–NiCr and Ni–20Cr coatings on nickel-based superalloy at 900 °C", Surf. Coat. Technol., Vol. 201, No. 18-19, pp.792-800.

[25] Vicenzi J., Villanova D.L., Lima M.D., Takimi A.S., Marques C.M., Bergmann C.P.,(2006), "HVOF - coatings against high temperature erosion (300 °C) by coal fly ash in thermoelectric power plant," Materials & Design, Volume 27, Issue 3, pp236-242.

[26] Suarez M., Bellayer S. , Traisnel M. , Gonzalez W., Chicot D. , Lesage J., Puchi-Cabrera E.S., Staia M.H. , (2008), "Corrosion behavior of Cr3C2–NiCr vacuum plasma sprayed coatings," Surface & Coatings Technology, Vol. 202, Issue 18, pp.4566–4571.

[27] Espallargas N., Berget J., Guilemany J.M., Benedetti A.V., Suegama P.H., (2008), "Cr3C2–NiCr and WC–Ni thermal spray coatings as alternatives to hardchromium for erosion–corrosion resistance," Surface and Coatings Technology, Volume 202, Issue 8, 15 January 2008, pp. 1405-1417.

[28] Matthews S., B James., Hyland M., (2008), "Erosion of oxide scales formed on Cr3C2–NiCr thermal spray coatings," Corrosion Science, Volume 50, Issue 11, pp. 3087-3094.

[29] Souza R.C., Voorwald H.J.C., Cioffi M.O.H.,(2008), "Fatigue strength of HVOF sprayed Cr3C2–25NiCr and WC-10Ni on AISI 4340 steel," Surface and Coatings Technology, Volume 203, Issues 3-4, , pp. 191-198.

[30] Subhash Kamal, Jayaganthan R., Satya Prakash, (2009), "Evaluation of cyclic hot corrosion behaviour of detonation gun sprayed Cr3C2–25%NiCr coatings on nickel- and iron-based superalloys," Surface and Coatings Technology, Volume 203, Issue 8, , Pages 1004-1013.

[31] Matthews S., James B., Hyland M., (2009), "High temperature erosion of Cr3C2-NiCr thermal spray coatings — The role of phase microstructure," Surface and Coatings Technology, Volume 203, Issue 9, pp.1144-1153.

[32] Subhash Kamal, Jayaganthan R. , Parkash S., (2009), "High temperature oxidation studies of detonation-gun-sprayed Cr3C2–NiCr coating on Fe- and Ni-based superalloys in air under cyclic condition at 900 0C," Journal of Alloys and Compounds Vol. 72, Issues 1-2, , pp. 378-389.

[33] Matthews S., James B., Hyland M., (2009), "The role of microstructure in the mechanism of high velocity erosion of Cr3C2–NiCr thermal spray coatings: Part 1 — As-sprayed coatings," Surface and Coatings Technology, Volume 203, Issue 8, pp. 1086-1093.

[34] Matthews S. James, B., Hyland M., (2009), "The role of microstructure in the mechanism of high velocity erosion of Cr3C2–NiCrthermal spray coatings: Part 2 — Heat treated coatings," Surface and Coatings Technology, Volume 203, Issue 8, pp.1094-1100.

Degradation of Pulverized Coal Burner Nozzles: A Review

Pardeep K. Jindal[1] and Buta S. Sidhu[2]

[1]Department of Mechanical Engineering, Guru Gobind Singh College of Engineering and Technology, Talwandi Sabo, Punjab - 151 302, India

[2]Department of Mechanical Engineering, Yadavindra College of Engineering, Bathinda Punjabi University Guru Kashi Campus, Talwandi Sabo, Punjab -151 302, India

E-mail:- pjindal@rediffmail.com

Abstract

Erosion of metal parts is a common problem in industry, such as in coal fired turbines, fluidized beds and boiler tubes. The Pulverized Coal Burner Nozzles (PCBNs) are subjected to highly deleterious conditions due to erosion by solid fuel (pulverized coal) in air passing through the tip and due to the extreme temperatures encountered in the burning or combustion zone of the furnace. The present review paper deals with some of the case studies made in various thermal power plants. The PCBNs are found to degrade rapidly because of high temperature in the furnace and continued exposure to high velocity solid fuel. The fuel roping has also been observed to be the cause of rapid degradation of the nozzles. To improve the material degradation resistance against high temperature erosion problem, possibility of design modification and application of new materials / coatings, resistant to erosion can be explored. Hardfacing of the nozzle surface may also be one of the remedy to improve the material degradation resistance.

Keywords: *Erosion, Erosion-corrosion, Pulverized coal burner nozzle*

1. INTRODUCTION

Solid particle (impingement) erosion (SPE) is defined as a progressive loss of original material from a solid surface due to continued exposure to impacts by solid particles. This material damage is a serious problem in several fields of technology, especially in the aerospace engineering and process industries [8]. Over the past half century, many models have been proposed to evaluate the rate of material removal under various eroding conditions. In the electric power industry, solid particle erosion costing an estimated US$150 million a year in kind of lost efficiency, forced outages and repair costs [12].

High temperature erosion (HTE) is one of the main failure modes of coal-fired power plant boilers all over the world and has attracted worldwide attention. Because of the low quality, high ash proportion and high sulfur content of the coals generally used, the HTE of the circulating fluidized bed (CFB) boiler appears even more serious [7].

Erosive, high temperature wear of heat transfer pipes and other structural materials in coal boilers are recognized as being the main cause of downtime at power generating plants, accounting for 50% to 75% of the total arrest time. Maintenance costs for replacing broken pipes in such installations are also very high, and can be estimated at up to 54% of the total production costs [4].

The coal used in Indian power stations has large amounts of ash (about 50%) containing abrasive mineral species, such as hard quartz (up to 15%), which increases the erosion propensity of coal [5]. Further, Indian coal proved to be exceptional in that it had significant amounts of alkali feldspars, (K, Na)$AlSi_3O_8$ and a garnet, minerals usually thought of as trace components of a coal. The garnets in the Indian coals were found to follow the general formula (Mg, Fe_2+)$3Al_2Si_3O_{12}$ [15]. The ash and flue gases analysis of Guru Nanak Dev Thermal Plant, Bathinda (Punjab) as reported by [9], confirms the presence of these constituents in Indian coal.

Metals and alloys still constitute the most-important group among engineering materials and demand for metallic materials with higher strength and special properties is on the increase with the advancement of technology. However, a serious drawback of metallic material (and of other materials too) is the deterioration in properties originating from the interaction with the

environments. Often this leads to a premature failure of metallic components with the allied hazards of plant shutdown and loss of economy, environmental pollution and risk to human lives [10]. It is important to understand the nature of all types of environmental degradation of metals and alloys as vividly as possible, so that preventive measures against metal loss and failures can economically be devised to ensure safety and reliability in the use of metallic components [10].

High temperature erosion-corrosion is a major cause of wear in both fluidized bed combustors and gas turbines and much effort has been put into understanding the phenomena and reducing wear rates. A number of different erosion-corrosion mechanisms have been proposed over the years to describe the different wear regimes [14].

2. PULVERIZED COAL FIRING SYSTEM

In high pressure, coal fired boilers, which are generally used in power generation systems, the pulverized coal is fed along with the primary air. The pulverized coal with primary air enters the furnace of the boiler from the four corners, at different heights (Figure1). This Coal-air mixture is fired by the Pulverized Coal Burner Nozzles (PCBN).

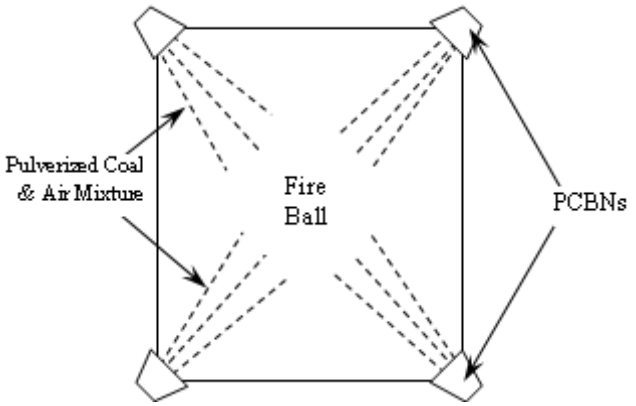

Fig.1 Plan of furnace of boiler, showing arrangement of PCBNs

The pulverized coal burner nozzles are subjected to highly deleterious conditions due to erosion by solid fuel (pulverized coal), in air passing through the tip and due to the extreme temperatures encountered in the burning or combustion zone of the furnace. In the construction of nozzle tips, baffle or splitter plates are disposed within the tip to provide directional force to the solid fuel and air mixture, particularly upon tilting of nozzle. These plates and the supporting box like structure are rapidly eroded by the solid fuel mixture projected through the tips under pressure. In addition, these elements of the tip as well as the outer box-like portion of the tip, through which air is passed under pressure, is subject to the heat of the flame as the nozzle is positioned in the burning or combustion zone. The latter described elements warp and crack from the heat encountered even in normal operation of the furnace. Although the useful life of recently used burner nozzle tips made of stainless steel is considerably longer than the formerly used tips, the outer portions of the tips are still often destroyed by cracking, burning and melting due to the heat affected zones adjacent the welds [1].

With a viewpoint of further analysis and to understand such problems, the survey was carried out in some of the thermal power plants. Two of the power plants are in district Bathinda (G.N.D.T.P., Bathinda and G.H.T.P., Lehra Mohabbat), one is at Ropar (G.G.S.S.T.P., Ropar) and another thermal power plant selected for survey is at Panipat (T.D.L.T.P., Panipat).

During the survey of these Thermal Power Plants of Northern Region of India, the damaged nozzles found in very bad condition, due to high temperature erosion problem, which can easily be inferred from the macrographs of nozzles presented in Figure 2.

Eroded burner nozzle tips (PCBNs) causes poor fuel distribution exiting the nozzle tip or outlet, which results in flame variations. These flame variations range from sub-stoichiometric fuel rich zones, where the reducing atmosphere contributes to slagging and water wall erosion, to high oxygen zones, which potentially create high thermal generation oxides of nitrogen. Unit control is difficult with these wide variations at each burner of a multiple burner unit [2]. Poor fuel distribution results in reduced combustion efficiencies. As per the survey, these nozzles are generally replaced every year. It leads to a direct material wastage cost, also the eroded nozzle causes poor fuel distribution, which in turn results in reduced combustion efficiencies.

Figure 3 shows the PCBN fitted inside the boiler at Guru Nanak Dev Thermal Plant, Bathinda. The severe erosion problem may sometimes erode the PCBNs completely and erosion may further affect the water wall. Once the water wall is eroded, it may lead to the

breakdown, which results in huge loss of economy. It further results in reduced lifetime of certain components and high maintenance costs.

Looking at the condition of the eroded nozzle in Figure 2(b), the extent of erosion is more on one side of the nozzle. This problem seems to be due to the fuel roping. Fuel roping is believed to be caused by centrifugal flow patterns established by elbows and pipe bends. Fuel roping may be one of the main reason for enhancing the erosion rate and also it affects the uniform distribution of fuel, exiting the nozzle tip. The condition of damaged nozzles at T.D.L.T.P., Panipat (Figure 2e) further supports this opinion, as the damaged nozzles were not in such a bad condition as there were in other plants. At T.D.L.T.P., Panipat, some measures to break fuel ropes were taken.

Fluidized bed combustor (FBC) boilers are of continuously increasing interest worldwide, as an attractive alternative to conventional stoker-type boilers for the generation of electricity, because of attractive operating efficiency, fuel flexibility and clean exhaust gases. The metal wastage of heat exchanger tubes in FBCs by erosion-corrosion (E-C) mechanisms has become a problem of significant importance [13].

The erosion rate of a material is dependent on several factors, including target material properties and erosion test conditions of angle, velocity, temperature, particle flux and erodent. Velocity is a critical test variable in erosion and can easily overshadow changes in other variables, such as target material, impact angle etc.

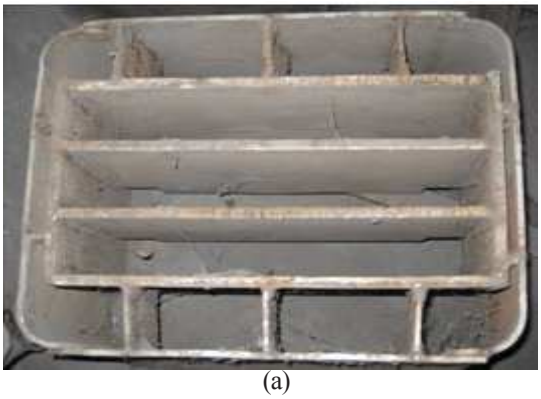

(a)

(b)

(c)

(d)

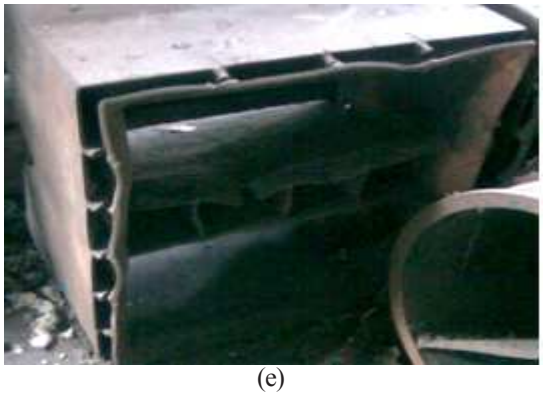

(e)

Fig. 2 Macrographs of fresh & damaged PCBNs collected from various plants - (a) Fresh PCBN of GNDTP, Bti, (b) Damaged PCBN of GNDTP, Bti, (c) Damaged PCBN of GHTP, Lehra Mohabbat, (d) Damaged PCBN of GGSSTP, Ropar, (e) Damaged PCBN of TDLTP, Panipat.

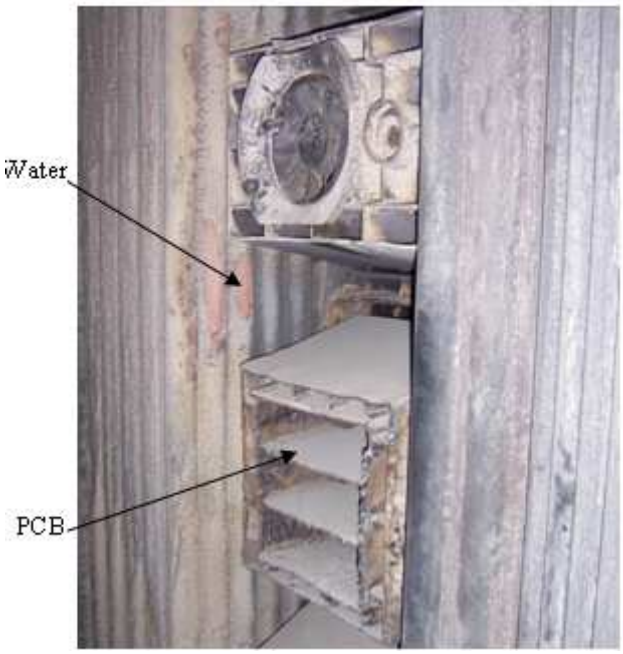

Fig. 3 Inside view of PCBN in furnace at GNDTP, Bti

Erosion rate has been shown to follow an empirical power law relationship with velocity:

$$\text{Erosion Rate} = kV^n$$

Where, 'V' is velocity, 'k' is a constant and 'n' has values between 2 and 3.5 for metallic materials. Brittle materials tend to have a larger 'n' range, from 2 to 6.5 [6]. A lot of research work is being carried out in the field of material degradation problem of boiler tubes due to erosion and corrosion. The velocity of pulverized coal and air mixture is very high at the points from where it enters the boiler furnace, which results in high rate of erosion of PCBN.

3. REMEDIAL MEASURES

The different case studies show that the material degradation problem of PCBN is a very severe problem. There could be different remedial measures to improve the material degradation resistance of PCBNs. Application of new materials or coatings on the surface of the PCBN may be one of the solutions. The high temperature erosion resistant alloy materials may be chosen for coating. Hardfacing [3] may be one of the alternative for depositing high temperature erosion resistant material on the surface of PCBN. Some design modifications to capture the problem of fuel roping, as at T.D.L.T.P., Panipat, can also be reviewed upto some extent.

REFERENCES

[1] Bauer T.E. *et.al.* (1974), United States Patent No. 3,823,875.

[2] Bowen P. (2000), United States Patent No. 6,105,516.

[3] Gregory E.N. (1978), "Hardfacing", Wear, Vol. 11, pp. 129-134.

[4] Hidalgo V.H. *et.al.* (2001), "High temperature erosion wear of flame and plasma-sprayed nickel–chromium coatings under simulated coal-fired boiler atmospheres", Wear, Vol. 247, pp. 214-222.

[5] Krishnamoorthy P.R. and Seetharamu S. (1989), "The wear life of pipe bends and other components under pulverized coal erosion" LIPREX-89, Hyderabad, India.

[6] Lindsley B.A. and Marder A.R. (1999), "The effect of velocity on the solid particle erosion rate of alloys", Wear, Vol. 225-229, pp. 510-516.

[7] Liu S.G. *et.al.* (2007), "High temperature erosion properties of arc-sprayed coatings using various cored wires containing Ti–Al intermetallics", Wear, Vol. 262, pp. 555-561.

[8] Pekko P. (2000), "Tetrahedral amorphous carbon deposited with the pulsed plasma arc-discharge method as a protective coating against solid impingement erosion", Diamond and Related Materials, Vol. 9, pp. 1524-1528.

[9] Sidhu B.S. (2003), "Studies on the role of coatings in improving resistance to hot corrosion and degradation", Ph.D. thesis.

[10] Sidhu B.S. and Prakash S. (2006), "Erosion-corrosion of plasma as sprayed and laser remelted St-6 in a coal fired boiler", Wear, Vol. 260, pp. 1035-1044.

[11] Sidhu B.S. and Prakash S. (2007), "Analytical Studies on the Behavior of Ni- and Co-Base Shrouded Plasma Spray Coatings at Elevated Temperature in Air", Oxid. Met., Vol. 67, pp. 279-298.

[12] Stein K.J. *et.al.* (1999), "Erosion of thermal spray MCr–Cr C cermet coatings", Wear, Vol. 224, pp. 153-159.

[13] Wang B.Q. (1996), "Erosion-corrosion of thermal sprayed coatings in FBC boilers", Wear, Vol. 199, pp. 24-32.

[14] Wellman R.G. and Nicholls J.R. (2004), "High Temp Erosion-Oxidation Mechanisms, Maps and Models", Wear, Vol. 256, Issues 9-10, pp. 907-917.

[15] Wells J.J. *et.al.* (2005), "The nature of mineral matter in a coal and the effects on erosive and abrasive behavior", Fuel Processing Technology, Vol.86, pp. 535-550.

Remedies Measure Against Hot Corrosion of Boiler Tube Steels: A Review

Hazoor S. Sidhu[1] Gursham Lal[2] and Buta S. Sidhu[1]

[1]Department of Mechanical Engineering,Yadavindra College of Engineering, Punjabi University Guru Kashi Campus, Talwandi Sabo, Bathinda, Punjab -151 001, India

[2]Department of Mechanical Engineering, Baba Hira Singh Bhattal Institute of Engineering and Technology Lehragaga, Punjab - 148 031, India

E-mail:- hazoors@yahoo.com

Abstract

Power plants are one of the major industries suffering from severe corrosion problems resulting in the substantial losses. Materials degradation due to corrosion, erosion and wear is the major problem in power generation equipment, gas turbine, fluidized bed combustion, industrial waste incinerators etc. Some super alloys have been developed, but they are unable to have different properties to meet the demand of today's industry. Extensive research is going on throughout the word in this exciting field. There are several technique and alloys available commercially. Selection of right method and alloy for a particular application is vital to get the desired service life. This paper reviews the various most commonly used methods and alloys to control the degradation of materials.

Keywords: *Corrosion resistant material, Fuel additive, Hot corrosion, Protective coatins*

1. CORROSION

Hot corrosion is an accelerated form of oxidation, which occurs when metals are heated in temperature range 700-9000C in the presence of sulphate deposits formed as a result of reaction between sodium chloride and sulphur compounds in gas phase around the metals. Hot corrosion observed in boilers, diesel engine, mufflers of I.C. engines and gas turbines. The hot corrosion process is markedly dependent upon parameters such as alloy composition, gas composition, deposit composition and temperature.

2. PROBLEM OF HOT CORROSION IN POWER PLANTS

Power plants are one of the major industries suffering from severe corrosion problems resulting in the substantial losses. For instance steam temperature of boilers is limited by corrosion and creep resistance of boiler component, which effects the thermal efficiency of boilers. Consequently thermal efficiency decreases, hence electricity production is reduced [1]. These facts emphasis the need to develop more and more corrosion resistant materials for such applications. Although corrosion problems can not be completely remedied, it is estimated that corrosion related costs can be reduced by more than 30% with development and use of better corrosion control technologies [2].

Except for most gaseous fuels, combustion of fossil fuels produces solid, liquid and gaseous compounds that can be corrosive to structural components and heat transfer surfaces. In addition deposits of solid and liquid residues in gas passage can alter the heat transfer characteristics of system with potentially severe effect on system efficiency and tube wall temp. The composition of coal ash varies widely, but is composed chiefly of Si, Al, Iron and calcium compounds with smaller amounts of Mg, Ti, Na and K compounds [3].

Coal ash corrosion starts with deposition of fly ash on surfaces that operate predominantly at temperature from 54^0 to 73^0C. these deposits may be loose and powdery or slag type masses that are more adherent. Over an extended period of time, volatile alkali and sulphur compounds condense on fly ash and react with it to form complex alkali sulphides such as $KAl(SO_4)_2$ and $Na_3Fe(SO_4)_3$ at boundary between metal and deposit. The reaction that produce alkali sulphates are believed to be depend in part on catalytic oxidation of SO_2 toSO_3 in the outer layer of fly ash deposit [3].

3. MAJOR CAUSES OF BOILER TUBE FAILURE

The failure of boiler tubes is one of the major causes of power plant outages. A substantial amount is lost due to these failures. On an average minimum shut down of 24 hours is required to attend to a tube leakage in boiler. The major reasons of boiler tube leakage are Caustic gauging, Hydrogen embrittlement, Overheating due to high internal oxides, Localized corrosion under oxides, Loss of efficiency due to heavy build up of oxides, Pitting attack [4].

The strength of boiler tube depends upon stress level as well as on the temperature of exposure in the creep range. An increase in either can reduce time to rupture. The failure had resulted due to carryover of boiler feed water into super heater section of boiler due to upstream problem such as malfunctioning of separators in steam drum. The tri sodium phosphate from carryover water had deposited at bends of suspension coil of super heater section resulting in chokage. The ultimate failure had taken place due to long term overheating [5].

The accelerated corrosion that may be experienced by super heater tubes is typically on the leading surface of first row of tubes facing the combustion gas, the second and third rows may also suffer accelerated attack, but it is not usually so severe. The corrosion morphology consists of pits, fairly large (5-10mm across) with relatively smooth bottoms. After a while, the pits will link up and the corrosion will begin to look like a rough general attack [6-7].

4. REMEDIES MEASURE AGAINST HOT CORROSION

4.1 Fuel Selection

The use of ash less or sulphur free fuel is perhaps the most direct means of minimizing fire side corrosion. Factors considered in selecting coals for thermal power plants are firing qualities of coal are of prime importance and influence the design of combustion chamber, type of combustion equipment and lay out of heat transfer parts of thermal power plants. Coals with low volatile content have slower burning characteristics but generate high fuel bed temperature. Coal with high volatile content on the other hand, have a high grate of burning and hence require a large combustion chamber for combustion of volatiles. Such coals are very useful for thermal power plants to meet sudden increase of load. They quickly liberate their combustible volatile gases that rapidly burn off to increase furnace temperature to boost up steam productivity. Coal can be desulphurized prior to combustion by the use of bacteria. The micro organisms oxidize both inorganic and organic sulphur of coal. The process has been developed at INEL, USA) and 95% of inorganic sulphur and less than half of organic sulphur can be removed by this process [8].

Sulphur capture in combustion process to be more difficult because calcium sulphate, the reaction product of SO_2 and additive lime, is unstable at high temperature of pulverized coal combustion. It is possible to retain sulphur by the application of fluidized combustion in which coal burns at much reduced combustion temperature. Fluidized bed combustion is however primarily intended for the utilization low grade, low volatile coals in smaller capacity units, which leaves the task of sulphur capture for majority of coal fired boilers to flue gas desulphurization [9].

4.2 Design Aspects

Avoid hot spots (improve temperature distribution), adjustment of firing rates, amount of excess air, air temp., amount of re circulated flue gas, tube size and spacing, furnace configuration, size and direction of flue gas passages, avoid excessive deposition of ash and slag by the use of soot blowers.

By controlling the various process parameters (air/ fuel ratio, temperature, pressure etc.) of boiler and gas turbines were also useful to some extent in combating oil ash corrosion. The low excess of combustion air can control hot temperature of boilers to some extent. As a matter of fact excess of oxygen promotes formation of SO_3 and V_2O_5 (melting point 675^0C) instead of lower oxides V_2O_3-V_2O_4 (melting point 2000^0C). The industrial practice generally does not allow operating with low excess of combustion air, consequently the use of additives turns out to be the only effective means to prevent corrosion at elevated temperatures [10].

4.3 Chemical Additive

The use of fuel additives such as‘ lime stone, dolomite, alumina etc. minimize corrosion. These are injected into

furnace gases or blow onto heat transfer surfaces through soot blowers. Vanadium corrosion can be reduced by keeping super heater temperature below 600^0C , by dosing alkaline additives to fuel. Alkaline additive $MgCl_2$ added in 0.6 to 0.8 kg per ton of fuel [11].

The use of MgO as a fuel additive to combat Vanadic corrosion is widely accepted in practice for boilers and turbines operating on residual or low grade fuels. Tin oxide is inherent to chemical reaction with wide range of vandate and vandate-sulphate melts at 700^0C and 800^0C. SnO_2 is very useful against vandate and vandate-sulphate hot corrosion at moderate temp.(800^0C). CaO and $CaSO_4$ addition is also useful at higher temperature 800^0C and 900^0C [10].

Wet pretreatment of coal and use of mineral additivesare the two control methods. In wet pretreatment sample of coal were treated with aluminium solutions to adjust the levels of Na, Al and copper. With wet method aluminium reduces the sodium level and the stickness of sodium silicates from coal was also reduced by Al. With use of mineral additives, sodium could be captured by clay minerals, particularly Kaolin. For coal based power plant boilers, 10-20 kaolin making 2-3 wt% of the feed was estimated to effectively reduce ash problems [12].

The introduction of low NO_x burners to coal fired power stations can change the nature of ash deposition with in boilers. Lower peak flame temperature and delayed mixing of combustion air have reduced the rate of mineral transformations. The resulting ash is finer and less sticky than ash produced with conventional burners, reducing the proportion of soluble bottom ash and increasing the load on electrostatic precipitators [13].

4.4 Periodic Cleaning of Coal or Coal Derived Fuel

For high pressure boilers a very high standard quality of water treatment is expected to un keep the chemical parameters. Despite of all the care taken, the magnetite layer grows over years and deposits start accumulating. These deposits restrain heat transfer, resulting in overheating and subsequent failure of tubes. Tube cleanliness is important due to high operating temp. reduce the temp. elevation that can be tolerated without exceeding the metal creep limits. High temp. are conducive to chemical corrosion which can proceed beneath internal deposits where soluble boiler water constituents can concentrate. In NTPC 1998 during post operational boiler cleaning 3 Mt of iron and copper deposits were removed. The cleaning was carried out successfully and overall efficiency of boiler has improved from 86.34% to 86.995%. [14].

4.5 Selection of Better Corrosion Resistance Materials of Construction

A large number of Fe, Ni and Co based alloys exist today especially designed for good resistance to oxidation, sulphidation or corrosion by ash/salt deposits. Selection of high chromium contents alloy, austenitic steels rather than low alloy steels is also suitable. Low Cr ferritic steels are a good choice provided the higher limit of bed temperature is restricted to about 775K. Austenitic steels such as 304, 316, 321, and 347 demonstrate good performance upto 925K with or without sorbent (lime stone) addition. For bed temperature as high as 1175K, high strength Ni based alloys appears to be suitable, provided bed is operated without lime stone addition or dolomite. This is because with lime stone addition, Ni based alloys can suffer from intergrannular grain boundary corrosion. For metal temperature exceeding 925K in beds of lime stone, it is therefore necessary to use an iron base austenitic steels, particularly type 347 upto 1075K, above this temperature it is necessary to use allow strength super alloy such as GE 2541 as a cladding material to protect a high strength alloy base [15].

The oxidation rates depend heavily upon chromium content, the 12% Cr steels that have Cr content near to max specified exihibiting very much better corrosion resistance than steels with 9% Cr Thin walled components of 95 Cr. Steels may offer no advantage over the 125 Cr steels in terms of service life despite the inherently higher stress ruptue strength of 9% Cr steels [16]. Iron-base, Ni-base and Co-base superalloys show excellent corrosion reistance in hot ash corrosion environment [10]. HR-160, 556 230, 242 superalloys are considered for power generation, gas turbines gasifiers [17].

No alloy is immune to hot corrosion attack indefinitely although there are some alloy compositions that require along initiation time at which hot corrosion moves from initiation stage to propagation stage. Superalloys have been developed for high temperature applications. However these alloys are not always able to meet both high temperature strength and high temperature corrosion

resistance simultaneously, so the need to be protected from corrosion. The high temp. protecting system must meet several criteria, provide adequate environment resistance, be chemically and mechanically compatible with substrate, be practically applicable, reliable and economically viable [18].

4.6 Protective Coatings

The different coating techniques are applied to protect the critical surface areas from corrosive gases including co-extrusion, chromising, weld overlay and thermal spray coatings. The coatings provide the way of extending the limits of use of materials at upper end of their performance capabilities by allowing mechanical properties of substrate materials to be maintained while protecting them against corrosion. Thermal spraying, high velocity Oxy fuel Coating, Laser surface alloying, Thermal barrier coating, Ion beam assisted depositing, Physical vapor deposition and chemical vapor deposition are the methods of applying coatings on the substrates [19].

The porosity content is the lowest in HVOF sprayed sample. The high velocity processes give very low levels of porosity due to high velocity at which particles impinge upon substrate. Moreover due to high velocity of particles in HVOF, interaction time of particles with atmosphere is very less which could result in lower oxide content of coatings. The parameters of spraying for high velocity processes should be optimized to produce coatings with low levels of porosity along with low levels of oxides in sprayed coating [20].

Ni_3Al coating were obtained on boiler tube steels through a plasma spray process and this coating was very effective in decreasing the corrosion rate in air and molten salt at 900^0C in case of ASTm-SA210 grade A1 and ASTm-Sa213-T-11 type of steel wheras coating was least effective for ASTM-SA213-T22 steel. Uncoated ASTM SA213 T22 steel showed very poor resistance to hot corrosion [21].

Hot corrosion studies were conducted on uncoated as well as plasma spray coated superalloy of Fe-based (32Ni-21Cr-0.3Al-0.3Ti-1.5Mn-1.0Si-0.1C-bal.Fe) with coating NiCrAlY, Ni-20Cr, Ni3 Al and satellite 6 at temperature of 900^0C in molten salt. All these overlay coatings showed better resistance to hot corrosion as compared to that of uncoated superalloy. NiCrAlY coating was found to be most protective followed by Ni-20Cr coating. Stellite6 was least effective but still decreased weight gain to around 60% of that of bare superalloy [22].

Cr_2C_3-NiCr, NiCr, WC-Co and stellite6 metallic coatings were sprayed on ASTM SA-210 grade A1 steel by HVOF process and hot corrosion studies at 900C in molten salt showed that NiCr coating was found to most protective followed by Cr_2C_3 -NiCr coating. WC-Co coating was least effective to protect the substrate steel [23].

5. CONCLUSION

The factors i.e Fuel selection, Design aspects, Chemical additive, Periodic cleaning of coal or coal derived fuel, Selection of better corrosion resistance materials of construction, Protective coatings decreases the hot corrosion rate of boiler tube steels. The applicability of these factors is very difficult in some cases. The coatings show the significant improvements in hot corrosion resistance.

REFERENCES

[1] Uusitalo, M.A., Vuoristo, P.M.J. and Mantyla, T.A., (2003), "High Temperature Corrosion of Coatings and Boiler Steels in Oxidizing Chlorine-containing Atmosphere," Mater. Sci. Eng. A, Vol. 346, pp. 168-177.

[2] Picas, J.A., Forn, A., Igartua, A. and Mendoza, G., (2003), "Mechanical and tribological properties of high velocity oxy-fuel thermal sprayed nanocrystalline CrC-NiCr coatings," Surf. Coat. Technol., Vol.174 –175, pp. 1095–1100.

[3] Metals Handbook, (1975), "Failure analysis and Prevention," Vol.10, ASM Publication, Metals Park OH, USA.

[4] Sanayal S.k., Bhakta U.C., Sinha A., (2000), "Cases of corrosion in power plant components at NTPC," NACE International, Vol. 2, pp 537-551.

[5] Bhattacharya S., Amir Q.M., C. Kannan, S.B. Mahapatra (2000), "Overheating failure of superheater suspension tubes of a captive poer plant boiler," NACE International, Vol. 2, pp 611-620.

[6] Stringer J., (1997) "High temperature corrosion problems in coal based power plant and possible solutions," Elseveir Proced. Corrosion CORCON-97, Mumbai, vol. 1, pp 13-23.

[7] Chattopadhyay P. (2006), " Boiler operation engg," Tata McgrawHill, pp. 739.

[8] Chattopadhyay P. (2006), " Boiler operation engg," Tata McgrawHill, pp. 254.

[9] Beer J.M. (2000), "Combustion technologies developments in power generation in response to environment challenges," Process in Energy and Combustion Science, Vol. 26 (Issue 4-6), pp. 301-327.

[10] Gitanjaly, S. Parkash, (2000) "Review on effect of additives on hot corrosion. NACE International," Vol.1, pp. 174-182.

[11] Chattopadhyay P. (2006), " Boiler operation engg," Tata McgrawHill, pp. 772.

[12] Vuthaluru H.B. (1999), "Remediation of ash problems in pulverized coal fired boiler," Fuel Vol. 78 (Issue 15), pp. 1789-1803.

[13] Wigley F., Williamson J., Rilly G., (2007), "The effect of mineral additives on coal ash deposition," Fuel Processing Technology, Vol. 88 (Issue 11-12 Dec), pp. 1010-1016.

[14] Varadan J. R., (1997) "Post operational boiler chemical cleaning, an experience at NTPC-Ramagundam," NACE International, Vol. 2, pp. 621-631.

[15] Chattopadhyay P. (2006), " Boiler operation engg," Tata McgrawHill, pp.992.

[16] Quadakkers W.J., Theile M., Ennis P.J., Teichmann H., (1997) "High temperature corrosion of boiler tubes steels in simulated coal fired plant atmosphere containing water vapors," Elseveir Proced. Corrosion CORCON-97. Mumbai, Vol.1, pp. 199-207.

[17] Paul L., Ishwar V. R, George Y. L., (1997) "High temperature corrosion behavior and application of modern superalloys," Elseveir Proced. Corrosion CORCON-97, Vol. 2, pp. 493-502.

[18] Sidhu T.S., Aggarwal R.D., Parkash S. (2004), "Hot corrosion of some superalloys and role of HVOF spray coatings-a review," Surface and Coating Technology, Vol. 198 (1-3) pp 441-46.

[19] Sidky, P.S. and Hocking, M.G., (1999), "Review of Inorganic Coatings and Coating Processes For Reducing Wear and Corrosion," Brit. Corros. J., Vol. 34, No. 3, pp. 171-183.

[20] Calla E., Modi S.C., (1997) "Corrosion protection by Ss-316 coating by thermal spray processes" Elseveir procedding Corrosion CORCON-97, Mumbai, vol. 2, pp 816-830.

[21] Sidhu B.S., Parkash S. (2003), "Evaluation of corrosion behavior of plasma sprayed Ni3Al coating on steel in oxidation and molten salt environment at 900C," Surface and Coating Technology, Vol. 166 (1-3) pp 89-100.

[22] Singh H., Puri D., Parkash S. (2003), "Some studies on hot corrosion performance of plasma sprayed coatings on a Fe based superalloy," Surface and Coating Technology, Vol. 192 (1) pp 27-38.

[23] Sidhu H.S., Sidhu B.S, Parkash S. (2006), "Cyclic hot corrosion of High Velocity Oxy Fuel sprayed coatings on steel at 9000C," Corrosion, Vol. 62 (11), pp 1028-1038.

High Temperature Corossion Behaviour of Ni-based Thermal Spray Coatings: A Review

Sukhpal Singh Chatha, Rakesh Bhatia, Hazoor S. Sidhu and Buta S. Sidhu
Department of Mechanical Engineering, Yadavindra College of Engineering, Punjabi University Guru Kashi Campus, Talwandi Sabo, Bathinda, Punjab -151 302, India
E-mail:- sukhpal_chatha@yahoo.com

Abstract

High temperature corrosion is chemical deterioration of a material under very high temperature conditions. This non-galvanic form of corrosion can occur when a metal is subject to a high temperature atmosphere containing oxygen, sulfur or other compounds capable of oxidising the material concerned. Nickel-Chromium coatings provide a way of extending the limits of use of materials at the upper end of their performance capabilities, by protecting them against wear or corrosion. This paper reviews the developments and applications of these thermal spray coatings for corrosion/ erosion-corrosion under different types of environments.

Keywords: *Erosion, Hot corrosion, NiCr, Oxidation, Thermal spray*

1. INTRODUCTION

Corrosion is the most severe problem that causes huge losses to energy sector in general and to the efficiency of boiler tubes in particular. In order to suppress the problem the use of protective coatings is a way out for meeting the requirements of high temperature strength and corrosion resistance of components operating at elevated temperature and in corrosive-erosive environment such as fuel-fired boilers, waste incineration boilers, and electric furnaces. The Nickel Chromium coatings, due to their high resistance to high temperature corrosion are recommended for high temperature applications. The addition of other elements, namely Cr, Al, and Si, have improved the corrosion resistance of these coatings due to the formation of more protective oxide layers such as Cr_2O_3, Al_2O_3, or SiO_2, respectively [1-5].

In this paper author has made the efforts to compile the available literature on Nickel based coatings as reported.

2. STUDIES ON Ni-BASED COATINGS

Hot corrosion studies of air plasma sprayed NiCoCrAlY, NiCoCrAlY+1% Hf, NiCoCrAlY+1% Si, NiCrAlY, CoCrAlY coatings on CM 247 LC super alloy at 900^0C in the corrosive environments of $95\%Na_2SO_4+5\%NaCl$ and $90\%Na_2SO_4+5\%NaCl+5\%V_2O_5$ were conducted by Gurrappa[6], using crucible immersion technique. The coating of composition 22Co-18Cr-12Al-0.5Y was found to exhibit maximum life among the investigated coatings in both the environments.

Lee *et al.* [7] reported that corrosion resistance of HVOF sprayed Ni-Cr-W-Mo-B coating improved by increasing the annealing temperature. Thermal spray processes such as high velocity oxy fuel (HVOF) and plasma spray are often used to apply high-chromium, nickel coatings [8].Yamada *et al.* [9] reported that corrosion resistance of detonation gun sprayed Ni-50Cr was highest among the Ni-20Cr, Ni-50Cr and Cr coated boiler tubes in actual refuse incineration plant as well as in laboratory tests. When nickel is alloyed with chromium, this element oxidizes to Cr_2O_3 which could make it suitable for use upto about 1200^0C, although in practice use is limited to temperature below about 800^0C [10].

Usitalo *et al.* [11] investigated that the homogeneous and dense laser-melted HVOF Ni-Cr coatings with high chromium content are better and protect the ferritic and austenitic boiler steels in hot corrosive environment. It was further reported that corrosive species were able to penetrate through some of the HVOF coatings and attack the substrate via interconnected network of voids and oxides at splat boundaries [12]. Laser-melted Ni-57Cr, HVOF coating did not suffer any corrosion in oxidising atmosphere of 500 vppm HCl, 3% O_2, 14% CO_2, 20%

H_2O and Argon as balance due to an oxide layer formed during the laser treatment [13].

Ni-20Cr metallic coatings were deposited on 9Cr-1Mo type steel using HVOF and APS techniques. Sundararanjan *et al* [14] observed the formation of protective oxide scale of Cr_2O_3 on the coating surfaces at four steam temperatures in the range of 600-750^{0}C. The diffusion of nickel from the coatings to the substrate and the diffusion of iron from the substrate to the coatings for longer exposures to steam oxidation were noticed. The rate of diffusion of Ni and Fe were almost similar and diffusion increased with the increase in the temperature and duration [15]. The diffusion of iron caused formation of Fe_2O_3 scale, the reason for non-protectiveness of coatings for longer exposure times [16]. Coatings containing high nickel and chromium offer better ccorrosion resistance[17].

Uusitalo *et al.* reported that in HVOF sprayed Ni/Cr and Fe_3Al coatings, the corrosion was more severe in oxidising environments as compared to the corrosion in reducing environment in the presence of 40% Na_2SO_4-40%K_2SO_4-10NaCl-10KCl salt. In reducing conditions materials with high chromium content were found to be able to form a protective layer containing chromium, sulphur and sodium. The corrosion resistance of this layer increased with increasing chromium content [18].

Corrosion mechanism of HVOF deposited NiCrBSi coatings by immersing the specimens in 3.5% NaCl with pH adjusted to 3 by addition of acetic acid was studied by Zhao *et al.* [19]. They concluded that the corrosion first occurred on the surface of the coating around the particles that had not melted during spraying and the defects such as pores, inclusions and microcracks. Corrosion resistance can be improved by remelting the coating.

Singh *et al.* conducted hot corrosion studies using shrouded plasma spray process on NiCrAlY, Ni-20Cr, Ni_3Al, and Stellite-6 metallic coatings deposited on a Ni-based superalloy after exposure to molten salt at 900°C, under cyclic conditions. The thermogravimetric technique was used to establish the kinetics of corrosion. All the coatings were found to be successful but the NiCrAlY coating provided maximum protection against corrosion, which may be attributed to the formation of oxides, and spinels of nickel, aluminum, chromium, or cobalt [20]. Further same coatings were deposited on boiler tube steels by Singh et al. [21] for examining the degradation behaviour in the platen super heater of the coal fired boiler. All the coatings were found to be effective and Stellite-6 coating provided maximum protection against degradation followed by NiCrAlY, Ni-20Cr and Ni_3Al. Further these coatings are examined by Singh *et al.*[22] on boiler tube steels in air at 9000C. Coatings were found to be beneficial in increasing oxidation resistance in air. The superior oxidation resistance of the Stellite-6 coating is attributed to the presence of $CoCr_2O_4$, which reduces diffusion rates, and thus oxidation rates. The oxidation resistance of the Ni_3Al coating is better than the Ni-20Cr and NiCrAlY coatings due to the presence of a chromium-rich continuous layer just below the oxidized bond coat. Further these coatings were deposited on a Ni-base superalloy(Superni 600). NiCrAlY coating provided the best protection against corrosion which was attributed to the simultaneous formation of an additional protective oxide Al_2O_3, along with the Cr_2O_3 and $NiCr_2O_4$ phases, which grows very slowly and is thermodynamically stable [21].

Singh *et al.* deposited Cr_2C_3–NiCr, NiCr, WC–Co and stellite-6 metallic coatings on ASTM SA-210 gradeA1 steel by the HVOF process to examine hot corrosion behaviour after exposure to molten salt at 900^{0}C under cyclic conditions. LPG was used as the fuel gas. The thermo-gravimetric technique was used to establish kinetics of corrosion. All these coatings showed better resistance to hot corrosion as compared to that of uncoated steel. NiCr Coating was found to be most protective followed by Cr_2C_3–NiCr coating. WC–Co coating was least effective to protect the substrate steel. It was found that the formation of Cr_2O_3, NiO, $NiCr_2O_4$, and CoO attributed for the hot corrosion resistance in the coatings [23].

Singh *et al.* investigated degradation of plasma sprayed Ni-20Cr coating on boiler tube steels, namely low carbon steel ASTM-SA210-GradeA1 (GrA1), 1Cr-0.5Mo steel ASTM-SA213-T-11(T11), and 2.25Cr-1Mo steel ASTM-SA213-T-22(T22) steels in the platen superheater zone of a coal fired boiler at around 755°C for 10 cycles, each100 h. Coated steels showed lower degradation (erosion-corrosion)rate than uncoated steels. Ni-20Cr coated T11 steel showed lowest rate of degradation [4].

Sidhu *et al.* deposited NiCrBSi, Cr_3C_2 -NiCr, Ni-20Cr, and Stellite-6 coatings on an Fe-based superalloy by the high-velocity oxyfuel (HVOF) thermal spray process. The hot corrosion behavior of the coatings in an aggressive environment of Na_2SO_4-60%V_2O_5 at 900°C under cyclic conditions was studied. Due to the formation of oxides and spinels of nickel, chromium, or cobalt, Ni-20Cr coating was found to be the most protective followed by Cr_3C_2–NiCr, NiCrBSi and Stellite-6 [24].

Singh *et al.* investigated cyclic-oxidation behavior of Ni –22Cr –10A1 –1Y and Stellite-6 coatings, deposited on boiler-tube (ASTM-SA210-Grade A1, ASTM-SA213-T-11 and ASTM-SA213-T-22)using shrouded plasma-spray process at 900^0C. Both coatings were found to be beneficial in increasing the resistance to oxidation in air. Coated GrA1 steel gave the highest resistance followed by T11 and T22 steels. The Stellite-6 coating had the best resistance to oxidation due to the presence of $CoCr_2O_4$ in its scale [25]. Further the same substrate was coated using high velocity oxyfuel (HVOF)-sprayed NiCr coating. Coatings were developed by two different techniques using wire and powder as feed materials. It was found that the HVOF wire spraying process offers a technically viable and cost-effective alternative to HVOF powder spraying process for applications in an energy generation power for having better resistance to erosion [26].

Hot corrosion studies of Cr_3C_2-NiCr, NiCr, WC-Co and Stellite-6 alloy coatings sprayed on ASTM SA213-T11 steel using the HVOF process in molten salt at $900\ ^0$C under cyclic conditions were conducted by Singh et al.[27]. Liquid petroleum gas was used as the fuel gas. The thermo-gravimetric technique was used to establish the kinetics of corrosion. NiCr Coating was found to be most protective followed by the Cr_3C_2-NiCr and WC-Co coatings. The formation of Cr_2O_3, NiO, $NiCr_2O_4$, and CoO in the coatings were suggested to the reason for better hot-corrosion resistance.

Sidhu *et al.* investigated HVOF sprayed NiCrBSi, Cr_3C_2-NiCr, Ni-20Cr, and Stellite-6 coatings on a nickel-based superalloy(Superni 601) at 900 °C in the molten salt (Na_2SO4-60%V_2O_5) environment under cyclic oxidation conditions. The thermogravimetric technique was used to establish kinetics of corrosion. Ni-20Cr coated superalloy imparted maximum hot corrosion resistance, whereas Stellite-6 coated indicated minimum resistance. The hot corrosion resistance of all the coatings may be attributed to the formation of oxides and spinels of nickel, chromium, or cobalt [28].

Singh *et al.* investigated solid particle erosion behavior of the HVOF deposited NiCr and Stellite-6 coatings on boiler tube steels. The study was conducted using an air jet erosion test rig at a velocity of 26 m/s and impingement angle of 30° and 90°, on uncoated as well as HVOF spray coated boiler tube steel (GrA1) at 250°C. The coatings were harder as compared to substrate steel. The NiCr coating performed better than Stellite-6 coating during solid particle erosion for both impact angles. The NiCr coating showed fine, uniform and layered microstructure [29].

Sidhu *et al.* investigated hot corrosion behaviour of Cr_3C_2-NiCr and NiCrBSi coatings formed by the high velocity oxy-fuel (HVOF) process on Superni 718 superalloy in the Na_2SO_4-V_2O_5 molten salt environment at 900^0C under cyclic conditions. Both coatings proved to effective due to the formation of protective oxides of chromium/silicon at the surface and at the splat boundaries of the coatings [30].

Sidhu *et al.* evaluated the oxidation and hot corrosion resistance of HVOF sprayed WC-NiCrFeSiB coating deposited on Ni-based superalloy (Superni 75) and Fe-based superalloy (Superfer 800H). The coated as well as uncoated specimens were exposed to air and molten salt (Na_2SO_4-25%NaCl) environment at 800^0C under cyclic condition. The WC-NiCrFeSiB coating provided necessary resistance against oxidation and hot corrosion to both the nickel and iron based superalloys in the given environmental conditions at 800^0C [31].

Singh *et al.* deposited Ni-20Cr alloy powder on three Ni based super alloys; Superni 75, Superni 600 and Superni 601 by shrouded plasma spray process. Oxidation kinetics was established for the uncoated as well as the coated super alloys in the air at 900^0C under cyclic conditions for 50 cycles using thermogravimetric technique. All the coated superalloys nearly followed the parabolic rate law of oxidation. The coating was found to be successful in maintaining its integrity with the superalloy substrates in all cases [32].

Vicenzi *et al.* investigated the hot and cold erosive wear mechanisms of HVOF and plasma-sprayed NiCr-

based coatings. Erosion tests were carried out in specially developed equipment, with possible variations in temperature and attack angle. The results showed that NiCr coatings are ductile, a property similar to monolithic metallic materials. The porosity influenced both the amount of incrusted alumina particles and oxidation. The increase in temperature caused higher oxidation and erodent incrustation [33].

X. OU *et al.* investigated the oxidation and lower temperature hot corrosion (LTHC) behaviour of Ni-Cr coatings produced by high velocity arc spray (HVAS) in simulated boiler conditions at 650°C. The protection effect of an Al coating deposited by HVAS onto the Ni-Cr coating was also investigated. It was observed that the oxidation rates are almost superposed in both air and in simulated coal-fired gas (containing SO_3) as long as no salt was present on the surface. When the surface is coated with salt (75%K_2SO_3 + 25%Na_2SO_3) the rate curve for LTHC of the Ni-Cr coated surface shows a parabolic shape in the simulated coal-fire flue gas. The Al coating on the Ni-Cr enhances resistance to LTHC [34].

TAO *et al.* characterized the high velocity air-fuel (HVAF) sprayed conventional and nanostructured NiCrC (80%NiCr-20%CrC) coatings. The results show that nanostructured NiCrC coating possesses a more uniform and denser microstructure, much higher microhardness and better fracture toughness than its conventional counterpart [35]. The enhanced grain boundary diffusion in the nanostructured coating not only promotes the formation of a denser Cr_2O_3 scale with a higher rate, but also helps to mitigate the Cr depletion at the metal/scale interface. The less porosity of the nanostructured coating is also thought to be beneficial to the anti-corrosion properties [36].

Mahesh *et al.* characterized NiCrAl coatings on superalloys sprayed by HVOF process. The observed microstructral characteristics, higher bond strength, and hardness of HVOF sprayed NiCrAl coating show that it may act as an effective barrier to provide high temperature protection to the superalloys [37].

Zhang *et al.* examined tribological properties of Ni–Cr–B–Si–RE alloy coatings, thermal spray welded onto steel substrate for characterizing the critical normal loads and sliding speed on the wear behavior of a Ni–Cr–B–Si–RE alloy. The worn surfaces of the Ni–Cr–B–Si–RE alloy coatings were examined. The results show that an adhered oxide debris layer was formed on the worn surface in friction which contributed to decreased wear. Wear rate of the coatings increased with the load, but decreased with the sliding speed Wear mechanism is dominated by a large amount of counterpart material transferred to the coating [38].

Bala et al. investigated deposition of Ni–50Cr powder on two boiler steels SA-213-T22 and SA516 (Grade 70) by cold spray process. The hot corrosion performance of coated as well as bare boiler steels was evaluated in an aggressive environment of Na_2SO_4–60% V_2O_5 under cyclic conditions at an elevated temperature of 900°C. Results showed that the Ni–50Cr coating provided adequate protection to the steels and the oxide scales remained intact till the end [39].

3. CONCLUSION

Corrosion is the most severe problem that causes huge losses to energy & power sector. Nickel based coatings can provide the effective means to combat with high temperature corrosion and oxidation. NiCr coatings can be successfully deposited on boiler steel and on other Ni and Fe based alloys by thermal spray processes. The hot corrosion resistance of all the coatings is attributed to the formation of oxides and spinels of nickel, aluminium, chromium, or cobalt. Corrosion resistance of NiCr coatings can further be increased by post treatment.

REFERENCES

[1] Uusitalo, M.A., Vuoristo, P.M.J. and Mantyla, T.A. (2003) "High Temperature Corrosion of Coatings and Boiler Steels in Oxidizing Chlorine-containing Atmosphere", Mater. Sci. Eng. A, Vol. 346, pp. 168-177.

[2] Sidhu B.S., Prakash S., (2005) "Nickel-chromium plasma spray coatings: A way to enhance degradation resistance of boiler tube steels in boiler environment", J. Therm.Spray Technol.,Vol.15, pp.131-140.

[3] Sidhu T.S., Prakash S.,and Agrawal R.D.(2006)"Hot Corrosion Resistance of High-Velocity Oxyfuel Sprayed Coatings on a Nickel-Base Superalloy in Molten Salt Environment", J. Therm.Spray Technol, vol.15(3) pp. 387-389.

[4] Singh H., Puri D., Prakash S. (2005)"Studies of plasma spray coatings on a Fe-base superalloy, their structure and high temperature oxidation behaviour",Anti-Corrosion Methods and Materials,Vol.52(2) pp.84 – 95.

[5] Sidhu H. S., Sidhu B. S., Prakash S. (2007)" Comparative characteristic and erosion behavior of NiCr coatings deposited by various high-velocity oxyfuel spray processes", Journal of Materials Engineering and Performance,Vol. 15, pp.699-704.

[6] Gurrappa I. (1999) "Hot Corrosion Behavior of CM 247 LC Alloy in Na2SO4 and NaCl Environments", Oxid. Met., Vol. 51, No. 5, pp. 353-382.

[7] Lee. C.H., and Min K.O. (2000) "Effects of heat treatment on the microstructure and properties of HVOF-sprayed Ni-Cr-W-Mo-B alloy coatings" ,Surf. Coat. Technol., Vol.132, pp. 49-57.

[8] Tuominen J., Vuoristo P., Mantyla T., Ahmaniemi S., Vihinen J. and Andersson P.H. (2002)"Corrosion Behavior of HVOF-Sprayed and Nd-YAG Laser-Remelted High-Chromium, Nickel-Chromium Coatings", J. Therm. Spray Technol., Vol. 11, No. 2, pp. 233-243.

[9] .Yamada K., Tomono Y., Morimoto J., Sasaki Y. and Ohmori A. (2002)"Hot Corrosion Behavior of Boiler Tube Materials in Refuse Incineration Environment" ,Vacuum, Vol. 65, No. 3-4, pp. 533-540.

[10] Hidalgo V. H., Varela J. B., Menéndeza A. C. and Martýnez S. P. (2001) "High temperature erosion wear of flame and plasma-sprayed nickel–chromium coatings under simulated coal-fired boiler atmospheres", Wear, Vol. 247, pp. 214–222.

[11] Uusitalo M.A., Vuoristo P.M.J., Mantyla T.A. (2002) "High temperature corrosion of coatings and boiler steels in reducing chlorine-containing atmosphere," Surf. Coat. Technol., Vol. 161, pp. 275-285.

[12] Uusitalo M.A., Vuoristo P.M.J., Mantyla T.A. (2002) "Elevated temperature erosion-corrosion of thermal sprayed coatings in chlorine containting environments", Wear, Vol. 252, pp. 586-594.

[13] Uusitalo M.A., Vuoristo P.M.J. and Mantyla T.A. (2003) "High Temperature Corrosion of Coatings and Boiler Steels in Oxidizing Chlorine-containing Atmosphere", Mater. Sci. Eng. A, Vol. 346, pp. 168-177.

[14] Sundararajan T., Kuroda S., Itagaki T. and Abe F. (2003) "Steam Oxidation Resistance of Ni-Cr Thermal Spray Coatings on 9Cr-1Mo Steel. Part 1: 80Ni-20Cr", ISIJ Int., Vol. 43, No.1, pp. 95-103.

[15] Sundararajan T., Kuroda S., Itagaki T. and Abe F. (2003) "Steam Oxidation Resistance of HVOF Thermal Sprayed Ni-Cr Coatings", Thermal Spray 2003: Advancing the Science & Applying the Technology, (Ed.) C, Moreau and B. Marpie, pp. 495-502.

[16] Sundararajan T., Kuroda S., Itagaki T. and Abe F. (2003) "Steam Oxidation Resistance of Ni-Cr Thermal Spray Coatings on 9Cr-1Mo Steel. Part 2: 50Ni-50Cr", ISIJ Int., Vol. 43, No.1, pp. 104-111.

[17] Chidambaram D., Clayton C.R. and Dorfman M.R. (2003) "Evaluation of the electrochemical behavior of HVOF-sprayed alloy coatings—II", Surf. Coat. Technol., Vol. 192, No. 2-3, pp.178-283.

[18] Uusitalo M.A., Vuoristo P.M.J. and Mantyla T.A. (2004) "High Temperature Corrosion of Coatings and Boiler Steels below Chlorine-containing Salt Deposits", Corros. Sci., Vol. 46, No. 6, pp. 1311-1331.

[19] Zhao W.M., Wang Y., Dong L.X., Wu K.Y. and Xue J. (2005)"Corrosion mechanism of NiCrBSi coatings deposited by HVOF", Surf. Coat. Technol., vol.190(no.2-3).

[20] Singh H., Puri D., Prakash S. (2005)"Corrosion Behavior of Plasma-Sprayed Coatings on a Ni-Base Superalloy in Na2SO4-60 Pct V2O5 Environment at 900 °C", Metallurgical and Materials Transactions A, Vol. 36, pp.1007-1015.

[21] Singh H., Prakash S., Puri DPhase., D.M. (2006) "Cyclic Oxidation Behavior of Some Plasma-Sprayed Coatings in Na2SO4 -60%V2 O5 Environment", Journal of Materials Engineering and Performance, Vol. 15(6) pp. 729-741

[22] Sidhu B. S., Prakash S.(2007) "Analytical Studies on the Behavior of Nickel-and Cobalt-Base Shrouded Plasma Spray Coatings at Elevated Temperature in Air", Oxid. Met., vol. 67, pp. 279–298.

[23] Sidhu H. S., Sidhu B. S., Prakash S.(2005)"Comparative characteristic and erosion behavior of NiCr coatings deposited by various high-velocity oxyfuel spray processes", Journal of Materials Engineering and Performance, Vol. 15, pp. 699-704.

[24] Sidhu T.S., Prakash S., Agrawal R.D.(2005)"Performance of High-Velocity Oxyfuel-Sprayed Coatings on an Fe-Based Superalloy in Na2 SO4 -60%V2O5 Environment at 900 °C Part II:Hot

Corrosion Behavior of the Coatings",Journal of Materials Engineering and Performance, Vol.15(1), pp.122-129.

[25] Sidhu B. S., Prakash S.,(2005)"High-Temperature Oxidation Behavior of NiCrA1Y Bond Coats and Stellite-6 Plasma-Sprayed Coatings", Oxid. Met., Vol. 63, pp.241-259.

[26] Sidhu H. S.,. Sidhu B. S, Prakash S. (2006) "Comparative Characteristic and Erosion Behavior of NiCr Coatings Deposited by Various High-Velocity Oxyfuel Spray Processes", Journal of Materials Engineering and Performance, Vol. 15, No.6, pp.699-704.

[27] Sidhu H.S., Sidhu B.S., Prakash S.(2006) "Hot Corrosion Behavior of HVOF SprayedCoatings on ASTM SA213-T11 Steel", J. Therm.Spray Technol., Vol.16, No.3, pp. 349–354.

[28] Sidhu T.S., Prakash S., Agrawal R.D. (2006) "Hot Corrosion Resistance of High-Velocity Oxyfuel Sprayed Coatings on a Nickel-Base Superalloy in Molten Salt Environment", J. Therm.Spray Technol., Vol.15, No.3, pp.387-399.

[29] Sidhu H. S., Sidhu B. S., Prakash S.(2007) "Solid particle erosion of HVOF sprayed NiCr and Stellite-6 coatings", Surf. Coat. Technol. Vol.202, pp.232-238.

[30] Sidhu T.S., Prakash S., Agrawal R.D. (2007) " Study of Molten Salt Corrosion of High Velocity Oxy-Fuel Sprayed Cermet and Nickel-Based Coatings at 9000 C", Metallurgical And Materials Transactions A,Vol. 38A, pp.77-85.

[31] Sidhu T.S., Malik A., Prakash S., Agrawal R.D.(2007) "Oxidation and Hot Corrosion Resistance of HVOF WC-NiCrFeSiB Coating on Ni- and Fe-based Superalloys at 800 0C", J. Therm.Spray Technol., Vol. 16(5-6),pp.844-849.

[32] Singh H., Puri D., Prakash S., Maiti R.(2007) "Characterization of oxide scales to evaluate high temperature oxidation behavior of Ni–20Cr coated superalloys", Materials Science and Engineering, Vol. 464, pp.110-116.

[33] Vicenzi J., Marques C.M., Bergmann C.P.(2008) "Hot and cold erosive wear of thermal sprayed NiCr-based coatings: Influence of porosity and oxidation", Surf. and Coat. Technol., Volume 202, pp. 3688-3697.

[34] Xue-mei OU, SUN Z., SUN M., Duan-lian ZOU(2008) "Hot-corrosion mechanism of Ni-Cr coatings at 650°C under different simulated corrosion conditions", Journal of China University of Mining and Technology, Vol.18, pp. 444-448.

[35] Tao K., Zhang J., Cui H., Zhou X., Zhang J.(2008) "Fabrication of conventional and nano structured NiCrC coatings via HVAF technique", Transactions of Nonferrous Metals Society of China Vol. 18,pp. 262-269.

[36] Mahesh R.A., Jayaganthan R., Prakash S.(2009) "Microstructural characteristics and mechanical properties of HVOF sprayed NiCrAl coating on superalloys", Journal of Alloys and Compounds, Vol. 468, pp. 392-405.

[37] Tao K., Zhou X., Cui H., Zhang J.(2009) "Oxidation and hot corrosion behaviors of HVAF-sprayed conventional and nanostructured NiCrC coatings", Transactions of Nonferrous Metals Society of China, Vol.19, pp. 1151-1160.

[38] Zhang Z., Wang Z., Liang B.(2009) "Wear characterization of thermal spray welded Ni–Cr–B–Si–RE alloy coatings",Journal of Materials Processing Technology, Vol. 209, pp. 1368-1374.

[39] Bala N., Singh H., Prakash S.(2010) "Accelerated hot corrosion studies of cold spray Ni–50Cr coating on boiler steels"Materials& Design, Vol. 31, pp. 244-253.

A Study on Turning of Al(6063)/5 Vol% SiC and Al(6063)/10 Vol% SiC-MMC

H.S. Bains[1] and A. Manna[2]

[1]Department of Mechanical Engineering, Sant Longowal Institute of Engineering & Technology, Sangrur, India

[2]Department of Mechanical Engineering, Punjab Engineering College, Chandigarh, India

Email: kgpmanna@rediffmail.com

Abstract

Metal matrix composite is an advanced engineering material possesses several characteristics that make them useful in situations where low weight, high strength, high stiffness and ability to operate at elevated temperatures are required. These materials are difficult to machine, however, consisting of hard abrasive ceramic reinforcing medium set within a more ductile matrix material. This paper presents results from a series of turning tests in which a number of different cutting tool materials were used to machine an Al(6063)/5 vol% SiC and Al(6063)/10 vol% SiC Metal Matrix Composites. The influence of the cutting speed on tool wear was established for each tool material. It was found that carbide tools, both coated and uncoated sustained significant levels of tool wear after a short period of machining. The best overall performance was achieved using a titanium coated carbide insert.

Keywords: *Metal matrix composites, Cutting tool materials*

1. INTRODUCTION

The demand for a material to have high strength and high toughness and capable of operating effectively under adverse conditions has led to the developement of new generations of materials known as Metal Matrix Composites(MMC).These are the advance materials generally reinforced with SiCp or Al_2O_3 in the form of continious or discontinious fibers,whiskers or particulates of the ceramic material. The matrix can be any suitable material, but aluminium, magnesium, titanium, and some super alloys are the most popular.These advance composites are considered excellent canditates for high temperature applications but only difficut to machine which resist its wide spread application [1-5].The density of most MMC's is about one third that of steel,so that the specific strength and stiffness of these materials is high.These properties are important in automotive and aerospace industries because of potential for large reductions in weight. The presence of hard SiCp led to rapid tool wear, which is not surprising as SiC is harder than WC, a common cutting tool materials.The machining of MMC's using these conventional methods often involves frequent and expensive tool changes and there for increased job completion time. Machining processes such as turning,milling and drilling of MMC's , therefore, require the use of carbide,diamond or hard nitride coated tools. Even then machining times tend to be 2-4 times greater than for the unreinforced matrix matrial because because of increased tool wear,the necessatity to use reduced feed rates ,and the need to achieve good surface finish: the latter is necessary because of fracture behavior of matrix material composite is sensative to surface finish. In particular,a poor finish on a continious-fibre reinforced MMC's component can led to longitudinal fibre fracture and delamination.

The difficulties associated with the machining of MMC's should be minimised if these materials are to be used more extensively.The machinability of MMC's is now considered to be one of the most important areas of manufacturing science. MMC's are the new engineering materials,comprehensive machinabilty data have as yet to be established and this has aroused some research interest. The result outlinesd in this paper are based on an investigation involving the machining of an aluminium /silicon MMC by conventional turning on a lathe machine.A range of cutting tool materials were used for the turning test on different vol% of SiCp reinforced in aliminium(6063) and measurement were made of tool wear and surface finish.Test were performed over a range of cutting speed and at two feed rates using tools having two different nose radius.The result obtained have enabled an assesment to be made of the influence of each cutting tool materials on the machinabilty of the Al/ SiCp metal matrix composite.

2. PREPARATION OF WORK-PIECE

The matrix material used is an Al-Mg-Si wrought alloy matrix reinforced with SiCp of size 100µm.commercial Al(6063) alloy reinforced with 5, & 10 vol% SiCp .The matrix alloy was first melted in a graphite crucible in electric furnace. The matrix alloy was preheated at 300°C for 1-2 hours before melting and before mixing the SiCp was preheated at 300°C for 1 hour to make the surface of SiCp oxidized. The furnace temperature was raised above the liquidus temperature to melt the alloy completely at 750°C and was then cooled down just below the liquidus temperature to keep the slurry in a semi solid state. At this stage the preheated SiCp were added and mixed manually. The mixing was done for a short time period of 1-1.5 minutes. The composite slurry was reheated to a fully liquid state and then automatic mechanical mixing was done for 30 minutes at a stirring rate of 220 rpm.In this experiment, the molten composite was transferred from the crucible into the mild steel mould with diameter 50mm and length 250mm.

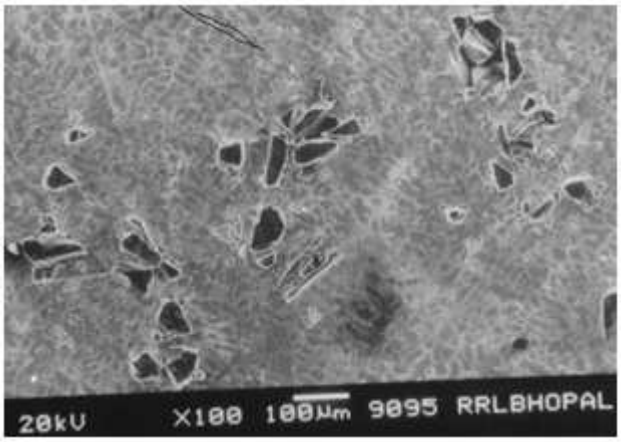

Fig.1 SEM of Al(6063)/5 vol% SiC-MMC W/P

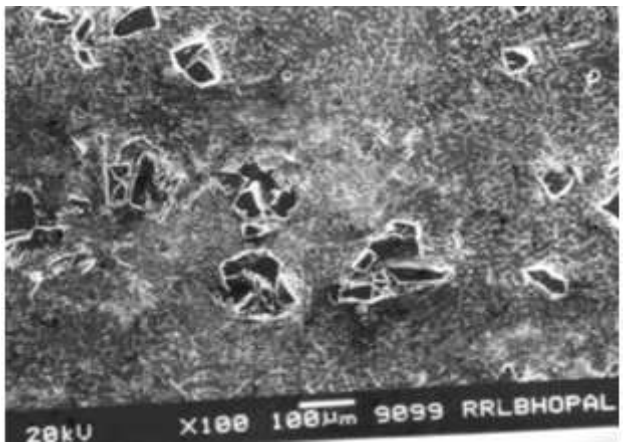

Fig.2 SEM of Al(6063)/10 vol% SiC-MMC W/P

3. SCHEME OF EXPERIMENT

In the present experimental study, analyze the effect of cutting speed and feed rate on tool wear keeping depth of cut constant during turning of Al(6063)/5 vol% SiC and Al(6063)/10 vol% SiC metal matrix composites. Present experimental study attempts to characterize the wear mechanism of coated and uncoated tungsten carbide tools in the machining of MMCs.The results could be applied to design better carbide tools and selection of cutting tool for machining of Al/SiC-MMC. HMT centre lathe machine is used for experimentation. The cutting tools used in this experimental study were coated and uncoated cemented carbide, specification CNMG 120408 TTS and CNMG 120408-PM-TiN coated. Tool holder specification was PCLNR 2525 M12 used for holding the insert during machining.

Machining parameters, cutting speed, feed rate were varied and depth of cut was kept constant for tool wear study. The cutting speed was derived from the measured spindle speed and diameter of surface of work-piece. All tests were carried out in dry environment. All the turning tests were performed over a range of cutting speed varying from 75 m/min to 225 m/min and feed rate varying from 0.1mm/rev to 0.75 mm/rev. Depth of cut was kept constant i.e. 0.5 mm throughout the experiment. The cutting tool flank wears were measured using tool maker microscope of resolution 0.01 mm.

4. RESULTS AND DISCUSSION

The turning tests was performed on a HMT Lathe machine using a range of cutting speeds 75-225 m/min. Feed rate of 0.1 - 0.75 mm/rev were used for turning tests. Each experiment repeated thrice and three measurement of flank wear were taken for further analysis.

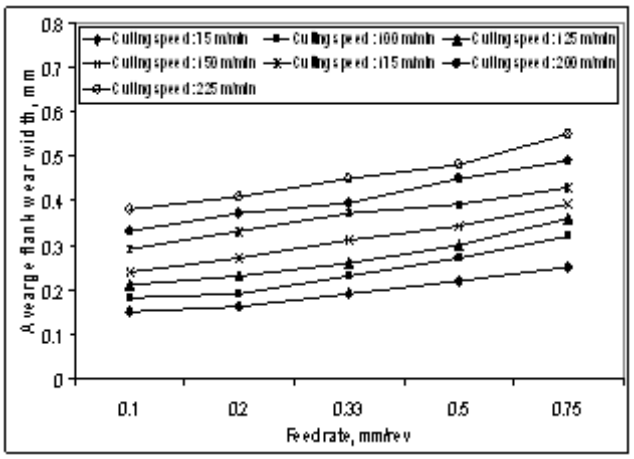

Fig 3 Influence of feed rate on flank wear at different cutting speeds during turning of Al/SiCp 5% vol-MMC without use of coolant by CNMG 120408 TTS insert

Figure 3 shows influence of feed rate on flank wear at different cutting speeds during turning of Al/SiCp 5% vol metal matrix composite without use of coolant. From the Figure 3, it is clear that when the feed is tripled e.g. from 0.1mm/rev to 0.33 rev/mm, cutting tool flank wear increases from 0.15 mm to 0.19 mm at constant 0.5mm depth of cut, 75 m/min cutting speed, whereas for the same change of feed rate, when the cutting speed is tripled i.e. from 75m/min to 225 m/min, the flank wear goes up from 0.19 to 0.45 mm for same depth of cut. Thus, when feed rate increases three times, flanks wear increases by 1.2 times. But when cutting speed increases three times, flank wear increases 2.3 times. Therefore, it is evident that flank wear is more susceptible to cutting speed as compared to feed rate, It is better to increase feed rate rather than increasing the cutting speed during machining of Al/5 vol%SiC-MMC. From the experimental results, it can be observed that when cutting speed is doubled, i.e. from 100m/min to 200 m/min flank wear goes up by 1.8 times (i.e from 0.18 to 0.33mm) at constant feed of 0.1mm/rev and 0.5mm depth of cut.

Figure 4 shows influence of feed rate on flank wear at different cutting speeds during turning of Al/ 10 vol.% SiC-MMC without use of coolant. From the Figure 4, it is clear that when the feed is tripled i.e. from 0.1mm/rev to 0.33 mm/rev, cutting tool flank wear increases from 0.17 mm to 0.24 mm at constant 0.5mm depth of cut, 75 m/min cutting speed, whereas for the same change of feed rate, when the cutting speed is tripled i.e. from 75m/min to 225 m/min, the flank wear goes up from 0.24 to 0.54 mm. Thus, when feed rate increases three times, flanks wear increases by one and half times.

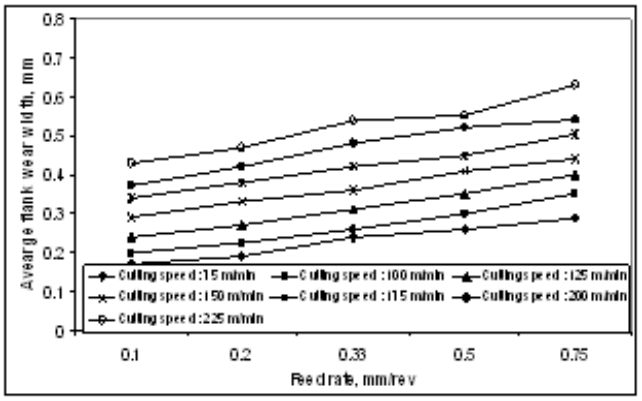

Fig 4 Influence of feed rate on flank wear at different cutting speeds during turning of Al/ 10 vol% SiC- MMC without use of coolant by CNMG 120408 TiN-Coated insert

But when cutting speed increases three times, flank wear increases to double the rate. Thus it is evident that flank wear is more susceptible to cutting speed as compared to feed rate, hence, it is better to increase feed rate rather than increasing the cutting speed during machining of Al/ 10 vol.% SiC-MMC. From the experimental results, it can be observed that when cutting speed is doubled, i.e from 100m/min to 200 m/min flank wear goes up by 1.8 times i.e. from 0.2 to 0.37mm at constant 0.1mm/rev feed rate and 0.5mm depth of cut.

5. CONCLUSIONS

i. The results from the flank wear tests indicate that the uncoated carbide tools are unsuitable for machining the MMC's because of SiC volume fraction present as reinforcement in the metal matrix composites.

ii. The Vol % together with the cutting speed were found to be the major factors affecting the flank wear during turning of Al/SiC-MMCs. This may be due to considerable increase in cutting force and change in feed rate. At the interface of particulate and matrix, there is a coordinate deformation which causes increase in shear angle and reduction in chip thickness.

iii. Abrasion was the main tool wear mechanism although edge chipping was observed at low cutting speed. This could be because of formation of adhesion of aluminum layer on the tool tip. This layer is not present in case of coated tools. Coated cutting tools performed better than uncoated cutting tools in terms of tool wear for all material machined.

REFERENCES

[1] A Manna and B Bhattacharaya, "A study on Different Tooling Systems During Machining of Al/SiC MMC", Journal of Materials Processing Technology, Vol.123, 2002, pp. 476-482

[2] L.A. Looney, J.M. Monaghan and P. O'Reilly, D. M. R. Taplin, "The Turning of An Al/SiC Metal Matrix Composite", Journal of Materials Processing Technology, Vol. 33, 1992, pp.453-468.

[3] N.P. Hung, S.H. Yeo and B.E. Oon, "Effect of Cutting Fluid on the Machinability of Metal Matrix Composites", Journal of Materials Processing Technology, Vol. 67, 1997, pp.157-161.

[4] A Manna and B Bhattacharaya, "A Study Onmachinability of Al/SiC MMC", Journal of Materials Processing Technology, Vol.140, 2003, pp.711-716.

[5] Alakesh Manna and B.Bhattacharyya, " Influence of Machining Parameters on the Machinability of Particulate Reinforced Al/SiC-MMC", International Journal of Advanced Manufacturing Technology, Vol 25, 2005, pp. 850-856.

Stress Analysis of Spur Gear using FEM Method

Sunil Kumar[1], K. K. Mishra[2] and Jatinder Madan[3]

[1]Yadavindra College of Engineering, Punjabi University Guru Kashi Campus, Talwandi Sabo, Bathinda - 151 302, Punjab

[2]Department of Mechanical Engineering, Sant Longowal Institute of Engineering & Teechnology, Longowal - 148 106, Punjab

[3]Department of Mechanical Engineering, Sant Longowal Institute of Engineering & Teechnology, Longowal - 148 106, Punjab

E-mail: sunilbaghla@yahoo.co.in

Abstract

This paper is about generating CAD model of spur gear using Pro/Program toolkit of Pro-E and to investigate validity of spur gear design by determining contact and bending stresses. It has been observed that contact and bending stresses are a major source of wear and tooth breakage respectively and subsequent failure of a gear. In present work, a program has been developed which by taking few input parameters from the user generates CAD model of the spur gear as output. This CAD model has been further utilized for analysis in terms of contact and bending stress determination. Current methods of calculating gear contact stresses use Hertz's equations, which were originally derived for contact between two cylinders. The results of FEM analyses using ANSYS10.0 are presented and compared with those obtained using Hertz's equations. Bending stresses have also been determined using three dimensional FEM analysis procedure using ANSYS 10.0 and comparison has been made with conventional methods. Results, both for contact and bending stress analysis have been found to be quite close to those obtained using mathematical formulae. Automation for gear design and analysis attempted in this work pertains to generation of CAD model and, contact and bending stress analysis. It has been concluded that, further work for automated design and failure analysis can be achieved with greater level of confidence.

Keywords: *Bending stresses,CAD model, Contact stresses,Gear failure, Spur gear*

1. INTRODUCTION

With increased use of computer hardware and software in design as well as manufacturing, most of the design and analysis is being done with the help of these tools. In computer aided design greater use is now made of CAD modeling software's and analysis tools. One of the major components of the present day machines is gear. Design and analysis of gear has been taken in this study.

Gears are a means of changing the rate of rotation of a machinery shaft. They can also change the direction of the axis of rotation and can change rotary motion to linear motion. Unfortunately, mechanical engineers sometimes shy away from the use of gears and rely on the advent of electronic controls and the availability of toothed belts, since robust gears for high-speed and/or high-power machinery are often very complex to design. However, for dedicated, high-speed machinery such as an automobile transmission, gears are the optimal medium for low energy loss, high accuracy and low play [1].

A gearbox as usually used in the transmission system is also called a speed reducer, gear head, gear reducer etc., which consists of a set of gears, shafts and bearings that are factory mounted in an enclosed lubricated housing. Speed reducers are available in a broad range of sizes, capacities and speed ratios. Their job is to convert the input provided by a prime mover into an output with lower speed and correspondingly higher torque. [2]

The increasing demand for quiet power transmission in machines, vehicles, elevators and generators, has created a growing demand for a more precise analysis of the characteristics of gear systems. In the automobile industry, the largest manufacturer of gears, higher

reliability and lighter weight gears are necessary as lighter automobiles continue to be in demand. Designing highly loaded spur gears for power transmission systems that are both strong and quiet requires analysis methods that can easily be implemented and also provide information on contact and bending stresses, along with transmission errors. The finite element method is capable of providing this information, but the time needed to create such a model is large.

In order to reduce the modeling time, a preprocessor method that creates the geometry needed for a finite element analysis may be used, such as that provided by Pro/Engineer. Using API toolkit of Pro/Engineer one can generate model of three-dimensional gears easily. In Pro/E, the geometry is saved as a file and then it can be transferred from Pro/E to ANSYS [3, 4].

2. LITERATURE REVIEW

Some of the papers related to stress analysis of mechanical bodies including gears have been discussed in this chapter. Heinrich Rudolph Hertz [6] was among the first to formulate and solve the problem of contact between two elastic bodies. Hertz's theory was expanded by Boussinesq. He studied the deformation of a semi-infinite solid due to pressure exerted on a small area of its plane surface. Lund-berg [7] developed a general theory of elastic contact between two semi-infinite bodies, in which the effect on the stresses in the presence of a tangential load is taken into consideration. Mindlin [8] investigated the distribution of the tangential load across the area of contact when one elastic body slides over another. Fischer-Cripps [9] addressed the issue by utilizing the finite-element method to compute the radius of curvature of the contact surface for both elastic and elastic-plastic contacts.

Significant development in analysis of strength properties of gear transmissions follows the achievements in computational design, simulation of meshing, and tooth contact analysis made by Litvin *et al* [10]. The development of the precise FEM model of gear tooth requires accurate determination of tooth profile with consideration of the selected machining process of gear fabrication [11].

3. OBJECTIVES

i. Propose a program for generating 3 D model of the spur gear using API (Application Program Interface) of Pro- Engineer.
ii. Analyze contact stresses developed in two cylinders using ANSYS.
iii. Analyze bending stresses developed in spur gear and pinion using ANSYS.
iv. Comparison of results with AGMA standards both for contact and bending stresses.

4. MODELING OF SPUR GEAR

For performing stress analysis of gears, one has to first make 3D model of it. It is a well known fact that preparing the model of the part like a gear is very difficult and time consuming in analysis software like ANSYS. However, one can make the model in any other third party CAD software and bring the solid model to ANSYS for doing the analysis.

Preparing a 3D model of a part like gear in CAD software like Pro-E also requires lot of manual input. However this process can be automated using programming facility available in the software. This would definitely reduce the time required for preparing a 3D model in a significant manner. Same has been attempted as a part of this paper, with specific attention on spur gear with involute profile. As a result of this program only few parameters are required to be input to get 3D model of a spur gear. This model can be further utilized for analysis in ANSYS. Figure 1 shows the model of spur gear.

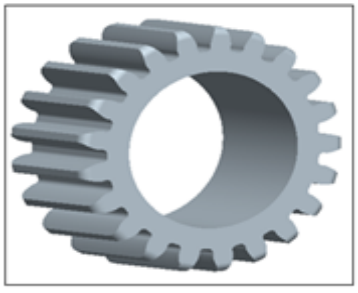

Fig. 1 CAD model of the spur gear

5. AUTOMATION OF GEAR PROCESS

Procedure for automation of gear process is explained in this section. First step would be to create a Pro/Program. This can be done by selecting Program from the main menu and then choosing the Edit Design.

Fig. 2 Input required for gear design

The user merely has to regenerate the gear ring. When he does, the system will prompt him to either use current values or to enter new ones. Simply select Enter, Select All, and then answer the questions that are asked. Information shown in Figure 2 in between the input and end input lines need to be entered when asked by the program. Once all the information is answered, the gear is regenerated and new spur gear is created with required specifications.

6. CONTACT STRESS ANALYSIS AND COMPARISON

The calculation is carried out under a plane strain condition with a Young modulus $2.07e^{11}$ Pa and Poisson's ratio of 0.3 using eight-node iso-parametric elements (Figure 3). Two circular discs with a radius 76.2mm.

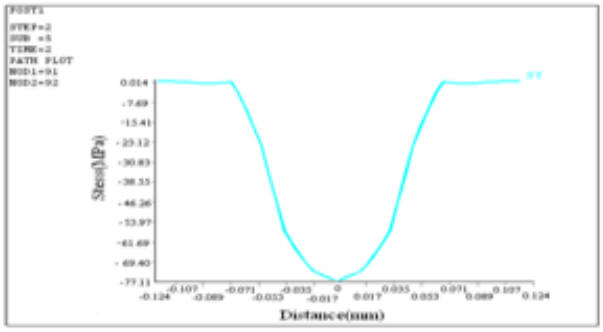

Fig. 3 Contact stresses determined using ANSYS

The comparison of contact stress from FEM and the Hertzian theoretical formula are shown in Figure 4 in which the two distributions lie very close. The red color line represents the value from the theoretical Hertz equation and blue color points represent the results from ANSYS10.0. It is observed that results for ANSYS are very close to mathematical results.

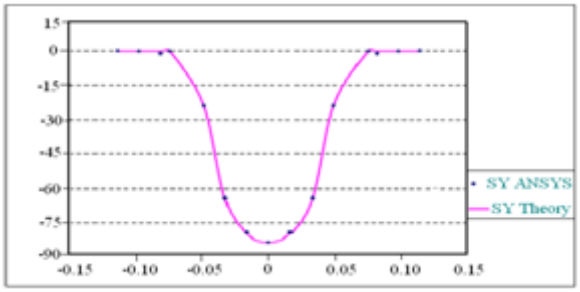

Fig. 4 Comparison of contact stress from FEM and the Hertzian theoretical formula

7. BENDING STRESS ANALYSIS AND COMPARISON

There are various no of teeth taken by changing number of teeth. All other parameters will be constant only diametral pitch will be varied. Material used is carbon steel and value of young modulus & Poisson ratio respectively is $2.07e^{11}$Pascal & 0.292 [5]. The transmitted load applied is 1500 N.

The comparison of results has been shown in Table 1. When referred to Table 1, the maximum value of the tooth stress obtained using ANSYS has been given. For 21 numbers of teeth, there is only a difference of 0.07% between stress values obtained by the AGMA and ANSYS.

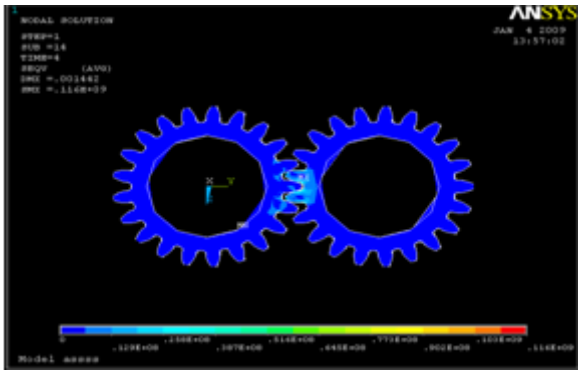

Fig. 5 Von-mises stresses in the spur gear

For cases of 23, 26 and 29 number of teeth, the difference in percentage terms between two methods is 1.01, 0.46 and 1.75 respectively, which is well within the acceptable limits. From these results, it was found that for all the cases give results obtained using ANSYS are in close approximation of the value obtained by the other method using AGMA standards. These differences are believed to be caused by factors such as the mesh pattern and the restricted conditions on the finite element analysis, and the assumed position of the critical section in the standards.

Table 1Comparison of Stresses between ANSYS and AGMA Standard

No. of Teeth	Stresses (ANSYS)	Stresses (AGMA)	Difference	% Difference
21	116	116.08	0.08	0.07
23	100	101.02	1.02	1.01
26	84.9	84.41	0.49	0.46
29	32.6	33.18	0.56	1.75

8. CONCLUSION

A method to generate 3D model of a spur gear has been developed using Pro/Program module of the Pro-E Wildfire. It takes only a few parameters of the gear as input to generate a complete 3D model of the gear as input. Purpose of such a program is to significantly reduce the time required for preparing a 3D model of the gear.

It models a gear with the help of mathematical calculation taken from literature. One can just change the input parameters to get CAD model of a new gear. With the help of this program automation to prepare 3D model of the gear has been achieved. This CAD model of the gear can be used for carrying out stress analysis, which has been done in this thesis.

ANSYS has been used to find contact stresses between two cylinders and results were compared with the Hertzian contact stresses. It has been found that results obtained using ANSYS are very close to a Hertzian contact stresses. Finite element method like ANSYS can be used because of the high level of accuracy. This would definitely reduce the time required for doing such an analysis as with the use of FEM systems one can achieve automation which is not possible in conventional methods.

Finite element method has been further used to calculate the bending stress between two gears. This study has been performed by taking different number of gears, which have been modeled using a program developed as part of this thesis. These results are then compared with the results obtained using AGMA standard. It has been found that use of ANSYS gives results with good accuracy witch in the acceptable limits.

It is further concluded in this thesis that preparing 3D model together with use of FEM viz. a viz. ANSYS can be used to significantly reduce the time required for design and analysis. This study would be useful for achieving automation of gear design and analysis, though presently limited automation has been attempted, the work can be further extended for achieving greater level of automation.

REFERENCES

[1] J. E. Shigley, "Mechanical Engineering Design", 2nd ed., McGraw-Hill Inc., New York, 1972.

[2] G. W. Michalec, "Precision Gearing Theory and Practice", 1st Ed., John Wiley and Sons, New York, 1966.

[3] Y. Nakasone, "Engineering Analysis with ANSYS Software", Elsevier Butterworth- Heinemann, UK, 2006.

[4] K.J. Bathe and C.L. Wilson, "Numerical Methods in Finite Element Analysis", Prentice Hall, Inc., Englewood Cliffs, NJ, 1976.

[5] B.J. Hamrock and S.R. Jacobson, "Fundamentals of Machine Elements", Eurasia Publishing House, India, 1985.

[6] http://en.wikipedia.org/wiki/Heinrich_Rudolf_Hertz (Accessed on 20th Nov., 2008).

[7] G. Lundberg, "Elastic Contact between Two Semi-Infinite Bodies", Forsch Ingenieurwes, Vol.10, 1939, pp. 201-211.

[8] R. D. Mindlin, "Compliance of Elastic Bodies in Contact, Journal of App. Mech., Vol. 16, 1949, pp.121-125.

[9] A. C. Fischer, "The Hertzian Contact Surface", Journal of Materials Science, Vol. 34, 1999, pp. 129-137.

[10] F.L. Litvin, A. Fuentes, C. Zani, M. Pontiggia and R.F. Handschuh, "Face-Gear Drive With Spur Involute Pinion: Geometry", Generation by a Worm, Stress Analysis, Comput. Methods Appl. Mech. Eng. Vol 191, No.25-26, 2002, pp.2785-2813.

[11] V.B. Math and S. Chand, "An Approach to the Determination of Spur Gear Tooth Root Fillet", ASME J. Mech. Des., Vol.126, No.2, 2004, pp. 336-340.

Concept and Guidelines of Design for Manufacturability: A Shift from Traditional Design Concept

Roshan Lal Virdi[1], Khushdeep Goyal[2] and Jatinder Madan[3]

[1&2]Department of Mechanical Engineering, Yadvindra College of Engineering, Punjabi University Guru Kashi Campus, Talwandi Sabo, Bathinda - 151 302, Punjab

[3]Department of Mechanical Engineering, Sant Longowal Institute of Engineering & Teechnology, Longowal - 148 106, Punjab

E-mail:- khushgoyal@yahoo.com

Abstract

In this century, during the time of global competition the communication between design and manufacturing is decreasing day by day. Instead of traditional over the wall approach between design and manufacturing, the companies are giving stress on design it right first time approach. In this new approach the designers are using new CAD software and tools to reduce the iterations between design and manufacturing to make products easy to manufacture. The one such important technique is Design for Manufacturability analysis. With this technique, designers are able to decrease the manufacturability problems at design stage of a product only. This not only reduces the time of manufacturing, but also gives edge on the competitors. In the present paper, we have described this emerging area of DFM, its concept and general guidelines for DFM.

Keywords: *Design process, DFM, Guidelines*

1. INTRODUCTION

Design for manufacture (DFM) is the technique of designing products with keeping in view manufacturing concepts. Its goal is to reduce costs required to manufacture a product and improve the ease with which that product can be made [1, 2]. The concept of DFM can be linked with a Frenchman, LeBlanc, who in 18th Century gave the concept of interchangeable parts in manufacturing of muskets. He successfully implemented manufacturability concepts involving tolerances and he succeeded to develop a back manufacturing process for muskets, which were repeatability manufactured with hand. After implementation of DFM, the muskets could be manufactured easily, and with much less cost and very few manufacturing errors. But, it was in the late 1990s when DFM became popular [2].

1.1 Importance of DFM

Design for manufacturability is the process of proactively designing products to

i. Optimize all the manufacturing functions: fabrication, assembly, test, procurement, shipping, delivery, service, and repair, and

ii. Assure the best cost, quality, reliability, regulatory compliance, safety, time-to-market, and customer satisfaction [3].

2. TRADITIONAL DESIGN APPROACH

The traditional design approach was "I designed it; you build it". Design engineers were either working alone or along with other design engineers only. The traditional approach was also called over the wall approach, where design engineers after making the design just passed the design to manufacturing engineers, as shown in Figure 1. The manufacturing people either ask design people to change the design or struggle to manufacture the product that was not designed for manufacturability. Mostly this delayed the time to launch the product in market, which means a huge loss. In addition to poor quality of design, product cost also affects in a great way. Researchers have shown that design costs nearly 10% while more than 80% of manufacturing costs are determined at design stage [4]. It means manufacturing people cannot control more than 20% of the cost of the product, whereas design people controls more than 80% of cost. Therefore traditional approach results in high product costs.

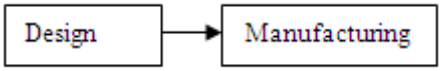

Fig. 1 Traditional design approach

3. DFM CONCEPT

Figure 2 explains the concept of DFM. First step of the new DFM process is idea generation [5]. Ideas are fleshed out into a proposal and presented to top management (or a new-product review committee comprised of key executives of all the functional areas) for screening. For major product ideas/ concepts that pass screening, management assigns representatives from relevant functional areas to a multifunctional project team for this particular new product endeavor. The team members select a leader (who might or might not be the product manager) to organize and monitor the project, guiding it through the critical path schedule developed by the team. All members do as many tasks as possible in parallel (concurrently) to shorten the product development cycle. For example, product managers can conduct focus groups on concept evaluation at the same time that engineering is conducting technical feasibility studies. The dotted line from the concept development and evaluation box to project cancellation box indicates that Concepts testing poorly should be considered for elimination as early as possible rather than investing more resources in their development [6].

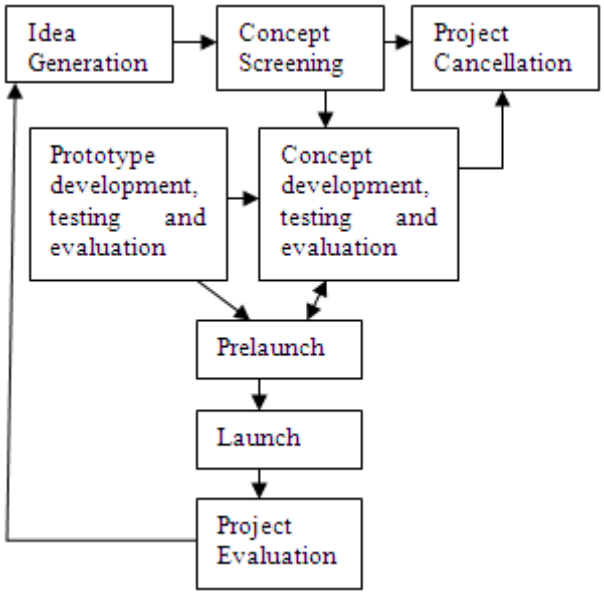

Fig. 2 DFM Approach [6]

Many industries have implemented DFM successfully. Documented evidence [6, 7] of the success of DFM indicates the possibility of:

i. Reducing product assembly time by up to 61%.
ii. Reducing the number of assembly operations by as much as 53%.
iii. Reduction of 68% in the number of assembly defects.
iv. Cutting the time to market by as much as 50%.

4. SOME KEY DESIGN FOR MANUFACTURABILITY GUIDELINES

4.1 Understand Manufacturing Problems/Issues of Current/Past Products

In order to learn from the past and not repeat old mistakes, it is important to understand all problems and issues with current and past products with respect to manufacturability, introduction into production, quality, repairability, serviceability, regulatory test performance, and so forth [3,4]. This is especially true if previous engineering is being "leveraged" into new designs.

4.2 Design for Easy Fabrication, Processing, and Assembly

Designing for easy parts fabrication, material processing, and product assembly is a primary design consideration. Even if labor "cost" is reported to be a small percentage of the selling price, problems in fabrication, processing, and assembly can generate enormous costs, cause production delays, and demand the time of precious resources.

4.2.1 Adhere to Specific Process Design Guidelines

It is very important to use specific design guidelines for parts to be produced by specific processes such as welding, casting, forging, extruding, forming, stamping, turning, milling, grinding, powdered metallurgy (sintering), plastic molding, etc. Some reference books are available that give a summary of design guidelines for many specific processes. Many specialized books are available devoted to single processes.

4.2.2 Avoid Right/Left Hand Parts

Avoid designing mirror image (right or left hand) parts. Design the product so the same part can function in both

right and left hand modes. If identical parts cannot perform both functions, add features to both right and left hand parts to make them the same.

Another way of saying this is to use "paired" parts instead of right and left hand parts. Purchasing of paired parts (plus all the internal material supply functions) is for twice the quantity and half the number of types of parts. This can have a significant impact with many paired parts at high volume.

At one time or another, everyone has opened a brief case or suit case upside down because the top looks like the bottom. The reason for this is that top and bottom are identical parts used in pairs.

4.2.3 Design Parts with Symmetry

Design each part to be symmetrical from every "view" (in a drafting sense) so that the part does not have to be oriented for assembly. In manual assembly, symmetrical parts cannot be installed backwards, a major potential quality problem associated with manual assembly. In automatic assembly, symmetrical parts do not require special sensors or mechanisms to orient them correctly. The extra cost of making the part symmetrical (the extra holes or whatever other feature is necessary) will probably be saved many times over by not having to develop complex orienting mechanisms and by avoiding quality problems.

It is a little known fact that in felt-tipped pens, the felt is pointed on both ends so that automatic assembly machines do not have to orient the felt.

4.2.4 If Part Symmetry is not Possible, Make Parts Very Asymmetrical

The best part for assembly is one that is symmetrical in all views. The worst part is one that is slightly asymmetrical which may be installed wrong because the worker or robot could not notice the asymmetry. Or worse, the part may be forced in the wrong orientation by a worker (that thinks the tolerance is wrong) or by a robot (that does not know any better).

So, if symmetry cannot be achieved, make the parts very asymmetrical. Then workers will less likely install the part backward because it will not fit backward. Automation machinery may be able to orient the part with less expensive sensors and intelligence.In fact, very asymmetrical parts may even be able to be oriented by simple stationary guides over conveyor belts.

4.2.5 Design for Fixturing

Understand the manufacturing process well enough to be able to design parts and dimension them for fixturing. Parts designed for automation or mechanization need registration features for fixturing. Machine tools, assembly stations, automatic transfers and automatic assembly equipment need to be able to grip or fixture the part in a known position for subsequent operations. This requires registration locations on which the part will be gripped or fixtured while part is being transferred, machined, processed or assembled.

4.2.6 Minimize Tooling Complexity by Concurrently Designing Tooling.

Use concurrent engineering of parts and tooling to minimize tooling complexity, cost, and delivery lead time and maximize throughput, quality and flexibility.

4.2.7 Specify Optimal Tolerances for a Robust Design

Design of Experiments can be used to determine the effect of variations in all tolerances on part or system quality. The result is that all tolerances can be optimized to provide a robust design to provide high quality at low cost.

5. CONCLUSION

The DFM concept is more than 100 years old, but it was only in later 1990s when it became popular. Its advantages over traditional design concepts are that industries can improve product efficiency by minimizing costs, which results in high profits, lesser time to market which ultimately gives edge over the competitors. In this paper the concept of DFM is discussed and along-with a number of DFM guidelines are also discussed to minimize the number of parts in a product for ease of manufacturing. It is now clear that by properly implementing DFM at design stage more than 80% of the cost of product can be easily controlled. The design guidelines discussed in this paper can be used to finalize guidelines for any kind of manufacturing process.

REFERENCES

[1] J.J. Bralla, "Design for Manufacturability Handbook", 2nd Edition, McGraw-Hill, New York, 2009.
[2] M.O. Driscoll, "Design For Manufacture", Journal of Materials Processing Technology, Vol. 122, 2002, pp 318-321.
[3] D.M. Anderson, "Design for Manufacturability and Concurrent Engineering", CIM Press, California, 2008.
[4] D.M. Anderson, "Design for Manufacturability: Optimising Cost", Quality and Time-to-Market, Paperback, CIM Press, California, 2008.
[5] L. Gorchels, "The product Manager's Handbook, NTC Business Book, USA, 1997.
[6] A.M. Belay, "Design for Manufacturability and Concurrent Engineering for Product Development", Journal of WASET, Vol. 49, 2009, pp 240-246.
[7] G. Boothroyd and P. Dewhurst, Website, www.dfma.com.

Numerical Investigation of Laminar Heat Transfer in a Plate-fin Heat Exchanger with Single V-shaped Obstacle

Munish Gupta[1], K.S. Kasana[2] and R.Vasudevan[3]
[1]Department of Mechanical Engineering, Guru Jambheshwar University of Science and Technology, Hisar, Haryana, India.
[2]Department of Mechanical Engineering,N.I.T Kurukshetra, India.
[3]RCAM Labs, SMU, Dallas, USA
E-mail-mcheeka@rediffmail.com

Abstract

A numerical investigation of laminar flow and heat transfer in a plate-fin heat exchanger with V-shaped obstacle mounted on the triangular fins is carried out in the present work. The computational domain taken is a triangular channel. The finite difference method and Marker-And-Cell algorithm has been implemented for all compuatations. The heat transfer characteristics are presented for Reynolds number 250. The V-shaped obstacle is having an angle 2â= 30º. The computational results reveal that the significant increase in heat transfer due to the longitudinal vortices formed by the V- shaped obstacle. The average heat transfer enhancement with obstacle is found to be 10% more than without the obstacle, along with moderate pressure drop.

Keywords: *Heat transfer augmentation, Ribs, Vortex generator*

1. INTRODUCTION

During recent years, serious attempts are made to apply passive methods for heat transfer enhancement in the compact heat exchangers used in automotive industry, air-conditioning,internal cooling of gas turbine blade, electronic chip cooling etc. In single phase internal flows commonly used passive heat transfer enhancement technique is the use of ribs, baffles, wings or winglet placing them as obstacle in the channel (for cooling/ heating).These obstacles produces vortex generators which disturbs the flow structure and causes heat transfer enhancement either locally or globally depending upon the type of vortices produced. Two types of vortices are produced longitudinal or transverse. Longitudinal vortices are better for heat transfer than transverse vortices [1].

2. REVIEW OF LITERATURE

A large number of experimental and computational studies has been carried out for the use of longitudinal vortex generators (LVG's) in heat transfer enhancement. Jacobi [2] has given a state of art review through the use of longitudinal vortices (LV's).The first systematic study of the use of vortex generator (wing and winglet) for heat transfer enhancement was reported by Fiebig and his coworkers [3, 4].They used liquid crystal thermography to measure the heat transfer enhancement. They found increase in local heat transfer coefficient was in order of several hundred percent and a mean heat transfer enhancement of more than 50%. Biswas *et. al.* [5] numerically studied the developing laminar mixed convection in a rectangular channel with wing-type vortex generators at Reynolds numbers of 500 and 1815. The channel wall did not have a hole under the delta wing. Biswas and Chattopadhyay [6] further extended this numerical model by including the hole under the delta wing for forced convection heat transfer. It was concluded that the delta wing with hole was slightly inferior that without hole but realistic. Biswas [7] numerically investigated the flow structure and heat transfer in a channel with a built-in-winglet type vortex generator in a fully developed laminar flow. The computed results were compared with the experimentally obtained results measured by hot-wire-anemometer. Vasudevan [8] numerically studied the potential of triangular fins having delta winglets mounted on their slant surfaces has been computed. Liou *et al.* [9] experimentally predicted detailed local Nusselt number distributions in the first pass of a sharp turning two-pass square channel with twelve different configurations of longitudinal vortex generator. The delta wing was found to be the best creating

enhancement of 170% with 30% increase in friction factor. Sohankar [10] studied 3-dimensional unsteady flow and heat transfer in a channel with inclined block shape vortex generators mounted on one side of a channel flow for different Reynolds numbers, Re= 400 and 1500. Sohankar [11] studied the unsteady flow and heat transfer using LES and DNS for a channel with two angled ribs as a vee-shaped vortex generator to enhance heat transfer. Hiravennavar *et al.* [12] investigated the flow structure and heat-transfer enhancement by a winglet pair of finite thickness. It was found that the winglet of finite thickness was superior to the zero thickness winglet. Wu *et al.* [13] presented numerical results on laminar convection heat transfer in a channel with a rectangular winglet pair punched out from the lower wall of the channel. The effect of the punched holes and the thickness of the rectangular winglet pair to the heat transfer were numerically studied. Wu [14] in extension to his earlier paper Wu *et al.* [13] presented the influences of main parameters of longitudinal vortex generator (LVG) on the heat transfer enhancement and flow resistance in a rectangular channel. Tian *et al.* [15] performed three dimensional simulations on laminar heat transfer and fluid flow characteristics of a channel with rectangular winglet pair (RWP) and delta winglet pair (DWP). The numerical results indicated that the application of LVG's enhanced heat transfer of the channel. Gupta *et al.*[16] performed a numerical study on a winglet pair in a triangular channel.

The present work concentrates on the study of steady flow heat transfer in a three dimensional flow in a triangular channel with V-shaped vortex generator mounted on the fin surface for Re=250 and Pr=0.71.

3. GEOMETRY AND MATHEMATICAL FORMULATION

The physical problem considered in this study is a three dimensional triangular channel flow (i.e., a part of a plate-fin cross flow compact heat exchanger).Two angled ribs as a V-shaped vortex generator are mounted on the fin surface. The geometry of the plane channel is similar to [8, 16] .The computational domain and grid for the ribbed channel is shown in Figure1.The flow is described in a coordinate system(x, y, z) in which the x-axis is aligned with the inflow, streamwise direction, the z-axis is in the spanwise direction and the y-axis is perpendicular to x and z axes. The V-shaped obstacle is attached on the fin surface and its angle with main flow direction is â.The length of the vortex generator is denoted by L1and the height of the vortex generators H1=0.14142.The sides of the channel are denoted L, H and B in the x,y,z direction.The leading edge of the obstacle is at X=2.66 from the inlet.

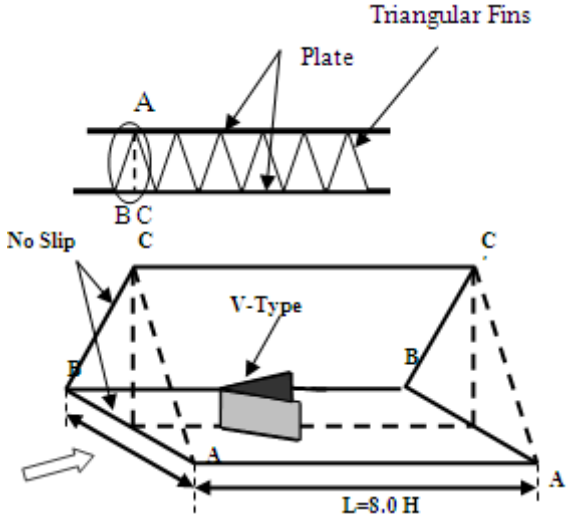

Fig.1 Computational domain with V-shape obstacle

All geometrical lengths are non-dimentionalized by H, the channel height. Velocities are scaled by U_{av}, the inflow velocity and pressure by ñU_{av}^2 .The dimensionless temperature is defined as è= $(T-T_\alpha)/(T_w-T_\alpha)$, where Tw is the constant wall temperature and T_α is the constant inflow temperature. The Reynolds number is calculated as Re=U_{av}H/õ.The staggered grid type arrangement is used. The detail is given in ref. [16].The simultaneously developing flow is considered. The uniform flow u=U, v = w = è = 0) was considered at the inlet. At the outlet boundary condition given by Orlanski [17] is considered. For the surfaces no-slip boundary conditions are considered. No slip boundary conditions on the surface of the obstacle are considered.

The continuity, momentum and energy equations in the dimensionless form for incompressible flow with constant fluid properties are considered as given below.

Continuity equation

$$\frac{\partial U}{\partial X}+\frac{\partial V}{\partial Y}+\frac{\partial W}{\partial Z}=0.0$$

Momentum equations

$$\frac{\partial U}{\partial \tau}+\frac{\partial (U^2)}{\partial X}+\frac{\partial (UV)}{\partial Y}+\frac{\partial (UW)}{\partial Z}=\frac{\partial P}{\partial X}+\frac{1}{\mathrm{Re}}\left(\frac{\partial^2 U}{\partial X^2}+\frac{\partial^2 U}{\partial Y^2}+\frac{\partial^2 U}{\partial Z^2}\right)$$

$$\frac{\partial V}{\partial \tau}+\frac{\partial (UV)}{\partial X}+\frac{\partial (V^2)}{\partial Y}+\frac{\partial (VW)}{\partial Z}=\frac{\partial P}{\partial Y}+\frac{1}{\mathrm{Re}}\left(\frac{\partial^2 V}{\partial X^2}+\frac{\partial^2 V}{\partial Y^2}+\frac{\partial^2 V}{\partial Z^2}\right)$$

$$\frac{\partial W}{\partial \tau}+\frac{\partial (UW)}{\partial X}+\frac{\partial (WV)}{\partial Y}+\frac{\partial (W^2)}{\partial Z}=\frac{\partial P}{\partial Z}+\frac{1}{\mathrm{Re}}\left(\frac{\partial^2 W}{\partial X^2}+\frac{\partial^2 W}{\partial Y^2}+\frac{\partial^2 W}{\partial Z^2}\right)$$

Energy equation

$$\frac{\partial \theta}{\partial \tau}+\frac{\partial (\theta U)}{\partial X}+\frac{\partial (\theta V)}{\partial Y}+\frac{\partial (\theta W)}{\partial Z}=\frac{1}{\mathrm{Re}^{*}\,\mathrm{Pr}}\left(\frac{\partial^2 \theta}{\partial X^2}+\frac{\partial^2 \theta}{\partial Y^2}+\frac{\partial^2 \theta}{\partial Z^2}\right)$$

The above equations were discretized with finite difference method. The Marker and cell method is used to solve the equations [18, 19].

4. RESULTS AND DISCUSSION

The effectiveness of a V-shaped vortex generator is numerically evaluated for Reynolds number 250.

Three parameters of interest in the present study are bulk temperature, Nusselt number and friction factor. The bulk temperature, given by the relation

$$\theta_b(x)=(\Sigma U\theta)/(\Sigma U)$$

It a the direct measure of the thermal energy associated with the flow. The heat transfer is measured by local Nusselt number which can be written as

$$Nu = \left(\frac{\partial \theta / \partial n}{\theta b - \theta w}\right)$$

The combined spanwise Nusselt number can be found by taking the average along the periphery. The friction factor, f is computed by pressure drop (p1-p2) across the length of the channel, as

$f = ((p1-p2)/ (0.5* \tilde{n}U_{av}2)) *(H/\triangle x)$

The fluid flows and strikes the obstacle and the pressure difference in the upstream and downstream direction takes place.Beacuse of this the counter clockwise longitudinal vortices are formed which comes in the centre of the obstacle. These vortices churn the fluid causing the increase in the mixing of the near wall fluid with the fluid in the core region. Due to the mixing the heat transfer is enhanced and this can be seen from the increase in the bulk temperature as shown in Figure2.

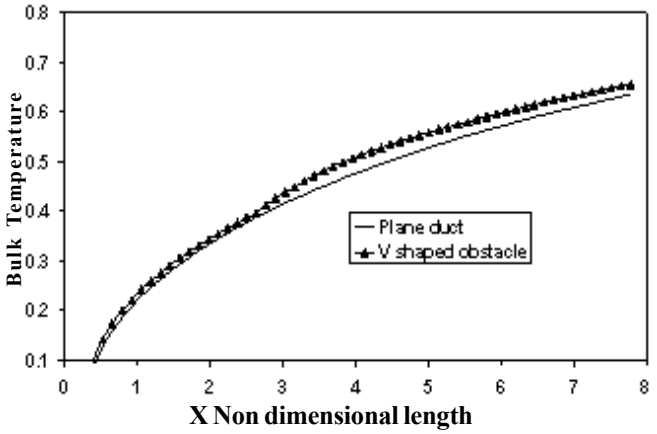

Fig.2 Bulk temperature variation along the axial direction

The local Nusselt number contours of the fin surfaces ABA' B' and BCB'C' are shown in Figures 3 and 4.The combined spanwise Nusselt number with and without obstacle is shown in Figure 5.The overall heat transfer enhancement w.r.t plane duct is found to be about 10%.

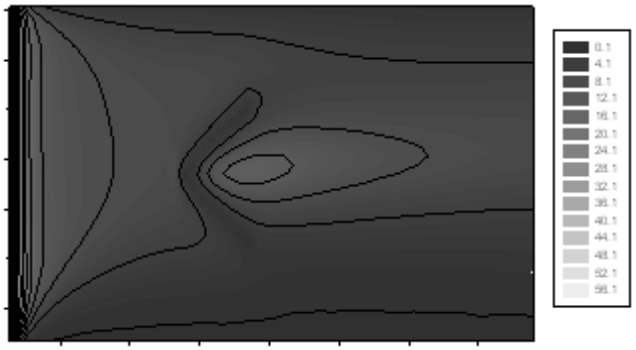

Fig. 3 Local Nusselt number for the surface ABA' B'

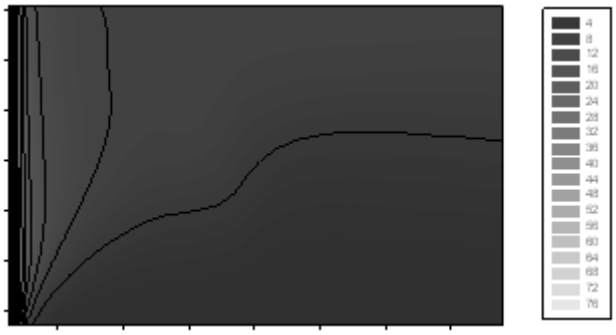

Fig. 4 Local Nusselt number for the surface BCB' C'

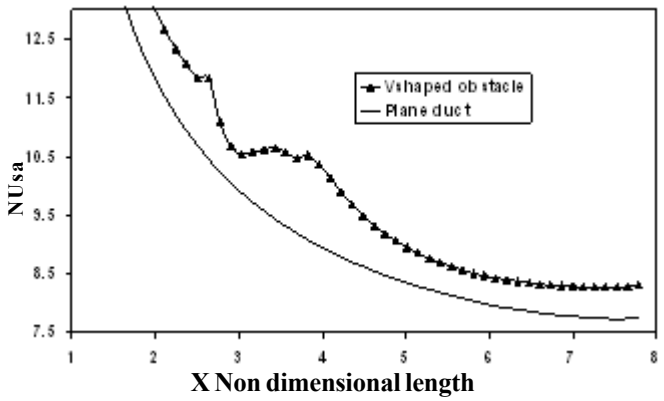

Fig. 5 Combined spanwise average nusselt number along axial direction of the channel

Finally it is well known that the enhancement in heat transfer is associated with penalty in terms of increase in friction factor leading to higher pressure drop. The distribution of friction factor along the axial direction is presented in Figures where it is clear that the presence of obstacle involves increases value of friction factor. The rise in friction factor persists even at far downstream location. Increase in friction factor even at the exit is 15% more than the plane duct.

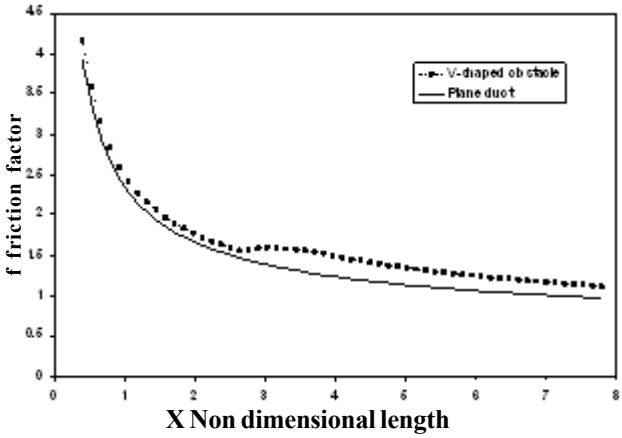

Fig. 6 Friction factor along the axial direction

5. CONCLUSION

Estimate of heat transfer enhancement in a channel due to the presence of the V-shaped obstacle was obtained using numerical simulations. The order of average enhancement with obstacle is about 10% w.r.t plane duct.However, as expected the enhancement is associated with increases friction factor.

REFERENCES

[1] Fiebig M., (1995) Embedded vortices in internal flow: heat transfer and pressure loss enhancement, International Journal of Heat and Fluid Flow, Vol. 16, pp.376–388.

[2] Jacobi A.M., Shah R.K., (1995) Heat transfer surface enhancement through the use of longitudinal vortices: a review of recent progress, Experimental Thermal and Fluid Science, Vol. 11, pp.295–309.

[3] Fiebig, M., Kallweit, P., and Mitra, N. K., (1986) "Wing Type Vortex Generators for Heat Transfer Enhancement", Heat Transfer 1986, Proc. Eighth Int. Heat Transfer Conf., Hemisphere, New York., Vol. 6, pp.2909-2913.

[4] Fiebig M, Kallweit P, Mitra N and Tiggelbeck S (1991) Heat Transfer Enhancement and Drag by Longitudinal Vortex Generators in Channel Flow. Exp. Thermal Fluid Sci., 4:pp. 103-114.

[5] Biswas, G., Mitra, N. K., and Fiebig, M., (1989) "Computation of Laminar Mixed Convection Flow in a Channel with Wing Type Built-in Obstacles", J. Thermophysics. Vol.3, pp. 447-453.

[6] Biswas, G., and Chattopadhyay, H., (1992) "Heat Transfer in a Channel with Built-in Wing-Type Vortex Generators", Int. J. Heat Mass Transfer, , Vol.35, pp.803-814.

[7] Biswas G, Torri K, Fujii D and Nishino K (1996) Numerical and experimental determination of flow structure and heat transfer effects of longitudinal vortices in a channel flow. International journal of Heat Mass Transfer, 39:pp.3441-3451.

[8] Vasudevan R., Eswaran V.,and Biswas G., (2000) "Winglet-Type Vortex Generators For Plate Fin Heat Exchangers Using Triangular Fins", Numerical Heat Transfer, Part A, Vol. 58, pp.533-555.

[9] Liou, T.M., Chen, C.C., and Tsai, T.W., (2000), "Heat Transfer and Fluid Flow in a Square Duct with 12 Different Shaped Vortex Generators," Journal of Heat Transfer, Vol. 122, pp. 327-335.

[10] Sohankar, A., and Davidson, L. (2001) "Effect of Inclined Vortex Generators on Heat Transfer Enhancement in a Three-Dimensional Channel", Numerical Heat Transfer, Part A, Vol.39, pp. 443-448.

[11] Sohankar (2007) Heat transfer augmentation in a rectangular channel with a vee-shaped vortex generator. International Journal of Heat and Fluid Flow, 28:pp. 306–317.

[12]Hiravennavar, S.R., Tulapurkara and E.G., Biswas, G., (2007) "A note on the flow and heat transfer enhancement in a channel with built-in winglet pair", International Journal of Heat and Fluid Flow, Vol.28, pp.299–305.

[13]Wu, J.M and Tao, W.Q., (2008a) "Numerical study on laminar convection heat transfer in a rectangular channel with longitudinal vortex generator. Part A: Verification of field synergy principle." International Journal of Heat and Mass Transfer, Vol. 51, pp.1179-1191.

[14]Wu, J.M and Tao, W.Q., (2008b) "Numerical study on laminar convection heat transfer in a rectangular channel with longitudinal vortex generator. Part B: Parametric study of major influence factors."." International Journal of Heat and Mass Transfer, Vol. 51

[15]Tian T.L., Ling H.Y., Gang L.Y.and Quan T.W., (2009) "Numerical study of fluid flow and heat transfer in a flat-plate channel with longitudinal vortex generators by applying field synergy principle analysis", International Communications in Heat and Mass Transfer, Vol. 36, pp.111–120.

[16]Gupta M., Kasana K.S. & Vasudevan R.,(2009) "Numerical study of effect on flow structure and heat transfer with a rectangular winglet Pair in a plate-fin heat Exchanger", Journal of Mechanical Engineering Science, Proc. IMechE U.K., Part-C, Vol.223,No. 9, pp 2109-2115.

[17]Harlow, F.H. and Welch, J.E., (1965) "Numerical Calculation of Time Dependent Viscous Incompressible Flow of Fluid with Free surface". Phys. Fluids., Vol.8, pp.2182-2188.

[18] Hirt, C.W. and Cook, J.L., (1972) "Calculating Three Dimensional Flows around Structures and over Rough Terrain", J. Comput. Phys., Vol. 10, pp.324-340.

[19] Orlanski, I., (1976) "A Simple Boundary Condition for unbounded Flows", J. Comput. Phys., Vol.21, pp.251-269.

[20] Fiebig, M., Brockmeier, U., Mitra, N. K. and Guntemann, T., (1989) "Structure of Velocity and Temperature Fields in Laminar Channel Flows with Longitudinal Vortex Generators", Numerical Heat Transfer- Part A, vol. 15,pp 103-114.

Mathematical Modeling of Exhaust Emission of a Spark Ignition Engine on LPG

Jagtar Singh, Kulwant Singh and Gurdeep Singh
Department of Mechanical Engineering, SLIET Longowal (Deemed University), Punjab, India
E-mail:- jagtarsliet@gmail.com

Abstract

Conventional fuels such as gasoline and diesel are causing serious environmental issues due to their high amount of pollutants. Moreover, emissions such as nitrogen oxides (NOx), carbon dioxide (CO_2), Hydrocarbons (HC) and so on have adverse impacts on the human body. In the present work, an attempt was made to use LPG (Liquefied petroleum gas) as substitute for conventional fuels in spark ignition engine. Varying the loads, rotational speed and fuel, a two-stroke single cylinder engine was tested. Mathematical models were developed to determine the effect of these variables on exhaust emissions. It was observed that the exhaust emission of nitrogen oxides (NOx), reduced by 63.27% and CO_2 decreased by 45.92% by using LPG as a fuel.

Keywords: *Conventional fuel, Design matrix, Exhaust emission,IC engine,Liquefied petroleum gas*

1. INTRODUCTION

Control of pollutant emissions from fuel burning engines is of major environmental concern worldwide, especially for engineers who design engine components with the aim of minimizing the exhaust emissions. Many hydrocarbon and other fuels have been tried upon IC engine, right from their inception till date in quest of alternate fuels. Even though petrol and diesel fuels are on front line of usage, laboratory and field investigations are still going on other fuels to find their suitability of substitution if not for now, but on exhaustion of prime hydrocarbons [1]. As far as low emission fuels are concerned, gaseous fuels appeared to be capable of performing a prominent role. Various gases fuels such as biogas, producer gas, hydrogen, LPG and CNG (compressed natural gas) are suitable for internal combustion engines. But LPG and CNG are considerable better alternatives because of their simpler structure with low carbon content, resulting in reduction of exhaust emissions drastically. In India, LPG is relatively more easily available compared to CNG [2]. Hence in the present work LPG was taken as gaseous fuel. The performance and drivability of LPG operating vehicles is essentially the same as gasoline operating vehicles [3]. The displacement of air by LPG causes reduction in power of 4% if compared to an equivalent gasoline counterpart. Moreover, the evaporative cooling rate and increase in air density when gasoline fuel is used provides the added power.

Engines powered by LPG are easier to start than gasoline engines in cold weather due to the earlier vaporization rate of LPG before being introduced into the engines. Furthermore LPG decreases soot formation in addition to reduction of mechanical abrasiveness and chemical degradation of the engine oil. Higher octane rating of LPG (110 to 120) allows higher compression ratio and thus help to resist engine knocks better than gasoline. However, a liter of LPG consists of 28% less energy than a liter of gasoline, which means that more consumptions of LPG is needed to provide same vehicle power than that of a gasoline engine. According to the research, LPG fueled vehicle owners need to install a slightly bigger tank in order to achieve the same driving range as gasoline vehicles [4].

The major objective of this study is to develop the model of exhaust emissions by varying the spark ignition engine parameters such as load, rpm and type of fuel. Two different levels are considered for each factor as Table 1.

2. PLAN OF INVESTIGATION

The investigations were planned according to the steps given below:

2.1 Design of Experiment

A two level factorial design of ($2^3 = 8$) eight trials, which is a standard statistical tool to investigate the effects

of number of parameters on the required response, was selected for determining the effect of three independent SI engine parameters. The commonly employed method of varying one parameter at a time, though popular, does not give any information about interaction among parameters. The selecting of two level factorial design also helped in reducing experimental runs to the minimum possible.

2.2 Identifying Critical Process Control Variables

Load (L), speed of engine (R) and type of fuel used (F) were identified as critical SI engine parameters for carrying out the experiment work and to find their effect on exhaust emissions. All remaining variables were kept constant.

2.3 Selection of Two Levels of Engine Parameters

The working range covering the lowest and the highest level of the variables was carefully selected by carrying out the trial runs so as to maintain defect free experimentation. Upper and lower levels of the variables were found out.

The direct and indirect parameters except under consideration were kept constant. The upper level was coded as (+1) and lower level as (-1) or simply (+) and (-). For the factors with a continuous determination region, this can always be done with the aid of transformation with in the variation interval.

$$X_j = \frac{X_{jn} - X_{j0}}{j_j} \qquad (1)$$

Where, X_j, X_{jn}, and X_{jo} are the coded, natural and basic value of the parameter respectively. J_j and j are the variation and number of parameters respectively. The units, symbols used and limits of engine parameters are given in Table 1.

2.4 Development of Design Matrix

The design matrix developed to conduct the experimentation as shown in Table 2 For the sake of further simplicity the parameters from X_1 to X_3 were represented by subscripts 1 to 3 through out this work. The signs under the columns 1, 2, 3 were arranged in standard Yate's order [5].

Table 1 Experiment Factors and Levels

Factor	Description	Low Level	High Level	Type
A	Load	01 kg	03 kg	Numeric
B	Engine rotation speed	800 rpm	3200 rpm	Numeric
C	Type of fuel	LPG	Petrol	Categorical

3. EXPERIMENTAL DETAIL

The experiment was conducted in th Thermal Engineering lab, SLIET Longowal, District Sangrur, Punjab. Before running the original experiment, few pilot runs were carried out to observe the response variable (exhaust emission) and to check the variability in the system. These runs provided consistency in the experimental data. The experiment was conducted in a random order as planned.

Table 2 Design Matrix

S.No	L 1	F 2	r 3
1	+	+	+
2	-	+	+
3	+	-	+
4	-	-	+
5	+	+	-
6	-	+	-
7	+	-	-
8	-	-	-

A Scooter engine is used as the test engine for analysis. Some modifications of the engine are made so that it is possible to switch between LPG and gasoline as the burning fuel and to ease the experiment process. For instance, a mixer is introduced in the generator set so that it is compatible to both LPG and gasoline fuel. The mixer allows air and LPG to mix together to obtain the correct ratio before entering the combustion chamber. It is a cross flow type mixer, which is connected to the LPG steel tank via a flexible hose. Besides that, due to fact that LPG has lower velocity flame and hence burns slower compared to gasoline, shortening the gap between the electrode and insulator nose advanced the spark timing. Spark advance control timing gives the maximum engine efficiency by continuously adjusting the spark timings to deliver peak combustion pressure. For the purpose of data collection of pollutant emissions from the engine using both LPG and gasoline, a commercial

portable exhaust gas analyzer was employed to measure the content of exhaust gas emissions such as NOx, CO_2, and HC at different loads in a closed environment.

The engine was running at different variables during each run order (for example: on maximum speed and at maximum load 3 kg; the petrol as a fuel used). The emission exhausted by the engine in each block and replicate was considered as the response variable.

The complete set of eight trials was repeated thrice for the sake of determining the 'variance of optimization parameter' and 'variance of adequacy' for this model. The experiments were performed in a random order in order to avoid any systematic error.

3.1 Selection of Mathematical Model

The models of the type Y = f (L, R, R) could be developed to facilitate the prediction of a response within the specified dimensional tolerance for a particular set of direct process parameters.
Assuming a linear relationship in the first instance and taking into account all the possible two factor interaction and confounded interactions, it could be written as:

$$Y=b_o+b_1L+b_2R+b_3F+b_{12}LR+b_{13}LF+b_{23}RF \quad (2)$$

Where: LF= combination of type of load and fuel
RF = combination of type of rpm and fuel
LR = combination of load and rpm

3.2 Development of Model

Models were developed by the method of regression. Adequacy of the model and significance was tested by the analysis of variance technique and student's't' test

3.2.1 Evaluation of the Coefficients

The regression coefficients of the selected model were calculated using Equation 3. This is based on the method of least squares [8]. Various coefficients are to be based on Table 3.

$$b_j = \frac{\sum_{i=1}^{N} X_{ji} Y_i}{N}, j = 0,1,2---,k \quad (3)$$

Where,
X_{ji} = Value of a factor or interaction in coded form
Y_i = Average value of response parameter
N = Number of observations
K = Number of coefficients of the model.

Table 3 Coefficients of Model

Sl.No.	Coefficient	Due to
1	b0	Combined effect of all Parameters
2	b1	Load
3	b2	Type of Fuel
4	b3	Engine Spedd rpm
5	b12	Interaction of L & F
6	b13	Interaction of L & r
7	b23	Interaction of F & r

Table 4 Analysis of Variance

Degrees of Freedom		Variance of Adequacy	Variance of Response	'F' Ratio Model	'F' Ratio Table	Adequacy of Model
f	N	S^2ad	S^2Y	$F = \frac{S^2ad}{S^2Y}$	At 4,8,0.5	Whether $F_m < F_t$
4	8	1.62	4.187	0.386	3.8	yes

3.2.2 Adequacy of the Developed Model

The adequacy of the model was determined by the analysis of variance technique. The regression coefficients were determined by the method of least square, from which the F-ratio for the polynomial was found. The variance of the response and the adequacies were calculated. The 'F'- ratio of the model were compared with the corresponding 'F'- ratio from the standard table and it was found that the model is adequate within 95% level of confidence, thus justifying the use of assumed polynomials.

After calculating the coefficients of model, it must be tested for its fitness. Thus adequacy of the model was tested using analysis of variance technique. For this, variance of optimization parameter (S^2y) was determined. Details of the analysis of variance are given in Table 4.

3.2.3 Significance of Coefficients

The statistical significance of the coefficients can be tested by 't' test. The level of significance of a particular parameter can be assessed by the magnitude of the 't' value associated with it. Higher the value of 't', the more significant it becomes. 't' values for the given coefficients of the models were calculated using following formula:

$$t = \frac{lb_j I}{S_{bj}} \qquad (4)$$

Where,

$lb_j I$ = absolute value of coefficients

S_{bj} = standard deviation of coefficients

$$S_{bj} = \sqrt{\frac{S^2 y}{N}}$$

Calculated 't' values were compared with the t-table value and statistically insignificant terms of the models were dropped. The value of 't' from the standard table for eight degree of freedom and 95% confidence level is 2.306. Coefficients having calculated 't' value less than or equal to 't' value from the standard table for eight degree of freedom and 95% confidence level, are the members of reference distribution i.e. due to the intrinsic variations of the experimentation and hence, they can not be significant.

4. RESULTS AND DISCUSSION

The proposed model for the prediction of NOx, CO_2 and HC emissions was obtained by dropping statistically in-significant terms from the developed models.

$$Y_{NO_x} = 27.375 + 6.125\ L + 7.875\ f + 2.875\ Lf$$

The hypothesis adopted for identifying the parameters, which were mainly and predominantly responsible for the interaction effect in a confounded pattern was to first drop those interactions that were due to the parameter having insignificant effects and if there were still two or more interactions left in the confounded pattern then the interaction due to parameter which the most predominant effect was selected. The mathematical models furnished above can be used to predict the exhaust emissions of two stroke SI engine.

Figure 1-3, shows the emission of NO_x v/s speed-load, type of fuel-load and type of fuel-rpm respectively. It was observed that at maximum range of speed-load, the emission of NO_x was 47.6 ppm and at minimum range of speed-load it was13.25 ppm. When maximum range of fuel- load was used then 44.25ppm and at minimum range fuel-load it was 16.25ppm. So the graph shows that the emission of NO_x reduces to 48.58% by using LPG as a fuel and applying maximum load. Further by decreasing load to minimum, the approximate emission of NO_x was decreases 63.27 %.

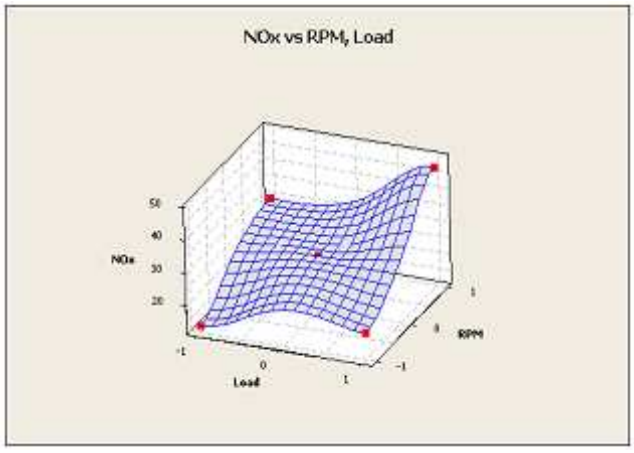

Fig.1Emission of NO_x v/s RPM and Load

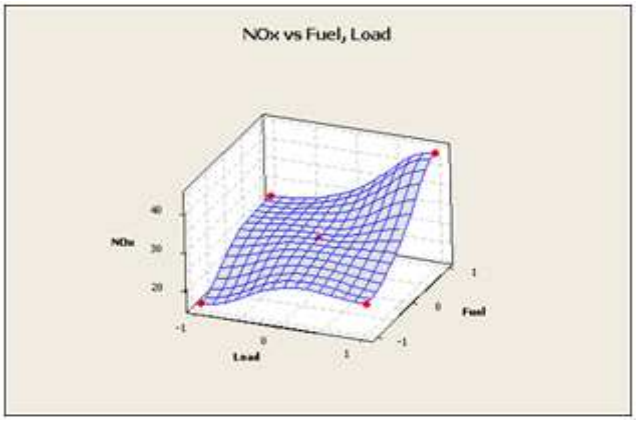

Fig.2 Emission of NOx vs Type of fuel – Load

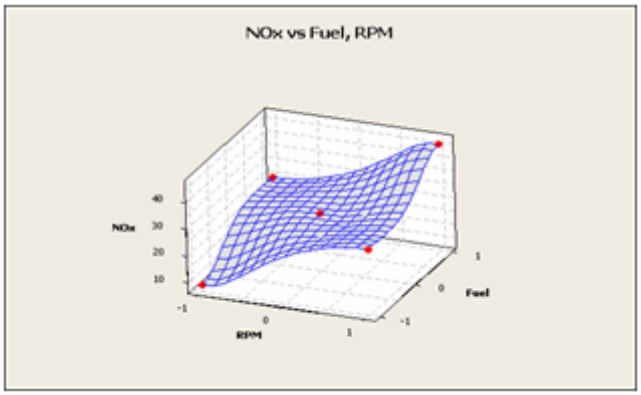

Fig. 3 Emission of NOx v/s type of fuel and rpm

Figure 4-5 shows the emission of CO_2 v/s speed- load, type of fuel-load respectively. It was observed that at maximum range of speed-load emission of CO_2 5.59%, by keeping minimum speed, load remains same at maximum range, it was 3.75% .By keeping maximum range of fuel-load was used then 5.69% and at minimum range fuel-load it was 3.077% which shows percentage decrease of 45.92%.

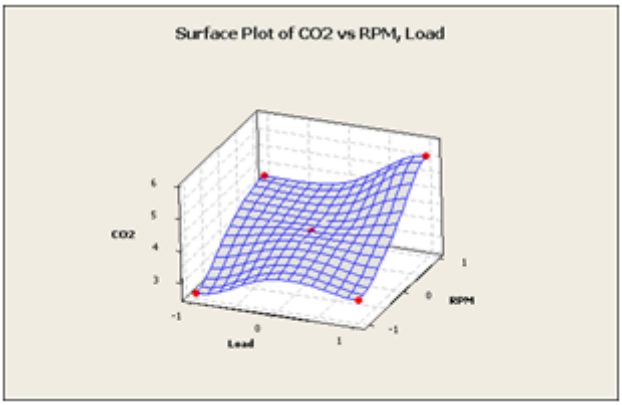

Fig. 4 Emission of CO_2 v/s Speed – Load

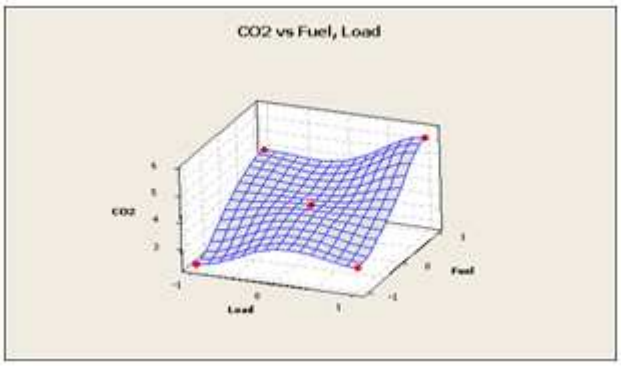

Fig.5 Emission of CO_2 v/s Fuel-Load

Figure 6 shows the emission of HC v/s fuel-load. It was observed by maximum load and petrol as a fuel, the emissions of HC was 1598.25 ppm, at the same load and LPG as a fuel, the emissions was 9951.25 ppm, which shows the increase of 80% HC.

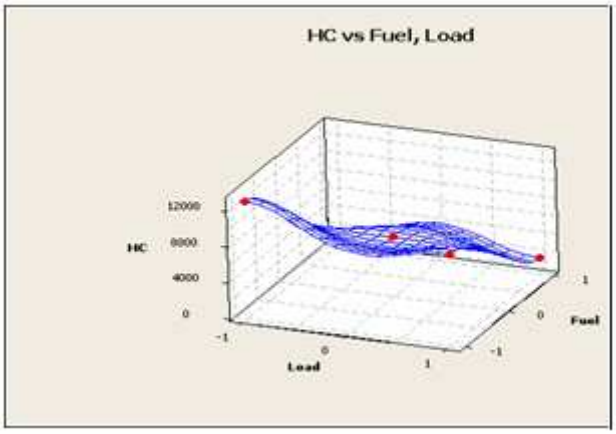

Fig. 6 Emission of HC v/s Fuel -Load

Figure 7 shows the emission of HC v/s fuel-rpm. By keeping maximum speed and petrol as a fuel the emissions of HC was 1283.13 ppm and by considering LPG as fuel the emission of HC was 10505.87ppm, which means increase of approx. 87%.

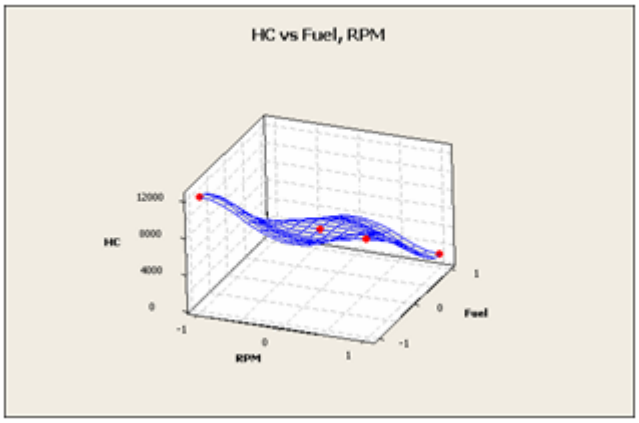

Fig. 7 Emission of HC v/s Fuel - Speed

High HC emission normally denotes excessive unburned fuel caused by a lack of ignition or by incomplete combustion. LPG gas, which enters the combustion chamber in gaseous form, may be forced out of the exhaust during the engine scavenging process to force exhaust air out so that fresh air can replace them. Some of the unburnt propane may be flushed into the exhaust and causes the HC emission level of LPG system to be high. Besides that, another reason for the high HC emission of LPG fuel system might be due to improper timing or dwelling in the combustion chamber.

5. CONCLUSIONS

On the basis of the present work following conclusions drawn:

i. Two level factorial designs is found to be effective tool to investigate the interaction effect of parameters on the required response.
ii. Proposed model is adequate at 95% confidence level, thus justifying the use of assumed polynomials.
iii. The emissions of Nitrogen Oxide (NO_x) is decreased 63.27% when we using LPG as a fuel.
iv. The emission of CO_2 is decreased 45.92% when we using LPG as a fuel.
v. The emission of Hydrocarbon (HC) increases 87% when we using LPG as a fuel.

REFERENCES

[1] V Ashok, Sikander Mohammed and Mohammed Najmul Islam Khan, "Experimental Investigation on use of Welding Gas (acetylene) on SI Engine", Advances in Energy Research, 2006, pp. 11-16.
[2] PB.Reddy, N Kapilan and RP. Reddy, "Experimental Investigation of Esters Mahua Oil as An Alternative Fuel for Dual Fuel Engine", Journal of Institute of Engineers (India). Mechanical Engineering Division, Vol 89, 2008, pp.7-11.
[3] S. R. Turns, "Introduction to Combustion", McGraw-Hill Inc., Singapore, 1996.
[4] National Propane Gas Association 2005, Liquefied Petroleum Gas 48 Years Old, National Propane Gas Association, United States, Viewed, 22 March 2005, http://www.npga.org/files/public/BPN_LPG_Early_History_1-53.pdf
[5] D. C. Montgomery, "Design and Analysis of Experiments", Wiley India (P) Ltd., 4435/7, Ansari Road, Daryganj, New Delhi, 2007.
[6] M.A.D. Santos, "Energy Analysis of Crops used for Producing Ethanol and Co_2 Emissions", Energy Planning program, Brazile.
[7] Southern Technologies, "Environmental Concerns for Combustion Equipment", Southern Technologies Inc, Florida, United States. http://www.southerntechnologies.com/emissions.htm., 2005
[8] Prabhjot Singh, Gurdeep Singh and Manpreet Singh, "Analysis of Exhaust Emissions of SI Petrol Engine using LPG", A Project Report Submitted to Mechanical Engineering Department, SLIET Longowal, Punjab, India.
[9] V.P. Sethi and K.S.Salariya, " Exhaust Analysis and Performance of Single Cylinder Diesel Engine Run to Dual Fuel", Journal of Institute of Engineers (India). Mechanical Engineering Division, Vol 85, No.1, 2004, pp.1-7.

Improvement of Carbon-carbon Composite Properties using VGCNFs/CNTs

Dhruv Bansal[1] and M. L. Bansal[2]
[1]University of Alabama Birmingum, USA
[2]Department of Civil Engineering, College of Agricultural Engineering & Technology, CCS,
Haryana Agicultural University, Hisar

Abstract

The effect of adding VGCNFs and surfactant to the Carbon/phenol composite on its flexural strength and flexural modulus was studied. For this two sets of composites were made, in set - I the concentration of surfactant was varied from 0%, 12 % and 50 % keeping the concentration of VGCNFs constant at 1 %. In set –II the concentration of VGCNFs was varied from 0 %, 0.5 % and 1 % keeping the concentration of surfactant constant at 12.5 %. A composite was also made by directly mixing 1% VGCNFs to the phenol resin with no surfactant. Addition of 1% VGCNF with 12.5% surfactant treatment gave the maximum flexural strength of 0.56GPa and maximum flexural modulus of 48GPa and the maximum short beam strength of 39 MPa.

Keywords: *Carbon composites, Flexural modulus, Flexural strength,VGCNF*

1. INTRODUCTION

Carbon -Carbon composites are advanced composites used for variety of applications. They were initially developed for American defense and space industry funded by American government [1]. In carbon composites carbon fibers are bonded together in carbon matrix. The matrix could be obtained by either chemical vapor deposition of the carbon particles, chemical vapor infiltration or carbonization of thermo-set or thermoplastic pitches which are infiltrated into the fibrous skeleton to obtain the carbon fiber reinforced composite. They have unique properties of low density, high thermal conductivity and shock resistance, low thermal expansion and high modulus [2].

The mechanical, electrical and thermal properties of the composites are enhanced by using vapor grown carbon nano fibre / carbon nano tube (VGCNFs/CNTs) either as reinforcement of as a filler compounded with thermo-sets or thermoplastics. Range of properties of Carbon - carbon composites as compared to ferrictic steel are compared as in Table1.

Different properties of fillers VGCNFs and CNTs used for making C/C composites are compared as in Table 2By varying the feedstock composition and furnace operating conditions, different thickness of VGCNF's can be produced. VGCNFs are hollow core single or double layer graphite planes nanofibers [3].

Table1Range of Properties of Carbon - Carbon Composites as Compared to High Performance Metal Alloys

Property	Carbon-Carbon	Ferritic Steel
Compressive Strength	100-150	240-400
Density	1.3-2.5	7.5-7.7
Tensile Strength	~900	500-800
Thermal Expansion	-2-2 × 10^{-6}	12-15× 10^{-6}
Thermal Conductivity	20-150	23-27
Thermal Shock Resistance	150-170	5.5
Young's Modulus	~300	200-205

The three fold increase in tensile strength and modulus can be achieved with even more in the case of compressive strength. The most important contribution of the VGCNFs/CNTs is that they make the plastics conducting. Resistivity as low as 0.15 can be achieved by fiber loading of 15% and a percolation threshold of below 1% is possible. Also a tenfold improvement in thermal properties can be achieved as in the case of epoxy resins. In short, well dispersed and uniformly distributed VGCNF/CNT with high aspect ratio, strong adhesion between fiber and matrix interface for better mechanical properties and lower cost are key factors in producing high quality VGCNF/CNTs/polymer composites for widespread commercial use. It was observed that the diffraction pattern of the graphitized VGCNFs is somewhat symmetric due to graphitization

of concentric outer layer of pyrolytic carbon of VGCNFs [4]. Single walled nanotubes are individual cylinders of 1-2 nm in diameter which are actually a single molecule. Multi walled nanotubes are collection of several concentric graphene cylinders, a "Russian doll" structure, where weak Waals forces bind the tubes together [5]. All failure modes in nanofillers reinforced composites were reported [6]. In the present manuscript the effect of adding VGCNFs and surfactant to the Carbon/phenolic composite on its flexural strength and flexural modulus was studied.

Table 2 Typical Properties of VGCNFs and CNT

Property	VGCNFs	SWNTs	MWNTs
Diameter (nm)	50-200	0.6-1.8	5-50
Length (μm)	50-100	-	-
Aspect Ratio	250-2000	100-10000	100-10000
Density (g/cm^3)	2	~ 1.3	~ 1.75
Thermal Conductivity (W/mK)	1950	3000-6000	3000-6000
Electrical Resistivity (ohm.cm)	10^{-4}	10^{-3} to 10^{-4}	2×10^{-3} to 10^{-4}
Tensile Strength (Gpa)	2.92	50-500	10-60
Tensile Modulus (GPa)	240	1500	1000

2. EXPERIMENTAL DETAILS

Two sets of composites were made in set - I the concentration of surfactant was varied from 0%, 12 % and 50 % keeping the concentration of VGCNFs constant at 1 %. In set - II the concentration of VGCNFs was varied from 0 %, 0.5 % and 1 % keeping the concentration of surfactant constant at 12.5 %. A composite was also made by directly mixing 1% VGCNFs to the phenolic resin with no surfactant.

2.1 Desizing and Surfactant Treatment

Eight plies measuring 6 inches by 6 inches of carbon satin fabric were cut for each composite and desized using acetone (completely immersed) for 15 hours followed by surfactant (Triton X-100) treatment for 24 hours. Surfactant concentration was taken with respect to the volume of acetone used. After that fabrics were dried in air.

Set-I

1% VGCNF	0% surfactant
1% VGCNF	12.5% surfactant
1% VGCNF	50% surfactant

Set-II

12.5% surfactant	0% VGCNF
12.5% surfactant	0.5% VGCNF
12.5% surfactant	1% VGCNF

2.2 Spraying of VGCNF'S & Drying Dispersion of VGCNF'S

A known weight of VGCNFs according to the required concentration was dispersed in DMF using ultrasonic bath for two intervals of 7 minutes each. The dispersion ratio of 0.5 grams of VGCNFs per 75 ml of DMF was maintained.

2.2.1 Spraying and Drying

The prepared dispersion was sprayed on the eight fabric layers by means of an air spray gun giving a fine uniform layer of VGCNFs on the fabric plies. After spraying the wet sheets were dried in furnace for 30 min at 160^{0}C to evaporate the DMF from the plies (Boiling pt. of DMF is 153 ^{0}C).

2.3 Making of Composite by Hand Layup

VGCNFs sprayed plies were made into a composite by infusing about 200 grams of phenolic resin mixed with catalyst in the ratio 100:8. The composite was left under vacuum for 24 hours to get the prepreg.

2.4 Curing

The prepreg formed was cured in the curing press by applying a pressure of 40 psi and the temperature was varied from 60^{0}C to 90^{0}C at the rate of 10^{0}C/2 hours. So, it took eight hours to cure the composite.

2.5 Flexure Testing

Small strips of required dimensions were cut depending on the thickness and flexure testing was done to get the flexural strength and flexural modulus according to ASTM C393. Obtained results were analyzed.

3. RESULTS AND DISCUSSION

3.1 Effect On Flexural Strength of Different Surfactant Concentration Keeping VGCNF Concentration Constant at 1%

Addition of 12.5 % surfactant to 1% VGCNF increased the flexural strength by 16.5% compared to sample without surfactant. However, doubling the concentration of surfactant to 50% did not have any appreciable effect on the strength as compared to 12.5% surfactant increasing it to 13%.

3.2 Effect on Flexural Strength of Different VGCNF Concentration Keeping Surfactant Concentration Constant at 12.5%

Adding 0.5% VGCNF of the weight of the resin used in the composite decreased or had no significant effect on the flexural strength of the composite as compared to the sample with no VGCNFs but adding 1 % VGCNFs to the composite increased the strength by 18.75% as compared to composite with no VGCNF.

Directly mixed VGCNF to phenolic resin composite however gave the highest strength at 660MPa.

3.3 Effect on Flexural Modulus of Different Surfactant Concentration Keeping VGCNF Concentration Constant at 1%

Addition of 12.5% surfactant to 1% VGCNF increased the flexural modulus of the composite by 20.68%. Doubling the concentration to 50% didn't show appreciable increase as compared to flexural modulus of 12.5% surfactant treated composite.

3.4 Effect on Flexural Modulus of Different VGCNF Concentration Keeping Surfactant Concentration Constant at 12.5%

Addition of 0.5% VGCNF decreased the modulus by 42.3% and addition of 1% VGCNF decreased the flexural modulus by 11.53% as compared to composite with 12.5% surfactant treatment and no VGCNFs. Directly mixed VGCNF composite strangely gave the highest value of flexural modulus of 54GPa.

Addition of 1% VGCNF with 12.5% surfactant treatment gave the maximum short beam strength of 39 MPa which was 14.3% more as compared to the composite made with no surfactant used.

With the further increase in surfactant concentration to 50 % the short beam strength decreased to 27.5 MPa which was about 29.48% lower than the maximum value obtained.

4. CONCLUSION

Addition of 1% VGCNF with 12.5% surfactant treatment gave the maximum flexural strength of 0.56GPa and maximum flexural modulus of 48GPa and the maximum short beam strength of 39 MPa.

REFERENCES

[1] W. Torsten and B. Gordon, "Carbon-carbon Composites: A Summary of Recent Developments and Applications", Materials and Design, Elsevier Science Ltd. Oxford, Engl., 1997.

[2] Tibbetts, G. Gray, Lake, L. Max , Karla Strong and P. Brian Rice, "A Review of the Fabrication and Properties of Vapor-grown Carbon Nanofiber/ Polymer Composites", Composites Science and Technology, Elsevier Ltd., Oxford, OX5 1GB, United Kingdom, 2007.

[3] AI-Saleh, H. Mohammed and Uttandaraman Sundararaj, " A Review of Vapor Grown Carbon Nanofiber/Polymer Conductive Composites", Carbon, Elsevier Ltd, Oxford, OX5 1GB, United Kingdom, 2009.

[4] S.R. Dhakate, R. B. Mathur and T.L. Dhami, "Development of Vapor Grown Carbon Fibers (VGCE) Reinforced Carbon/carbon Composites", Journal of Materials Science, Kluwer Academic Publishers, Dordrecht, 3311 GZ, Netherlands, 2006.

[5] O. Breuer, Uttandaraman Sundararaj, "Bir Returns from Small Fibers: A Review of Polymer/carbon Nanotube Composites", Polymer Composites, John Wiley and Sons Ltd., Chichester, West Sussex, PO19 8SQ, United Kingdom, 2004.

[6] E.T. Thostenson, C.Li and T.W. Chou, "Nanocomposites in Context", Composites Science and Technology, Elsevier Ltd., Oxford, OX5 1GB, United Kingdom, 2005.

Effect of Mechanical Stress on the Generation of Thermo - EMF for Copper - Constantan Thermocouple

Jaspal Singh and S.S. Verma
Department of Physics, Sant Longowal Institute of Engineering and Technology (Deemed to be University), Longowal, Sangrur -148 106, Punjab
E-mail: jaspalsliet@yahoo.com

Abstract

The mechanical stress on the thermoelectric materials may cause some interactions with the phonon waves controlling the heat transfer in metals but at the same time the electron wave (electrical conductivity) may remain unaffected. This paper presents the effect of mechanical stress on the generation of thermo-emf for Copper-Constantan thermocouple. The generation of thermo emf is studied for the temperature difference between cold and hot junction in a wide temperature range of 22^0C to 282^0C from the waste heat recovery point of view. The load in a range from 250-500gm is applied individually and simultaneously on both the thermoelectric wires. The increasing load results in the enhancement of thermo-emf for a specified temperature range.

Keywords: *Mechanical stress, Thermoelectricity, Thermocouple, Thermo-emf*

1. INTRODUCTION

Thermoelectricity is an old technique to convert the heat into electricity by the advent of thermocouples and in present day of energy crisis thermoelectricity is proposed strongly a mean for the utilization of low grade waste heat available all around us [1-4]. Thermo-emf strongly relates to electrical & thermal conductivities of thermocouple materials. For better performance, electrical conductivity should be more where as thermal conductivity should be less but both these properties go hand in hand. A lot of heat energy gets wasted in various energy producing and utilizing devices, especially in cars with gasoline engines and in residential systems. Only 25% fuel energy is utilized and the remaining gets waste as heat and residential systems [1-4]. With the growing energy crisis, efforts are to be made to utilize waste heat. Besides waste heat utilization for electric generation, it will also prevent some unexpected effects of waste heat in various devices/instruments. The main advantages of thermoelectric conversion such as pollution free, no moving parts, no toxic materials, simple designing, reliable and no complexity of equipments implementation make it more attractive as compared to any other techniques. Due to these all beneficial aspects, researchers are continually trying to improve the performance of thermocouples and hence to enhance the generation of thermo-emf. Nanotechnology is the latest to improve the thermoelectric performance such as by the silicon nano-wires [5].

One of the important aspects of thermoelectricity is the coefficient of performance of a thermocouple, which is also known as the figure-of-merit and is denoted by

ZT and its expression is: $ZT =$, where 'á' is the

Seebeck coefficient in 'μV/K'; 'σ', the electrical conductivity of thermoelectric materials in Simen meter-1(Sm^{-1}); 'λ', the thermal conductivity of the materials in $WK^{-1}m^{-1}$ and 'T' , the temperature difference between hot and cold junctions of a thermocouple. It is clear that the figure-of-merit of a thermocouple is affected directly by the electrical conductivity but inversely by the thermal conductivity of the thermoelectric material. Hence to improve the coefficient of performance, the electrical conductivity should be increased whereas the thermal conductivity should be reduced.

It is proposed by researchers [6-8] that heat is transferred inside the thermocouple wires in the forms of phonon waves along with electron motion. The effect of mechanical stress on the thermo-emf generation for particular thermocouples have been discussed earlier also by many workers [6-8]. In present research work, we also investigated the effect of mechanical stress on the

coefficient of performance (ZT) of a copper-constantan thermocouple. A Copper-Constantan thermocouple with its specifications given below in table 1 was selected in the present investigations due to its easy market availability and cheap cost to realize its use in waste heat recovery. However, characterization of thermocouple materials is important to determine the effect of material compositions to finalize the maximum performance. The present investigations will conclude the effect of mechanical stress in order to utilize waste heat by the advent of cheap thermocouple with maximum thermo-emf generation conditions.

Table1Specifications of the Thermocouple

Physical Quantity	Copper- Constantan	
	Copper	Constantan
Length	55.5×10^{-2} m	55.5×10^{-2} m
Radius	2.35×10^{-4} m	1.015×10^{-4} m
Area of cross section	1.74×10^{-7} m^2	3.23×10^{-8} m^2
Resistance	0.150 ohm	1.221 ohm
Resistivity	4.7×10^{-8} Ωm	7.1×10^{-8} Ωm
Electrical Conductivity	2.134×10^{7} Sm^{-1}	1.41×10^{7} Sm^{-1}

2. EXPERIMENTAL PROCEDURE

All the experiments are performed in a well refined arrangement as shown in Figure 1. The whole experimental setup is discussed as follows:

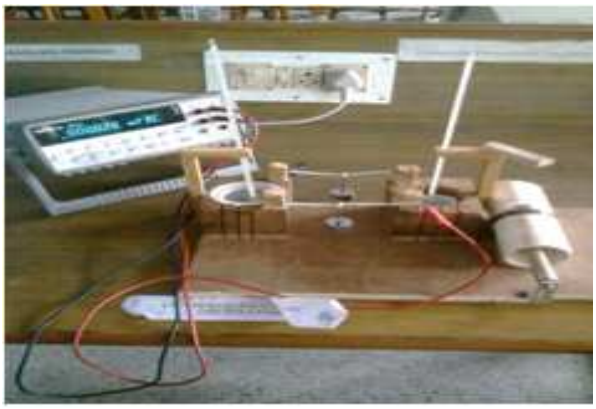

Fig. 1: Experimental set up

2.1 Heating and Cooling Arrangement

Mercury (Hg) having boiling point about 357^{0}C with all suitable properties of best heat transfer/contact is used to maintain the temperature of hot junction. First of all, mercury is heated in a crucible (THIASIL®) at the electric hot plate up to a temperature of 340^{0}C and then put in a wooden block (Figure 1). The hot mercury crucible is fitted with a thermometer and one end of the thermocouple is dipped in this to make it as a hot junction. Cold junction is maintained in contact with water at room temperature in other crucible. The fresh tap water is poured time to time to maintain a constant temperature (28^{0}C). Thus, thermo-emf measurements are possible for a junction temperature difference in the temperature range of 500 to 310^{0}C.

2.2 Thermo EMF Measurements

The thermo-emf produced across the thermocouple at various temperatures is measured using a digital multi-meter (HP 34401A) with a reading capacity up to six decimal places.

2.3 Application of Mechanical Stress

The mechanical stress (force/area) is applied, represented in the present investigations in terms of load on both insulated thermoelectric wires using normal steel hangers. The 50gm weights are repeated to extend the range from 250gm to 500gm. The normal fixers are used to get hold of the wooden blocks in order to prevent any possible movement.

3. RESULTS AND DISCUSSION

First of all, the thermo-emf for the selected copper-constantan thermocouple is investigated under the normal conditions i.e. without any load. Figure 2 shows the experimental curve of thermo-emf with temperature difference under normal conditions. Without any stress the maximum experimental value of thermo-emf equal to 3.647mv is obtained for a temperature difference of 62^{0}C and 0.216mv is minimum at the temperature difference of 22^{0}C. Erratic behavior of thermo-emf generation at higher temperature difference of thermocouple junctions may be assigned to a competition between phonon wave mode and electron mode of heat transfer.

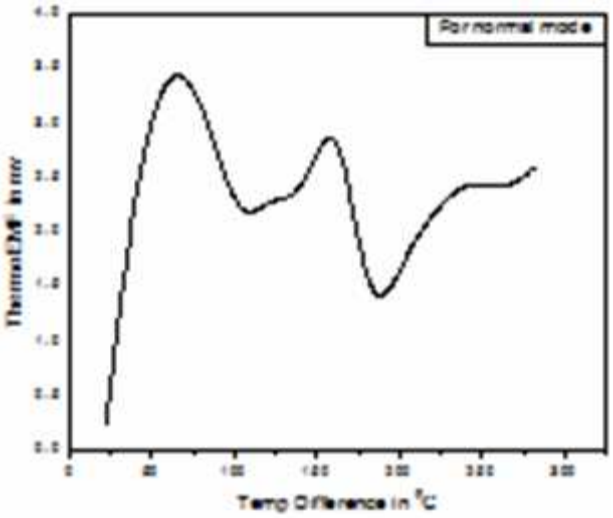

Fig. 2 Thermo-emf generation without load

When a load is applied, the results shown in Figure 3 indicate that with a load of 250gm, 300gm, 350gm or 400gm, the thermo emf enhances in the higher temperature range (from a temperature difference of 182 ^{0} to 282^{0}C). Below the temperature difference of 182^{0}C, the thermo-emf falls in comparison to normal mode expect for few temperatures in between. But for the load of 400gm, the thermo-emf is more than the normal modes up to the temperature difference of 102^{0}C. Approximately, a similar behavior is observed for the load of 460gm.

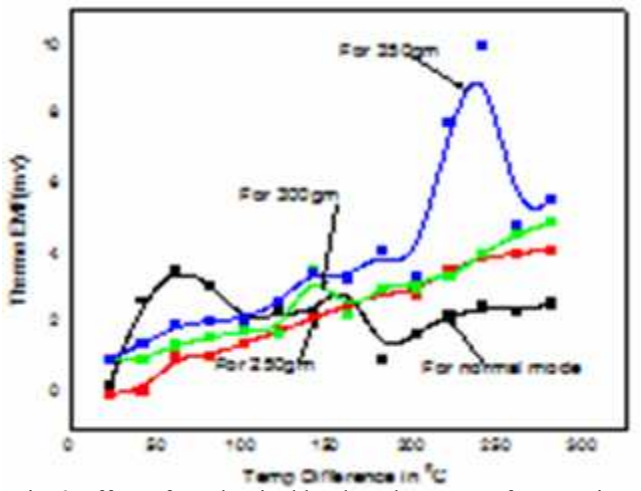

Fig. 3 Effect of mechanical load on thermo-emf generation

Similar observations for higher mechanical load are shown in Figure 4. The remarkable effect is for a load of 500gm, for which the thermo emf enhances for the entire temperature range. In this case, the maximum thermo-emf value is 5.5116mv at 150^{0}C temperature of the hot junction and minimum is 2.1102mv at the 50^{0}C temperature of the hot junction

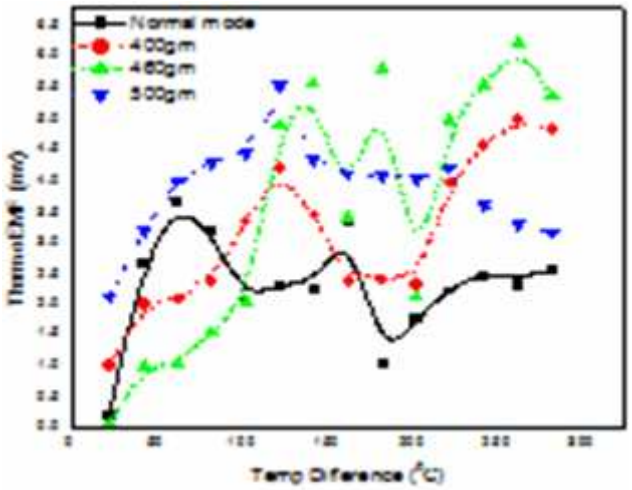

Fig. 4 Effect of mechanical load on thermo-emf generation

For a quick reference, the neutral temperatures (the temperature of the hot junction at which the thermo-emf is maximum) with load applied are given below in Table2.

4. CONCLUSIONS

i. Applications of mechanical stress do affect the generation of thermo-emf and this effect is different for different load applications. As for a load of 500gm, the thermo-emf is more at all temperature ranges in comparison to normal mode (without load).
ii. Load effects for loads of 250gm to 400gm are considerable only up to the higher temperature range of 210^{0}C of the hot junction with some erratic ariations at few temperatures in between.
iii. The load of 460gm becomes more effective up to a temperature difference of 130^{0}C of the hot junction.
iv. Finally, it is very clear that small loads (i.e., stress) are effective only in the higher temperature ranges but higher loads (i.e., stress) is better for the entire temperature range.

Table 2 Stress Vs Neutral Temperatures

Sl. No.	Load (gm)	Stress [10^4 N/m^2]		Neutral Temp (^{0}C)	Corresponding EMF (mv)
		Cooper	Constantan		
1	No Load	No Stress	No Stress	90	3.647
2	250	1412.9	7573.8	310	4.211
3	300	1695.4	9088.7	310	4.972
4	350	1978.0	10603.4	270	10.011
5	400	2260.6	12118.2	310	4.832
6	460	2599.7	13935.9	290	6.209
7	500	2825.7	15147.8	150	5.517

REFERENCES

[1] K.Qiu and A.C.S.Hayden, "Development of a Thermoelectric Self Powered Residential Heating System", Journal of Power Sources, Vol.180, 2008, pp. 884-889.

[2] Hyeung-Sik Choi *et.al,* "Development of a Temperature Controlled Car - Seat System Utilizing Thermoelectric Device", Applied Thermal Engineering, Vol.27, 2007, pp.2841-2849.

[3] K. Murakami *et. al,* "Development of Waste Heat Recovery System from Transformer with Bi-Te Thermoelectric Modules", http://home.agh.edu.pl/~ets2004/proceedings/Murakami.PDF.

[4] V. Leonov and R.J.M. Vullers, "Wearable Thermoelectric Generators for Body Powered Devices", Journal of Electronics Materials DOI: 10.1007/s11664-008-0638-6.

[5] Jin-cheng Zheng, "Recent Advances on Thermoelectric Materials", Front. Phys. China, Vol. 3, 2008, pp.269-279.

[6] A.J. Mortlock, "The Effect of Tension on the Thermoelectric Properties of Metals", Australian Journal of Physics, Vol. 6, 1953, pp.410.

[7] E. S. Morgan, "The Effect of Stress on the Thermal EMF of Platinum-Platinum/lS Rhodium Thermo-couples", J . Appl. Phys., J. Phys. D, Vol.1, 1968, pp. 1421.

[8] V.V. Chernysh and B.S. Cuamba, "Thermo EMF in Ll-Dl Germanium Models under Strong Hydrostatic Stress", Eduardo Mondlane University, Mozambique, XIII International Forum on Thermoelectricity, 10-13 February 2000.

A Futuristic Model for Activity Comfort using Artificial Neural Network (ANN)

P. Pul Singh, Jitendra Yadav, M. K. Bhiwapurkar, V. H. Saran and S. P. Harsha
MIED, Indian Institute of Technology, Roorkee, India
E-mail:- ppsingh.iitr@gmail.com

Abstract

A study was conducted in trains (Indian Railways) to measure the onboard vibrations, noise and a subjective rating of discomfort using a 7-point scale was evaluated with a questionnaire survey to assess the discomfort of approximately 100 passengers' performing sedentary activities (reading and writing). The results revealed that approx. 15-25% of the passengers reported their experience in performing sedentary activities as "Somewhat comfortable" whereas 20-29% as "Somewhat uncomfortable" due to vibrations and jerks. The accelerations (longitudinal, lateral and vertical), anthropometric parameters, noise level and assigned values of sitting postures and activities data treated as inputs and response of passengers as desired outputs were analyzed using a back propagation neural network model to predict the discomfort level of the passengers. Results of the analysis showed good correlation (91.8%) between passengers' rating and output of ANN. So, the developed ANN model can be used to predict activity comfort for futuristic train design.

Keywords: *Activity comfort, ANN, Low frequency vibrations, Questionnaire survey*

1. INTRODUCTION

Trains serve the purpose of transportation and also for provide working place to carry out sedentary activities like reading, writing, etc. There are, however, several important factors inside the train environments that hamper the performance of such activities. Some of the main sources of disturbance, apart from other train passengers, are noise and vibrations generated from the train itself. Although there are standards available for evaluation of ride comfort in vehicles none of these standards consider the effects of vibrations on sedentary activities.

A field study on Swedish inter-city trains (Khan and Sundstrom, 2004 [2]) which include both a questionnaire survey and vibration measurements found satisfactory vibration levels according to ISO 2631- 1.

All the studies indicate the importance of considering the context and seated posture when comfort is assessed in a vibrating environment. A few vibration studies, however, have been conducted in Great Britain and Japan (Suzuki *et.al.,* 2000) [3]. Train passengers exposure of noise has been studied with the focus on masking different sources of sound (Khan, 2003) [4]. A study on evaluation of neural network model on individual thermal comfort has been done (Weiwei L *et.al* 2006) [1].

The obejective of present study is to developing a futuristic model for activity comfort where the responses of the passengers can be predicted by artificial neural network.

2. MATHEMATICAL MODEL USING ANN

Artificial Neural Network (ANN) is an interconnected group of artificial neurons. These neurons use a mathematical or computational model for information processing. ANN is an adaptive system that changes its structure based on information that flows through the network. ANN is able to learn by example. Each neuron can take many input signals, then, based on an internal weighting system, produces an output signal which is generally input to another neuron.

2.1 Back Propagation Model

The back propagation method is a technique used in training multilayer neural networks in a supervised manner. The back propagation method, also known as the error back propagation algorithm, is based on the error-correction learning rule. It consists of two passes through the different layers of the network: a forward pass and a backward pass. In the forward pass, an activity pattern is applied to the input nodes of the network, and its effect propagates through the network layer by layer. Finally, a

set of outputs is produced as the actual response of the network. During the forward pass the synaptic weights of the networks are all fixed. During the backward pass, the synaptic weights are all adjusted in accordance with an error-correction rule. The actual response of the network is subtracted from a desired response to produce an error signal. This error signal is then propagated backward through the network. The synaptic weights are adjusted to make the actual response of the network move closer to the desired response in a statistical sense. The weight adjustment is made according to the generalized delta rule to minimize the error the system.

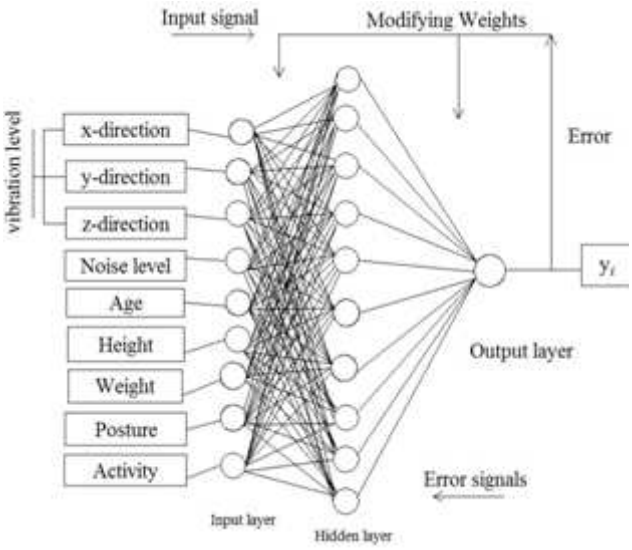

μ_o, h_o

Fig.1 Multi layer 9-10-1 BP neural network model

From the above Figure 1, a 9-10-1 multi layer back propagation network (Weiwei Liu *et.al* [1]), where 9 input layer units, are vibration levels (x, y and z-directions, in m/s^2), noise level, anthropometric parameters (age, height and weight) of the passengers, assigned values for sitting postures (lap and table) and activities (reading, writing and etc., shown in the table 2) and 10 hidden layer units and ANN response is output.

NOMENCLATURE

u_j - Summation at hidden unit
h_j - Output parameter of hidden layer
y_k - Summation at output unit
o_k - Output parameter
w_{ij} - Weight from input layer to hidden layer
v_{jk} - Weight from hidden layer to output layer
x_i - Input parameter of input layer
η - Learning rate
- Momentum
- Are biases at input and hidden layers respectively

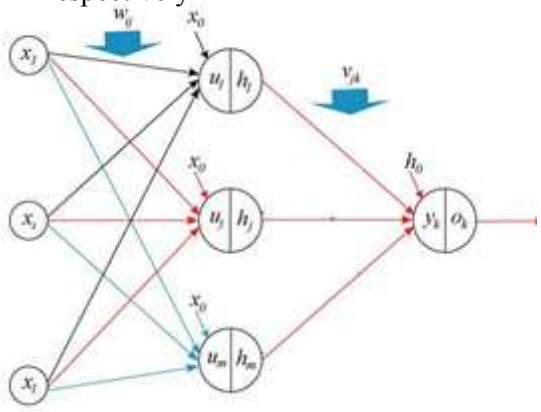

Fig. 2 Architecture of back propagation

2.2 Transfer Function

Summing function at hidden unit,

$u_j = \sum_{i=0}^{n} w_{ij} x_i + x_0$ and $y_k = \sum_{i=0}^{n} v_{jk} h_j + h_0$ at output unit and Log sigmoid transfer function at hidden unit is $h_j = \frac{1}{1+e^{-u_j}}$ and at output unit is $o_k = \frac{1}{1+e^{-y_k}}$

2.3 Training Function
Gradient Descent Method

Gradient based methods are one of the most widely used error minimization methods used to train back propagation networks. The error function is,

$$E(w) = \frac{1}{2}\sum_{i=0}^{N}[t_k - o_k]^2 \quad \text{.....(1)}$$

$$\frac{\partial E(w)}{\partial w_i} = \frac{\partial}{\partial w_i}\frac{1}{2}\sum_{i=0}^{N}[t_k - o_k]^2 \quad \text{.....(2)}$$

$$w_i(t+1) = w_i(t) - \eta\frac{\partial E(w)}{\partial w_i}$$

Back propagation training rule for output unit

$$\text{Delta rule}: \frac{\partial E}{\partial v_{jk}} = \frac{\partial E}{\partial y_k}\frac{\partial y_k}{\partial v_{jk}} = \frac{\partial E}{\partial y_k}h_j$$

$$\delta o_k = \frac{\partial E}{\partial y_k} = \frac{\partial E}{\partial o_k}.\frac{\partial o_k}{\partial y_k} = \frac{\partial E}{\partial o_k}.o_k(1-o_k)$$

where, $o_k = \frac{1}{1+e^{-y_k}}$;

$$\frac{\partial E}{\partial o_k} = \frac{\partial}{\partial o_k}\left(\frac{1}{2}\sum(t_k - o_k)^2\right) = -(t_k - o_k)$$

$$\delta o_k = -(t_k - o_k).o_k.(1-o_k)$$

$$\frac{\partial E}{\partial v_{jk}} = -(t_k - o_k).o_k.(1-o_k)h_j = \delta o_k.h_j$$

$$\Delta v_{jk}^{new} = \Delta v_{jk}^{old} - \eta \delta o_k.h_j \quad \text{.....(3)}$$

Similarly Backpropagation training rule for hidden unit is given by

$$\frac{\partial E}{\partial w_{ij}} = \frac{\partial E}{\partial u_j}\frac{\partial u_k}{\partial w_{ij}} = \frac{\partial E}{\partial u_j}x_i$$

And finally the weights are updated using equation (4)

$$\Delta w_{ij}^{new} = \Delta w_{ij}^{old} - \eta \delta h_j.x_i \quad \text{.....(4)}$$

2.4 Adaption Learning Function

Momentum (μ) can be added to BP method learning by making weight changes equal to the sum of a fraction of the last weight change and the new change suggested by the gradient descent BP rule. With momentum a network can slide through such a minimum error value.

$$\Delta w$$

.....(5)

3. METHODOLOGY

The study was conducted on various Indian railway passenger trains e.g. super fast, express, mail etc with AC chair car class of travel in three tiers AC on Haridwar to Saharanpur route. The study was performed in two parts simultaneously. The first part consisted of a questionnaire survey about the influence of vibration on various sedentary activities and postures adopted in these activities. The second part consisted of vibration and noise measurements.

3.1 Vibration and Noise Measurement

The main objective of the vibration measurements was to investigate the vibration levels that are present in contemporary passenger trains. The transmission of the vibration to the whole body is higher for the seated passengers who are using armrest, backrest and place both feet on the floor, therefore, the abilities to perform sedentary activities satisfactorily are very much dependent on the vibrations of the floor. The present study used a tri-axial accelerometer (KISTLER 8393B10) for measurements on the floor. The tri-axial accelerometer was mounted directly on the floor of the train using adhesive material and the signal sent to a laptop via a data acquisition card (NI 6008). The vibrations were recorded in each of the three primary axes viz, longitudinal(X), lateral(Y) and vertical (Z). The vibration samples are acquired with sampling rate of 2K for 15 minutes, Figure 3. The noise level inside train compartment was also measured using sound level meter (B&K) are shown in Table 2.

Fig. 3 Onboard vibration measurement setup

Normally window side seat was considered for vibration measurement. The trains considered and data measured in the study are shown in table 1. Since three different trains were used in the measurement study they would most likely also differ in frequency spectra due to their dynamic properties.

3.2 Questionnaire Survey

The questionnaire survey was also conducted simultaneously with vibration measurement on selected four trains e.g. 2017, 2055 and 2053. Approximately 50

printed questionnaires were distributed randomly to the passengers of each train either in English or Hindi language as per passenger's preference, Figure 4.

Fig. 4 Questionnaire respondent by passenger

In order to obtain a broad and representative base for the data the questionnaires were handed out to more than 100 randomly selected passengers on the trains. We have collected physical parameters (age, height and weight), level of discomfort of activities and postures (lap and table) using 7-point scale, where its two extreme points are "very comfortable" and "very uncomfortable" as shown in Figure 5.

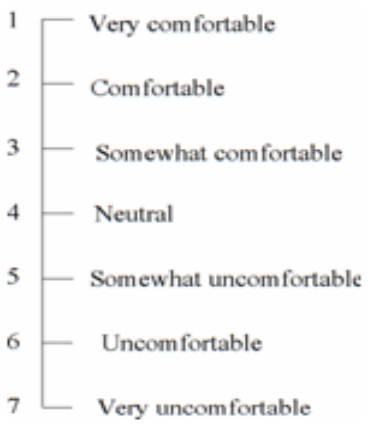

Fig.5 Seven point subjective comfort level

3.3 Assigned Values

The values are assigned based on the responses given by the passengers. The total average responses values of each activities based on different postures is divided by total number of points on the scale and the values are shown in the Table 1.

Table 1 Assigned Values

Description	Type	Assigned Values
Posture	Table	0.8
	Lap	0.6
Activity	Reading	0.7
	Writing	0.6
	Eating /Drinking	0.3
	Resting/Sleeping	0.4

3.4 Analysis of Data

The measured data, questionnaire data and assigned values were analysed using Back Propagation Neural Network. From all the data, for validation purpose 20% of the data randomly selected from each train with different activities and postures were trained to predict the responses of the passengers. A Multi layer 9-10-1Back Propagation Neural Network Model (Figure 1) has been trained the data using log sigmoid function as a transfer function, Gradient Descent Method as a training function and Learning Gradient Descent Momentum as an adaption learning function. The trained data got good correlation with 91.89% as shown in Table 3.

4. RESULTS AND DISCUSSION

The data will be divided in to the three different stages, are training, validation and testing where the 60-75% of the data goes for training (Figure 6), 15-20% for validation (Figure 7) and 15-20% for testing (Figure 8) and the overall correlation between output and target shown in Figure 9. If the value of regression, R=0, then there is no correlation between the output and target and R=1, there is a good correlation. For training the regression value is 81.9%, for validation 96.44% and for testing it is 99.96%.

The overall correlation between the output of the ANN and the subjective ratings is 91.8%, is considered to be good (Figure 7). So the conclusion is that an ANN predicted the human response with good correlation.

Table 2 Measured Data in Different Trains

Sl. No.	Train No.	Train Name	Station From	Station To	Class	Vibration Level (m/s^2)			Noise Level
						x-direction	y-direction	z-direction	(dBA)
1	2053	Jan-Shatabdi Exp.	Haridwar	Roorkee	CC	0.4	0.42	0.54	62-67
2	2055	Jan-Shatabdi Exp.	Tapri	Roorkee	CC	0.29	0.36	0.44	60-68
3	2017	Dehradun Shatabdi Exp.	Tapri	Haridwar	CC	0.67	0.86	0.94	65-72

Table 3 Input Values and Corresponding Predicted Output Values by ANN

Sl. No	Vibration level(m/s^3)			Noise level (dB)	Age	Height(cm)	Weight(kg)	Posture	Activity	Response of passengers	ANN Response
	x	y	z								
1	0.29	0.36	0.44	68	49	175.7	84	0.6	0.4	3	2.876
2	0.29	0.36	0.44	68	24	168	63	0.8	0.6	5	4.844
3	0.29	0.36	0.44	68	54	158.5	56	0.6	0.3	6	5.265
4	0.29	0.36	0.44	68	59	163	67	0.6	0.3	4	4.562
5	0.29	0.36	0.44	68	53	165	85	0.8	0.7	4	4.166
6	0.29	0.36	0.44	68	35	157	59	0.6	0.6	5	5.012
7	0.29	0.36	0.44	68	40	165	63	0.6	0.4	6	5.986
8	0.4	0.42	0.54	67	61	154.94	71	0.8	0.6	6	5.597
9	0.4	0.42	0.54	67	48	167.64	58	0.8	0.3	2	2.35
10	0.4	0.42	0.54	67	54	167.64	78	0.8	0.6	5	3.772
11	0.4	0.42	0.54	67	53	165.1	64	0.8	0.7	2	2.425
12	0.4	0.42	0.54	67	54	167.64	78	0.6	0.4	5	4.906
13	0.4	0.42	0.54	67	45	160	64	0.6	0.7	4	4.121
14	0.4	0.42	0.54	67	48	175	63	0.6	0.4	3	3.012
15	0.67	0.73	0.94	72	49	177.8	72	0.8	0.7	2	2.619
16	0.67	0.73	0.94	72	32	173	75	0.8	0.6	5	4.742
17	0.67	0.73	0.94	72	32	173	75	0.6	0.4	4	4.024
18	0.67	0.73	0.94	72	23	165.1	120	0.8	0.3	5	4.769
19	0.67	0.73	0.94	72	19	165.1	60	0.6	0.7	4	4.058
20	0.67	0.73	0.94	72	26	157	68	0.6	0.4	6	6.235
21	0.67	0.73	0.94	72	36	160	76	0.8	0.3	5	4.639

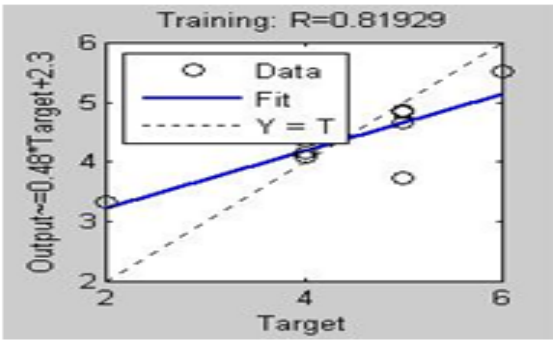

Fig.6 Training of Data

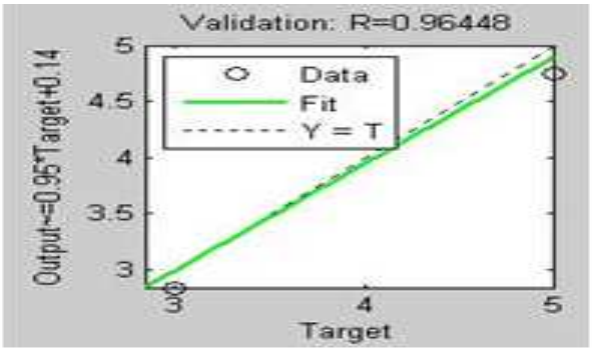

Fig.7 Validation of Data

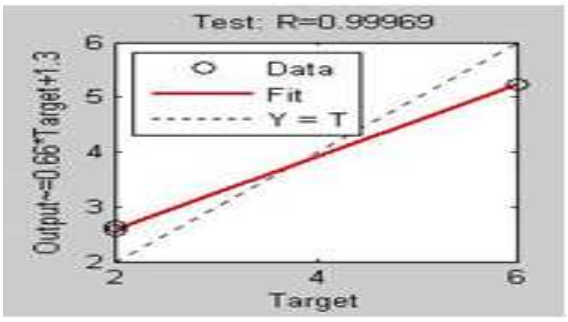

Fig. 8 Testing of Data

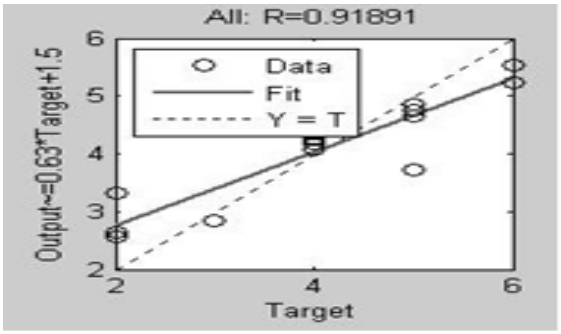

Fig.9 the overall Correlation between the output of the ANN and the subjective ratings is R=91.8%

5. CONCLUSION

An Artificial Neural Network (ANN) model for predicting sedentary activities comfort was developed based on the back propagation algorithm with gradient descent method as training the network. Compared with the experimental data from the questionnaire survey, the results of an ANN showed a good correlation (91.8%) with the subject's rating on comfort level. So, the developed neural network model can be used to predict activity comfort for futuristic train design.

REFERENCES

[1] Weiwei Liu, Zhiwei Lian and Bo Zhao, "A Neural Network Evaluation Model for Individual Thermal Comfort", Energy and Buildings, Vol. 39, 12th December 2006, 2007, pp.1115-1122.

[2] J. Sundstrom, "Contextual Studies of Truck Drivers Sitting", Licentiate Thesis, Chalmers University of Technology, Gothenburg.

[3] H. Suzuki, "Research Trends on Riding Comfort Evaluation in Japan", Proceedings of the Institution of Mechanical Engineers Part F - Journal of Rail and Rapid Transit, Vol. 212, 1998, pp. 61-72.

[4] S.M. Khan, "Effects of Masking Sound on Train Passenger Aboard Activities and on other Interior Annoying Noises", Acta Acustica, Vol. 89, 2003, pp. 711-717.

[5] A. Brindisi and A. Concilio, "Passengers Comfort Modeling Inside Aircraft",Journal of Aircraft, Vol. 45, No. 6, November-December 2008.

[6] C. Corbridge, M.J. Griffin and P.R. Harborough, "Seat Dynamics and Passenger Comfort", Institution of Mechanical Engineers, J Rail and Rapid Transit, Vol.203, 1989, pp.57- 64.

[7] W. Jaschinski, H. Heuer and H. Kylian, "A procedure to Determine the Individually Comfortable Position of Visual Displays Relative to the Eyes", Ergonomics, Vol. 42, 1999, pp. 535-549.

[8] S. Khan and J. Sundstrom, "Vibration Comfort in Swedish Inter-City Trains - A Survey on Passenger Posture and Activities", Proceedings of the 17th International Conference in Acoustics (ICA), Kyoto, Japan, 2004, pp. 3733-3736.

[9] Volker Mellert, Ingo Baumann, Nils Freese and Reinhard Weber, "Impact of Sound and Vibration on Health, Travel Comfort and Performance of Flight Attendants and Pilots", Institute of Physics, Oldenburg University, 26111 Oldenburg, Germany, 25 October 2007.

[10] S.K. Lee and H.C. Chae, "The Application of Artificial Neural Networks to the Characterization of Interior Noise Booming in Passenger Cars", Proc. InstnMech. Engrs, Part D: J. Automobile Engineering, Vol. 218, 2004.

Application of Acoustic Emission Technique in Surface Texture Monitoring during Turning Operation

G. Priyadarshini[1], Manpreet Bains[2], Bhuvnesh Bhardwaj[1], P. K. Singh[1] and Rajesh Kumar[1]

[1]Department of Mechanical Engineering, Sant Longowal Institute of Engineering and Technology, Longowal, Punjab-148 106, India

[2]Department of Mechanical Engineering, H.C.T.M. Kaithal, Haryana -136027, India

E-mail: rajesh_krs@rediffmail.com

Abstract

In this paper an acoustics based non-contact and indirect monitoring technique has been investigated to study the surface texture of work-piece and monitoring tool condition during turning operation. The acoustic emission (AE) signals, were acquired from tool post jig, and found to have the parametric features in 10–1000 Hz frequency domain for variable machining conditions. Machining was performed on mild steel work-piece. The tool used in the study was high speed steel (HSS). Results show that at lower feed rate/rev, AE-RMS value was less and surface roughness (Ra) value of the machined surface was also less i.e. better quality surface was obtained. With a sharp tool, power of the observed acoustic emission was low and surface roughness (Ra) value obtained for the finished surface was high but increase in tool radius results in higher acoustic emission and lower surface roughness (Ra) value of the finished surface.

Keywords: *Acoustic emission, Root mean square value, Turning, surface roughness*

1. INTRODUCTION

Acoustic emission (AE) is basically the stress waves generated by the sudden release of energy in deforming materials. If analysed properly, the charecteristics of the sound observed during machining can be advantegious in monitoring the process parameters. It has been successfully used in laboratory tests to detect tool wear and fracture in single-point turning operations. Dornfeld et al. pointed out the possible sources of AE during metal-cutting processes [1]. Methods have been developed for monitoring tool wear [2,3] in turning [4], milling [5], drilling [6], boring [7], grinding [8], and forming [9] oprations. Once acoustic emission signatures thresholds and bandwidth are established for a specific configuration, the AE signal and AE root mean square (RMS) may be monitored and compared to nominal values to detect abnormal events.

Surfaces obtained from machining processes are more vulnerable to damage of surface integrity than the surfaces obtained from cold working and polishing processes. However, by proper selection of machining parameters, quality surface finish and good surface integrity may be obtained. Routara et al. investigated the Influence of machining parameters (spindle speed, depth of cut and feed rate) on the quality of surface produced in CNC end milling in a conventional way. Analysis of AE signal can be helpful in simplifying the measurement process and controlling machining parameters. Kamarthi et al. dealt with the representational and analysis issues of AE signals in turning processes [10]. The effectiveness of the wavelet representation of AE signals was studied in the context of flank wear estimation problem in turning processes. A set of turning experiments was conducted in which the flank wear was monitored through AE signals. Specially designed neural network architecture was used to relate AE features to flank wear. Many researchers have focused their research on the development of methods for on-line monitoring of cutting tool breakage[7]. Li presented a real-time tool breakage detection method for small-diameter drills using AE and current signals. The features of tool breakage were obtained from the AE signal using typical signal processing methods. The relationship between the AE signal and tool wear is not so simple. Kim et al. observed the purely progressive tool wear in turning operations. As a result, they found that in most experimental results the refined mean level (RML) of the averaged AE signal increases at first with an increase of flank wear, and then stays at an approximately constant level even with further increase of flank wear while the fluctuation of the RML across the constant level becomes rather high.

During the last decade, some time-frequency methods have received growing attention and gained reliable acceptance in the field of condition monitoring. The method is usually based on visual observation of contour

plots. The progression of faults can be observed from the changes of the distribution features in the contour plots. Wavelet decomposition were also used for the purpose. Different problems may require the use of different time-frequency techniques. The raw AE signal usually contains high frequency components; therefore it requires signal acquisition equipment capable of signal sampling at high frequency. An appropriate method for analyzing the AE signal based on the root mean square of the signal is often used, this allows with the traditional signal processing systems with much lower sampling frequency to be used for data analysis. The RMS value of the AE signal, which presents the signal energy and has lower frequency content, has been the basis of the analysis carried out by Jemielniak and Otman. However, one should be aware of the nature of the AE signals and be careful when extracting results from the system to avoid processing incorrect or distorted results.

In this paper an acoustics based technique has been investigated to study the the effect of cutting parameters during turing operation on surface texture of machined work-piece. The acoustic emission (AE) signals were acquired from tool post jig, under variable machining conditions. Both the RMS value and Fourier transform of the AE signal were used to analyse the workpiece-tool interaction and average surface roughness (Ra) of the machined surface. This study is useful in identifying suitable conditions for good surface finish with the help of acoustic signals generated during the machining operation.

2. EXPERIMENTAL DETAILS

Experiments were conducted to study the effect of different cutting parameters on surface roughness of the finished product. Mild steel (MS) was selected as work-piece material. High speed steel (HSS) tool (nose radius 0.6mm) was used to machine the work-piece. Experiments were performed on conventional lathe centre which was having selectable automatic feed and spindle speed (rpm). Experimental set-up is shown in Figure 1. Machining was done at a cutting speed of (395rpm) 28.92m/min and diametral depth of cut (DOC) of 1mm with varying feeds. Effect of change in feed in the range of F1 (0.06mm/rev) to F5 (0.09mm/rev) on AE-RMS and Ra were obsered. The recorded signals were processed in MATLAB. The root mean square values of the raw acoustic emission signals for the selected cutting parameters were obtained.

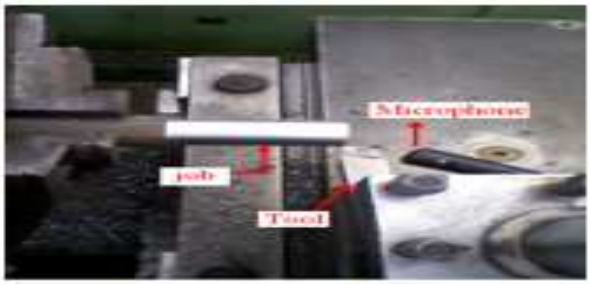

Fig. 1 Experimental set-up used for machining mild steel on conventional lathe centre

After machining, the measurements of average surface roughness were made on a Surfcorder. For each machined surface, three measurements of surface roughness were taken at different locations and the average value was used in the analysis.

3. RESULTS AND DISCUSSION

For the mentioned cutting parameters,values of AE-RMS and Ra are tabulated and shown in Table 1.

Table 1Values of AE-RMS and Surface Roughness Corresponding to Different Feed

Feed, mm/rev	AE-RMS, x dB	Two most dominating frequencies in acoustic signal obtained from Fourier transform, Hz		Surface roughness, Ra , µm
0.06	0.0571	25	975	1.94
0.071	0.059	25	975	2.2713
0.076	0.062	25	975	2.279
0.082	0.0653	55	950	2.288
0.09	0.0668	55	950	3.34

The graph for AE-RMS vs. feed shown in the above table is plotted in Fig. 2 which shows that as the feed increases, AE-RMS value increases. For a depth of cut of 1mm and a cutting speed of 28.92m/min, the graph for acoustic-rms vs. surface roughness is plotted and shown in Figure 3. From the plot in Figure 3, it is evident that the surface roughness (Ra) increases, when there is increase in AE-RMS value. AE-RMS value has increased due to incresed value of feed force. Plot between feed and surface roughness is also drawn and is shown in Figure 4. This plot (Fig. 4), shows that as the feed increases, surface roughness increases.

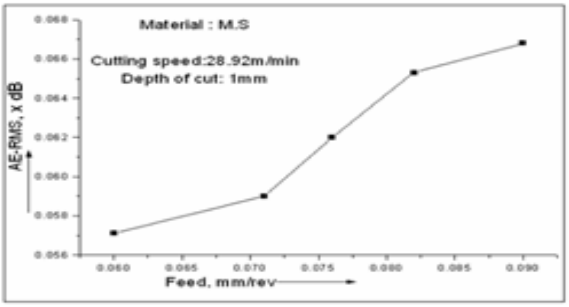

Fig. 2 AE-RMS vs. feed for mild steel at a speed of 28.92m/min.

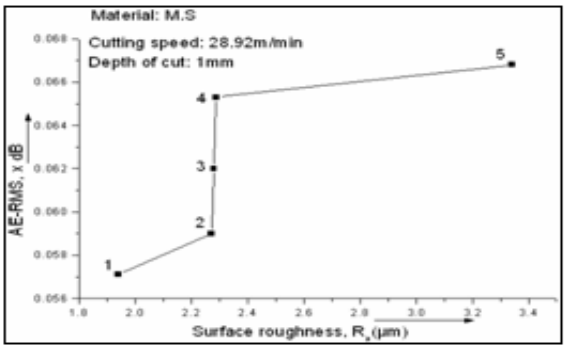

Fig. 3 AE-RMS vs. surface roughness for mild steel

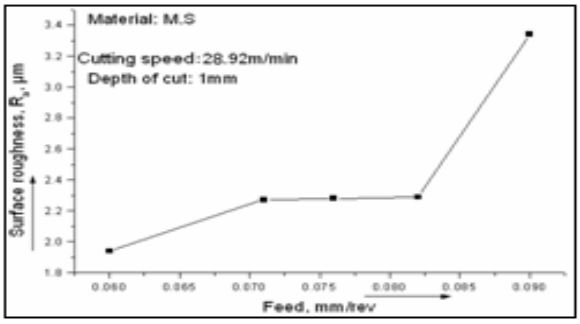

Fig. 4 Surface roughness vs. feed for mild steel

Investigations on tool with increased nose radius (1.2mm) reveals that for the the same cutting speed, DOC and feed, the value of AE-RMS increases but at the same time Ra value decreases. The acoustic emission (AE) signals, which were acquired from tool post jig, are found to have the parametric features in 10–1000 Hz frequency domain for the variable machining conditions. The dominating frequency indicates the charecteristics of acoustic emission which is dependent on tool-workpiece material ineraction under the machining condition.

3. CONCLUSION

The experimental results and analysis reveal that the acoustic emission while metal machining can be very useful in identifying relative surface quality of the product and hence in selection of proper cutting parameters. When machining MS workpiece with a sharp HSS tool at a cutting speed of 28.92m/min and diametral depth of cut of 1mm in varying feed range of 0.06mm/rev to 0.09mm/rev, as the feed increases values of AE-RMS increases along with increase in the value of Ra. Keeping other conditions same, tool with incresed nose radius results in high AE-RMS and low Ra value. Investigations shoe that the power of acoustic emission technique can be effectively used in online condition monitoring of machining parameters.

REFERENCES

[1] D.A. Dornfeld and G. Byrne, "Tool Condition Monitoring-the Status of Research and Industrial Application", CIRP, Vol. 44, No. 2, 1995, pp.541-567.

[2] M.S. Lan and D.A. Dornfeld, "In-process Tool Fracture Detection", J. Eng. Mater. Tech., ASME, Vol. 106, No.2, 1981, pp.111-118.

[3] E. Emel, "Tool Wear Detection by Neural Network Based AE Sensing In: Control of Manufacturing Processes", ASME, New York, 1991, pp. 425-428.

[4] J.Y. Chung and D.A. Blaser, "Transfer Function Method of Measuring in a Duct System with Flow", J. Acoustic Society of America, Vol. 67, 1980, pp. 1559- 1566.

[5] A. Yan, T.I.El-Wardany and M.A. Elbestawi, "A Multi-ssensor Strategy for Tool Failure Detection in Milling", Int. J. Mach. Tools Manufact., Vol. 35, No.3, 1995, pp.383-398.

[6] S.R.Ravishankar and C.R.L.Murthy, "Characteristics of AE Signals Obtained during Drilling Composite Laminates", NDT Int., Vol. 33, 2000, pp.341-348.

[7] X. Li and J. Wu, "Wavelet Analysis of Acoustic Emission Signals in Boring", Proceedings of the I Mech E, Part B, J.of Engg., Manufacture, Vol. 214, No.5, 2000, pp. 421-424.

[8] J. Webster, I.Marinescu, R. Bennet and R. Lindsay, "Acoustic Emission for Process Control and Monitoring of Surface Integrity during Grinding", CIRP Ann., Vol. 43, 1994, pp. 299-304.

[9] A.F. Seybert, "Two-sensor Methods for the Measurement of Sound Intensity and Acoustic Properties in Ducts", J.of the Acoustic Society of America, Vol. 83, No.6, 1988, pp. 2233-2239.

[10] S. Kamarthi, S. Kumara and P. Cohen, "Wavelet Representation of Acoustic Emission in Turning Process", Intell. Eng. Syst. Artif. Neural Netw., Vol. 5, 1995, pp. 861-866.

Indian Journal of Engineering, Science, and Technology (IJEST)

(ISSN: 0973-6255)
(A half-yearly refereed research journal)

Information for Authors

1. All papers should be addressed to The Editor-in-Chief, Indian Journal of Engineering, Science, and Technology (IJEST), Bannari Amman Institute of Technology, Sathyamangalam - 638 401, Erode District, Tamil Nadu, India.
2. Two copies of manuscript along with soft copy are to be sent.
3. A CD-ROM containing the text, figures and tables should separately be sent along with the hard copies.
4. Submission of a manuscript implies that : (i) The work described has not been published before; (ii) It is not under consideration for publication elsewhere.
5. Manuscript will be reviewed by experts in the corresponding research area, and their recommendations will be communicated to the authors.

Guidelines for submission

Manuscript Formats

The manuscript should be about 8 pages in length, typed in double space with Times New Roman font, size 12, Double column on A4 size paper with one inch margin on all sides and should include 75-200 words abstract, 5-10 relevant key words, and a short (50-100 words) biography statement. The pages should be consecutively numbered, starting with the title page and through the text, references, tables, figure and legends. The title should be brief, specific and amenable to indexing. The article should include an abstract, introduction, body of paper containing headings, sub-headings, illustrations and conclusions.

References

A numbered list of references must be provided at the end of the paper. The list should be arranged in the order of citation in text, not in alphabetical order. List only one reference per reference number. Each reference number should be enclosed by square brackets.

In text, citations of references may be given simply as "[1]". Similarly, it is not necessary to mention the authors of a reference unless the mention is relevant to the text.

Example

[1] M.Demic, "Optimization of Characteristics of the Elasto-Damping Elements of Cars from the Aspect of Comfort and Handling", International Journal of Vehicle Design, Vol.13, No.1, 1992, pp. 29-46.

[2] S.A.Austin, "The Vibration Damping Effect of an Electro-Rheological Fluid", ASME Journal of Vibration and Acoustics, Vol.115, No.1, 1993, pp. 136-140.

SUBSCRIPTION

The annual subscription for IJEST is Rs.600/- which includes postal charges. To subscribe for IJEST a Demand Draft may be sent in favour of IJEST, payable at Sathyamangalam and addressed to IJEST. Subscription order form can be downloaded from the following link http:// www.bitsathy.ac.in./ ijest.html.

For subscription / further details please contact:

IJEST
Bannari Amman Institute of Technology
Sathyamangalam - 638 401, Erode District, Tamil Nadu Ph: 04295 - 221289
Fax: 04295 - 223775 E-mail: ijest@bitsathy.ac.in Web:www.bitsathy.ac.in/ijest.html

Published by

BANNARI AMMAN INSTITUTE OF TECHNOLOGY
Sathyamangalam - 638 401 Erode District Tamil Nadu India
Ph: 04295-221289 Fax: 04295-223775
www.bitsathy.ac.in E-mail: ijest@bitsathy.ac.in

BANNARI AMMAN INSTITUTE OF TECHNOLOGY
Stay Ahead

TÜV CERT EN ISO 9001 Certificate : 3410021309
RWTÜV